CHROMOGENIC SENSORS BASED ON CALIX[4]PYRROLE-STRAPPED CALIX[4]ARENE

Mr. Preecha Thiampanya

A Dissertation Submitted in Partial Fulfillment of the Requirements
for the Degree of Doctor of Phisiosophy Program in Chemistry
Department of Chemistry
Faculty of Science
Chulalongkorn University
Academic Year 2011

เซ็นเซอร์เปลี่ยนสีได้จากคาลิกซ์[4]เอรีนคาดด้วยคาลิกซ์[4]พิร์โรล

นายปรีชา เทียมปัญญา

วิทยานิพนธ์นี้เป็นส่วนหนึ่งของการศึกษาตามหลักสูตรปริญญาวิทยาศาสตรดุษฎีบัณฑิต
สาขาวิชาเคมี ภาควิชาเคมี
คณะวิทยาศาสตร์ จุฬาลงกรณ์มหาวิทยาลัย
ปีการศึกษา 2554

Thesis Title	CHROMOGENIC SENSORS BASED ON CALIX[4]PYRROLE-STRAPPED CALIX[4]ARENE
By	Mr. Preecha Thiampanya
Field of Study	Chemistry
Thesis Advisor	Associate Professor Buncha Pulpoka, Ph.D.

Accepted by the Faculty of Science, Chulalongkorn University in Partial Fulfillment of the Requirements for the Doctoral Degree

…….. Dean of the Faculty of Science
(Professor Supot Hannongbue, Dr.rer.nat.)

THESIS COMMITTEE

…….. Chairman
(Assistant Professor Warinthorn Chavasiri, Ph.D.)

…….. Thesis Advisor
(Associate Professor Buncha Pulpoka, Ph.D.)

…….. Examiner
(Associate Professor Nuanphun Chantarasiri, Ph.D.)

…….. Examiner
(Associate Professor Nongnuj Muangsin, Ph.D.)

…….. Examiner
(Assistant Professor Wanlapa Aeungmaitrepirom, Ph.D.)

…….. External Examiner
(Assistant Professor Tienthong Thongpanchang, Ph.D.

ปรีชา เทียมปัญญา : เซ็นเซอร์เปลี่ยนสีได้จากคาลิกซ์[4]เอรีนคาดด้วยคาลิกซ์[4]พิร์โรล (CHROMOGENIC SENSORS BASED ON CALIX[4]PYRROLE-STRAPPED CALIX[4]ARENE) อ. ที่ปรึกษาวิทยานิพนธ์หลัก : รศ.ดร.บัญชา พูลโภคา, 162 หน้า.

ได้สังเคราะห์และพิสูจน์เอกลักษณ์ของสารประกอบ1,3-ไดพารา-ไนโตรฟีนิลเอโซคาลิกซ์[4]เอรีน-คาลิกซ์[4]พิร์โรล (**9**) ด้วยเทคนิคทางสเปกโทรสโกปี สำหรับใช้เป็นเซ็นเซอร์เปลี่ยนสีได้ จากการศึกษาการเกิดสารประกอบเชิงซ้อนกับแอนไอออนของ ลิแกนด์ **9** ด้วยเทคนิคการเปลี่ยนแปลงสีและยูวีวิซิเบิลสเปกโทรโฟโตเมทรี พบว่าสัญญาณยูวีวิซิเบิลสเปกโทรโฟโตเมทรีของลิแกนด์ **9** เกิดการเปลี่ยนแปลงความยาวคลื่นสูงสุดจาก 395 นาโนเมตรเป็น 600 นาโนเมตรเมื่อแอนไอออนเป็น F^-, AcO^-, BzO^- และ $H_2PO_4^-$ จากการเปลี่ยนแปลงดังกล่าวอาศัยการเกิดปรากฏการณ์การเคลื่อนที่ของอิเล็กตรอนภายในโมเลกุลเปลี่ยนแปลงไปเมื่อมีความจำเพาะในการเกิดสารประกอบเชิงซ้อนกับแอนไอออน ทำให้สามารถจำแนกแอนไอออนดังกล่าวที่มีรูปร่างแตกต่างกันแต่มีสมบัติความเป็นเบสที่ใกล้เคียงกันได้ นอกจากนี้ยังพบว่าลิแกนด์ **9** ยังมีความสามารถในการเกิดสารประกอบเชิงซ้อนแบบจำเพาะกับไอออนโลหะ Ca^{2+} โดยใช้หน่วยจับเป็นเอโซคาลิกซ์[4]เอรีนคราวน์อีเทอร์ เมื่อตรวจสอบสมบัติเป็นตัวรับไอออนแพร์ของลิแกนด์ **9** กับสารประกอบ CaF_2 โดยเทคนิคโปรตอนนิวเคลียร์แมกเนติกเรโซแนนซ์ (เอ็นเอ็มอาร์) พบว่าไม่เกิดการเปลี่ยนแปลงสัญญาณทางสเปกโทรสโกปีใดๆเลย จากนั้นไทเทรตสารละลาย F^-, AcO^-, BzO^- และ $H_2PO_4^-$ ลงในสารประกอบเชิงซ้อน **9**·Ca^{2+} เพื่อศึกษาสมบัติตัวรับไอออนแพร์ของลิแกนด์ **9** พบว่า AcO^- และ BzO^- เกิดสมบัติตัวรับไอออนแพร์กับสารประกอบเชิงซ้อน **9**·Ca^{2+} โดยเปลี่ยนแปลงค่าการดูดกลืนแสงสูงสุดของสารประกอบเชิงซ้อน **9**·Ca^{2+} แต่ F^- และ $H_2PO_4^-$ ทำให้ค่าการดูดกลืนแสงสูงสุดของสารประกอบเชิงซ้อน **9**·Ca^{2+}เกิดการย้อนกลับเป็นลิแกนด์ **9** นอกจากนี้นำสารประกอบ 1,3-ไดพารา-ไนโตรฟีนิลเอโซคาลิกซ์[4]ไดอะซีโตฟีโนน (**7**) ที่ไม่มีหน่วยจับคาลิกซ์ [4]พิร์โรล มาศึกษาการเกิดสารประกอบเชิงซ้อนเปรียบเทียบกับกับลิแกนด์ **9** พบว่าลิแกนด์ **7** เมื่อเกิดอันตรกิริยากับแอนไอออนที่จำเพาะจะไม่เกิดปรากฏการณ์การเคลื่อนที่ของอิเล็กตรอนภายในโมเลกุลและมีรูปแบบของการเกิดสารประกอบเชิงซ้อนเป็นตัวรับไอออนแพร์ที่แตกต่างกับลิแกนด์ **9**

ภาควิชา เคมี ลายมือชื่อนิสิต.....

สาขาวิชา เคมี ลายมือชื่อ อ.ที่ปรึกษาวิทยานิพนธ์หลัก.....

ปีการศึกษา 2554

5073843123 : MAJOR CHEMISTRY
KEYWORDS: CALIX[4]ARENE, CALIX[4]PYRROLE, ANION, ION-PAIR, CROMOGENIC SENSOR, SYNTHESIS

PREECHA THIAMPANYA: CHROMOGENIC SENSORS BASED ON CALIX[4]PYRROLE-STRAPPED CALIX[4]ARENE. THESIS ADVISOR: ASSOC. PROF. BUNCHA PULPOKA, Ph.D, 162 pp.

A new chromogenic sensor 1,3-di-*p*-nitrophenylazo-calix[4]arene-calix[4]pyrrole (**9**) was successfully synthesized and characterized by spectroscopic methodes. Anion binding abilities of ligand **9** was studied by UV-vis spectrophotometry and their color changes. Ligand **9** was found to bind F^-, AcO^-, BzO^- and $H_2PO_4^-$ to a different extent which ascribed to the internal charge transfer occurred upon deprotonation by anions. Then ligand **9** could be discriminate F^-, AcO^-, BzO^- and $H_2PO_4^-$ which have same basicity but different in their sizes and shapes. Ligand **9** also showed highly selective binding with Ca^{2+} using azocalix[4]crownether as a metal chelating unit. Ligand **9** has shown no binding situation with the ion-pair CaF_2 by using ^{1}H-NMR spectroscopy. A series of F^-, AcO^-, BzO^- and $H_2PO_4^-$ were titrated into the solution of complex **9**·Ca^{2+} to study ion pair binding properties of ligand **9**. In case of, AcO^- and BzO^- were found to induce a bathochromic shift in the spectrum of complex **9**·Ca^{2+} but F^- and $H_2PO_4^-$ gave back the spectrum of the free ligand **9**. 1,3-Di-*p*-nitrophenylazo-calix[4]diacetophenone (**7**) which was lack of the calix[4]pyrrole unit was used to compare the binding abilities with ligand **9**. Ligand **7** showed no internal charge transfer upon complexing with anions and gave different ion-pair binding as compared to ligand **9**.

Department: Chemistry Student's Signature .....
Field of Study: Chemistry Advisor's Signature .....
Academic Year: 2011

ACKNOWLEDGEMENTS

This thesis could not be accomplished without the extensive supports, suggestions, assistance, encouragement, kindness, profound and personal friendship throughout my doctoral degree career from my advisors, Associate Professor Dr. Buncha Pulpoka. In addition, I would like to thank Assistant Professor Dr. Warinthorn Chavasiri, Associate Professor Dr. Nuanphun Chantarasiri, Associate Professor Dr. Nongnuj Muangsin, Assistant Professor Dr. Wanlapa Aeungmaitrepirom and Assistant Professor Dr. Tienthong Thongpanchang for their input, interest, valuable suggestions, comments and acting as thesis examiners.

This thesis would not be successful without kindness and helps of a number of people in Supramolecular Research Unit and Organic Synthesis Research Unit. I am grateful to Professor Dr. Thawatchai Tuntulani, Associate Professor Dr. Vithaya Ruangpornvisuti, Associate Professor Dr. Nuanphun Chantarasiri, Assistant Professor Dr. Boosayarat Tamapatanagit and Assistant Professor Dr. Saowarux Fuansawadi. I am also grateful to Mr.Songtham Ruangchaithaweesuk and Dr. Chatthai Keawthong who acknowledge for valuable suggestion to solve problems arisen in my thesis.

I thank to the Supramolecular Chemistry Research Unit, the Organic Synthesis Research Unit, the Graduate School of Chulalongkorn University and the Department of Chemistry Faculty of Science Chulalongkorn University for financial supports. I wish to thank the Science and Technological Research Equipment Center of Chulalongkorn University for Elemental Analysis Results, Mr.Thapong Teerawatananond for his help to refined X-ray structure determination.

I would like to express my appreciation to the former and the current staffs in Supramolecular Chemistry Research Unit (Fai, Onn, Bumbim, Boy, Namm, Jik, Bird, Tao (boy), Tao (girl), Nu, J’ Koi, P’ Nok, P’ New, P’ Ball, P’ Dao, P’ Wan).

I thank to the Center for Petroleum, Petrochemicals, and Advanced Materials for their financial support of all my study in Ph.D program.

Finally, my love and thanks go to my family, especially my father and mother for their love, care, encouragement, kindness, financial support and other assistances throughout my life.

CONTENTS

Page

ABSTRACT IN THAI…….. iv

ABSTRACT IN ENGLISH…….. v

ACKNOWLEDGEMENTS…….. vi

CONTENTS……..…… vii

LIST OF TABLES……. xi

LIST OF FIGURES……..... xii

LIST OF SCHEMES……. xviii

LIST OF ABBREVIATIONS AND SIGNS……. xix

CHAPTER I INTRODUCTION……. 1

1.1 Supramolecular chemistry……. 1

1.2 Molecular recognition……... 1

1.3 Cation receptors…….... 3

1.4 Anion receptors……. 3

1.5 Ditopic receptors……... 4

1.6 Ion-pair receptors…….. 5

1.7 Binding site-signaling subunit approach……..... 7

1.8 Signaling Subunits……..... 7

1.9 Calixarene building block……..... 11

1.10 Chromogenic azocalix[4]arene…….. 12

1.11 Calix[4]pyrrole…… 15

1.12 Objectives of this research……..... 28

CHAPTER II EXPERIMENTAL SECTION…….. 30

2.1 General Procedures…….. 30

2.1.1 Analytical instruments……..... 30

2.1.2 Materials……..... 30

Page

2.2 Synthesis..... 31
2.2.1 Overall of synthetic pathways……. 31
2.2.2 Preparation of triethyleneglycol ditosylate (**1**)……... 33
2.2.3 Preparation of 2-(8-tosyltriethyleneglycol)acetophenone (**2**).... 34
2.2.4 Preparation of 1,3-calix[4]-diacetophenone (**3**)……..... 36
2.2.5 Preparation of 1, 3-calix[4]arene-bis-dipyrroethane (**4**)……... 38
2.2.6 Preparation of calix[4]arene-calix[4]pyrrole (**5**)……. 40
2.2.7 Preparation of calix[4]arene-*p*-nitrophenylazo-calix[4]pyrrole (**6**)…….. 42
2.2.8 Preparation of 1,3-di-*p*-nitrophenylazo-calix[4]-diacetophenone (**7**)..... 44
2.2.9 Preparation of 1,3-di-*p*-nitrophenylazo-calix[4]arene-bis-dipyrroethane (**8**)……..... 46
2.2.10 Preparation of 1,3-di-*p*-nitrophenylazo-calix[4]arene-calix[4]pyrrole (**9**)…… 48
2.3 Complexation studies..... 50
2.3.1 Anion complexation study of ligand **9** by using the UV-vis titration..... 50
2.3.2 Cation complexation study of ligand **9** by using the UV-vis titration..... 52
2.3.3 Anion complexation study of ligand **9** by using the ^{1}H NMR spectroscopy..... 52
2.3.4 Anion complexation study of ligand **7** by using the UV-vis titration..... 52
2.3.5 Cation complexation studyof ligand **7** by using the UV-vis titration..... 53
2.3.6 Anion binding study of ligand **9** in the presence of calcium ion by using UV-vis spectrophotometry..... 53
2.3.7 Anion complexation study of $9{\cdot}Ca^{2+}$ complex by using the ^{1}H-NMR spectroscopy..... 55

Page

CHAPTER III RESULT AND DISCUSSION……..... 56

3.1 Synthesis and characterization of
1,3-di-*p*-nitrophenylazo-calix[4]arene-calix[4]pyrrole (9)..... 56

3.1.1 Synthesis and characterization of 1,3-calix[4]-
diacetophenone (3)..... 56

3.1.2 Synthesis and characterization of
1,3-di-*p*-nitrophenylazo-calix[4]-diacetophenone (7)..... 58

3.1.3 Synthesis and characterization of
1,3-di-*p*-nitrophenylazo-calix[4]arene-bis-dipyrroethane (8)..... 60

3.1.4 Synthesis and characterization of
1,3-di-*p*-nitrophenylazo-calix[4]arene-calix[4]pyrrole (9)..... 61

3.1.5 Synthesis and characterization of
1,3-calix[4]arene-bis-dipyrroethane (4)..... 62

3.1.6 Synthesis and characterization of calix[4]arene-
calix[4]pyrrole (5)..... 63

3.1.7 Synthesis and characterization of calix[4]arene-*p*-
nitrophenylazo-calix[4]pyrrole (6)..... 64

3.2 Anion complexation studies of 1,3-di-*p*-nitrophenylazo-
calix[4]arene-calix[4]pyrrole (9)..... 66

3.3 Anion complexation studies of 1,3-di-*p*-nitrophenylazo-
calix[4]-diacetophenone (7)..... 75

3.4 UV-vis titration of ligand 9 with F^-, AcO^-, BzO^- and $H_2PO_4^-$..... 82

3.5 Cation complexation studies of 1,3-di-*p*-nitrophenylazo-
calix[4]arene-calix[4]pyrrole (9)..... 86

3.6 Anions binding properties of 1,3-di-*p*-nitrophenylazo-
calix[4]arene-calix[4]pyrrole (9) in the presence of calcium cation..... 92

3.7 Complexation studies of ligand 7 with AcO^-, BzO^-, F^- and
$H_2PO_4^-$ in the presence of Ca^{2+} using UV-vis spectrophotometry
and ^{1}H-NMR spectroscopy..... 103

Page

CHAPTER IV CONCLUSION……..... 105

REFERENCES……..... 107

APPENDICES…… 123

APPENDIX A..... 124

APPENDIX B..... 134

APPENDIX C..... 143

APPENDIX D..... 153

VITAE……..... 162

LIST OF TABLES

Table Page

2.1 Concentrations of anions ($X^- = F^-$, AcO^-, BzO^- and $H_2PO_4^-$) used in anion complexation studies with ligand **9** and the final ratios of guest:host X^-/L**9**)..... 51

2.2 Concentrations of anions ($X^- = F^-$, AcO^-, BzO^- and $H_2PO_4^-$) used in anion complexation studies with **9**·Ca^{2+}complex and the final ratio of guest:host (X^-/L**9**·**Ca**$^{2+}$)..... 54

3.1 Stability Constants (log β) of complexes of ligand **9** with anions in CH_3CN by the UV-vis Titration Method (T = 25 °C, I = 0.01 M Bu_4NPF_6)……..... 84

3.2 Geometry and basicity of various anions…….. 85

3.3 Stability constants (log β) of 1:1 complexes of ligand **9** with Ca^{2+} and ligand **9**·Ca^{2+} with anions in CH_3CN by the UV-vis titration method (T = 25 °C, I = 0.01 M Bu_4NPF_6)..... 98

A1 Crystal data and structure refinement for 1,3-di-*p*-nitrophenylazo-calix[4]-diacetophenone (7)..... 125

A2 Atomic coordinates [x 10^4], and equivalent isotropic displacement parameters [$Å^2$ x 10^3]. $U(eq)$ is defined as one third of the trace of the orthogonalized U^{ij} tensor..... 126

A3 Bond lengths [Å] and angles [°]..... 129

LIST OF FIGURES

Figure		Page
1.1	Supramolecular chemistry and molecular recognition represented by "*Lock and Key*" principle……..	2
1.2	Limiting ion-pair interactions relevant to receptor-mediated ion-pair recognition: (a) contact, (b) solvent-bridged, and (c) hostseparated. In this schematic, the anion is shown as "A^-'', the cation as ''C^+'', and the solvent is represented as ''S''……..	6
1.3	Operating principle for the binding site-signaling subunit approach.....	7
1.4	Structures of azophenol derivatives.....	9
1.5	Structures of azo-phenol thiourea derivative.....	10
1.6	Calix[4]arene conformations.....	12
1.7	Chromogenic azo-coupled calix[4]crowns.....	13
1.8	Chromogenic azo-coupled 1,3-di-pyrenyl-calix[4]arenes.....	14
1.9	(a) Azocalix[4]arene **9** coordinated with Ca^{2+} and (b) UV/vis spectra of **9** before and after adding $Ca(ClO_4)_2$, TBA^+F^- and $Ca(ClO_4)_2$ with TBA^+F^- in MeCN/$CHCl_3$ (*v*/*v* = 1000:4).....	15
1.10	Structure of octamethylcalix[4]pyrrole **10** (OMCP).....	16
1.11	1,3-Alternate conformation of (a) calix[4]pyrrole and (b) chloride complex of calix[4]pyrrole, which adopts a cone conformation in the solid state.....	16
1.12	Schematic representation showing various possible modification to the basic calix[4pyrrole core.....	18
1.13	Stucture of pentapyrrolic calix[4]pyrrole (**15**) (a) and Molecular model of compound **15**–acetate (b).....	19
1.14	(a) Structure of calix[4]pyrroles containing deep cavities and fixed walls **16** and (b) the molecular structure of the ethanol adduct of **16** in the cone conformation.....	20
1.15	Structure of (a) calix[4]arene-calix[4]pyrrole pseudo dimer and (b) its crystal structure.....	21

Figure Page

1.16 Structures of meso-octamethylcalix[4]pyrrole **10**, with strapped calixpyrroles containing phenyl **1**7, pyrrole **18** and furan **19** straps..... 22

1.17 Single crystal X-ray structure of the chloride complex of receptor **18**..... 22

1.18 Structures of (a) *cis*- and (b) *trans*-metalloporphyrin-strapped calix[4]pyrrole..... 23

1.19 Structures of chromogenic and fluorogenic strapped calix[4]pyrroles..... 25

1.20 (a) Structure of calix[4]arene-capped calix[4]pyrrole and (b) its crystal structure..... 25

1.21 (a) Proposed binding interactions involving crown-6-calix[4]arene-capped calix[4]pyrrole with Cs^+ and F^- salt and (b) crystal structureof its CsF complex..... 26

1.22 (a) Proposed binding interactions involving calix[4]pyrrole- calix[4]arene pseudodimer **20** with Cs^+ and F^- salt and (b) X-ray crystal structure of its CsF complex..... 27

1.23 Structure and function of each incorporated units of chromogenic 1,3-di-*p*-nitrophenylazo-calix[4]arene-strapped calix[4]pyrrole (**9**)..... 28

1.24 Structure of 1, 3-di-*p*-nitrophenylazo-calix[4]-diacetophenone (**7**)..... 29

2.1 Synthetic pathways of chromogenic calix[4]arene-strapped calix[4]pyrole (**9**)..... 32

3.1 ORTEP drawing of 1,3-di-*p*-nitrophenylazo-calix[4]-diacetophenone (**7**)..... 59

3.2 ORTEP drawing of calix[4]arene-calix[4]pyrrole (**5**)..... 64

3.3 Structure of calix[4]arene-*p*-nitrophenylazo-calix[4]pyrrole (**6**)..... 65

3.4 Wavelength changes of ligand **9** upon the addition of various anions. Condition:ligand **9** (0.02 mM)/CH_3CN; TBAX (100 equiv.)/CH_3CN..... 66

3.5 Colour change of ligand **9** (0.02 mM) with 100 equivalents of anions.... 67

Figure Page

3.6 Absorbance changes of ligand **9** upon the addition of various anions. Condition:ligand **9** (0.02 mM)/CH_3CN; TBAX (6 equiv)/ CH_3CN..... 68

3.7 Colour change of ligand **9** (0.02 mM) with 6 equivalents of anions (from left to right; ligand **9** only, **A** = ligand **9** + F^-, **B** = ligand **9** + AcO^-, **C** = ligand **9** + BzO^-, **D** = ligand **9** + $H_2PO_4^-$)..... 68

3.8 Electronic excitation of an azophenol chromophore..... 69

3.9 ^{1}H-NMR spectra (2-5 ppm) of ligand **9** (3.58 mM) in CD_3CN in the presence of different amounts of TBAF..... 70

3.10 ^{1}H-NMR spectra (5-9 ppm) of ligand **9** (3.58 mM) in CD_3CN in the presence of different amounts of TBAF..... 70

3.11 ^{1}H-NMR spectra (5-9 ppm) of ligand **9** (3.58 mM) in CD_3CN in the presence of different amounts of TBA^+AcO^-..... 71

3.12 ^{1}H-NMR spectra (2-5 ppm) of ligand **9** (3.58 mM) in CD_3CN in the presence of different amounts of TBA^+AcO^-..... 71

3.13 ^{1}H-NMR spectra (5-9 ppm) of ligand **9** (3.58 mM) in CD_3CN in the presence of different amounts of TBA^+BzO^-..... 73

3.14 ^{1}H-NMR spectra (2-5 ppm) of ligand **9** (3.58 mM) in CD_3CN in the presence of different amounts of TBA^+BzO^-..... 73

3.15 Wavelength changes of ligand **7** upon the addition of various anions. Condition: ligand **7** (0.02 mM)/CH_3CN; TBAX (10 equiv)/CH_3CN..... 75

3.16 Color change of ligand **7** (0.02 mM) with 10 equiv of anions (from left to right ligand **7** only, ligand **7** + F^-, ligand **7** + AcO^-, ligand **7** + BzO^-, ligand **7** + $H_2PO_4^-$)..... 76

3.17 Wavelength changes of ligand **7** upon the addition of various anions. Condition: ligand **7** (0.02 mM)/CH_3CN; TBAX (6 equiv)/ CH_3CN..... 76

Figure Page

3.18 Colour change of ligand **7** (0.02 mM) with 6 equiv of anions (from left to right ligand **7** only, ligand **7** + F^-, ligand **7** + AcO^-, ligand **7** + BzO^-, ligand + $H_2PO_4^-$)..... 77

3.19 ^{1}H-NMR spectra (6-10 ppm) of ligand **7** (0.65 mM) in CD_3CN in the presence of different amounts of TBAF..... 78

3.20 ^{1}H-NMR spectra (3-5 ppm) of ligand **7** (0.65 mM) in CD_3CN in the presence of different amounts of TBAF..... 78

3.21 ^{1}H-NMR spectra of ligand **7** (0.65 mM) in CD_3CN in the presence of different amounts of TBA^+AcO^-..... 79

3.22 ^{1}H-NMR spectra of ligand **7** (0.65 mM) in CD_3CN in the presence of different amounts of TBA^+BzO^-..... 79

3.23 Proposed binding mode of ligand **9** + anion (1 : 1)..... 81

3.24 Proposed binding mode of ligand **7** + anion (1 : 1)..... 81

3.25 UV-vis titration of ligand **9** (0.02 mM) in CH_3CN upon addition of F^- (0-6 equiv). (Inset) Absorbance at 395 nm as a function of F^- concentration, indicating in 1:1 and 1:2 ratios for ligand **9**: F^-..... 82

3.26 UV-vis titration of ligand **9** (0.02 mM) in CH_3CN upon addition of AcO^- (0-6 equiv). (Inset) Absorbance at 395 nm as a function of AcO^- concentration, indicating in 1:1 ratios for ligand **9**:AcO^-..... 83

3.27 UV-vis titration of ligand **9** (0.02 mM) in CH_3CN upon addition of BzO^- (0-6 equiv). (Inset) Absorbance at 395 nm as a function of BzO^- concentration, indicating in 1:1 ratios for ligand **9**:BzO^-..... 83

3.28 UV-vis titration of ligand **9** (0.02 mM) in CH_3CN upon addition of $H_2PO_4^-$ (0-6 equiv). (Inset) Absorbance at 396 nm versus the $H_2PO_4^-$ concentration..... 84

3.29 UV-vis spectra of ligand **9** (0.02 mM) before and after adding 300 equivalents of various metals nitrate in CH_3CN (a) and color changes upon addition of 300 equivalents of $Ca(NO_3)_2$ into the solution of ligand **9** (b)..... 86

Figure Page

3.30 ^{1}H-NMR spectra (5-12 ppm) of ligand **9** (1.3 mM) in CD_3CN (a) in the presence of 2 equivalents (b) and10 equivalents (c) of $Ca(NO_3)_2$..... 87

3.31 ^{1}H-NMR spectra (2-6 ppm) of ligand **9** (1.3 mM) in CD_3CN (a) in the presence of 2 equivalents (b) and 10 equivalents (c) of $Ca(NO_3)_2$..... 88

3.32 UV-vis spectra changes for time evolution of ligand **9** (0.02 mM) in CH_3CN in the presence of 300 equivalents of $Ca(NO_3)_2$..... 89

3.33 UV-vis spectra of ligand **9** (0.02 mM) upon titration with 2 equivalents of $Ca(NO_3)_2$ in CH_3CN..... 90

3.34 ^{1}H-NMR spectra of ligand **9** (3.58 mM) in $CDCl_3$ (a) and in the presence of excess CaF_2..... 91

3.35 Spectral changes in the UV-vis absorption of complex **9**·Ca^{2+} (0.02 mM) upon addition 6 equivalents of AcO^- in CH_3CN..... 93

3.36 Spectral changes in the UV-vis absorption of complex **9**·Ca^{2+} (0.02 mM) upon addition 6 equivalents of BzO^- in CH_3CN..... 93

3.37 ^{1}H-NMR spectra (5-11 ppm) of ligand **9** (1.3 mM) in CD_3CN (a) in the presence of 2.0 equiv. of $Ca(NO_3)_2$ (b) in the presence of 3.0 equiv. of TBA^+AcO^- (c) and ^{1}H-NMR spectra of complex **9**·Ca^{2+} (1.3 mM) in CD_3CN in the presence of 6 equiv of TBA^+AcO^- (d)..... 95

3.38 ^{1}H-NMR spectra (2.5-6 ppm) of ligand **9** (1.3 mM) in CD_3CN (a) in the presence of 2.0 equiv. of $Ca(NO_3)_2$ (b) in the presence of 3.0 equiv. of TBA^+AcO^- (c) and ^{1}H-NMR spectra of complex **9**·Ca^{2+} (1.3mM) in CD_3CN in the presence of 6 equiv. of TBA^+AcO^- (d)..... 96

3.39 UV-vis spectra of complex **9**·Ca^{2+} (0.02 mM) upon titration with 6 equiv. of AcO^- in CH_3CN..... 97

3.40 UV-vis spectra of complex **9**·Ca^{2+} (0.02 mM) upon titration with 6 equiv. of BzO^- in CH_3CN..... 97

Figure Page

3.41 (a) UV-vis spectra of complex **9**·Ca^{2+} (0.02 mM) upon titration with 6 equiv. of F^- in CH_3CN and (b) color change of solution of complex **9**·Ca^{2+} added with 6 equiv. of F^-..... 99

3.42 (a) UV-vis spectra of complex **9**·Ca^{2+} (0.02 mM) upon titration with 6 equiv. of $H_2PO_4^-$ in CH_3CN and (b) color change of solution of complex **9**·Ca^{2+} added with 6 equiv. of $H_2PO_4^-$..... 99

3.43 UV-vis spectra of ligand **9** (0.02 mM in CH_3CN) (black line), after adding 6 equivalents of F^- (red line) and then 2 equivalents of $CaNO_3$ (green line)..... 100

3.44 ^1H NMR spectra of **9** (2.0 mM) (a) after addition of 3 equiv. of F^- in CD_3CN (b) and excess $Ca(NO_3)_2$ were add to the **9**·F^- complex (c) and the pathway of color changed (inset)..... 101

3.45 The ion-pairing effect..... 102

3.46 Spectral changes in the UV-vis absorption of complex **7**·Ca^{2+} (0.02 mM) upon addition 6 equiv. of AcO^- and BzO^- in CH_3CN (a) and color changes of ligand **7** (0.02 mM) in CH_3CN after adding 2 equiv. of $Ca(NO_3)_2$ and addition 6 equiv. of AcO^- or BzO^- respectively (b)..... 103

3.47 ^1H-NMR spectra of ligand **7** (5.46 mM) upon titration with 3 equiv. of F^- in $CDCl_3$ and excess $CaNO_3$ was added to the **7**·F^- complex..... 104

LIST OF SCHEMES

Scheme Page

3.1	Synthetic pathway of 1,3-calix[4]-diacetophenone (**3**)……..…….	56
3.2	Synthetic pathway of 1**,**3-di-*p*-nitrophenylazo-calix[4]-diacetophenone (**7**)……	58
3.3	Synthetic pathway of 1,3-di-*p*-nitrophenylazo-calix[4]arene-bisdipyrroethane (**8**)……...	60
3.4	The synthesis of 1,3-di-*p*-nitrophenylazo-calix[4]arene-calix[4]pyrrole (**9**)…….	61
3.5	Synthetic pathway of 1,3-calix[4]arene-bis-dipyrroethane(**4**)…….	62
3.6	The synthesis of calix[4]arene-calix[4]pyrrole (**5**)……...	63
3.7	The synthesis of calix[4]arene-*p*-nitrophenylazo-calix[4]pyrrole (**6**)…..	64

LIST OF ABBREVATION AND SIGNS

A	Anion
Å	Angstrom
δ	Chemical shift
λ	Wavelength
AcO^-	Acetate ion
Anal	Analytical
Ar-	Aromatic
$BF_3{\cdot}OEt_2$	Boron trifluoride diethyl etherate
Bu_4NF	Tetrabutylammonium fluoride
Bu_4NCl	Tetrabutylammonium chloride
Bu_4NBr	Tetrabutylammonium bromide
Bu_4NI	Tetrabutylammonium iodide
Bu_4NCH_3COO	Tetrabutylammonium acetate
$Bu_4NPhCOO$	Tetrabutylammonium benzoate
Bu_4NPF_6	Tetrabutylammonium hexafluorophosphate
Bu_4NNO_3	Tetrabutylammonium nitrate
$Bu_4NH_2PO_4$	Tetrabutylammonium hydrogenphosphate
Bu_4NClO_4	Tetrabutylammonium perchlorate
BzO^-	Benzoate ion
°C	Degree celcious
CH_3CN	Acetonitrile
CD_3CN	Acetonitrile deuterated
$CDCl_3$	Chloroform deuterated
^{13}C-NMR	Carbon thirteen Nuclear Magnetic Resonance
$Ca(ClO_4)_2$	Calcium perchlorate
CsF	Cecium fluoride
Calcd	Calculate
DMAP	Dimethylaminopyridine

EDTA	Ethylenediamine tetraacetic acid
equiv	Equivalent
em	Emission
EtOAc	Ethyl acetate
g	Gram
^{1}H-NMR	Proton Nuclear Magnetic Resonance
HOMO	Highest Occupied Molecular Orbital
Hrs	Hours
Hz	Hertz
I	Ionic strength
IR	Infrared spectroscopy
J	Coupling constant
K	Degree Kelvin
L	Ligand
LUMO	Lowest Unoccupied Molecular Orbital
M	Molar
MALDI-TOF	Matrix Assistant Laser Desorption/Ionization-Time of Flight
MHz	Mega Hertz
mg	Milligram
mL	Milliliter
mM	Milli molar
mmol	Millimol
nm	Nanometer
p-	Para-position
ppm	Part per million
RT	Room temperature
s,d,t,m	Splitting patterns of ^{1}H-NMR (singlet, doublet, triplet and multiplet)
st	stretching
T	Temperature

TBAX	Tetrabutylammonium anion
TBAF	Tetrabutylammonium fluoride
$TBA^{+}AcO^{-}$	Tetrabutylammonium acetate
$TBA^{+}BzO^{-}$	Tetrabutylammonium benzoate
$TBAPF_6$	Tetrabutylammonium hexafluorophosphate
TFA	Trifluoro acetic acid
THF	Tetrahydrofuran
TLC	Thin layer chromatography
TsCl	Toluene-4-sulfonyl chloride
UV-vis	Ultraviolet-Visible Spectrophotometry
X^{-}	Anion

CHAPTER I

INTRODUCTION

1.1 Supramolecular chemistry

Research in the area of supramolecular chemistry which may be defined as "*chemistry beyond the molecule*" [1] is now an interesting branch of chemistry. These molecular systems result from the association of two or more chemical species held together by intermolecular forces, not by covalent bonds. Supramolecular chemistry is thermodynamically less stable, kinetically more labile and dynamically more flexible than ordinary molecules.

Supramolecular chemistry may be divided into two broad categories, supermolecules and supramolecular assemblies. Supermolecules come from intermolecular association of a few components. Supramolecular assemblies are polymolecular entities that result from the spontaneous association of a large number of components into a specific phase having more or less well-defined microscopic organization and characteristic. The development of supramolecular chemistry has led to a growing interest in the design and synthesis of macrocyclic molecules incorporating intermolecular cavities.

1.2 Molecular recognition

Molecular recognition is a critical component of intermolecular processes, including enzyme-substrate recognition, receptor-ligand binding, molecular self-assembly, and chemical sensing. The design of new hosts and/or guests is essential for providing insight into the factors governing molecular recognition and for preparing new materials with desirable properties.

Basically, molecular recognition is defined by energy and information involved in the binding and selection of substrate(s) by a given receptor molecule containing a specific function. Sometime, this idea is described as "*Lock and Key*" principle

(Figure1.1) [2]. The arrangement of binding sites in the host (lock) is complementary to the guest (key) both sterically (structurally) and electronically.

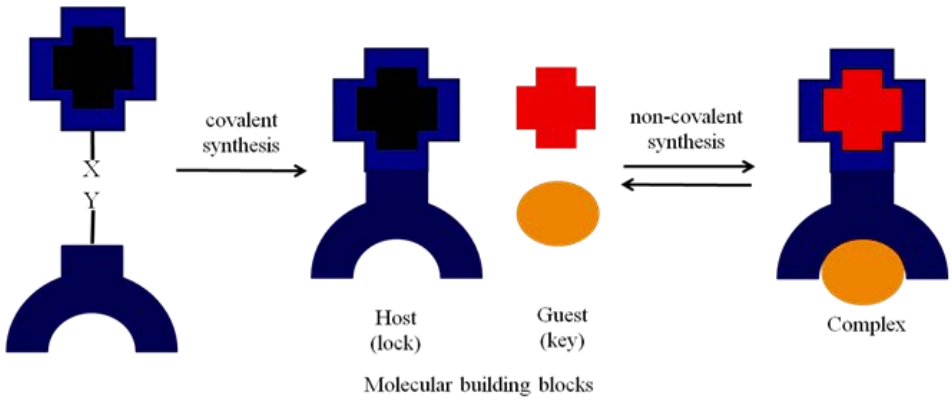

Figure 1.1 Supramolecular chemistry and molecular recognition represented by "*Lock and Key*" principle [2].

Molecular receptors are defined as organic structures held together by covalent bonds, that are able to bind ionic or molecular substrates (or both) by means of various intermolecular interactions such as electrostatic interaction, ion-dipole interaction, dipole-dipole interaction, hydrogen bonding, π-π stacking interaction, cation-π interaction, hydrophobic effects and close packing in the solid state, leading to an assembly of two or more species [3]. Design of receptor molecules depends on numerous types of complementary between host and guest such as geometry, size and electron cloud and interactions. Moreover, the large contact area and multiple interaction sites which lead to the strong overall bindings are also effected [1]. Molecular recognition can be divided into neutral substrate recognition, [4] cation recognition, [5, 6] and anion recognition [7-10].

Supramolecular chemists hope to probe fundamental aspects of molecular recognition through design and synthesis of completely artificial receptors, followed by examination of the structures and stabilities of artificial receptors and their complexes. Application of these kinds of synthetic receptors can be used in a number of areas, such

as medical analysis, detection of toxic compounds in environments, development of biosensors, separation of mixtures of compounds, including separation of enantiomers.

1.3 Cation receptors

Recognition of cation is one of the most interesting subjects in recent years. Due to various metal ions belong to metalloenzyme or it is well known that some heavy metal ions are toxic for organism, and early detection in the environment is desirable [11].

Some of many applications of cationic receptors are to get rid of metallic pollutants in the environment and to study a metal ion playing an important role in living systems. Over the last two decades, the search for new material as chemical receptor for metal ion has been an area of rapid development. Many molecular platforms such as crown ethers, [12, 13] cryptands, [14] cyclodextrins, [15] porphyrins [16] and calixarenes [17] are used to construct well-defined structures. Especially, attention has been paid on calixarene since it has binding ability toward alkaline and alkali earth metal ions that play various important roles in biochemistry and environmental science. A principle in the design of artificial receptors is based on using the proper binding sites and a proper cavity size. Their chemistry mainly depends on the hard-soft acid-base concept [18]. Ion-ion interactions, ion-dipole interactions and cation-π interactions play important roles in this kind of chemistry [1, 2].

1.4 Anion receptors

The design and synthesis of anion receptors possessing high affinity and adequate selectivity for various targeted substrates are also one of the most interesting subjects in recent year‟s which represents an ongoing challenge in the area of supramolecular chemistry. Anion recognition is often affected by hydrogen bonding interaction. Such interaction is weak which is one of the reasons that anion recognition is more challenging to achieve than cation complexation [19, 20]. Appreciated as being more difficult to achieve than cation recognition, this challenge continues to attract the attention of the

researchers within the molecular recognition community due to the important roles of anions play in various biological as well as environmental systems.

Compare to relatively well-developed cation receptors, [21] development of anion receptors is only emerging as a research area of significant importance [22]. The slow development of anion recognition can be related to some inherent differences between anions and cations:[23]

i. Anions are relatively large and therefore require (macrocyclic) receptors with a much larger binding site. The smallest anion, F^-, has the same ionic radius (1.33 Å) as a moderate size cation (K^+).
ii. Anions have many different shapes, e.g., spherical halides, linear SCN^-, trigonal planar NO_3^-, and tetrahedral $H_2PO_4^-$.
iii. Anions are more strongly hydrated than cations of equal size, whereas the solvation by organic solvents is generally less favorable.
iv. Several anions are presented only in a narrow pH window, e.g., $H_2PO_4^-$, and CO_3^{2-} anions in acidic and basic environment, respectively.

1.5 Ditopic receptors

The design of receptors for cations, and more recently anions, is a continuing challenge to supramolecular chemists. As its name, a ditopic receptor contains two binding cavities. These two cavities are probably for either the same or different ions. In the case that ditopic receptors are designed for two alkaline cations, [24] two transition metal cations, [25-27] or one organic salt with the same ends, [28-30] they are defined as "*homoditopic receptors*". On the other hand, the receptors for alkaline earth cation-transition metal cation, [31] alkaline cation-anion, [32-34] transition metal cation-anion [35-36] or organic ion-pair [37] are categorized as "*heteroditopic receptor*". [38]

The simultaneous complexation of cationic and anionic guest species by heteroditopic multisite receptor named "*ion-pair recognition*" is a new field of supramolecular chemistry which is the interface of cation and anion coordination [39]. The basic approach to develop receptors that recognize the salt as an associated ion-pair is to reduce the interference of anions during cation binding study or *vice versa*. These

heteroditopic receptors consist of two recognition moieties that are either directly linked to allow a highly efficient communication or connected by a flexible spacer to ensure an optimal approaching of the ion-pair. Therefore, these bifunctional receptors can be designed to exhibit novel co-operative or allosteric behavior, which one charged guest can enhance binding ability of another through hydrogen bonding, hydrophobic functionality, electrostatic force and conformation effects [40, 41].

1.6 Ion-pair receptors

For both cation and anion recognition are now well-established branches of supramolecular chemistry [42−49]. Ion pair receptors might also permit a greater level of control over ion recognition, extraction and through-membrane transport than simple ion receptors. In fact, in many cases, ion pair receptors containing binding sites for both cations and anions display affinities for ion pairs or their constituent pairs of ions that are enhanced relative to simple ion receptors. Often this is the result of allosteric effects, such as those derived from favorable electrostatic interactions between the co-bound ions [50−52]. However, in spite of their potential applications in various fields, such as salt solubilization, extraction, and membrane transport, the number of well characterized ion pair receptors remains limited. This could reflect a combination of synthetic challenges (the systems reported to date have not been easy to prepare) and experimental complexities associated with tracking multiple ionic species as well as the high inherent labiality of many ion pairs [50−52].

To effect anion recognition, most ion pair receptors take advantage of hydrogen bonding donors (urea, amide, imidazolium, pyrrole, and hydroxyl group), Lewis acidic sites (boron, aluminium and uranyl), and positively charged polyammonium groups [42−49]. In contrast, the majority of ion pair receptors rely on lone pair electron donors including crown ethers [53] and π-electron donors, such as functionalized calixarenes, for cation recognition [54,55].

In the limit, ion pair receptors can be classified as binding ion pairs in either a sequential or concurrent fashions. In the case of sequential binding, the receptor can bind one ion of the ion pair on its own. Once bound, this first ion enhances the affinity for the

other ion of the ion pair through an allosteric effect or by providing an additional binding driving force, commonly a direct or solvent-mediated electrostatic interaction with its counter ion [50−52]. By contrast, in the case of concurrent ion pair binding, the receptor literally forms a simultaneous complex with the anion and cation of the ion pair. Typically, this results in a complex where the two ions of the ion pair are in direct contact or spatially separated *via* one or more molecules of solvent or by the receptor skeleton [50−52].

Another way of classifying ion pair receptors is by how they bind the cations and the anions of targeted ion pairs. Here, three different binding modes can be defined. These limiting modes are depicted in Figure 1.2 and differ in how the ion pair is held within a host molecule. The first involves a contact ion pair, wherein the anion and the cation are in a direct contact (Figure 1.2(a)); the second, termed a solvent-bridged ion pair, is where one or more solvent molecules bridge the gap between the anion and the co-bound cation (Figure 1.2(b)), while the third consists of a host-separated ion pair, wherein the anion and the cation are bound relatively far from one another, usually by the receptor framework (Figure 1.2(c)) [53-55]. Depending on the identities of co-bound ions, the separation distance between ion pairs, the nature of the constituent recognition sites, and the nature of the solvents, a given receptor can bind a given ion pair in one or more of these limiting modes.

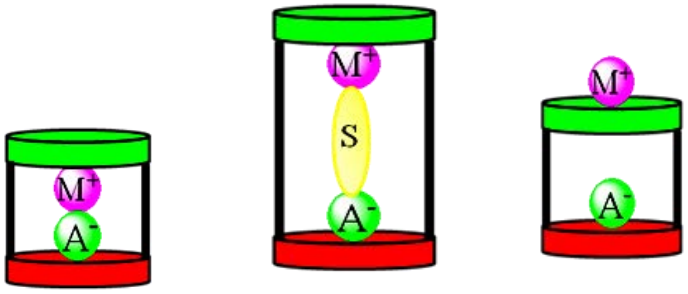

Figure 1.2 Limiting ion-pair interactions relevant to receptor-mediated ion-pair recognition: (a) contact, (b) solvent-bridged, and (c) host-separated. In this schematic, the anion is shown as "A^{-}"; the cation is denoted as "M^{+}"; and the solvent is represented as "S".

1.7 Binding site-signaling subunit approach

Many chemical sensors follow the approach of the covalent attachment of signaling subunits and binding sites as schematically shown in Figure 1.3. This has been the most widely used approach in the development of anion chemosensors and will surely be a fundamental approach in future developments. As shown in Figure 1.3, the coordination site binds anion in such a way that the properties of the signaling subunit are changed giving rise to variations either in its color (chromogenic chemosensor) or fluorescence behaviors (fluorogenic chemosensor).

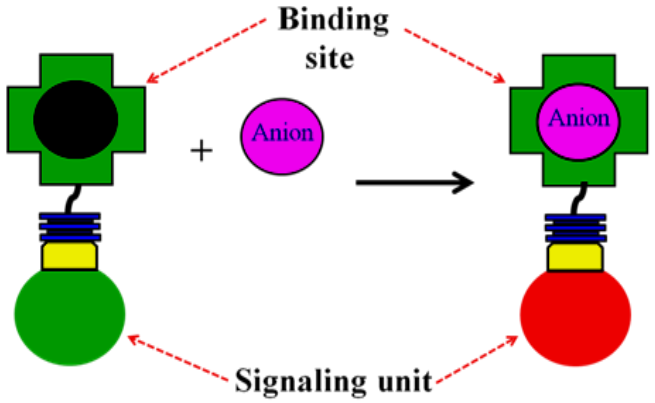

Figure 1.3 Operating principles for the binding site-signaling subunit approach.

1.8 Signaling Subunits

The role of the signaling subunits is to act as a signal transducer. That is, it translates chemical information taking place at the molecular level (the anion binding process) into a signal. It could be consider that, the use of spectroscopic signaling subunits able to transducer the coordination event into changes in either color or fluorescence behavior [56].

1.8.1 Chromogenic principles of sensing

Color changes as signaling events have been widely used because it requires the use of inexpensive equipment or no equipment at all as color changes can be detected by the naked eye [57]. In fact, there are many examples of analytical determinations whose final step involves the formation of a colored compound that is indication of the initial concentration of a certain analyze. This is so basically for cations and in a minor coverage for anions [58]. The chromogenic reagents use the same type of design principles as fluorogenic reagents do. Those involve the binding site-signaling subunit approach, the displacement approach, and the chemodosimeter approach.

1.8.2 Dyes as signaling subunits

Organic compounds become colored by absorbing electromagnetic radiation in the visible range (from 400 to 700 nm approximately), and investigations relates with the correlation between chemical structure and color in organic dyes are carried out extensively. It is soon recognized that many dyes contain systems of conjugated bonds, and it is the energy gap between the HOMO and the LUMO that is critical in determining the color of a certain organic dye. Thus, many conjugated systems have HOMO to LUMO differences in energy that correspond to visible light and it is well-established that the larger the conjugated system is, the shorter the difference between fundamental and excited states, resulting in a more bathochromic shift of the absorption band of lesser energy [59]. In addition to that basic conjugated backbone relates with the length of the conjugated system, there is a chemical mean of modifying the absorption wavelength by anchoring electron donor (NR_2, NHR, NH_2, OH, OMe, O^-, X^-, etc.) or electron acceptor (NO_2, SO_3H, SO_3^-, COOH, C=O, etc.) groups to the conjugated system [59]. When both an electron donor and an electron acceptor group are present and are connected through a conjugated system in a certain molecule, a charge transfer band can be observed. This corresponds to a charge transfer transition where, upon excitation with light, there is an important fraction of electronic charge that is transferred from the donor to the acceptor. What is important related to the design of chromogenic reagents is that the interaction of

anions with the donor or acceptors groups in those systems can result in a change in color. Thus, for instance, the interaction of an anion with a donor group will make this more donor, pumping more electrons to the conjugated system, enhancing the conjugation, and inducing a bathochromic shift. For most of the reported chromo sensors for anions, based on the binding site signaling subunit approach, containing anion binding sites and acceptor groups such as nitrophenyl, anthraquinone, azo dyes, etc., a shift to longer wavelengths was observed upon anion coordination.

1.8.3 The binding site containing azo dyes

Azo dye derivatives have been used as chromogenic subunits in the development of some chromogenic receptors for anion recognition. The UV-visible spectra of these chromogenic receptors consist of absorbance in the UV zone due to the presence of the aromatic rings and a charge transfer band, from a donor atom (nitrogen or oxygen) to the acceptor nitro group, centered around 450-480 nm and responsible for the orange-red color usually observed [59].

A family of azo-phenol receptors containing as anion coordination sites one unique phenol (as in **1**-**3**) or phenolthiourea groups (**4**-**6**) for anion sensing has been developed.

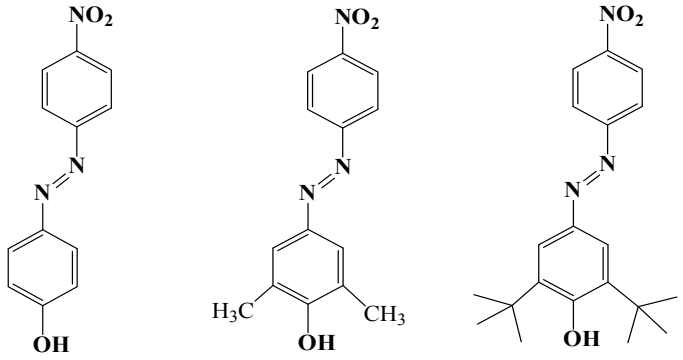

1 **2** **3**

Figure 1.4 Structures of azophenol derivatives.

In all cases, the phenol group was connected through a conjugated system with the acceptor nitrophenyl moiety. In the presence of certain anions, coordination with the phenol (*via* hydrogen bond) or deprotonation (proton transfer from the phenol to the anion) of the phenolic group was observed. With either coordination or deprotonation, the outcome was an enhancement of the donor character of the phenolic oxygen resulting in a red shift of the charge transfer band. Azo-phenols **1**-**3** were capable of selective detection of F^- over other anions tested ($H_2PO_4^-$, AcO^-, N_3^-, Cl^-, Br^-, and HSO_4^-) in dichloromethane solutions, by a change in color from yellow (λ_{max} = 390 nm) to bluish purple (for **1**, λ_{max} = 562 nm) or blue (for **2**, λ_{max} = 615 nm, and for **3**, λ_{max} = 632 nm) [60]. UV-vis and ^{19}F NMR experiments showed that the new absorption band at 615 nm was due to deprotonation of the phenolic group and formation of HF.

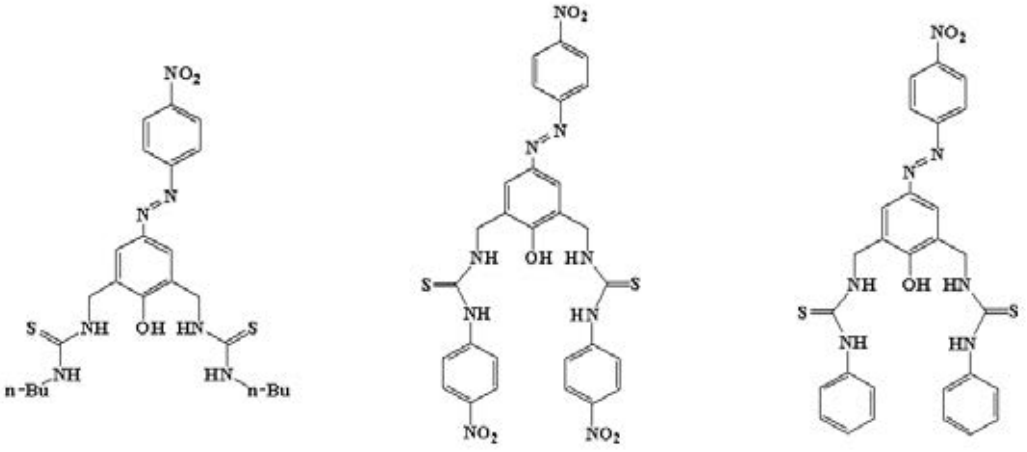

4 **5** **6**

Figure 1.5 Structures of azo-phenol thiourea derivatives.

Compound **4**, containing two thiourea groups and a phenol as a binding unit, gave color variation in the presence of F^-, $H_2PO_4^-$, and AcO^- in chloroform solutions [61]. Compound **4** showed an absorption maximum at 376 nm, and a new peak at 529 nm was found upon addition of those basic anions. For HSO_4^- and Cl^-, the color change was only detectable upon addition of 10 equivalents, whereas a large excess of Br^- or I^- resulted in

no color change. The color shift was assigned to the formation of strong complexes between **4** and the anions through hydrogen-bonding interactions between the anions and the protons of the thiourea and the phenolic-O*H*. The dual receptor **5** contains two backbones susceptible to color variation: the azophenol and the thiourea-nitrophenyl [62]. Compound **5** showed, in the absence of anions, one absorption maxima at 339 nm in chloroform. In the presence of $H_2PO_4^-$, with four oxygen atoms affecting both chromophores *via* multitopic hydrogen bonds, a pronounced color change was observed, while F^- and AcO^- had a relatively weaker effect. Thus, with $H_2PO_4^-$, the absorption band of **5** at 339 nm decreased while a new one gradually appeared at 374 nm (due to the anion interaction with the thiourea-nitrophenyl backbone) and at 538 nm (due to anion interaction with the azophenol). The color of the solution changed from light yellow to violet. No detectable color changes were observed upon addition of HSO_4^-, Cl^-, and Br^-. In the case of receptor **6**, color differentiation between the $H_2PO_4^-$, AcO^-, and F^- anions was not feasible because the new absorption band obtained upon complexation of the three anions with **6** was similar and centered at *ca.* 530 nm.

1.9 Calixarene building block

Calix[*n*]arene, a family of synthetic macrocyclic receptors consisting of cyclic arrays of *n* phenolic moieties linked by methylene groups, [63] was chosen as the putative host. This cyclic oligomer made up of phenol and formaldehyde provides new fascinating platforms [64]. The most famous calixarene is calix[4]arene because of (1) convenient preparation in large quantities, (2) easy chemical modification on both their lower and upper rims, and (3) unique structural properties, they have been ideal platforms for the development of complexing agents, not only for cations and molecules, but also anions. Calix[4]arene can adopt 4 conformations; cone, partial cone, 1,2-alternate and 1,3-alternate (Figure 1.6). Cone conformation is the most stable due to an array of hydrogen bond between the phenolic-O*H* groups at the narrow rim of the macrocycle. This conformation is particular useful because of its “bucket” shape leading to the rigidify cavity.

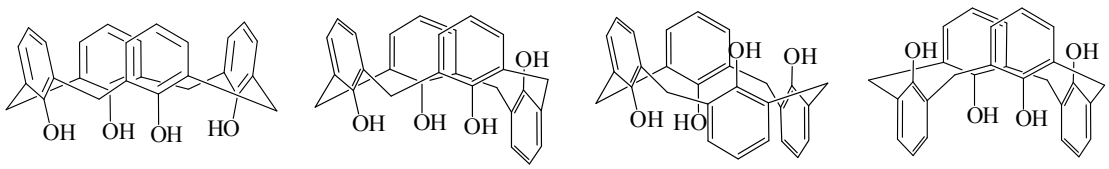

cone partial cone 1,2-alternate 1,3-alternate

Figure 1.6 Calix[4]arene conformations.

This cavity-containing molecule possesses hydroxyl groups on the lower rim and potentially free *para* position on the upper rim. The hydroxyl group provides convenient points for attachment of various moieties, as numerous other researchers have been demonstrated [65-66]. Calixarene with the appropriate appended groups are good candidates for probes because they have been shown to be highly specific ligands. In addition, their potential applications as sensing agents have received increasing interest. Indeed, the most significant feature of chemistry of these rigid macrocyclic molecules is their ability to bind selectively alkali, alkaline earth, transition metal cations [64] and a wide variety of anions inside the cavity [67].

Their potential application in the treatment of metal rich nuclear wastes has been investigated worldwide [68-69]. Calixarene-based receptors were found to form complexes with cationic or anionic species and also a variety of organic ion or organic compounds [70]. Furthermore, they are used as chemical sensors, [71] enzyme mimetic, [72] allosteric molecules [73] and peptide libraries [74].

1.10 Chromogenic azocalix[4]arene

Considering that azophenol dyes can be used as chromogenic anion sensors, [75-78] the deduced of azophenol can easily available azocalixarenes, containing one or more azophenol chromophores and different binding sites, would be ideal candidates for developing new chromogenic sensing systems for the ions. Shinkai *et al.* reported that calix[4]arene having a 4-(4-nitrophenyl)azophenol unit with three ethyl ester groups showed a lithium ion selectivity with respect to the UV-vis band shift [79]. Chang *et al.* reported a bathochromic shift of a *p-tert*-butylcalix[4]arene bearing a 1,3-diazophenol

unit upon calcium ion complexation [80]. Reinhoudt *et al.* also reported that a calix[4]arene with triamide and monoalkylated azophenol units on the lower rim gave a UV-vis band shift, in which the direction of the shift was dependent on the conformation of the calixarene [81].

Recently Jong Seung Kim and coworkers have described calixcrown-6 compounds carrying a pair of phenylazo moieties [82]. The azo-coupled calix[4]crown showed a red shift upon the addition of Ca^{2+} to the calixcrown carrying two OH groups and a blue shift for the calix[4]crown carrying two OR groups. For the compounds with two OR groups on the lower rim (Figure 1.7 (a)) and a fixed partial cone conformation (Figure 1.7 (b)), a blue shift caused by electrostatic interaction between the oxygen atoms of OR and the metal ion as well as a red shift caused by the π-metal complexation between the rotated calix benzene and the metal ion were observed.

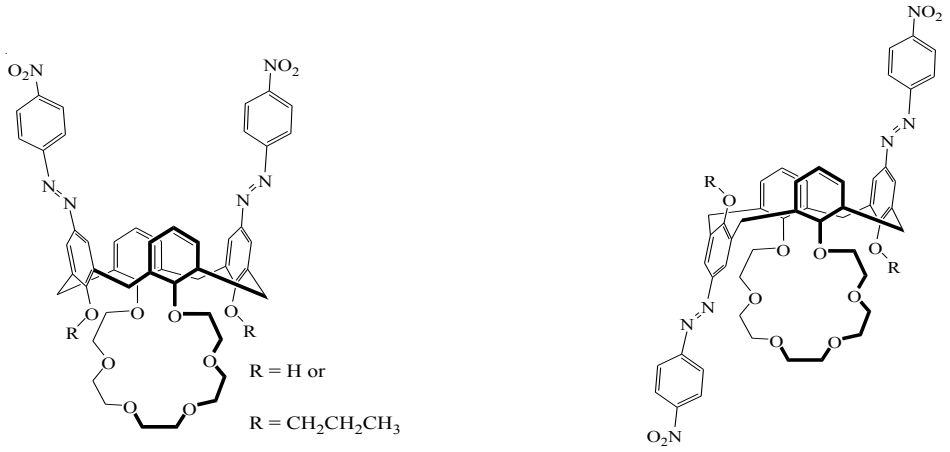

(a) (b)

Figure 1.7 Chromogenic azo-coupled calix[4]crowns.

A Bifunctional (fluorescence and visible light absorption) anion sensing compounds **7** and **8** based on calix[4]arene platform with 4-nitrophenylazo and pyrene, which is responsible for the different sensing property have been developed by Jong Seung Kim and coworkers [83]. The two NHs of the amide groups of **7** bind the fluoride

anion through the H-bonding. This changes the characteristic excimer emission and forms a new emission peak from a *static* excimer. In **8**, two OHs bind the fluoride anion, and this changes the characteristic absorption spectrum. From the DFT calculation supports the regioselective binding of the fluoride anion, which is responsible for the different sensing property.

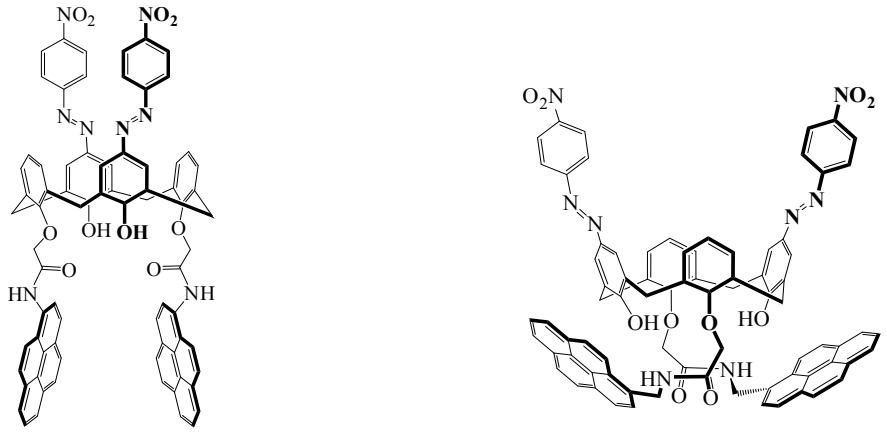

7 **8**

Figure 1.8 Chromogenic azo-coupled 1, 3-di-pyrenyl-calix[4]arenes.

Chung, Wen-Sheng and coworkers reported a bifunctional chromogenic calix[4]arene **9**, which contains both triazoles and hydroxyl azophenols as both cationic and anionic recognition sites and the azophenol moiety as a coloration unit, was designed and synthesized [84]. The recognition of Ca^{2+} by **9** gave rise to a marked color change from greenish to bright yellow, whereas the recognition of F^{-} by **9** showed a color change from light green to bluish. As a consequence of the UV-vis spectral behavior of **9** toward Ca^{2+} and F^{-} ions (Figure 1.9 (b)), contributes to the construction of a miniaturized and integrated molecular level device with logic gate function.

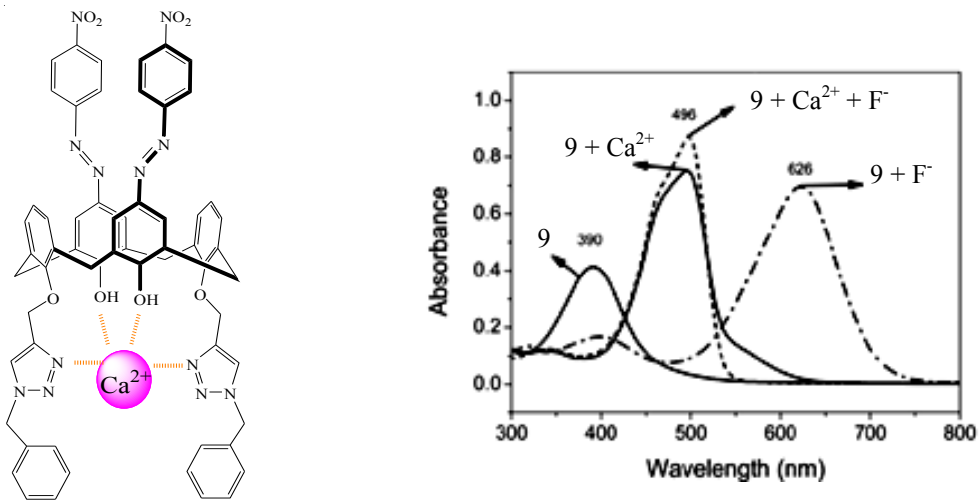

Figure 1.9 (a) Azocalix[4]arene **9** coordinated with Ca^{2+} and (b) UV/vis spectra of **9** before and after adding $Ca(ClO_4)_2$, TBA^+F^- and $Ca(ClO_4)_2$ with TBA^+F^- in $MeCN/CHCl_3$ (*v*/*v* = 1000:4).

1.11 Calix[4]pyrrole

Octamethylcalix[4]pyrrole (OMCP, **10**) (Figure 1.10), a tetrapyrrole macrocycle first prepared by Baeyer, [85] garnered significant attention recently due to its ability to bind small anions [86] and electroneutral molecules [87]. In 1996 Sessler and coworker reported the X-ray single crystal structure of calix[4]pyrrole obtained by slow evaporation of acetone and acetone/dichloromethane (1:1 v/v) solutions [86]. They also reported that the molecule of calix[4]pyrrole adopts a 1,3-alternate conformation in the solid state wherein adjacent rings are oriented in the opposite directions (Figure 1.11 (a)). In case of the complexation with anions, calix[4]pyrrole ligand adopts a cone-liked conformation such that the four NH protons can provide hydrogen bonds to the halide anion (Figure 1.11 (b)).

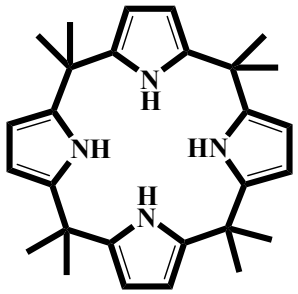

10

Figure 1.10 Structure of octamethylcalix[4]pyrrole **10** (OMCP).

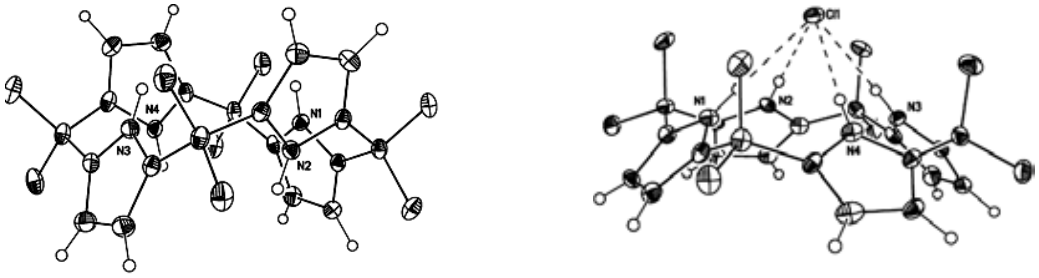

(a) (b)

Figure 1.11 1, 3-Alternate conformation of (a) calix[4]pyrrole and (b) chloride complex of calix[4]pyrrole, which adopts a cone conformation in the solid state.

After the discovery of its supramolecular properties, [88-90] OMCP has become the subject of numerous efforts devoted to understanding, improving, and tuning the binding affinity and selectivity toward anions by preparation of substituted OMCP [91-95] and further related compounds such as expanded calix[*n*]pyrroles, [96-99] calixbipyrrole, [100-101] strapped calixpyrrole, [102-104] calixpyrrole dimer, [105] and cryptand-like calixpyrrole [106]. Furthermore, OMCP has been applied in fabrication of HPLC supports for anion separation, [107] ion extractant, [108] and, most notably, optical [109-110] and electrochemical [111-112] anion sensors. This is mainly because calix[4]pyrroles, despite binding anions *via* hydrogen bonds, show unique affinity for

biologically important anions such as chloride and phosphate, even in the presence of competing media such as water and electrolytes [113].

In the years following the initial 1996 discovery of its anion binding properties, most modification of the calix[4]pyrrole skeleton focused on functionalzation of β-pyrrolic or meso-position [114]. Such peripheral modifications remain among the easiest changes to effect in calixpyrrole chemistry and some of the most versatile in terms of supporting calixpyrrole-based applications. One of the most effective ways of doing this is by producing strapped and other protected cavity system, wherein the anion binding domain is both effective defined and isolated more fully from solvent.

The isolation of the binding domain from the solvent matrix imparts a number of advantages in terms of substrate recognition. Firstly, such isolation can serve to enhance the affinity for a targeted guest or substrate by reducing guest-solvent and guest-counter cation interactions. Secondly, the modifications needed to effect such isolation usually produce binding domains of controlled size and shape that, in turn, generally give rise to greater inherent selectivity. Thirdly, in the specific case of calixpyrroles, these structural variations can be used to lock the conformation of the receptor into the so-called cone form, a conformation that is known to favour anion binding. Such a preorganized „locking" would thus be expected to enhance further the anion affinities.

The intellectual progression leading to the development of protected cavity calix[4]pyrroles is summarized in Figure 1.12. This schematic shows a series of sequential modifications. The simplest involves generation of a functionalized calix[4]pyrrole (**11**) bearing one (or more) "arms". The second one, illustrated by generalized structure **12**, embodies so-called deep cavity models, calix[4]pyrrole derivates that contain bulky *meso*-substituents. The third modification entails strapped systems, which are represented by structure **13**, while the fourth level of complexity involves capped models, such as generic system **14**.

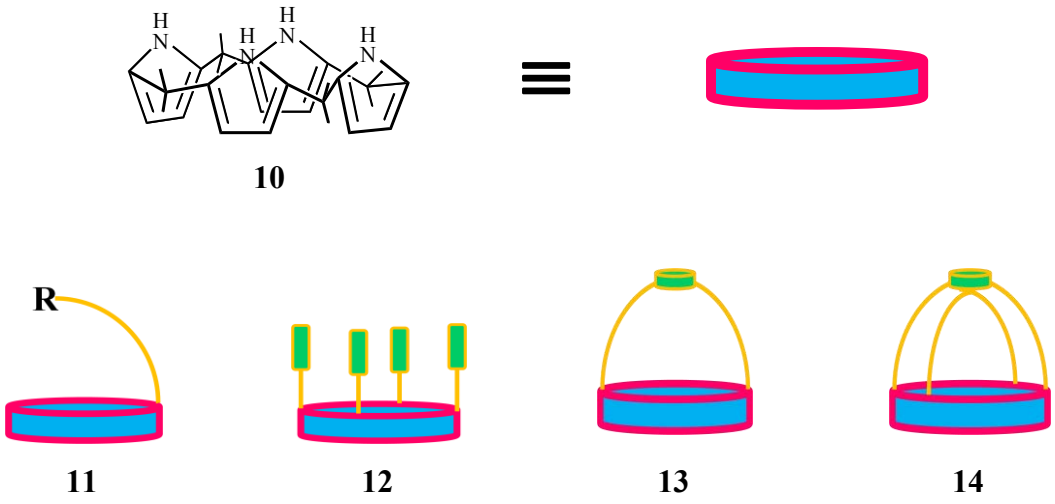

Figure 1.12 Schematic representation showing various possible modification to the basic calix[4pyrrole core [115].

Since the degree of preorganization is increasing along the progression from **11** to **14**, it might be expected that both the inherent anion selectivity and the thermodynamics of binding for appropriately sized anionic substrates would increase in a corresponding fashion. A number of functionalized calixpyrroles, including many of type **11** above, have been reported over the last decade. For instance, in work from Gale, P.A. and the group, the pentapyrrolic calix[4]pyrrole (**15**) (Figure 1.13(a)) was prepared and found to enhanced anion affinity as compared to the parent octamethylcalix[4]pyrrole macrocycle (**10**) [117]. ^{1}H-NMR titrations were conducted to compound **15** with the anion in deuteriated dichloromethane solution and the data compared with those obtained previously with compound **10**. The data show an enhancement in the anion complexation affinity of **15** as compared to the parent macrocycle **10**. Preliminary molecular modeling studies (using Spartan) [118] indicate the acetate complex of **15** to be more stable than the acetate complex of **10** by a significant margin.

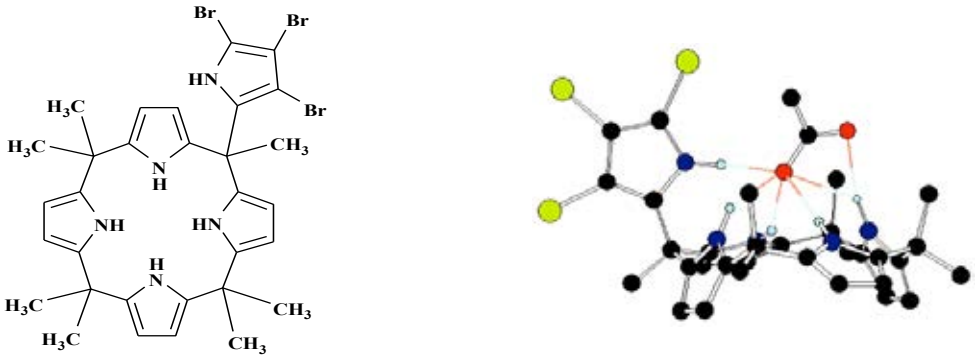

15

(a) (b)

Figure 1.13 Stucture of pentapyrrolic calix[4]pyrrole (**15**) (a) and Molecular model of compound **15**–acetate (b) [117].

Example of generalized system **12**, namely calix[4]pyrroles with deep cavities are fewer in number [119,120]. Typically, such systems have been prepared by „„appending"" substituted aryl groups onto the four meso-positions. This produces a sterically encumbered binding site that in favorable cases has been shown to display somewhat improved affinities and selectivity with regard to anion binding. Such as a prototypical system **16** (Figure 1.14(a)) obtained from the condensation of *p*-hydroxyacetophenone with pyrrole [121]. The configuration of **16** was confirmed by X-ray crystallographic analysis, a deep cavity structure was observed in the solid state, wherein the calixpyrrole core is in a so-called cone conformation (Figure 1.14(b)). These system show lower affinity for small anions, specifically Cl^- and $H_2PO_4^-$, in acetonitrile-water (99.5:0.5) than do simple unsubstituted calix[4]pyrrole **10**. On the other hand, increased selectivity and other binding effects ascribable to the "walls" of the cavity are observed. This, presumably, is due to a combination of electronic effects and steric interactions between the *meso*-aryl groups and the anion.

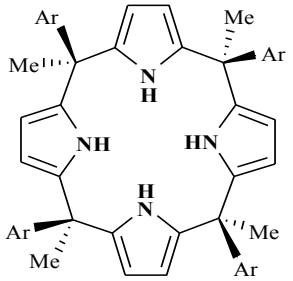

16

Ar = 4-hydroxyphenyl

(a)

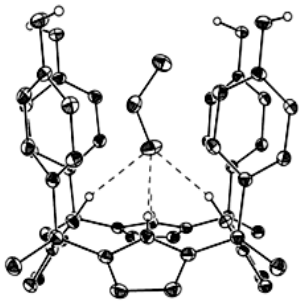

(b)

Figure 1.14 (a) Structure of calix[4]pyrroles containing deep cavities and fixed walls **16** and (b) the molecular structure of the ethanol adduct of **16** in the cone conformation [121].

However, since (i) receptors of type **14** could prove to be too rigid, thus reducing affinity, and because (ii) their greater complexity was expected to complicate synthesis, the initial decision was to focus on strapped systems; in this case the prediction was that large enhancements in the affinity would be seen as a direct consequence of inhibiting solvent–guest interactions. The first strapped system is a calix[4]arene-capped or strapped calix[4]pyrrole, calix[4]arene-calix[4]pyrrole pseudo dimer (Figure 1.12(a)), [122] was obtained as the result of a template mediated condensation between a keto-functionalized calixarene and pyrrole by Sessler and co-workers. From its ^{1}H-NMR spectroscopic studies, this receptor contained a strong hydrogen bonding between the pyrrole NH groups and the calixarene oxygen atoms. Addition of tetrabutylammonium fluoride to the ligand solution caused no change on the ^{1}H-NMR spectrum. The crystal structure shows that the pyrrole NH groups are within hydrogen bonding distance of the lower rim calixarene oxygen atoms (Figure 1.12(b)).

(a) (b)

Figure 1.15 Structure of (a) calix[4]arene-calix[4]pyrrole pseudo dimer and (b) its crystal structure [122].

After the first described of calix[4]arene-calix[4]pyrrole pseudo dimer by Sessler et al., various modifications of the strapped calix[4]pyrrole have been made in an effort to tune the binding characteristics of the parent system. Because of the strapped calix[4]pyrroles do indeed allow the inherent anion affinities of calix[4]pyrroles to be significantly modulated anion selectivity. Sessler and Lee have compared the anion complexation properties of octamethylcalix[4]pyrrole **10**, with strapped calix[4]pyrroles containing phenyl **1**7, pyrrole **1**8 and furan **1**9 straps linked *via* ester groups [Figure 1.16] [123].

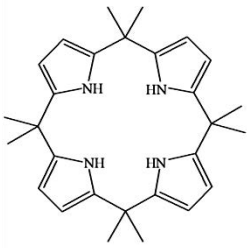

10

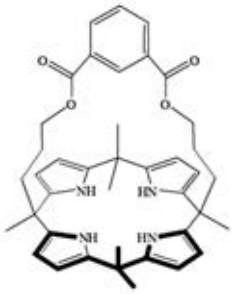

17

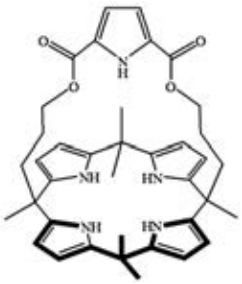

18

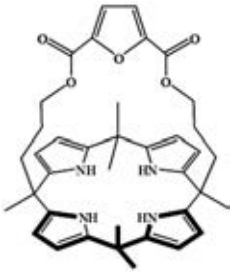

19

Figure 1.16 Structures of meso-octamethylcalix[4]pyrrole **10**, with strapped calixpyrroles containing phenyl **1**7, pyrrole **18** and furan **19** straps.

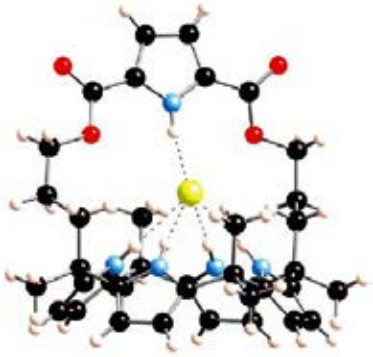

Figure 1.17 Single crystal X-ray structure of the chloride complex of receptor **18** [123].

The results show that the pyrrole strapped system **18** which contains an extra N*H* hydrogen bond donor has a 95× higher affinity for chloride in acetonitrile than the furan (**19**) and benzene (**17**) strapped systems. The result of a single crystal X-ray structure of the chloride complex reveals the hydrogen bonding interaction occurred from the calix[4]pyrrole and pyrrole group on the strap bound to chloride ion (Figure1.17).

In 2004, Lee and Panda were successfully synthesized strapped calix[4]pyrrole metalloporphyrin and used these molecule as a ditopic receptor model for anions [103,104]. The anion binding studies of these molecule revealed that only "*cis*" *meso*-carbon atoms isomer (Figure 1.18(a)) showed strong binding with fluoride in organic solvent, and the "*trans*" meso-carbon atoms isomer (Figure 1.18(b)) showed any appreciable binding with Cl^-, Br^-, and I^-. Then, these two different binding abilities of the two conformers of calix[4]pyrrole strapped porphyrin provide useful information in the design and synthesis of heteroditopic receptors, as well as Lewis acid assisted anion receptors.

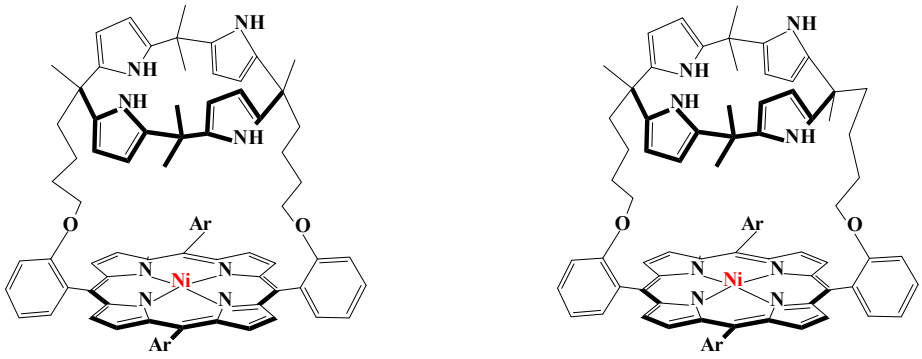

(a) (b)

Figure 1.18 Structures of (a) *cis*- and (b) *trans*-metalloporphyrin-strapped calix[4]pyrrole.

Nowadays, strapped calix[4]pyrrole is not only used for increasing the anion binding affinity and modulating the inherent anion selectivity. The introduction of built-in chromogenic reporter group in the calix[4]pyrrole would also be ideal for selective

sensing and detection of anions. Such systems would allow the detection of analytes *via* direct colorimetric or fluorometric means with higher affinity. Since the chromogenic or fluorescence sensors are useful detection methods for anion, development of chromogenic or fluorescence anion sensors based on calix[4]pyrrole would be worthwhile. Based on these considerations, the reported strapped calix[4]pyrrole systems bearing chromogenic or fluorogenic reporters were developed for selective sensing and detection of anions. Such systems would be potentially useful since they might permit the detection of analytes *via* direct optical or spectroscopic means. Lee *et al*. also reported the synthesis of anion receptors based on the strapped calix[4]pyrrole bearing acridine as fluorogenic moiety (Figure 1.19(a)) [124]. This designed system enhanced binding affinities for chloride and bromide anions with high selectivity and the fluorescence measurement indicated that the incorporated acridine moiety has minimal interaction with the anion. Sessler *et al*. synthesizing a strapped calix[4]pyrrole-coumarin (Figure 1.19(b)), [125] which a coumarin moiety served as a potential fluorophore located near the binding domain. This system was found to function as an INH logic gate, [126] wherein changes in cation and anion concentrations serve as the input and fluorescence intensity changes as the output [127]. Yoo *et al*. also synthesized calix[4]pyrrole bearing dipyrrolylquinoxaline as strapping element (Figure 1.19(c)) [128]. The receptors displayed a selective colorimetric response when exposed to the fluoride, dihydrogen phosphate, and acetate anions and an enhanced affinity as compared to a calix[4]pyrrole parent system. The incorporation of additional pyrrole subunits on the strap were expected to interact with the quinoxaline chromophore *via* a variety of second-order interactions, including through a conjugation and anion-π effects. These systems, which produce an, easy to see, visual response in the presence of certain anions, offer a further potential advantage.

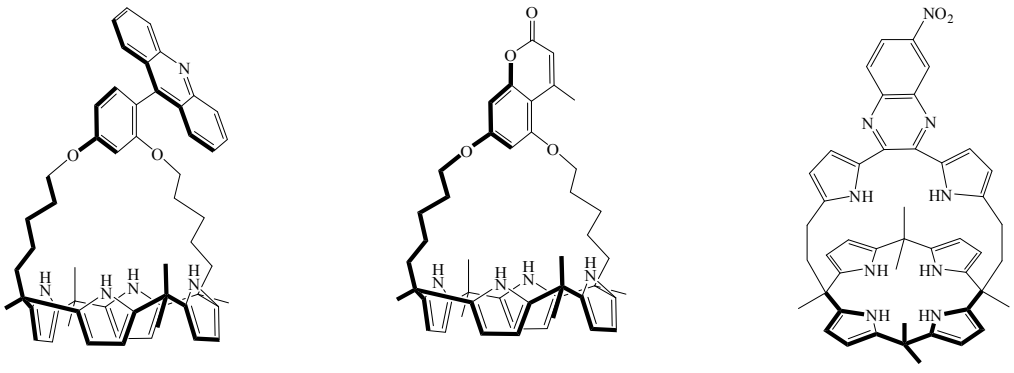

(a) (b) (c)

Figure 1.19 Structures of chromogenic and fluorogenic strapped calix[4]pyrroles.

Ruangchaitaweesuk [129] was success to synthesized calix[4]arene-capped calix[4]pyrroles by replacing the methylene bridges between 2 subunits with triethylene glycol chains. This calix[4]arene-calix[4]pyrrole pseudo-dimer (Figure 1.20(a)) can act as a ditopic receptor. The solid structure of calix[4]arene-capped calix[4]pyrrole was determined by single crystal X-ray crystallography (Figure 1.20(b)). Preliminary anion binding study was found that the calix[4]pyrrole moiety showed the greatest binding with fluoride anion in the cone conformation.

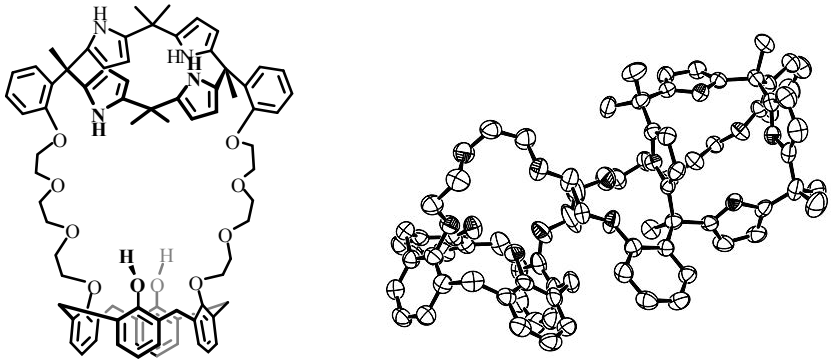

(a) (b)

Figure. 1.20 (a) Structure of calix[4]arene-capped calix[4]pyrrole and (b) its crystal structure [129].

Crown-6-calix[4]arene-capped calix[4]pyrrole (Figure 1.21(a)), [130] a new calix[4]arene-capped calix[4]pyrrole receptor containing both cation- and anion-recognizing sites, has been synthesized and characterized by Sessler and co-workers in 2008. The X-ray crystal structure (Figure 1.21(b)) and ^{1}H-NMR spectroscopic analysis supported the conclusion that crown-6-calix[4]arene-capped calix[4]pyrrole forms a stable 1:1 complex with CsF in spite of the large separation enforced between the anion and the cation.

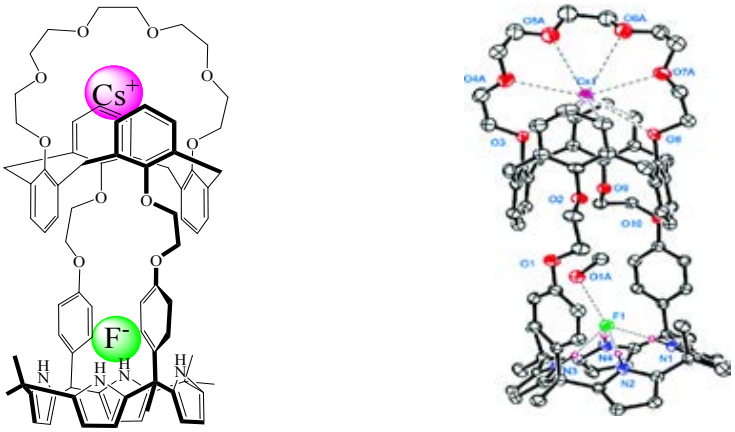

(a) (b)

Figure.1.21 (a) Proposed binding interactions involving crown-6-calix[4]arene-capped calix[4]pyrrole with Cs^{+} and F^{-} salt and (b) crystal structure of its CsF complex [130].

After that, in 2010 the same authors were also successfully synthesized the calix[4]pyrrole-calix[4]arene pseudo-dimer **20** (Figure 1.22(a)) bearing a strong anion recognition site, calix[4]pyrrole, and a strong cation-recognition site, crown ether unit [131]. The complexation study in 10% CD_3OD in $CDCl_3$ (v/v) by ^{1}H-NMR technique showed that this receptor bound neither the Cs^{+} cation nor the F^{-} anion when exposed to these species in the presence of other counterions; however, it formed a stable 1:1 solvent-separated CsF complex when exposed to these two ions in concert with one another in this same solvent mixture (Figure 1.22(b)). These findings reveal receptor **20**

to be a versatile ion-pair receptor whose binding behavior can be modulated *via* an appropriate choice of the counteranion.

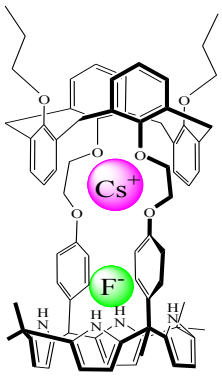

20

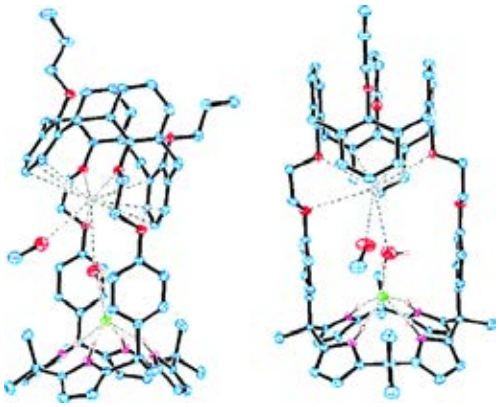

(a) (b)

Figure.1.22 (a) Proposed binding interactions involving calix[4]pyrrole-calix[4]arene pseudodimer **20** with Cs^+ and F^- salt and (b) X-ray crystal structure of its CsF complex [131].

1.12 Objectives of this research

The objectives of this research are i) to synthesized chromogenic sensor based on 1,3-di-*p*-nitrophenylazo-calix[4]arene-calix[4]pyrrole (**9**) and ii) to study its binding ability. The incorporation of a calix[4]pyrrole unit on calix[4]arene framework is aimed to serve for anion binding site and a crownether moiety is expected to acting as metal chelating unit. The azobenzene units are attached directly to the phenolic unit of calix[4]arene to enhance a hydrogen bonding upon anion binding and to serve as chromogenic signaling unit.

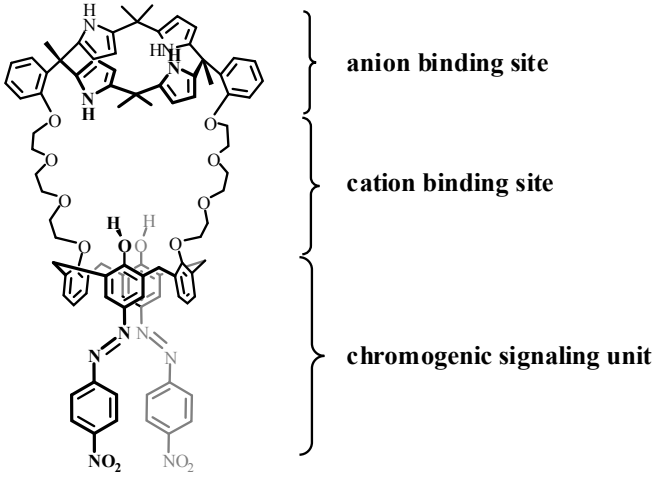

9

Figure 1.23 Structure and function of each incorporated units of chromogenic 1,3-di-*p*-nitrophenylazo-calix[4]arene-strapped calix[4]pyrrole (**9**).

In addition, ligand **9** combined the binding sites for both anionic and cationic species covalently in a neutral molecule. To understanding of molecular recognition processes involving anions and cations of this molecule so its binding ability and selectivity towards anions and cations or both of them, has also been investigated. The complexation determined by UV-vis spectrophotometry, ^{1}H-NMR spectroscopy and their color changes.

Furthermore, 1, 3-di-*p*-nitrophenylazo-calix[4]diacetophenone (**7**), which lack of calix[4]pyrrole binding unit was used to compare the binding abilities to ligand **9**. The complexation property of ligand **7** toward anions and cations or both of them also studied by UV-vis spectrophotometry, ^{1}H-NMR spectroscopy and their color changes.

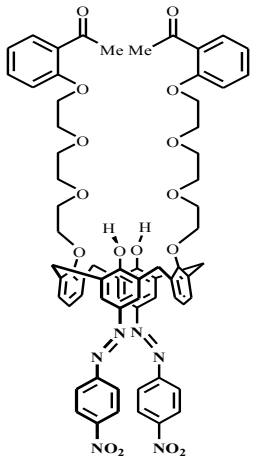

7

Figure 1.24 Structure of 1, 3-di-*p*-nitrophenylazo-calix[4]-diacetophenone (**7**)

CHAPTER II

EXPERIMENTAL SECTION

2.1 General Procedures

2.1.1 Analytical instruments

Nuclear magnetic resonance (NMR) spectra were recorded on a Varian 400 MHz nuclear magnetic resonance spectrometer. In all cases, samples were dissolved in deuterated chloroform. Elemental analysis was carried out on CHNS/O analyzer (Perkin Elmer's PE2400 series II). MALDI-TOF Mass spectra were recorded on a Biflex Bruker Mass spectrometer. Absorption spectra were measured by a Varian Cary 50 UV-Vis spectrophotometer.

2.1.2 Materials

All materials were standard analytical grade, purchased from Fluka, Aldrich or Merck and used without further purification. Commercial grade solvents such as acetone, hexane, dichloromethane, methanol and ethyl acetate were distilled before used. Acetonitrile was dried over CaH_2 and freshly distilled under nitrogen prior to use. Tetrahydrofuran was dried and distilled under nitrogen from sodium benzophenone ketyl immediately before used.

Column chromatography was carried out using silica gel (Kieselgel 60, 0.063-0.200 mm, Merck). Thin layer chromatography (TLC) was performed on silica gel plates (Kieselgel 60 F_{254}, 1 mm, Merck).

Starting materials such as *p-tert*-butylcalix[4]arene were prepared according to the literature procedure [132]. The compounds were characterized by ^{1}H-NMR spectroscopy, infrared spectroscopy, mass spectroscopy and elemental analysis.

2.2 Synthesis

2.2.1 Overall of synthetic pathways

The synthetic routes to prepare the chromogenic calix[4]arene-strapped calix[4]pyrrole sensor (**9**) was shown in figure 2.1. Pathway 1 started from 1,3-calix[4]diacetophenone (**3**) pass through the synthesis step of ligand **4** and ligand **5** and then the final step coupling with the benzenediazonium salt after that the undesired product **6** was then occurred. The pathway 2 was first coupling the benzenediazonium salt with 1, 3-calix[4]diacetophenone (**3**) and then a chromogenic sensor ligand **7** was obtained. The chromogenic calix[4]arene strapped calix[4]pyrrole (**9**) was successfully after condensation of pyrrole with ligand **8** in the presence of a catalytic amount of $BF_3{\cdot}OEt_2$.

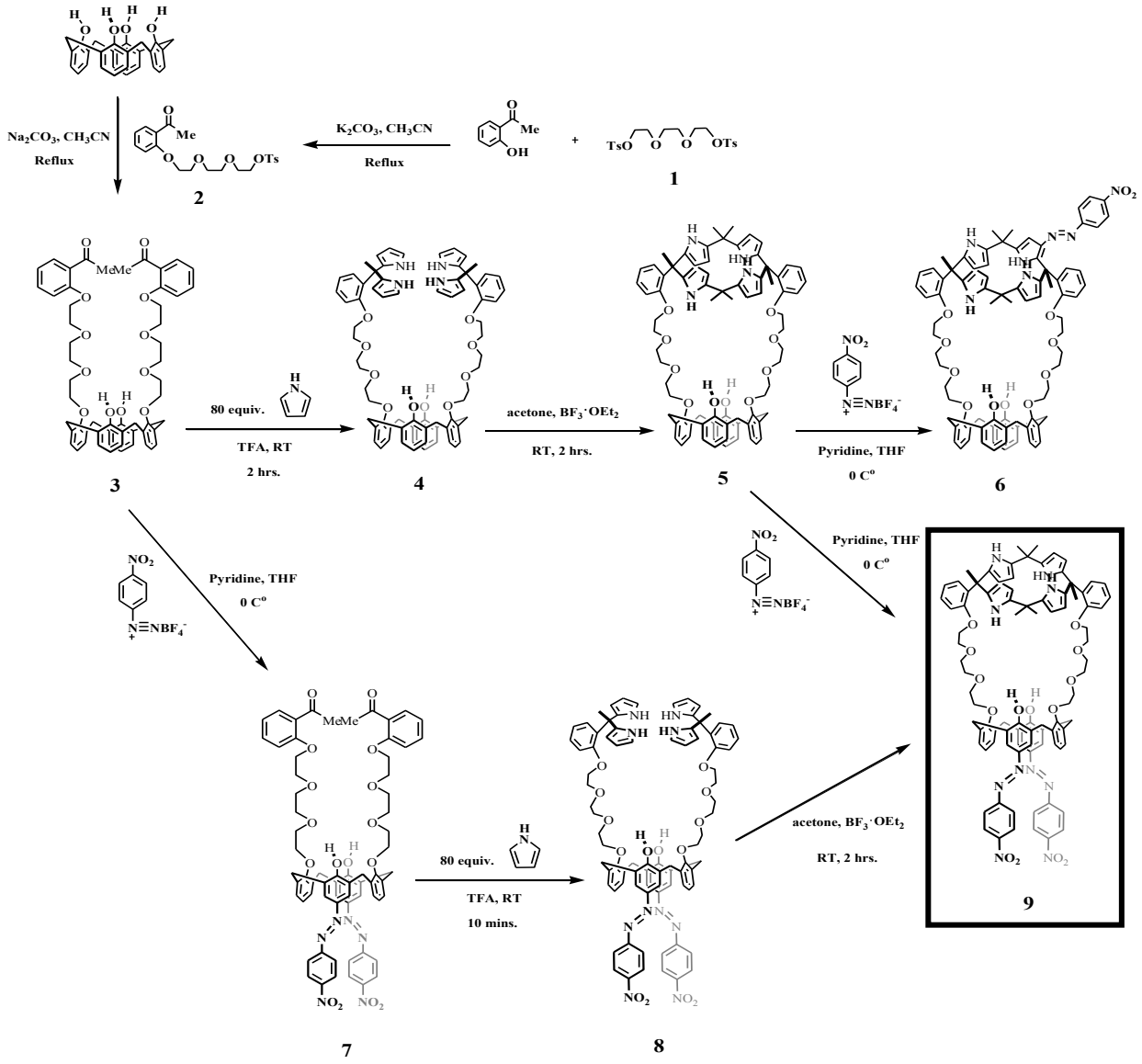

Figure 2.1 Synthetic pathways of chromogenic calix[4]arene strapped calix[4]pyrole (**9**).

2.2.2 Preparation of triethyleneglycol ditosylate (1)

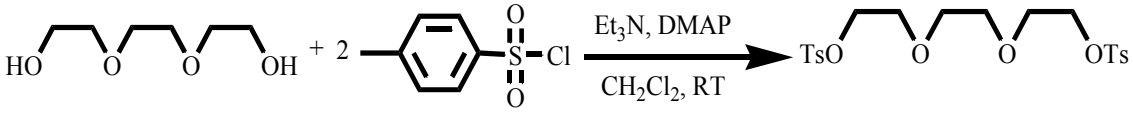

1

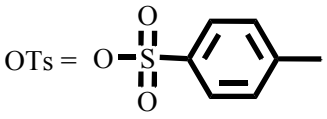

Into a 250 mL two-necked round bottom flask, a solution of triethyleneglycol (3.00 g, 28 mmol), triethylamine (11.8 mL, 85 mmol) and a catalytic amount of 4-dimethylaminopyridine (DMAP) in 50 mL of dichloromethane was chilled to 0 ˚C with an ice bath. The solution of tosylchloride (11.86 g, 62 mmol) in dichloromethane (100 mL) was then added drop wise. The reaction mixture was stirred for 4 hours at room temperature under nitrogen atmosphere. After the reaction was completed, the solution of 3 M hydrochloric acid was added until the pH of the solution reached to 1 and then extracted with dichloromethane (2×50 mL). The residue was dried over anhydrous Na_2SO_4, filtered and evaporated to dryness. The residue was dissolved in a minimum amount of dichloromethane and methanol was added to precipitate. Compound **1** was obtained as a white solid (7.66 g, 65% yield).

Characteristic data for 1:

^{1}H-NMR spectrum ($CDCl_3$, δ(ppm), 400 MHz): 7.77 (d, $J_{H\text{-}H}$ = 8.2 Hz, 4H, *o*-Ar***H***), 7.32 (d, $J_{H\text{-}H}$ = 8.2 Hz, 4H, *m*-Ar***H***), 4.10 (t, $J_{H\text{-}H}$ = 4.7 Hz, 4H, $SO_2OC\boldsymbol{H}_2CH_2OCH_2$), 3.60 (t, $J_{H\text{-}H}$ = 4.7 Hz, 4H, $SO_2OCH_2C\boldsymbol{H}_2OCH_2$), 3.50 (s, 4H, $SO_2OCH_2CH_2OC\boldsymbol{H}_2$), 2.42 (s, 6H, Ar-C***H***$_3$)

IR spectrum (KBr pellet (cm^{-1})): 3016-3083 (Aromatic C-H, st), 2800-3016 (Aliphatic CH, st), 1353 (S=O, st), 1150-1200 (C-O-C, st)

2.2.3 Preparation of 2-(8-tosyltriethyleneglycol)acetophenone (2)

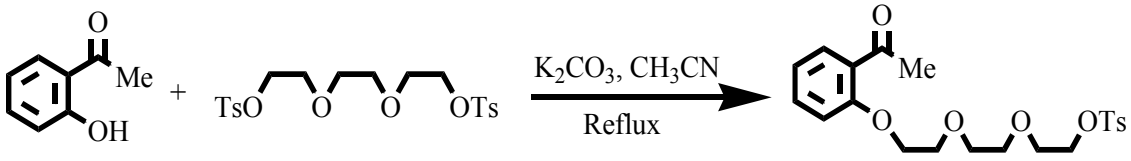

1 **2**

Into a 250 mL two-necked round bottom flask, 2-hydroxyacetophenone (1.36 g, 10 mmol) and K_2CO_3 (13.82 g, 100 mmol) were suspended in dried acetonitrile (50 mL). The mixture was stirred at room temperature under nitrogen atmosphere for 1 hour. A solution of triethyleneglycol ditosylate (**1**) (9.16 g, 20 mmol) in dried acetonitrile (100 mL) was then added drop wise. The reaction mixture was stirred and refluxed under nitrogen atmosphere for 18 hours. After the reaction was completed monitoring by TLC, the solution was allowed to cool to room temperature. The solvent was evaporated to dryness under reduced pressure. The obtained residue was dissolved in dichloromethane (100 mL) and extracted with 3 M HCl (1×100 mL) and water (2×100 mL), respectively. The combined organic layer was dried over anhydrous Na_2SO_4 and filtered off to give yellow oil. Compound **2** was purified by column chromatography (silica gel, CH_2Cl_2/EtOAc; 90:10) and obtained as colorless oil (2.53 g, 30%).

Characteristic data for 2:

^{1}H-NMR spectrum ($CDCl_3$, δ(ppm), 400 MHz): 7.82 (d, $J_{H\text{-}H}$ = 8.0 Hz, 2H, Ar_{tosyl}***H***), 7.77 (dd, $J_{H\text{-}H}$ = 1.6 and 4.0 Hz, 1H, Ar***H***), 7.47 (t, $J_{H\text{-}H}$ = 2.0, 4.0 Hz, 1H, Ar***H***), 7.36 (d, $J_{H\text{-}H}$ = 8.0 Hz, 2H, Ar_{tosyl}***H***), 7.03 (t, $J_{H\text{-}H}$, = 4.0 Hz, 1H, Ar***H***), 6.98 (d, $J_{H\text{-}H}$ = 4.0 Hz, 1H, Ar***H***), 4.25 (t, $J_{H\text{-}H}$ = 4.8 Hz, 2H, $SO_2OC\boldsymbol{H}_2$), 4.18 (t, $J_{H\text{-}H}$ = 4.8 Hz, 2H, $ArOC\boldsymbol{H}_2$), 3.91 (t, $J_{H\text{-}H}$ = 4.8 Hz, 2H, $C\boldsymbol{H}_2O$), 3.73-3.64 (m, 6H, $C\boldsymbol{H}_2O$), 2.66 (s, 3H,$COC\boldsymbol{H}_3$), 2.46 (s, 3H, $ArC\boldsymbol{H}_3$)

^{13}C-NMR spectrum ($CDCl_3$, δ(ppm), 400 MHz,) δ 199.6, 144.8, 133.6, 130.2, 129.8, 129.6, 129.5, 128.3, 127.8, 127.5, 120.6, 112.7, 70.6, 70.4, 69.4, 69.2, 68.6, 67.8, 31.9

IR spectrum (KBr pellet (cm^{-1})): 3016-3090 (Aromatic C-H, st), 2767 (Aliphatic CH, st), 1668 (C=O, st), 1359 (S=O, st), 1150-1200 (C-O-C, st)

Elemental analysis: *Anal.Calcd.* for $C_{21}H_{26}O_7S$: C, 59.70%; H, 6.20%
Found: C, 59.78%; H, 6.29%

MALDI-TOF mass: *Anal. Calcd* for $[C_{21}H_{26}O_7S]^+$ m/z = 422.4
Found m/z = 422.6 $[M]^+$

2.2.4 Preparation of 1,3-calix[4]-diacetophenone (3)

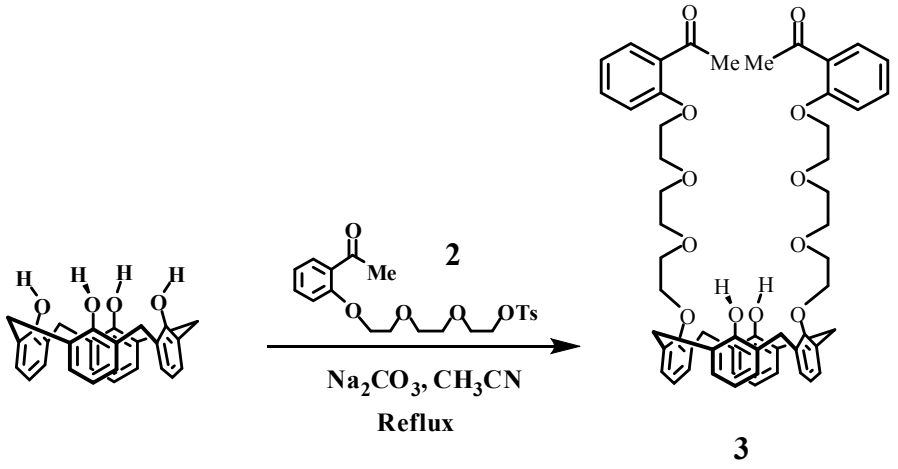

Into a 250 mL two-necked round bottom flask containing calix[4]arene (2.40 g, 5.7 mmol), Na_2CO_3 (6.00 g, 56.6 mmol) and acetonitrile (50 mL), a solution of 2-(8-tosyltriethyleneglycol)acetophenone (**2**) (4.78 g, 11.3 mmol) in acetonitrile (100 mL) was added drop wise. The reaction mixture was refluxed with stirring under nitrogen atmosphere for 7 days. After cooling to room temperature, the solvent was removed under reduced pressure to give yellow oil. The residue was dissolved in dichloromethane (100 mL) and extracted with 3 M HCl (1×100 mL) and water (2×100 mL), respectively. The combined organic layer was dried over anhydrous Na_2SO_4, filtered off and evaporated to dryness under reduced pressure. The residue was dissolved in a minimum amount of dichloromethane and methanol was added to precipitate 1,3-calix[4]-diacetophenone (**3**) as a white solid (4.47 g, 85%).

Characteristic data for (3):

^{1}H-NMR spectrum ($CDCl_3$, δ(ppm), 400MHz): 7.78 (t, J_{H-H} = 2.0 Hz, 2H, Ar***H***$COCH_3$), 7.72 (s, 2H, ArO***H***), 7.45 (t, J_{H-H} =8.0 Hz, 2H, Ar***H***$COCH_3$), 7.07 (d, J_{H-H} =7.6 Hz, 4H, Ar***H***OCH_2), 7.02 (t,J_{H-H} = 7.4 Hz, 2H, Ar***H***$COCH_3$), 6.89 (d, J_{H-H} = 7.6 Hz, 4H, Ar***H***OH), 6.86 (d, J_{H-H} = 8.8 Hz, 2H, Ar***H***$COCH_3$), 6.75(t, J_{H-H} = 7.4 Hz, 2H, Ar***H***OCH_2), 6.67 (t, J_{H-H} = 7.4 Hz, 2H, Ar***H***OH), 4.43 (AB system, J_{H-H} = 13.0 Hz, 4H, ArC***H***$_2$Ar), 4.19 (t, J_{H-H} = 4.2 Hz, 4H, OC***H***$_2$), 4.08 (t, J_{H-H} = 4.2 Hz, 4H, OC***H***$_2$), 3.99 (t,

$J_{H\text{-}H}$ = 4.2 Hz, 4H, OC***H***$_2$), 3.90-3.89 (m, 8H, OC***H***$_2$), 3.78-3.82 (m, 4H, OC***H***$_2$), 3.36 (AB system, $J_{H\text{-}H}$ = 13.0 Hz, 4H, ArC***H***$_2$Ar), 2.67 (s, 6H, ArCOC***H***$_3$)

^{13}C-NMR spectrum ($CDCl_3$, δ(ppm), 400 MHz,) δ 199.8, 158.3, 153.3, 151.7, 133.8, 133.1, 130.3, 128.9, 128.6, 128.2, 128.1, 125.3, 120.7, 118.9, 112.7, 75.5, 71.1, 70.7, 70.0, 69.5, 67.6, 32.2, 31.2

IR spectrum (KBr pellet (cm^{-1})): 3320 (OH, st), 3010 (Aromatic C-H, st), 2910-2810 (Aliphatic CH, st), 1710 (C=O, st), 1590 and 1495 (Aromatic C=C, st), 1250 (C-O-C, st)

Elemental analysis: *Anal.Calcd.* for $C_{56}H_{60}O_{12}$: C,72.71%; H, 6.54%
Found: C, 71.72%; H, 6.41%

MALDI-TOF mass: *Anal. Calcd* for $[C_{56}H_{60}O_{12}]^+$ *m/z* = 924.4
Found m/z = 947.6 $[M + Na]^+$

2.2.5 Preparation of 1, 3-calix[4]arene-bis-dipyrroethane (4)

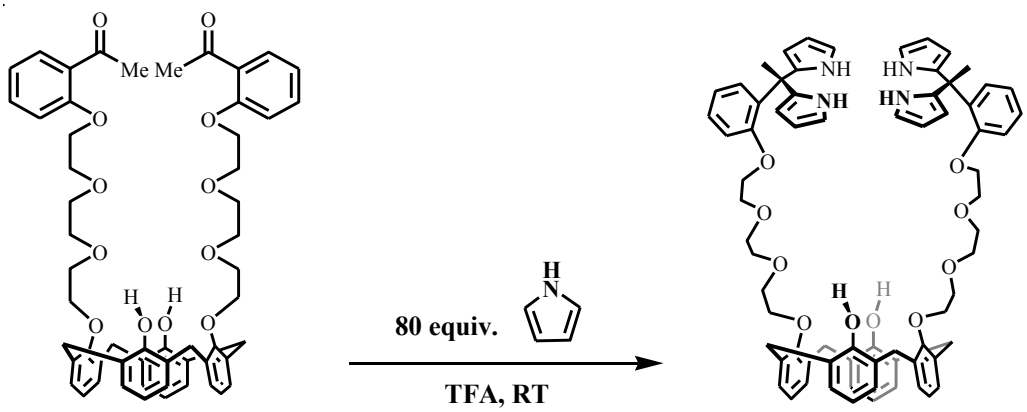

3 **4**

Into a 100 mL two-necked round bottom flask, a solution of 1,3-calix[4]-diacetophenone (**3**) (4.23 g, 4.6 mmol) in pyrrole (25.5 mL, 365 mmol) was degassed by bubbling with nitrogen for 15 minutes, and trifluoroacetic acid (TFA) (0.07 mL, 0.9 mmol) was then added. The solution was stirred in darkness for 10 minutes at room temperature. Then the reaction mixture was diluted with CH_2Cl_2 (100 mL), washed with 0.1 M $NaHCO_3$ (2×100 mL) and water (2×100 mL). The organic layer was dried over anhydrous Na_2SO_4 and the solvent was removed in vacuo. The obtained residue was purified by column chromatography over silica gel (CH_2Cl_2/EtOAc/NEt_3 = 95:4:1) to give 3.22 g of the 1, 3-calix[4]-bis-dipyrroethane (**4**) as a transparent viscous oil (61% yield).

Characteristic data for 4:

^{1}H-NMR spectrum ($CDCl_3$, δ(ppm), 400 MHz): 8.86 (s, 4H, N***H***), 7.74 (s, 2H, ArO***H***), 7.32-7.26 (m, 2H, Ar***H***), 7.22-7.17 (m, 2H, Ar***H***), 7.10 (d, $J_{H\text{-}H}$ = 7.6 Hz, 4H, Ar***H***OCH_2), 6.95 (t, $J_{H\text{-}H}$ = 8.0 Hz, 2H, Ar***H***C*Py*$_2CH_3$),6.90 (d, $J_{H\text{-}H}$ = 8.0 Hz, 4H, Ar***H***OH),6.75 (t, $J_{H\text{-}H}$ = 7.6 Hz, 2H, Ar***H***C*Py*$_2CH_3$), 6.71 (t, $J_{H\text{-}H}$ = 7.6 Hz, 4H, Ar***H***OCH_2), 6.60-6.64 (m, 4H, ***H***$_{Py}$), 6.09-6.13 (m, 4H, ***H***$_{Py}$), 5.90-5.94 (m, 4H, ***H***$_{Py}$), 4.44 (d(AB system), $J_{H\text{-}H}$ = 13.0 Hz, 4H, ArC***H***$_2$Ar), 4.15-4.19 (m, 4H, OC***H***$_2$), 3.96 (t, $J_{H\text{-}H}$ = 4.6 Hz, 4H, OC***H***$_2$), 3.87 (t, $J_{H\text{-}H}$ = 4.6 Hz, 4H, OC***H***$_2$), 3.78 (t, $J_{H\text{-}H}$ = 4.6 Hz, 4H, OC***H***$_2$), 3.70 (t, $J_{H\text{-}H}$ = 4.6 Hz, 4H,

OC***H***$_2$), 3.39 (d(AB system), $J_{H\text{-}H}$= 13.0 Hz, 4H, ArC***H***$_2$Ar), 3.36 (d, $J_{H\text{-}H}$ = 4.8 Hz, 4H, OC***H***$_2$), 2.67 (s, 6H, C***H***$_3$)

Elemental analysis: *Anal.Calcd.* for $C_{72}H_{76}N_4O_{10}$: C,74.72%; H, 6.62%; N, 4.80%
Found: C, 73.38%; H, 6.61%; N, 4.66%

2.2.6 Preparation of calix[4]arene-calix[4]pyrrole (5)

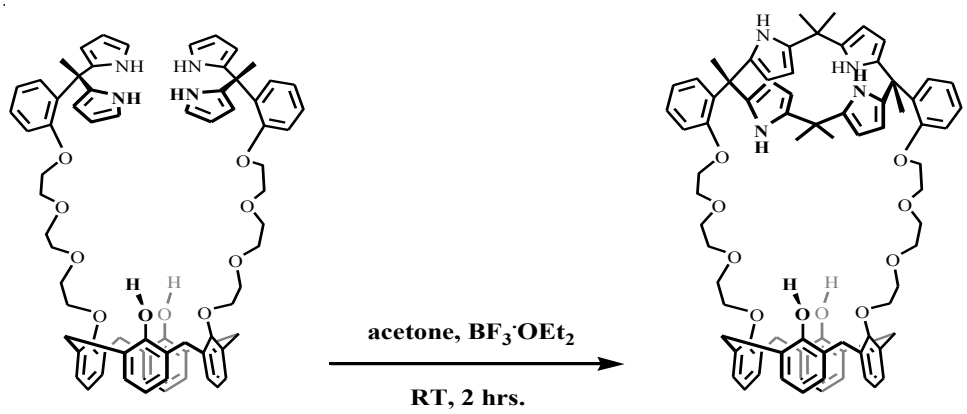

4 **5**

A solution of 1,3-calix[4]-bis-dipyrroethane (**4**) (0.13 g, 0.10 mmol) in acetone (30 mL) was added with $BF_3.OEt_2$ (0.01 mL, 0.04 mmol). The solution was stirred for 2 hours at room temperature. The solvent was removed by rotary evaporator under reduced pressure. The obtained residue was dissolved with CH_2Cl_2 (100 mL) and extracted with saturated $NaHCO_3$ solution (2×100 mL). The organic layer was dried over anhydrous Na_2SO_4 and the solvent was removed in vacuum. The residue was purified by silica gel pack using CH_2Cl_2/EtOAc (95:5) as eluent. The product contain fractions were combined and dried under reduced pressure. The obtained solid was dissolved in dichloromethane and recrystalized with methanol to give 0.05 g of **5** as a white solid (37% yield).

Characteristic data for 5:

^{1}H-NMR spectrum ($CDCl_3$, δ(ppm), 400 MHz): 7.98 (s(br), 4H, N***H***), 7.91 (s, 2H, ArO***H***), 7.23 (t, $J_{H\text{-}H}$ = 8.4 Hz, 2H, Ar***H***), 7.08 (d, $J_{H\text{-}H}$=7.6 Hz, 4H, Ar***H***), 6.94 (d, $J_{H\text{-}H}$= 7.6 Hz, 8H, Ar***H***)**,** 6.85 (d, $J_{H\text{-}H}$ = 8.0 Hz, 2H, Ar***H***), 6.78 (t, $J_{H\text{-}H}$ = 7.6 Hz, 4H, Ar***H***), 6.68 (t, $J_{H\text{-}H}$ = 7.6 Hz, 2H, Ar***H***), 5.91 (s, 4H, $\boldsymbol{H}_{Py}$), 5.67 (s(br), 4H, $\boldsymbol{H}_{Py}$), 4.40 (d(AB system), $J_{H\text{-}H}$ = 13.0 Hz, 4H, ArC$\boldsymbol{H}_2$Ar), 4.20 (t, $J_{H\text{-}H}$ = 4.8 Hz, 4H, OC$\boldsymbol{H}_2$), 4.09 (t, $J_{H\text{-}H}$ = 5.0 Hz, 4H, OC$\boldsymbol{H}_2$), 3.89 (t, $J_{H\text{-}H}$ = 4.6 Hz, 4H, OC$\boldsymbol{H}_2$), 3.83 (s, 4H, OC$\boldsymbol{H}_2$), 3.57 (s, 4H, OC$\boldsymbol{H}_2$), 3.39 (AB system, $J_{H\text{-}H}$ = 13.0 Hz, 4H, ArC$\boldsymbol{H}_2$Ar), 3.13 (s, 4H, OC$\boldsymbol{H}_2$), 2.09 (s, 6H, $Py_2CC\boldsymbol{H}_3Ar$), 1.55 (s, 12H, $Py_2C(C\mathbf{H}_3)_2$)

IR spectrum (KBr pellet (cm^{-1})): 3350 (N-H, st), 3065 (Aromatic C-H, st), 2980-2830 (Aliphatic CH, st), 1586 and 1495 (Aromatic C=C, st), 1250 (C-O-C, st)

Elemental analysis: *Anal.Calcd.* for $C_{78}H_{84}N_4O_{10}$: C,75.70%; H, 6.84%; N, 4.53%
Found: C, 75.65%; H, 6.73%; N, 4.56%

MALDI-TOF mass: *Anal.Calcd* for $[C_{78}H_{84}N_4O_{10}]^+$ m/z = 1236.6
Found m/z = 1259.7 $[M+ Na]^+$

2.2.7 Preparation of calix[4]arene-*p*-nitrophenylazo-calix[4]pyrrole (6)

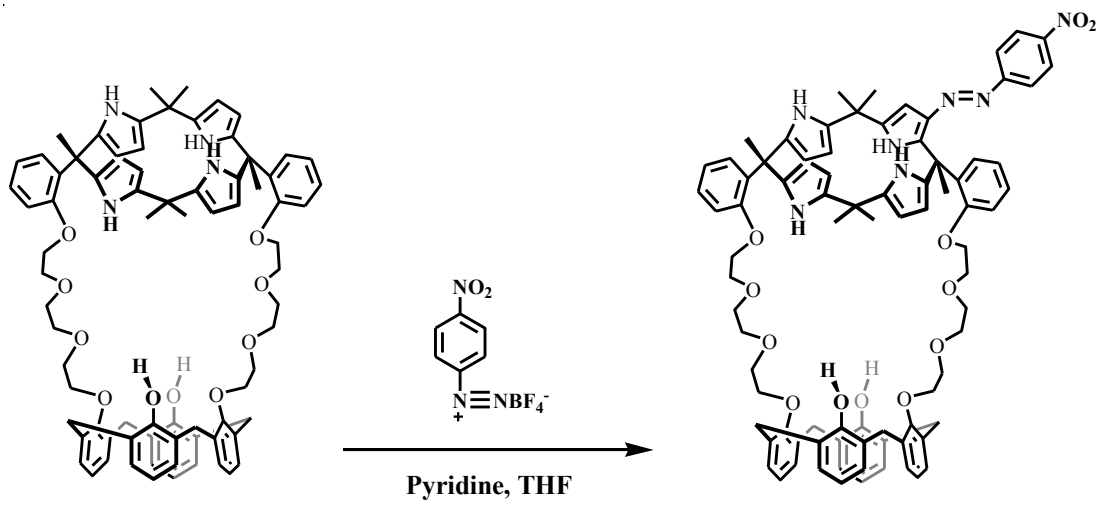

To a solution of **5** (0.18 g, 0.15 mmol) in tetrahydrofuran (THF; 200 mL), 4-nitrobenzenediazonium tetrafluoroborate (0.09 g, 0.37 mmol) was added. The reaction mixture was stirred for 30 minutes at 0 °C, and then pyridine (0.12g, 1.47 mmol) was added drop wise. The reaction mixture was stirred for an additional 8 hours at 0 °C, treated with 10% aqueous HCl solution (200 mL), and extracted with CH_2Cl_2 (2×100 mL). The combined organic layer was washed with 10% aqueous HCl solution (2×200 mL) and dried over anhydrous Na_2SO_4. Removing the organic solvent in vacuum afforded a reddish solid. Column chromatography on silica gel with EtOAc/hexane (30:70) as eluent gave 0.03 g of **6** (49% yield).

Characteristic data for 6:

^{1}H-NMR spectrum ($CDCl_3$, δ (ppm), 400 MHz): 8.64 (s(br), 4H, N***H***), 8.08 (d, 2H, J_{H-H} = 8.0 Hz, $NO_2Ar\boldsymbol{H_o}$), 7.82 (s, 1H, ArO***H***), 7.77 (s, 1H, ArO***H***), 7.60 (d, 2H, J_{H-H} = 8.2 Hz, $NO_2Ar\boldsymbol{H_m}$), 7.15 (t, J_{H-H} = 8.4 Hz, 2H, Ar***H***), 7.00 (d, J_{H-H}=7.6 Hz, 4H, Ar***H***), 6.85 (d, J_{H-H}= 7.6 Hz, 8H, Ar***H***), 6.78 (d, J_{H-H} = 8.0 Hz, 2H, Ar***H***), 6.69(t, J_{H-H} = 7.6 Hz, 4H, Ar***H***), 6.60 (t, J_{H-H} = 7.6 Hz, 2H, Ar***H***), 5.96 (s(br),4H, $\boldsymbol{H}_{Py}$), 5.86 (s, 1H, $\boldsymbol{H}_{Py}$), 5.81 (s, 1H, $\boldsymbol{H}_{Py}$), 5.33(s, 1H, $\boldsymbol{H}_{Py}$), 4.39 (t, J_{H-H} = 13.2 Hz,2H, OC$\boldsymbol{H}_2$), 4.25 (d(AB system),J_{H-H} = 13.2 Hz, 4H, *ArC*$\boldsymbol{H}_2$*Ar*), 4.15-4.08 (m, 2H, OC$\boldsymbol{H}_2$), 4.03-3.95 (m, 2H, OC$\boldsymbol{H}_2$), 3.91 (s(br),

2H, OC***H***$_2$), 3.85 (s(br), 2H, OC***H***$_2$), 3.79 (s(br), 2H, OC***H***$_2$), 3.71 (s(br), 2H, OC***H***$_2$), 3.64 (s(br), 2H, OC***H***$_2$), 3.52 (s(br), 2H, OC***H***$_2$), 3.34 (d(AB system), $J_{H\text{-}H}$ = 12.8 Hz, 4H, ArC***H***$_2$Ar), 3.27 (s, 2H, OC***H***$_2$), 3.11 (s(br), 2H, OC***H***$_2$), 2.97 (s(br), 2H, OC***H***$_2$), 2.15 (s, 3H, Py_2CC***H***$_3$Ar), 2.03 (s, 6H, (C***H***$_3$)$_2$CPy_2), 1.70 (s, 3H, Py_2CC***H***$_3$Ar), 1.52 (s, 3H, C***H***$_3$CPy_2), 1.42 (s, 3H, C***H***$_3$CPy_2)

IR spectrum (KBr pellet (cm^{-1})): 3352 (N-H, st), 3063 (Aromatic C-H, st), 2950-2850 (Aliphatic CH, st), 1588 and 1492 (Aromatic C=C, st), 1588 (N=N, st), 1326 (C-N, st) 1246 (C-O-C, st)

MALDI-TOF mass: *Anal.Calcd* for $[C_{84}H_{87}N_7O_{12}]^+$ *m*/*z* = 1386.6

Found m/*z* = 1387.8 $[M+ H]^+$

2.2.8 Preparation of 1,3-di-*p*-nitrophenylazo-calix[4]-diacetophenone (7)

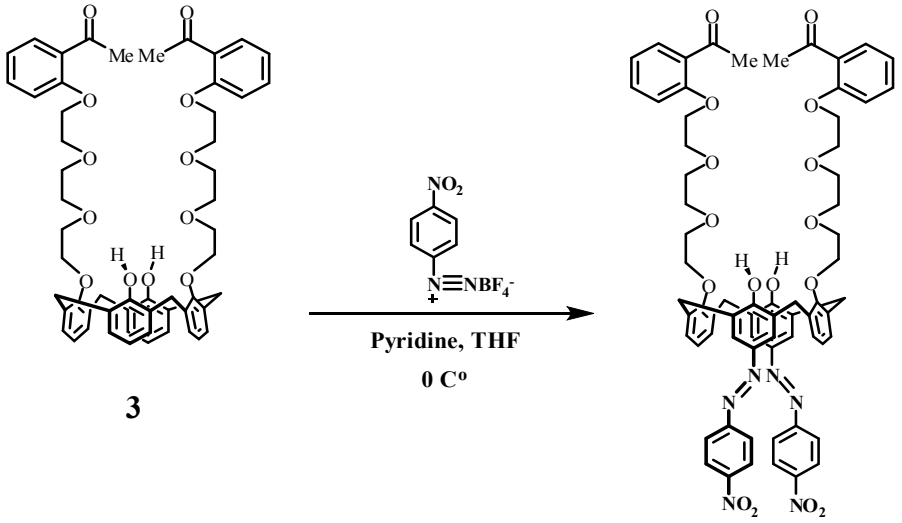

3 **7**

To a solution of **3** (0.75 g, 0.79 mmol) in tetrahydrofuran (THF; 200 mL), 4-nitrobenzenediazonium tetrafluoroborate (0.58 g, 2.44 mmol) was added. The reaction mixture was stirred for 30 minutes at 0 °C, and then pyridine (0.96 g, 12.17 mmol) was added drop wise. The reaction mixture was stirred for an additional 15 hours at 0 °C treated with 10% aqueous HCl solution (200 mL), and extracted with CH_2Cl_2 (2×100 mL). The organic layer was washed with 10% aqueous HCl solution (2×200 mL) and dried over anhydrous Na_2SO_4. Removing the organic solvent in vacuum afforded a reddish solid. Purification by column chromatography on silica gel with EtOAc/hexane (60:40) as eluent gave 0.18 g of **7** (49% yield).

Characteristic data for 7:

^{1}H-NMR spectrum ($CDCl_3$, δ(ppm), 400 MHz): δ 8.75 (broad s, 2H, ArO***H*)**, 8.35 (d, 4H, $J_{H\text{-}H}$ = 7.2 Hz , $NO_2Ar\boldsymbol{H}_o$), 7.95 (d, 4H, $J_{H\text{-}H}$ = 7.6 Hz , $NO_2Ar\boldsymbol{H}_m$), 7.77 (s, 4H, $Ar\boldsymbol{H}_m$), 7.70 (d, 4H, $J_{H\text{-}H}$ = 8.0 Hz, $Ar\boldsymbol{H}_m$), 7.35 (t, 2H, $J_{H\text{-}H}$ = 7.8 Hz, $Ar\boldsymbol{H}_p$), 6.98 (d, 2H, $J_{H\text{-}H}$ = 8.4 Hz, $Ar\boldsymbol{H}COCH_3$,), 6.92 (d, 2H, $J_{H\text{-}H}$ = 7.2 Hz, $Ar\boldsymbol{H}OCH_2$), 6.78 (t, 4H, $J_{H\text{-}H}$ = 7.0Hz, $Ar\boldsymbol{H}COCH_3$), 4.47 (d, AB system, 4H, $J_{H\text{-}H}$ = 13.2 Hz, $ArC\boldsymbol{H}_2Ar$), 4.22 (t, 4H, $J_{H\text{-}}$

$_{H}$ = 4.2 Hz, OC***H***$_2$), 4.02 (m, 8H, OC***H***$_2$), 3.84 (m, 8H,OC***H***$_2$), 3.77 (m 4H, OC***H***$_2$), 3.48 (d, AB system, 4H, $J_{H\text{-}H}$ = 13.2 Hz, ArC***H***$_2$Ar), 2.62 (s, 6H, ArCOC***H***$_3$)

^{13}C-NMR spectrum($CDCl_3$, δ(ppm), 400 MHz,) δ 199.7, 158.2, 158.1, 156.2, 151.6, 147.9, 145.6, 133.6, 132.4, 130.3, 129.4, 128.8, 128.2, 125.6, 124.7, 122.9, 120.7, 112.4, 75.5, 71.1, 70.7, 70.0, 69.6, 67.6, 32.1, 31.0

IR spectrum (KBr pellet (cm^{-1})): 3562-3038 (OH, st), 2918-2875 (Aliphatic C-H, st), 1668 (C=O, st), 1593 and 1453 (Aromatic C=C, st), 1518 (N=N, st), 1253 (C-N, st), 1114 (C-O, st)

Elemental analysis: *Anal. Calcd* for $C_{68}H_{66}N_6O_{16}$: C, 66.77%; H, 5.44%; N, 6.87%
Found: C, 66.78%; H, 5.50%; N, 6.96%

MALDI-TOF mass: *Anal. Calcd* for $[C_{68}H_{66}N_6O_{16}]^+$ *m*/*z* = 1222.5
Found m/*z* = 1223.83 $[M + H]^+$

2.2.9 Preparation of 1,3-di-*p*-nitrophenylazo-calix[4]arene-bis-dipyrroethane (8)

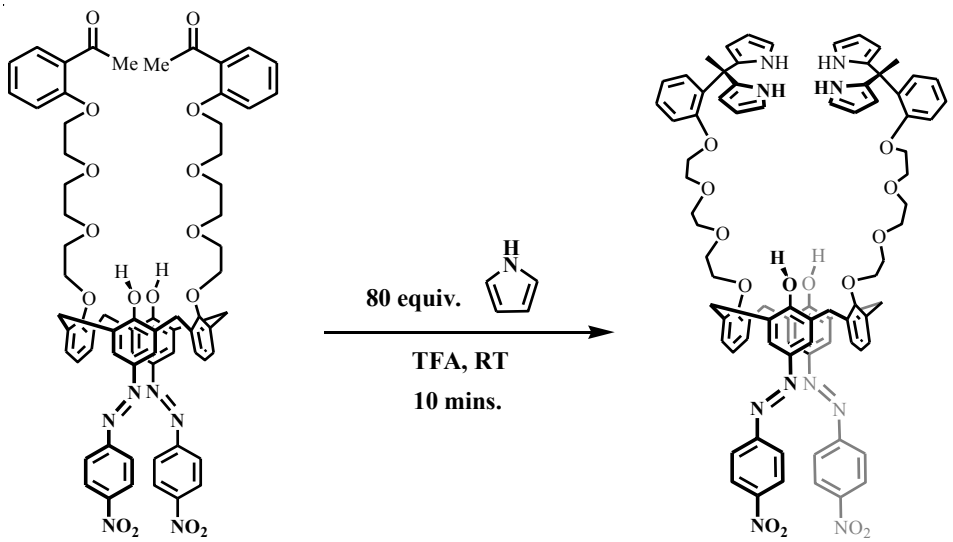

7 **8**

A solution of pyrrole (2 mL, 29 mmol) and **7** (0.20 g, 0.16 mmol) was degassed by bubbling with nitrogen for 15 minutes, and trifluoroacetic acid (TFA) (0.003 mL, 0.039 mmol) was then added. The solution was stirred in darkness for 10 minutes at room temperature. Then the reaction mixture was diluted with dichloromethane (15 mL), washed with 0.1 M $NaHCO_3$ (2×15 mL) and water (2×15 mL). The organic layer was dried over anhydrous Na_2SO_4 and the solvent was removed in vacuum. The obtained residue was purified by column chromatography over silica gel with CH_2Cl_2/EtOAc/NEt_3 (95:5:1) as eluent gave a red viscous oil **8** (0.091 g, 39%).

Characteristic data for 8:

^{1}H-NMR spectrum ($CDCl_3$, δ(ppm), 400 MHz): δ 8.74 (s (br), 4H, N***H***), 8.64 (s, 2H, ArO***H***), 8.29 (d, 4H, $J_{H\text{-}H}$ = 8.8 Hz, $NO_2Ar\boldsymbol{H_o}$), 7.89 (d, 4H, $J_{H\text{-}H}$ = 8.8 Hz, $NO_2Ar\boldsymbol{H_m}$), 7.73 (s, 4H, $Ar\boldsymbol{H_m}$), 7.05 (t, 2H, $J_{H\text{-}H}$ = 7.4 Hz, $Ar\boldsymbol{H_p}$), 6.92 (d, 2H, $J_{H\text{-}H}$ = 7.6 Hz, $Ar\boldsymbol{H_m}$), 6.81 (t, 2H, $J_{H\text{-}H}$ = 7.4 Hz, Ar***H***), 6.72 (t, 2H, $J_{H\text{-}H}$ = 7.8 Hz, Ar***H***), 6.59 (d, 2H, $J_{H\text{-}H}$ = 8.0 Hz, Ar***H***), 6.51 (s(br), 2H, Ar***H***), 5.98 (s, 4H, $\boldsymbol{H}_{Py}$), 5.80 (s, 4H, $\boldsymbol{H}_{Py}$), 4.40 (d, 4H, $J_{H\text{-}H}$ = 13.2 Hz, $ArC\boldsymbol{H}_2Ar$) 4.09 (t, 4H, $J_{H\text{-}H}$ = 4.0 Hz, $OC\boldsymbol{H}_2$), 3.87 (t, 4H, $J_{H\text{-}H}$ = 4.8 Hz,

OC***H***$_2$), 3.75 (t, 4H, $J_{H\text{-}H}$ = 4.2 Hz, OC***H***$_2$), 3.64 (t, 4H, $J_{H\text{-}H}$ = 4.4Hz, OC***H***$_2$), 3.59 (t, 4H, $J_{H\text{-}H}$ = 4.6 Hz, OC***H***$_2$), 3.44 (d, 4H, $J_{H\text{-}H}$ = 13.6 Hz, ArC***H***$_2$Ar), 3.21 (t, 4H, $J_{H\text{-}H}$ = 4.2 Hz, OC***H***$_2$), 1.98 (s, 6H, C***H***$_3$)

^{13}C-NMR spectrum ($CDCl_3$, δ(ppm), 400 MHz) δ 171.2, 158.1, 156.1, 151.6, 147.9, 145.6, 138.3, 134.9, 132.4, 129.4, 128.8, 128.1, 127.5, 125.6, 124.7, 122.9, 120.9, 116.9, 115.6, 112.3, 107.5, 104.3, 103.6, 75.3, 70.9, 70.4, 69.7, 69.4, 66.3, 60.4, 42.3, 31.1, 29.6, 29.2, 28.5, 21.1, 14.1

IR spectrum (KBr pellet (cm^{-1})): 3373 (NH, st), 3096 (Aromatic C-H, st), 2925-2861 (Aliphatic C-H, st), 1588 and 1460 (Aromatic C=C, st), 1520 (N=N, st), 1320-1207 (C-N, st), 1113-1024 (C-O, st)

Elemental analysis: *Anal. Calcd* for $C_{84}H_{82}N_{10}O_{14}$: C, 69.31%; H, 5.68%; N, 9.62%
Found: C, 69.38%; H, 5.73%; N, 9.68%

MALDI-TOF mass: *Anal.Calcd* for $[C_{84}H_{82}N_{10}O_{14}]^+$ *m*/*z* = 1454.6
Found m/*z* = 1455.06 $[M + H]^+$

2.2.10 Preparation of 1,3-di-*p*-nitrophenylazo-calix[4]arene-calix[4]pyrrole (9)

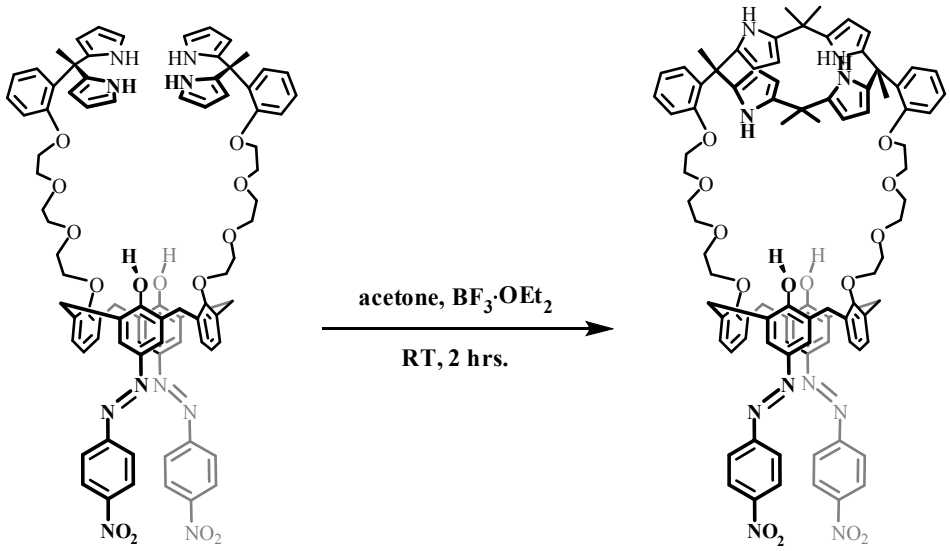

8 **9**

A mixture of **8** (0.09 g, 0.06 mmol) with dry acetone (15 mL) was stirred in a 100 mL two-necked round bottom flask and the solution was then added by $BF_3{\cdot}OEt_2$ (0.003 mL, 0.002 mmol). The solution was stirred for 2 hours at room temperature. The solvent was removed and the obtained residue was dissolved with CH_2Cl_2 (15 mL) then treated with saturated $NaHCO_3$ (15 mL) and extracted with water (2×15 mL). The organic layer was dried over anhydrous Na_2SO_4 and the solvent was removed to dryness. The residue was purified by silica gel with CH_2Cl_2/EtOAc (95:5) as eluent to provide a reddish solid of **9** (0.013 g, 14%).

Characteristic data for 9:

^{1}H-NMR spectrum ($CDCl_3$, δ(ppm), 400 MHz): δ 8.71 (s, 2H, ArO***H***), 8.30 (d, 4H, $J_{H\text{-}H}$ = 8.8 Hz, $NO_2Ar\boldsymbol{H_o}$), 8.10 (s(br), 4H, N***H***), 7.89 (d, 4H, $J_{H\text{-}H}$ = 8.8 Hz, $NO_2Ar\boldsymbol{H_m}$), 7.72 (s, 4H, $Ar\boldsymbol{H_m}$), 7.10 (t, 2H, $J_{H\text{-}H}$ = 8.0Hz, $Ar\boldsymbol{H_p}$), 6.94 (d, 4H, $J_{H\text{-}H}$ = 7.6 Hz, $Ar\boldsymbol{H_m}$), 6.80 (t, 4H, $J_{H\text{-}H}$ = 7.8 Hz, Ar***H***), 6.74 (d, 2H, $J_{H\text{-}H}$ = 8.0 Hz, Ar***H***), 6.71 (d, 2H, $J_{H\text{-}H}$ = 8.4 Hz, Ar***H***), 5.80 (s, 4H, $\boldsymbol{H_{Py}}$), 5.56 (s(br), 4H, $\boldsymbol{H_{Py}}$), 4.37 (d, 4H, $J_{H\text{-}H}$ = 12.8 Hz, $ArC\boldsymbol{H_2}Ar$),

4.16 (t, 4H, $J_{H\text{-}H}$ = 4.1 Hz, OC***H***$_2$), 4.01 (t, 4H, $J_{H\text{-}H}$ = 4.9 Hz, OC***H***$_2$), 3.77 (t, 4H, $J_{H\text{-}H}$ = 4.3 Hz, OC***H***$_2$), 3.70 (t, 4H, $J_{H\text{-}H}$ = 3.6 Hz, OC***H***$_2$), 3.49 (s(br), 4H, OC***H***$_2$), 3.45 (d, 4H, $J_{H\text{-}H}$ = 13.2 Hz, ArC***H***$_2$Ar), 3.01 (m, 4H, OC***H***$_2$), 1.98 (s, 6H, Py_2CC***H***$_3$Ar), 1.51 (s, 6H, $Py_2C(C$***H***$_3)_2$), 1.44 (s, 6H, $Py_2C(C$***H***$_3)_2$)

^{13}C-NMR spectrum ($CDCl_3$, δ(ppm), 400 MHz) δ 158.1, 156.3, 151.5, 148.0, 145.7, 137.7, 137.6, 132.5, 129.5, 128.7, 127.9, 125.7,124.7, 122.9, 121.0, 113.8, 103.9, 103.1, 75.2, 71.0, 70.3, 70.2, 69.8, 69.4, 67.6, 35.2, 33.7, 31.9, 31.1, 30.0, 26.7, 22.6,14.2, 14.1

IR spectrum (KBr pellet (cm^{-1})): 3290 (NH, st), 3060 (Aromatic C-H, st), 2920-2850 (Aliphatic C-H, st), 1582 and 1462 (Aromatic C=C, st), 1519 (N=N, st), 1343 (C-N, st), 1130-1110 (C-O, st)

Elemental analysis: *Anal. Calcd* for $C_{90}H_{90}N_{10}O_{14}$: C, 70.39%; H, 5.91%; N, 9.12%
Found: C, 70.43%; H, 5.93%; N, 9.29%

MALDI-TOF mass: *Anal.Calcd* for $[C_{90}H_{90}N_{10}O_{14}]^+$ *m*/*z* = 1534.7
Found m/*z*= 1534.65 $[M]^+$

2.3 Complexation studies

2.3.1 Anion complexation study of ligand 9 by using the UV-vis titration

Stock solution of ligand **9** with approximate concentration of 0.1 mM has been prepared by weighting an exact amount of ligand **9** on the Mettler Toledo model AT 201 balances and dissolving in CH_3CN with ionic strength kept constant at 10 mM using $TBAPF_6$. The stock solution was diluted with the same solvent system to provide an approximate 0.02 mM of concentration, named ligand solution. In the case of stock solutions of anions, actual concentrations of anion stock solutions could be determined by EDTA titration [133] before being diluted with $CH_3CN/TBAPF_6$ system to provide an optimal concentration for each complexation studies.

Used $CH_3CN/TBAPF_6$ as a blank then 2 mL of ligand **9** solution was placed in a spectrophotometric cell of 1-cm path length and its absorbance was recorded extending from 200 to 800 nm. An anion solution had been then added directly and successively into the cell by a microburette and then, the solution was stired for 30 seconds before recording its absorbance. Table 2.1 shows the concentrations of anion used in anions complexation and the ratio of anions:ligand **9**. The stability constants were refined from spectrometric data using the program Sirko [134].

Table 2.1 Concentrations of anions (X^- = F^-, AcO^-, BzO^- and $H_2PO_4^-$) used in anion complexation studies with ligand **9** and the final ratios of guest:host (X^-/L**9**).

Point	X^-/L9	[L9], mM	[X^-], mM	V of X^- (mL)	V total (mL)
1	0	0.0200	0.0000	0.00	2.00
2	0.08	0.0198	0.0016	0.02	2.02
3	0.16	0.0196	0.0031	0.04	2.04
4	0.24	0.0194	0.0047	0.06	2.06
5	0.32	0.0192	0.0062	0.08	2.08
6	0.40	0.0190	0.0076	0.10	2.10
7	0.48	0.0189	0.0091	0.12	2.12
8	0.56	0.0187	0.0105	0.14	2.14
9	0.72	0.0183	0.0132	0.18	2.18
10	0.88	0.0180	0.0159	0.22	2.22
11	1.04	0.0177	0.0184	0.26	2.26
12	1.20	0.0174	0.0209	0.30	2.30
13	1.36	0.0171	0.0232	0.34	2.34
14	1.52	0.0168	0.0255	0.38	2.38
15	1.68	0.0165	0.0278	0.42	2.42
16	2.00	0.0160	0.0320	0.50	2.50
17	2.32	0.0155	0.0360	0.58	2.58
18	2.65	0.0150	0.0397	0.66	2.66
19	2.96	0.0146	0.0432	0.74	2.74
20	3.35	0.0141	0.0473	0.84	2.84
21	3.76	0.0136	0.0512	0.94	2.94
22	4.14	0.0132	0.0547	1.04	3.04
23	4.57	0.0127	0.0581	1.14	3.14
24	5.35	0.0120	0.0642	1.34	3.34
25	6.16	0.0113	0.0696	1.54	3.54

2.3.2 Cation complexation study of ligand 9 by using the UV-vis titration

Stock solution of ligand **9** was prapared with approximate concentration of 0.1 mM containing ionic strength at 10 mM using $TBAPF_6$. The UV-vis titrations were carried out in the same manner as mentioned in 2.3.1. The stability constants were also refined from spectrometric data using the program SIRKO [134].

2.3.3 Anion complexation study of ligand 9 by using the ^{1}H-NMR spectroscopy

Typically, NMR tubes containing a solution of 0.65 mM of ligand **9** (0.325 mmol) in 0.5 mL of CD_3CN were directly added with 0.1 equivalent to 3 equivalents of tetrabutylammonium salts. The ^{1}H-NMR spectra were recorded after addition of anions and every 24 hours until the complexation reached to the equilibrium.

2.3.4 Anion complexation study of ligand 7 by using the UV-vis titration

Stock solution of ligand **7** with approximate concentration of 0.1 mM have also been prepared by measuring exact amount of ligand **7** on the Mettler Toledo model AT 201 balances and dissolving in CH_3CN with ionic strength kept constant at 10 mM using $TBAPF_6$. The stock solution were diluted with the same solvent system until a desired concentration of approximate 0.02 mM was obtained, named ligand solution. In the case of stock solutions of anions, actual concentrations of anion stock solutions could be determined by EDTA titration [133] before diluting with $CH_3CN/TBAPF_6$ system to provide an optimal concentration for each complexation studies. 2 mL of ligand solution were placed in spectrophotometric cell of 1-cm path length and its absorbance was recorded extending from 200 to 800 nm. An anion solution had then been added directly and successively into the cell by a microburette and, then, the solution was stired for 30 seconds before its absorbance was recorded.

2.3.5 Cation complexation study of ligand 7 by using the UV-vis titration

Stock solution of ligand **7** with approximate concentration of 0.1 mM and the ionic strength of 10 mM using $TBAPF_6$ was prepared. The UV-vis titrations were carried out in the same manner as mentioned in 2.3.1.

2.3.5.1 Anion complexation study of ligand 7 by using the ^{1}H-NMR spectroscopy

Typically, 0.1 equivalent until 3 equivalents of tetrabutylammonium salts were directly added into NMR tubes containing a solution of 0.65 mM of ligand **7** (0.325 mmol in 0.5 mL CD_3CN. The ^{1}H-NMR spectra were recorded after addition of anions and every 24 hours until the complexation reached to the equilibrium.

2.3.6 Anion binding study of ligand 9 in the presence of calcium ion by using UV-vis spectrophotometry

In a typical titration experiment, a stock solution of 0.1 mM of ligand **9** and 2 equivalents of $Ca(NO_3)_2$ in CH_3CN with ionic strength kept constant at 10 mM using $TBAPF_6$ was prepared. The stock solution was diluted with the same solvent system to obtain a desired concentration of approximate 0.02 mM. Then, 2 mL of complex **9**·Ca^{2+} (0.02 mM) were transferred into a spectrophotometric cell of 1-cm path length. An anion solution was then added directly and successively into the cell by a microburette and the solution was stired for 30 seconds after each addition. The absorbance was recorded extending from 200 to 800 nm. Table 2.2 shows the concentrations of anion which used in anion complexation and ratios of anion:host. The stability constants were refined from spectrometric data using the program Sirko [134].

Table 2.2 Concentrations of anions (X^- = F^-, AcO^-, BzO^- and $H_2PO_4^-$) used in anion complexation studies with **9**·Ca^{2+} complex and the final ratio of guest:host (X^-/L**9**·Ca^{2+}).

Point	X^-/L9·Ca^{2+}	[L9·Ca^{2+}], mM	[X^-], mM	V of X^- (mL)	V total (mL)
1	0	0.0200	0.0000	0.00	2.00
2	0.08	0.0198	0.0016	0.02	2.02
3	0.16	0.0196	0.0031	0.04	2.04
4	0.24	0.0194	0.0047	0.06	2.06
5	0.32	0.0192	0.0062	0.08	2.08
6	0.40	0.0190	0.0076	0.10	2.10
7	0.48	0.0189	0.0091	0.12	2.12
8	0.56	0.0187	0.0105	0.14	2.14
9	0.72	0.0183	0.0132	0.18	2.18
10	0.88	0.0180	0.0159	0.22	2.22
11	1.04	0.0177	0.0184	0.26	2.26
12	1.20	0.0174	0.0209	0.30	2.30
13	1.36	0.0171	0.0232	0.34	2.34
14	1.52	0.0168	0.0255	0.38	2.38
15	1.68	0.0165	0.0278	0.42	2.42
16	2.00	0.0160	0.0320	0.50	2.50
17	2.32	0.0155	0.0360	0.58	2.58
18	2.65	0.0150	0.0397	0.66	2.66
19	2.96	0.0146	0.0432	0.74	2.74
20	3.35	0.0141	0.0473	0.84	2.84
21	3.76	0.0136	0.0512	0.94	2.94
22	4.14	0.0132	0.0547	1.04	3.04
23	4.57	0.0127	0.0581	1.14	3.14
24	5.35	0.0120	0.0642	1.34	3.34
25	6.16	0.0113	0.0696	1.54	3.54

2.3.7 Anion complexation study of $9{\cdot}Ca^{2+}$ complex by using the ^{1}H-NMR spectroscopy

Typically, excess amounts (6 equivalents) of tetrabutylammonium salts were directly added into NMR tubes containinga solution of 0.65 mM of ligand **9** (0.325 mmol) with 2 equivalents of $Ca(NO_3)_2$ (0.650 mmol) in 0.5 mL of CD_3CN. The ^{1}H-NMR spectra were recorded after addition of anions and every 24 hours until the complexation reached to the equilibrium.

CHAPTER III

RESULTS AND DISCUSSION

3.1 Synthesis and characterization of 1,3-di-*p*-nitrophenylazo-calix[4]arene-calix[4]pyrrole (9)

3.1.1 Synthesis and characterization of 1,3-calix[4]-diacetophenone (3)

The synthetic pathway of 1,3-calix[4]-diacetophenone **3** (Scheme 3.1) started with a preparation of triethyleneglycol ditosylate **1** by tosylation of triethyleneglycol in the presence of triethylamine as base and a catalytic amount of DMAP in dichloromethane at room temperature for 4 hours. A white solid of compound **1** was obtained in 65% yield by precipitating with methanol. The ^{1}H-NMR spectrum of compound **1** showed the characteristic peaks of tosyl groups; a singlet of C*H*$_3$ at 2.42 ppm and two doublets of Ar*H* at 7.77 and 7.32 ppm ($J_{H\text{-}H}$ = 8.2 Hz).

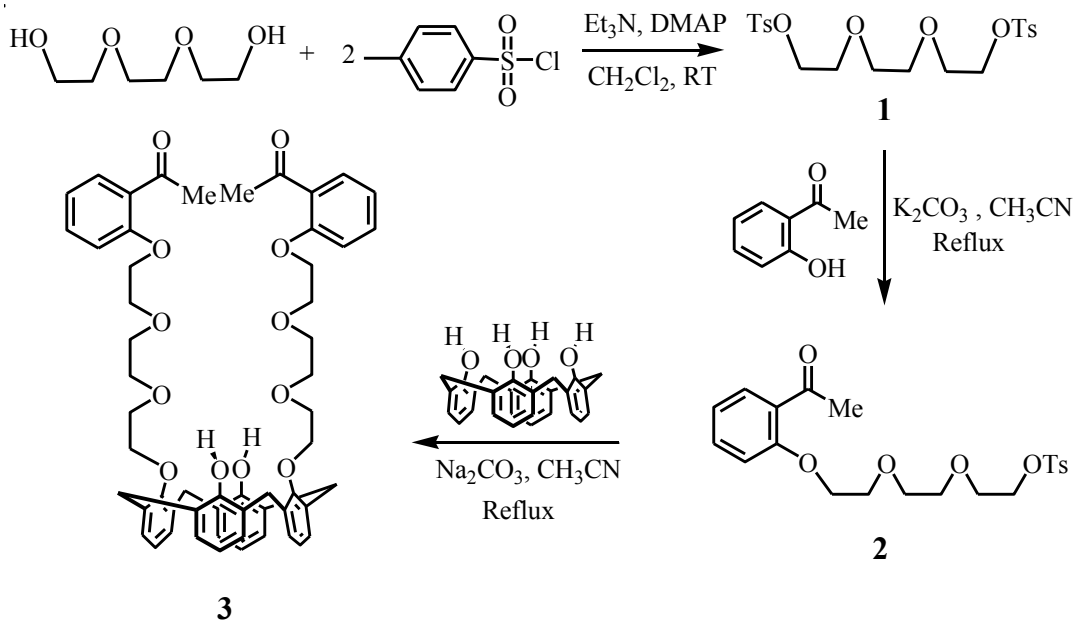

Scheme 3.1 Synthetic pathway of 1, 3-calix[4]-diacetophenone (**3**).

The nucleophilic substitution reaction of 2-hydroxyacetophenone with triethylene glycol ditosylate (**1**) using excess K_2CO_3 as base in acetonitrile provided 2-(8-tosyltriethyleneglycol)acetophenone (**2**) as a colorless oil (30% yield). The ^{1}H-NMR spectrum of **2** showed the characteristic peaks of tosyl groups; a singlet of C*H*$_3$ at 2.46 ppm and two doublets of Ar*H* at 7.82 and 7.36 ppm ($J_{H\text{-}H}$ = 8.0 Hz), and the characteristic peaks of the acetophenone unit, a singlet of C*H*$_3$ at 2.66 ppm, two doublets of Ar*H* at 7.77 and 6.98 ppm ($J_{H\text{-}H}$ = 4.0 Hz) and two triplets of Ar*H* at 7.47 and 7.03 ppm ($J_{H\text{-}H}$ = 4.0 Hz).

A condensation of 2 equivalents of 2-(8-tosyltriethyleneglycol)acetophenone (**2**) with calix[4]arene was carried out by using K_2CO_3 as a base in refluxing acetonitrile for 7 days. A white solid of ligand **3** was obtained in 85% yield by precipitation with methanol in dichloromethane. From the ^{1}H-NMR and ^{13}C-NMR spectrum, the substitution occurred in a distal manner due to the presence of only AB-system of methylene bridge protons of calix[4]arene unit (ArC*H*$_2$Ar) as two doublets at 3.36 and 4.43 ppm ($J_{H\text{-}H}$ = 13.0 Hz) and a singlet at 31 ppm in the ^{13}C-NMR. These evidences indicated that ligand **3** exists in cone conformation. Because of the adjacent phenyl rings of calix[4]arene in cone conformations were in a syn orientation. Consequently, only one ^{13}C-NMR signal at 31 ppm was presented for the methylene carbon atoms of calix[4]arene in this conformation [135]. Whereas in 1,3-alternate conformations, adjacent phenyl rings were in an anti orientation so two signals of ^{13}C-NMR at 31 and 37 ppm should be present [135]. The elemental analysis was also in accordance with the proposed structure of ligand **3**.

3.1.2 Synthesis and characterization of 1,3-di-*p*-nitrophenylazo-calix[4]-diacetophenone (7)

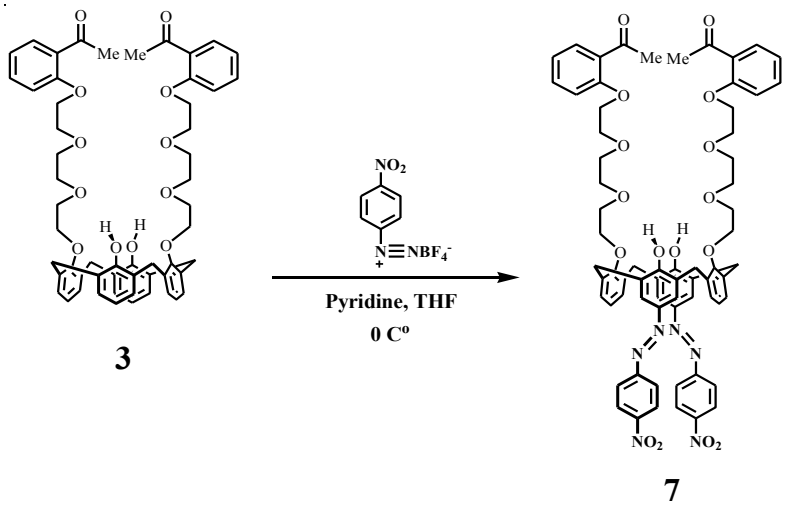

3 **7**

Scheme 3.2 Synthetic pathway of 1,3-di-*p*-nitrophenylazo-calix[4]-diacetophenone (**7**).

The synthesis of 1,3-di-*p*-nitrophenylazo-calix[4]-diacetophenone (**7**) was accomplished by treating 1,3-calix[4]-diacetophenone (**3**) with 4-nitrobenzenediazonium tetrafluoroborate in the presence of pyridine as a base and tetrahydrofuran as a solvent under 0 °C. After purification by column chromatography on silica (ethyl acetate/hexane = 60/40), ligand **7** was obtained as a reddish solid in 49 % yield. The ^{1}H-NMR spectrum of ligand **7** showed the characteristic peaks of azobenzene protons as two doublet peaks at 8.35 and 7.95 ppm and a downfield shift of hydroxyl protons from 7.72 ppm to 8.75 ppm. The singlet peak of meta-protons on the phenol rings at 7.77 ppm confirmed that the azo dye was connected to phenol ring at the para-position. The signal of methylene bridge protons of calix[4]arene unit (ArCH_2Ar) appeared as two doublets at 3.48 and 4.47 ppm ($J_{H\text{-}H}$ = 13.2 Hz). In addition, the elemental analysis and MALDI-TOF mass spectrum were in good agreement with the proposed structure.

Furthermore, the proposed structure was also confirmed by X-ray single crystal analysis. Suitable crystal was obtained by allowing a dichloromethane/methanol solution of ligand **7** to undergo slow evaporation at the temperature of 4 °C. The X-ray single crystal structure (Figure 3.1) revealed that ligand **7** adopts a pinch cone conformation and confirmed that two units of the azobenzene ring were connected to phenol rings in the para position. The *p*-nitrophenylazo moiety aligned approximately planar to phenolic unit of calix[4]arene framework allowing electron transfer by resonance.

(a) Top view

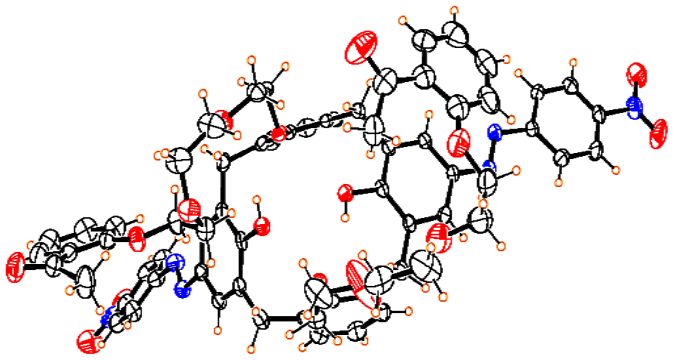

(b) Side view

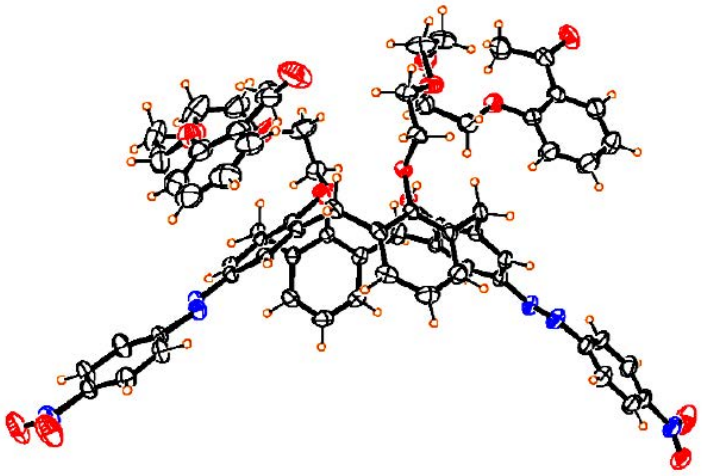

Figure 3.1 ORTEP drawing of 1,3-di-*p*-nitrophenylazo-calix[4]-diacetophenone (**7**).

3.1.3 Synthesis and characterization of 1,3-di-*p*-nitrophenylazo-calix[4]arene-bis-dipyrroethane (8)

Due to the highly selective anion binding of calix[4]pyrrole [136] and its easy modification of calix[4]arene to obtain a specific conformer and rigid cavity for a selective anion binding ability, 1,3-di-*p*-nitrophenylazo-calix[4]arene-bis-dipyrroethane (**8**) was synthesized to serve as the intermediate to further modification as depicted in Scheme 3.3.

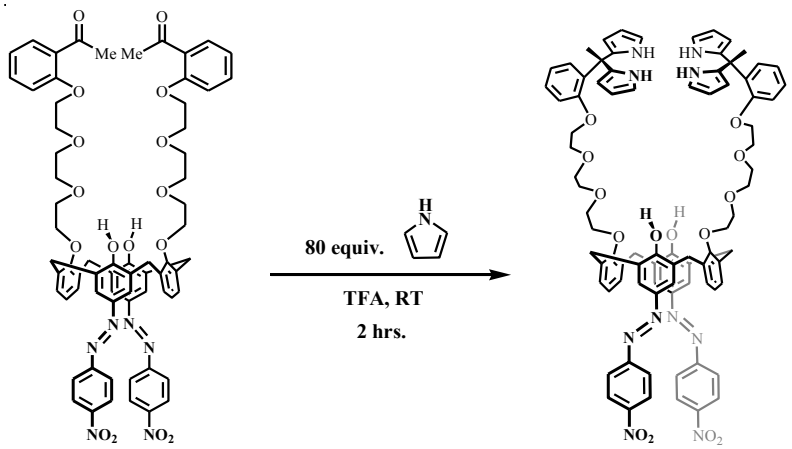

7 **8**

Scheme 3.3 Synthetic pathway of 1,3-di-*p*-nitrophenylazo-calix[4]arene-bisdipyrroethane (**8**).

The synthesis of 1,3-di-*p*-nitrophenylazo-calix[4]arene-bis-dipyrroethane (**8)** was accomplished by treating 1**,**3-di-*p*-nitrophenylazo-calix[4]-diacetophenone (**7**) with excess pyrrole (80 equiv.) in the presence of catalytic amount of trifluoroacetic acid for 10 minutes according to conventional procedure [137]. After purification by column chromatography on silica (dichloromethane/ethylacetate/triethylamine = 95:4:1), ligand **8** was obtained as a red viscous oil in 39% yield. The ^{1}H-NMR spectrum of ligand **8** showed the characteristic peaks of pyrrole-N*H* as a broad singlet at 8.74 ppm and three multiplets of the pyrrolic protons of the dipyrrolethane at 6.51, 5.98 and 5.80 ppm, respectively. In addition, elemental analysis result was in good agreement with the

proposed structure and the MALDI-TOF mass spectrum confirmed the presence of 1,3-di-*p*-nitrophenylazo-calix[4]arene-bisdipyrroethane (**8**).

3.1.4 Synthesis and characterization of 1,3-di-*p*-nitrophenylazo-calix[4]arene-calix[4]pyrrole (9)

The modification of intermediate **8** with dry acetone in the presence of a catalytic amount $BF_3{\cdot}OEt_2$ accomplished the azo-calix[4]arene-calix[4]pyrrole **9** by procedure as depicted in Scheme 3.4.

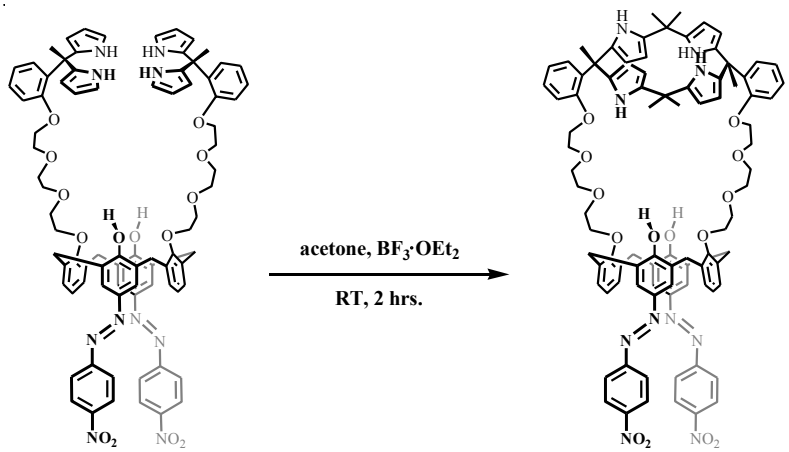

8 **9**

Scheme 3.4 The synthesis of 1,3-di-*p*-nitrophenylazo-calix[4]arene-calix[4]pyrrole (**9**).

1, 3-di-*p*-nitrophenylazo-calix[4]arene-bis-dipyrroethane (**8)** was condensed with dry acetone in the presence of $BF_3{\cdot}OEt_2$ at room temperature for 2 hours. Ligand **9** was separated by column chromatography on silica (dichloromethane/ethyl acetate = 95:5) to afford a reddish solid (14 %). The ^{1}H-NMR spectrum in $CDCl_3$ showed a broad signal of N*H* of calix[4]pyrrole unit at 8.10 ppm along with two singlet peaks of *β*-pyrrolic protons at 5.80 and 5.56 ppm and a singlet signal of O*H* of calix[4]arene framework at 8.71 ppm. Calix[4]arene exists in cone conformation due to a presence of doublet signal of ArCH_2Ar of calix[4]arene at 3.45 ($J_{H\text{-}H}$= 13.2 Hz) and 4.37 ppm ($J_{H\text{-}H}$= 12.8 Hz).

MALDI-TOF mass supported the presence of the desired ligand **9** with an intense m/z peak at 1534.43 [M^+] and the elemental analysis result was in good agreement with the proposed structure. The resonance of pyrrolic-N*H*s in CD_3CN appear at 8.19 and around 6.80-6.95 ppm in the form of two distinct singlets confirmed the configuration of calix[4]pyrrole unit exists in 1,3-alternate conformation. The two Ar-*H* of phenyl-triethyleneglycol spacers between calix[4]arene and calix[4]pyrrole in $CDCl_3$ were found to be split into two distinct doublets appearing at 6.94 and 6.74 ppm confirmed that link in trans geometry according to the previous report [137].

3.1.5 Synthesis and characterization of 1,3-calix[4]arene-bis-dipyrroethane (4)

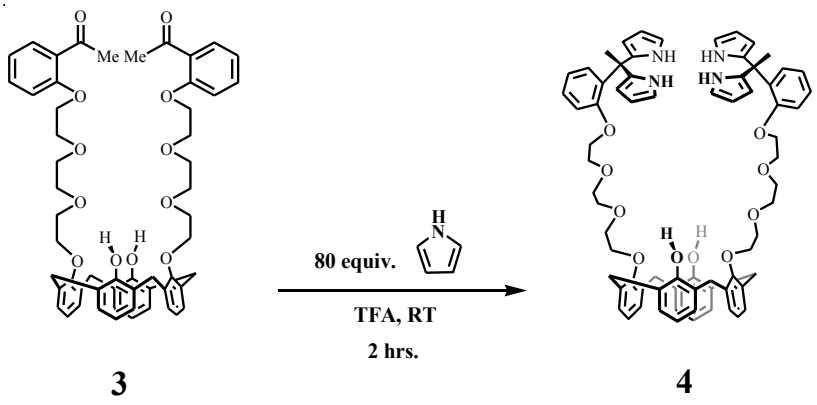

Scheme 3.5 Synthetic pathway of 1,3-calix[4]arene-bis-dipyrroethane(**4**).

The synthesis of 1,3-calix[4]arene-bis-dipyrroethane **4** was carried out by treating 1,3-calix[4]-diacetophenone (**3**) with excess pyrrole (80 equiv.) in the presence of catalytic amount of trifluoroacetic acid for 10 minutes according to conventional procedure [137]. After purification by column chromatography on silica gel (dichloromethane/ethyl acetate/triethylamine = 95:4:1), ligand **4** was obtained as a transparen viscous oil in 61% yield. The ^{1}H-NMR spectrum of ligand **4** in $CDCl_3$ showed the characteristic peaks of pyrrole-N*H* as a singlet at 8.86 ppm and three multiplets of the pyrrolic protons of the dipyrrolethane at 6.62, 6.11 and 5.92 ppm. On the

other hand, elemental analysis was not in good agreement with the structure due to its instability at room temperature.

3.1.6 Synthesis and characterization of calix[4]arene-calix[4]pyrrole (5)

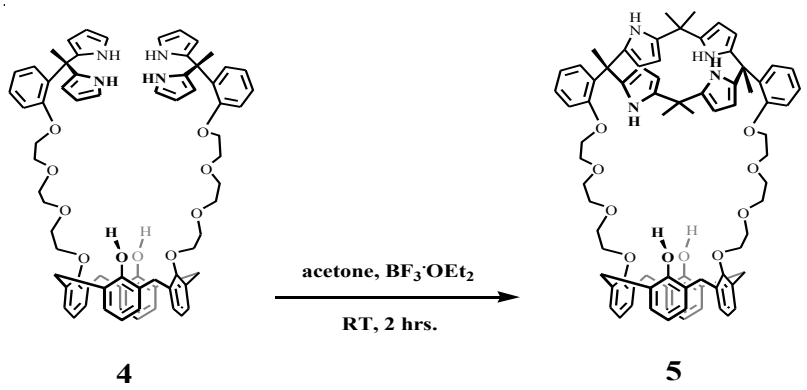

Scheme 3.6 The synthesis of calix[4]arene-calix[4]pyrrole (**5**).

The synthesis of ligand **5** was done by the condensation of 1,3-calix[4]arene-bisdipyrroethane (**4**) with dry acetone in the presence of $BF_3{\cdot}OEt_2$ as a catalyst at room temperature for 2 hours. The ligand **5** was separated on column chromatography and recrystalized with methanol to afford ligand **5** as a white solid (37%). The ^{1}H-NMR spectrum showed a broad signal of N*H* of calix[4]pyrrole moiety at 7.98 ppm accompanied by two singlet peaks of *β*-pyrrolic protons at 5.91 and 5.67 ppm, and the singlet signal of O*H* of calix[4]arene unit at 7.91 ppm. A doublet signal of Ar*CH*$_2$Ar of calix[4]arene at 3.39 and 4.40 ppm ($J_{H\text{-}H}$ = 13.0 Hz) suggested a cone conformation of calix[4]arene. MALDI-TOF mass spectrum supported the presence of desired ligand **5** showing an intense peak at m/z 1259.65 [M+Na$^+$] and the elemental analysis result was in accordance to the proposed structure.

The solid structure of ligand **5** determined by X-ray crystallography (Figure 3.2) has been reported by previous thesis [129]. In contrast to calix[4]arene, the calix[4]pyrrole unit adopted in 1,3-alternate conformation. Interestingly, one of the aromatic rings connected to calix[4]pyrrole point up the plane, while the other point down. Because of a strong hydrogen bonding of pyrrolic-N*H* to the oxygen of glycolic

chain, then calix[4]pyrrole unit bend down to the calix[4]arene and destroy the symmetry of the molecule.

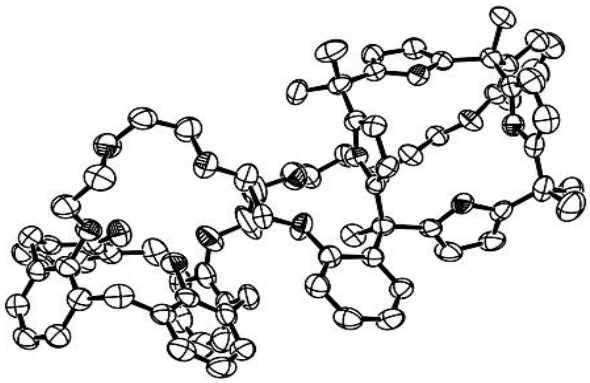

Figure 3.2 ORTEP drawing of calix[4]arene-calix[4]pyrrole (**5**) [127].

3.1.7 Synthesis and characterization of calix[4]arene-*p*-nitrophenylazo-calix[4]pyrrole (6)

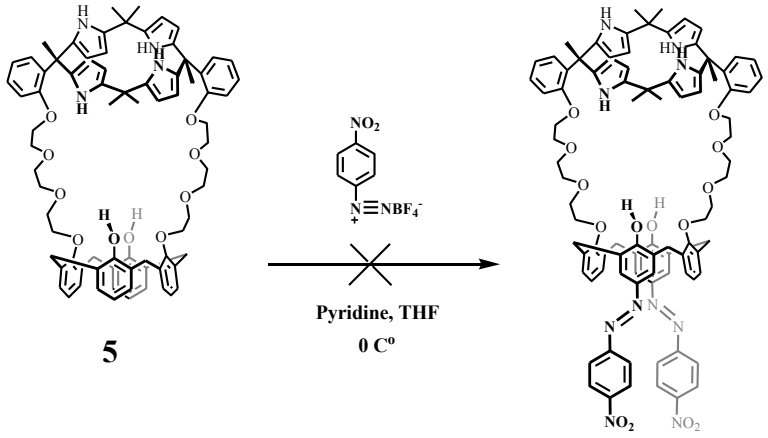

5 **9**

Scheme 3.7 The synthesis of 1,3-di-*p*-nitrophenylazo-calix[4]arene-calix[4]pyrrole (**9**).

The treatment of calix[4]arene-calix[4]pyrrole (**5**) with 4-nitrobenzenediazonium tetrafluoroborate in the presence of pyridine as a base in tetrahydrofuran under 0 °C. According to ^{1}H-NMR spectrum, the design ligand **9** did not occurred. After purification

by column chromatography on silica gel (ethyl acetate/hexane = 30:70) ligand **6** (Figure 3.3) was obtained as a reddish solid in 49% yield. The MALDI-TOF mass analysis of ligand **6** revealed signals of *m/z* = 1387.8, corresponding to the molecular ion $[M+H]^+$ as the major peak (calcd. mass M^+ = 1386.6). ^{1}H-NMR spectrum of ligand **6** recorded in $CDCl_3$ showed the characteristic peak of azobenzene protons as two of doublet peaks at 8.08 and 7.60 ppm. The pyrrole-N*H* was occurred at 8.64 ppm and *β*–pyrrolic protons showed three singlet at 5.86, 5.81 and 5.33 ppm. It is mentioning that both sets of resonances of pyrrole-N*H* and *β*–pyrrolic protons were downfield shifts (Δδ = 0.66 for N*H* and Δδ = 0.1-0.2 for *β*–pyrrolic) relative to calix[4]arene-calix[4]pyrrole (**5**). In addition, the three singlets of non equal intensity at 2.03, 1.52 and 1.42 ppm (6H, 3H and 3H, respectively) are assigned to the chemically-non-equivalent methyl protons of the calix[4]pyrrole unit. This is presumably as a result of mono-substitution on calix[4]pyrrole unit. However the signal of methylene-bridge and glycolic protons are complicated due the destroy a symmetry of the molecule by mono-substitution of azobenzene but the relative integration of the protons corresponding to the number of protons on that chain. Because of a scrambling was observed in the reaction, then the undesired ligand **6** was occurred, which due to the formation of a variety of substitution products on the reactive pyrrole *β*–position and phenol *para*-position.

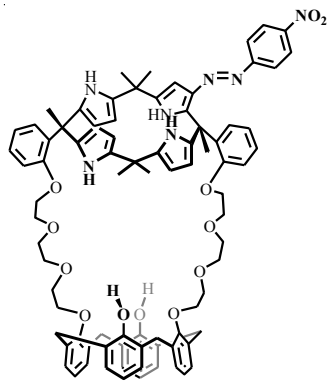

6

Figure 3.3 Structure of calix[4]arene-*p*-nitrophenylazo-calix[4]pyrrole (**6**).

3.2 Anion complexation studies of 1,3-di-*p*-nitrophenylazo-calix[4]arene-calix[4]pyrrole (9)

3.2.1 By using UV-vis spectrophotometry

Azocalix[4]arene-strapped calix[4]pyrrole **9** was designed to have calix[4]pyrrole for anion binding and azo-calix[4]arene to serve as sensoring unit along with enhancing anion binding by increasing hydrogen bonding ability of calix[4]arene platform. The anion binding ability of ligand **9** with F^-, Cl^-, Br^-, I^-, AcO^-, BzO^-, $H_2PO_4^-$, ClO_4^-, NO_3^- and PF_6^- was carried out using UV-vis spectrophotometry. 100 and 6 equivalents of tetrabutylammonium salts in acetonitrile solution were added into the 0.02 mM solution of ligand **9**. The anion recognition *via* H-bonding and/or deprotonating interactions could be easily monitored by induced wavelength and color changes.

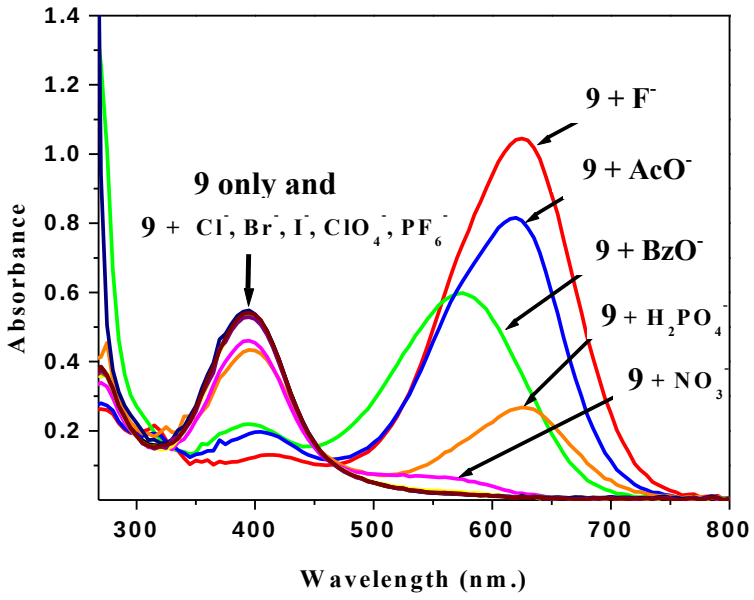

Figure 3.4 Wavelength changes of ligand **9** upon the addition of various anions. Condition: ligand **9** (0.02 mM)/CH_3CN; TBAX (100 equiv.)/CH_3CN.

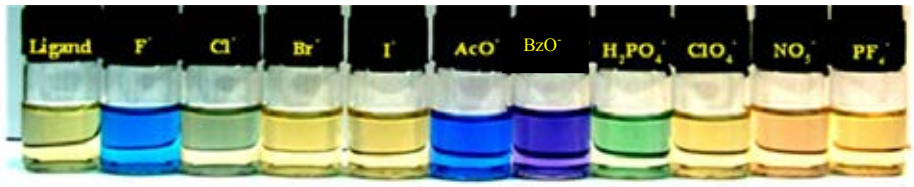

Figure 3.5 Color change of ligand **9** (0.02 mM) with 100 equivalents of anions.

Addition of 100 equivalents of the anions into ligand **9** solution gave a bathochromic shift, from 395 nm to around 600 nm only with F^-, AcO^-, BzO^-, $H_2PO_4^-$ and NO_3^- while Cl^-, Br^-, I^-, PF_6^- and ClO_4^- gave no effect on ligand solution (Figure 3.4). The magnitude of these bathochromic shifts is in the order of $F^- > AcO^- > BzO^- > H_2PO_4^- > NO_3^-$ while significant color changes from light orange to blue, deep blue, violet, green and orange were observed, respectively (Figure 3.5). The new absorption band showed at 624 nm for F^-, 620 nm for AcO^- and 624 nm for $H_2PO_4^-$, in which almost the same wavelength contrast to BzO^-, which showed the new absorption band at 575 nm. This result suggested that ligand **9** could enable to show colorimetric differentiation of F^-, AcO^-, BzO^- and $H_2PO_4^-$ of similar basicity [76, 138] but different in their size and shape.

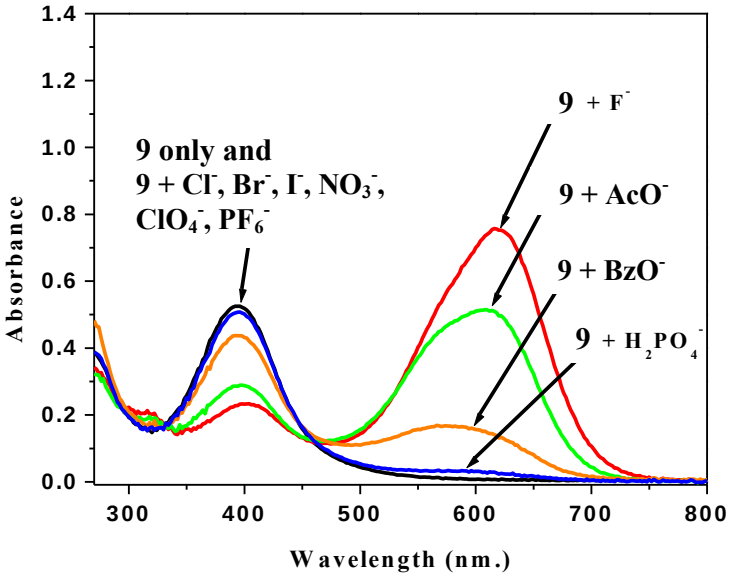

Figure 3.6 Absorbance changes of ligand **9** upon the addition of various anions. Condition: ligand **9** (0.02 mM)/CH_3CN; TBAX (6 equiv)/CH_3CN.

9 **A** **B** **C** **D**

Figure 3.7 Color change of ligand **9** (0.02 mM) with 6 equivalents of anions (from left to right; ligand **9** only, **A** = ligand **9** + F^-, **B** = ligand **9** + AcO^-, **C** = ligand **9** + BzO^-, **D** = ligand **9** + $H_2PO_4^-$).

Adding 6 equivalents of the anion into the solution of ligand **9** to study the anions binding affinity. UV-vis absorption band of ligand **9** in CH_3CN undergoes a red shift as only for F^-, AcO^-, BzO^- and $H_2PO_4^-$. The absorption band at 395 nm of ligand **9** decreases while the new absorption band gradually move to longer wavelengths reaching to a maximum at 615 nm for F^-, 607 nm for AcO^- and 575 nm for BzO^-. In case of $H_2PO_4^-$, the spectrum did not show a significant spectrum changes but show a small

shoulder around 600 nm. Dramatic changes in color were also induced upon addition of 6 equivalents of anions into the solutions of ligand **9**. Specifically, the initial light orange color solution of ligand **9** turned to light sky blue, blue, light pink and light yellow upon the addition of F^-, AcO^-, BzO^- and $H_2PO_4^-$, respectively (Figure 3.7).

It is known that the electronic excitation of an azophenol chromophore generally occurs through a charge transfer from the donor oxygen of the phenol to the acceptor substitute (NO_2) of the chromophore [61,139]. The mechanism of these phenomena was shown in Figure 3.8. Upon complex formation between ligand **9** and anions, the excited state would be more strongly stabilized by the anion binding, resulting in a bathochromic shift in the absorption maxima as well as in color changes [61,140].

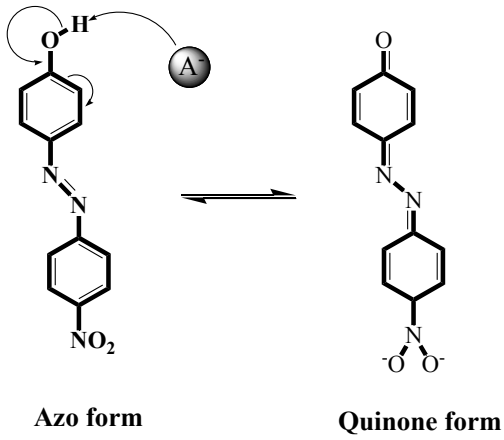

Figure 3.8 Electronic excitation of an azophenol chromophore.

3.2.2 By using ^{1}H-NMR spectroscopy

The binding ability of ligand **9** with a series of anions F^-, AcO^- and BzO^- was study by using ^{1}H-NMR titration experiments. The different amount of TBAF, TBA^+AcO^- or TBA^+BzO^- was added into the solution of ligand **9** (3.58 mM) then the ^{1}H-NMR spectrum in each experiment was then collected.

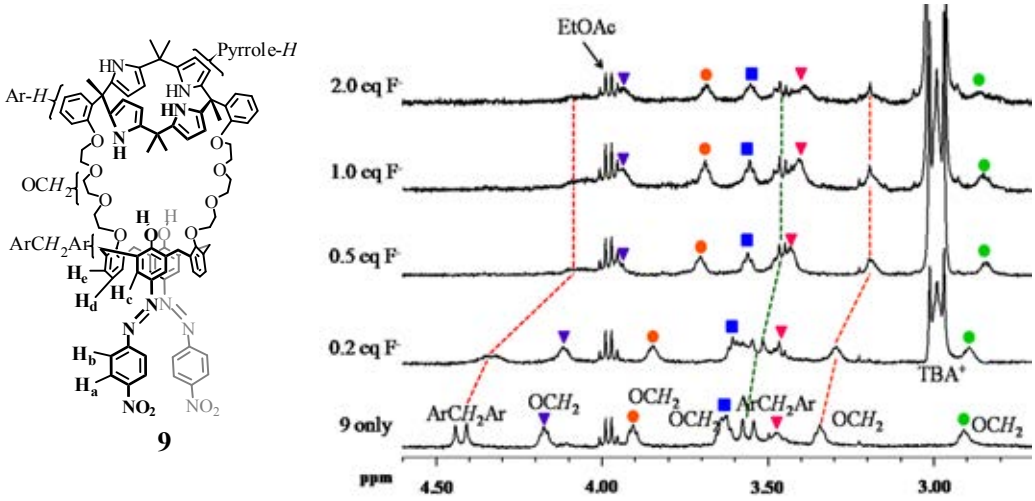

Figure 3.9 ^{1}H-NMR spectra (2-5 ppm) of ligand **9** (3.58 mM) in CD_3CN in the presence of different amounts of TBAF.

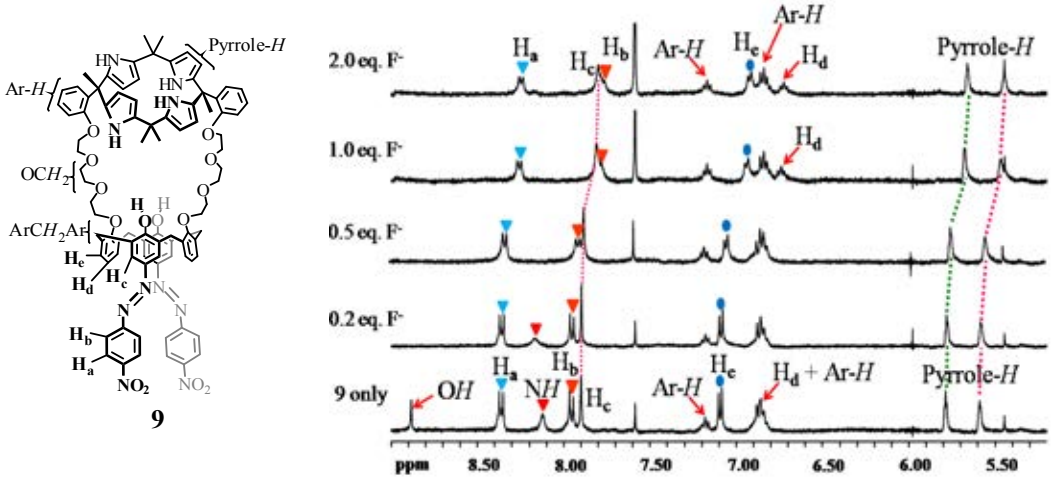

Figure 3.10 ^{1}H-NMR spectra (5-9 ppm) of ligand **9** (3.58 mM) in CD_3CN in the presence of different amounts of TBAF.

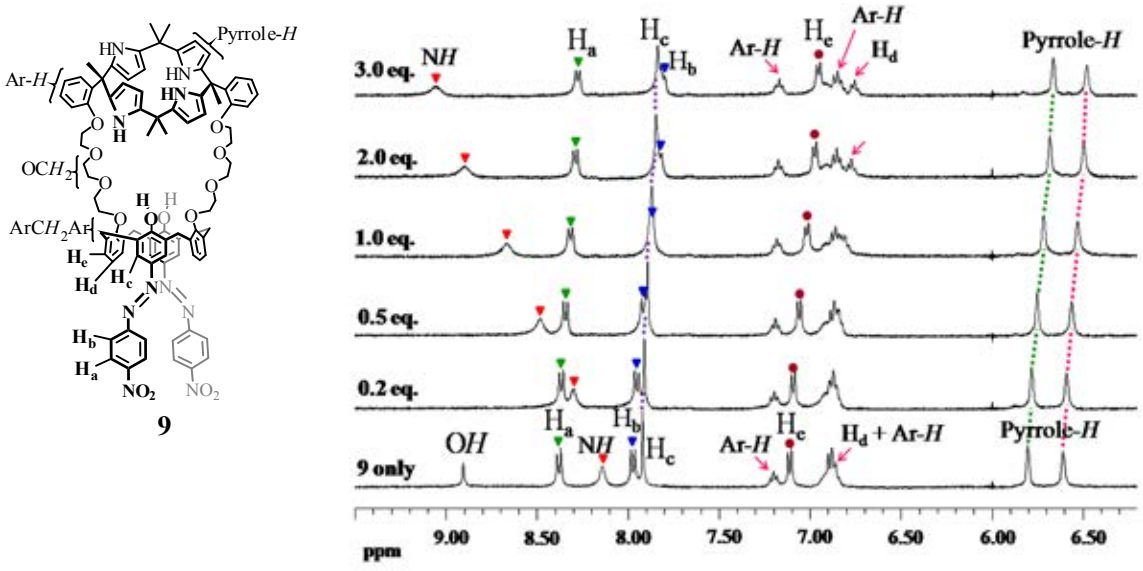

Figure 3.11 ^{1}H-NMR spectra (5-9 ppm) of ligand **9** (3.58 mM) in CD_3CN in the presence of different amounts of $TBA^{+}AcO^{-}$.

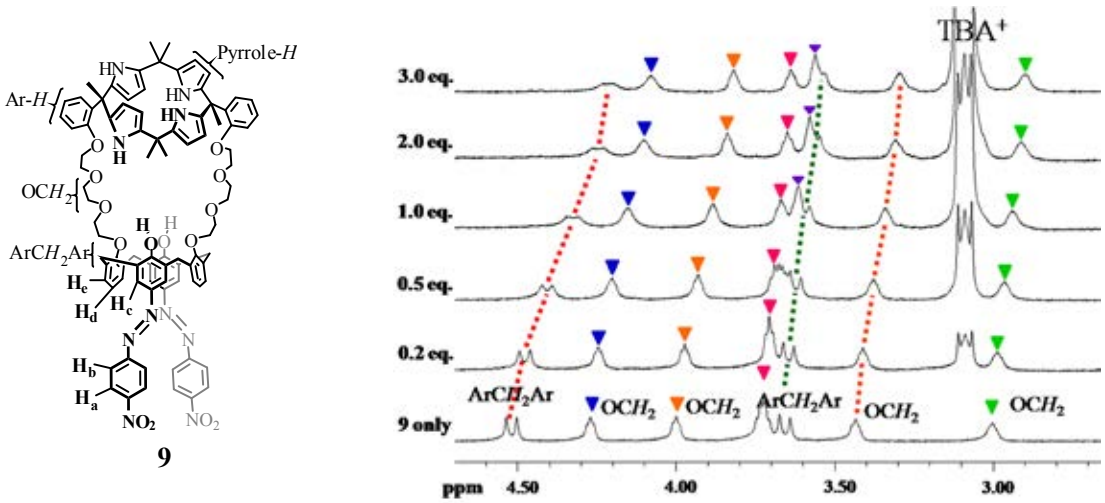

Figure 3.12 ^{1}H-NMR spectra (2-5 ppm) of ligand **9** (3.58 mM) in CD_3CN in the presence of different amounts of $TBA^{+}AcO^{-}$.

In order to comprehend the binding mode of ligand **9** with F^{-}, ^{1}H-NMR titration was carried out. Figure 3.9 and 3.10 show the ^{1}H-NMR spectra of ligand **9** (3.58 mM) with different amounts of TBAF in CD_3CN. It was revealed that the phenol protons of

azocalix[4]arene moieties at 8.80 ppm disappeared when only 0.1 equivalent of F^- was added into solution of ligand **9** along with displacement of H_c proton signal to upfield, from 7.82 ppm to 7.72 ppm. This indicates that phenol protons of ligand **9** were deprotonated by F^- as previously reported [141, 142]. Moreover, protons H_a and H_b of nitrobenzene units shifted upfield from 8.28 and 7.88 ppm to 8.26 and 7.80 ppm, respectively, which implies that the electron pushed from phenolate ion formed by deprotonation by F^- ion to nitro group. In addition, the H_d and H_e protons shifted upfield from around 6.86-6.72 and 7.02 ppm to 6.66 and 6.85 ppm which indicated that 1,3-alternate platform of azocalix[4]arene rearranged to accommodate F^- ion. Concerning the calix[4]pyrrole moiety, the N*H* protons shifted downfield from 8.04 ppm to 8.09 ppm at 0.1 equiv of F^- added and disappeared at 0.2 equiv of F^- added contrasting with *β*-pyrrolic protons without peak merging. This evidence suggests that calix[4]pyrrole unit participated in F^- binding by hydrogen bonding. From the ^{1}H-NMR evidence, it can be concluded that N*H* of calix[4]pyrrole unit in azocalix[4]arene strapped calix[4]pyrrole served as anions binding site and phenolic O*H* of calix[4]arene enhanced the anion binding abilities by hydrogen bonding and selectively signaled the anion detection.

I case of AcO^-, the signal of phenol protons also disappeared when only 0.2 equivalents was added into the solution of ligand **9**. The disappearance of phenol protons caused to the signal of H_a and H_b protons of azobenzene unit and H_c proton shifted upfield. Other protons signal such as N*H*, *β*-pyrrolic protons, H_d and H_e were also shifted into the same pattern as compared to the F^-. From these evidence of ^{1}H-NMR spectra concerning to AcO^- complexes with ligand **9**, it can also be described that the strapped azocalix[4]arene can modulate the inherent anion selectivity and increase the anion binding affinities of calix[4]pyrrole.

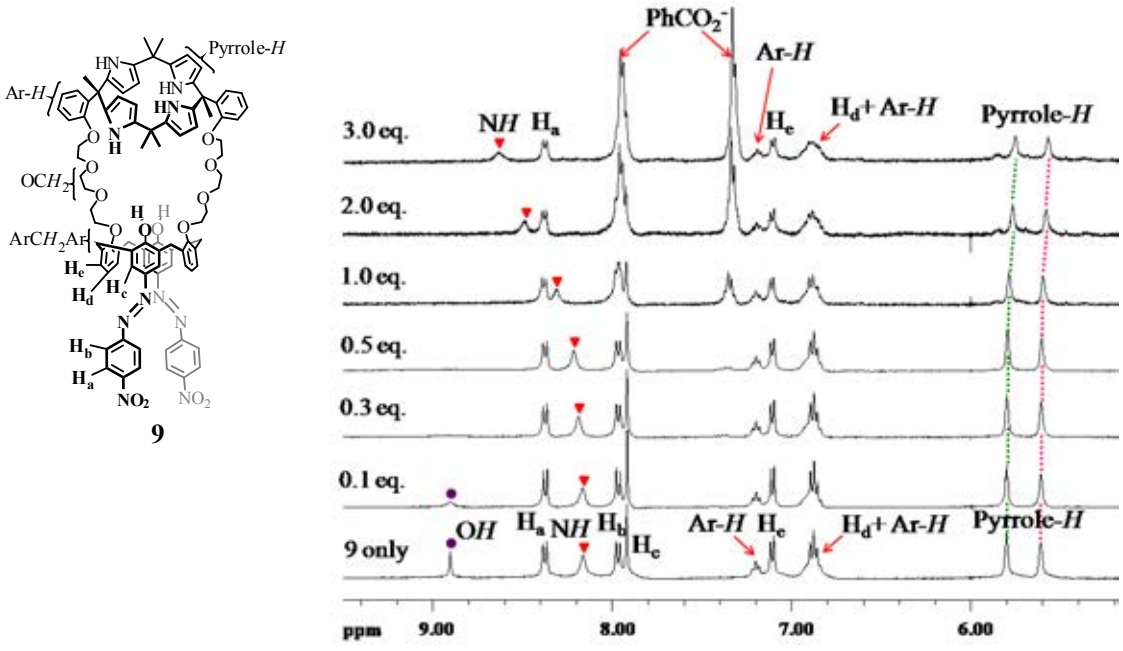

Figure 3.13 ^{1}H-NMR spectra (5-9 ppm) of ligand **9** (3.58 mM) in CD_3CN in the presence of different amounts of $TBA^{+}BzO^{-}$.

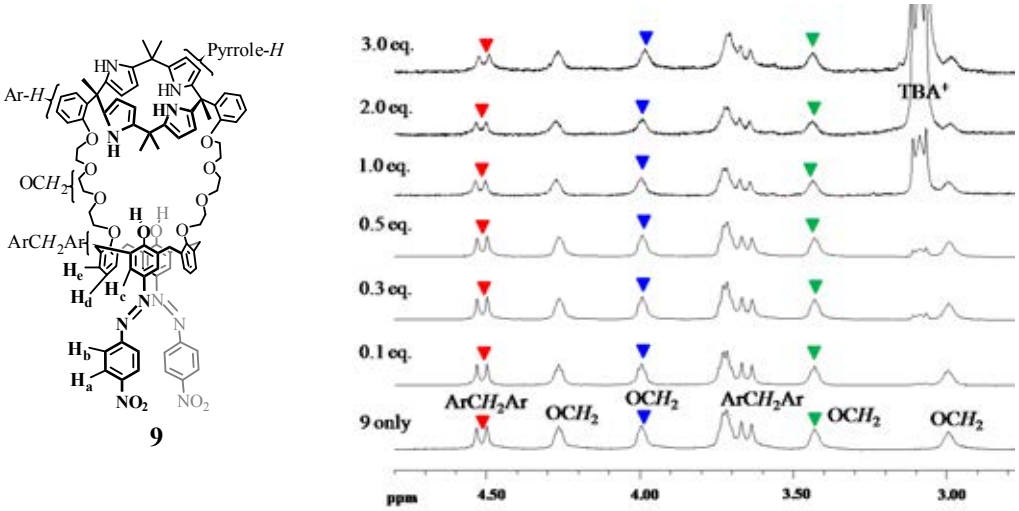

Figure 3.14 ^{1}H-NMR spectra (2-5 ppm) of ligand **9** (3.58 mM) in CD_3CN in the presence of different amounts of $TBA^{+}BzO^{-}$.

However, ^{1}H-NMR spectroscopy (Figure 3.13 and 3.14) shows a different complexation fashion of benzoate by ligand **9**. The phenolic protons of azocalix[4]arene

moiety at 8.80 ppm became broaden signal when only 0.1 equivalent of benzoate was added into solution of ligand **9** and disappeared after 0.2 equivalents was added without displacement of H_a and H_b protons. This implies that electron push was not occurred. Concerning calix[4]pyrrole unit, the N*H* protons of gradually shifted downfield from 8.16 ppm to 8.65 ppm while pyrrolic protons displaced upfield from 5.80 and 5.61 ppm to 5.75 and 5.57 ppm upon addition of benzoate salt solution until 3 equivalents. This suggests that ligand **9** bound benzoate ion by hydrogen bonding

3.3 Anion complexation studies of 1,3-di-*p*-nitrophenylazo-calix[4]-diacetophenone (7)

3.3.1 By using UV-vis spectrophotometry

1,3-Di-*p*-nitrophenylazo-calix[4]-diacetophenone (**7**), which lack of the calix[4]pyrrole unit was used to compare the anions binding properties with ligand **9.** The anion binding ability of azocalix[4]-diacetophenone **7** with F^-, Cl^-, Br^-, I^-, AcO^-, BzO^-, $H_2PO_4^-$, ClO_4^-, NO_3^- and PF_6^- (as a tetrabutylammonium salt) was carried out by using UV-vis spectrophotometry. 10 and 6 equivalents of tetrabutylammonium anion in acetonitrile solution were added into the 0.02 mM solution of ligand **7**. The anion binding via H-bonding and/or deprotonating can also be easily monitored by a wavelength and color changes.

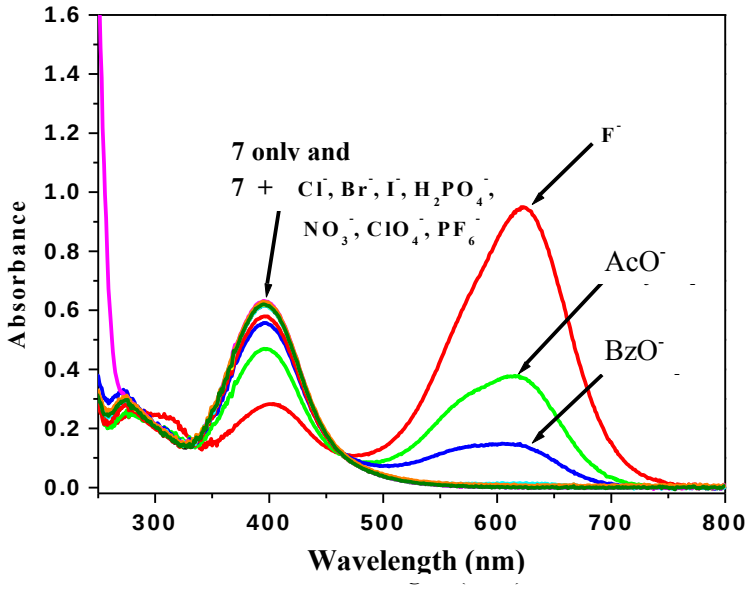

Figure 3.15 Wavelength changes of ligand **7** upon the addition of various anions. Condition: ligand **7** (0.02 mM)/CH_3CN; TBAX (10 equiv.)/CH_3CN.

7 F^- AcO^- BzO^- $H_2PO_4^-$ Cl^- Br^- I^- NO_3^- ClO_4^- PF_6^-

Figure 3.16 Color change of ligand **7** (0.02 mM) with 10 equiv of anions (from left to right ligand **7** only, ligand **7** + F^-, ligand **7** + AcO^-, ligand **7** + BzO^-, ligand **7** + $H_2PO_4^-$).

Addition 10 equivalents of 10 tetrabutylammonium salts into the solution of ligand **7** (0.02 mM), the bathochromic shifts occurred only for F^-, AcO^- and BzO^- (Figure 3.15). The light yellow color solution of ligand **7** changed to deep blue, deep blue and blue for F^-, AcO^- and BzO^-, respectively (Figure 3.16). In this case, the discrimination of F^-, AcO^- and BzO^- is quite hard due to the similarity of color changes.

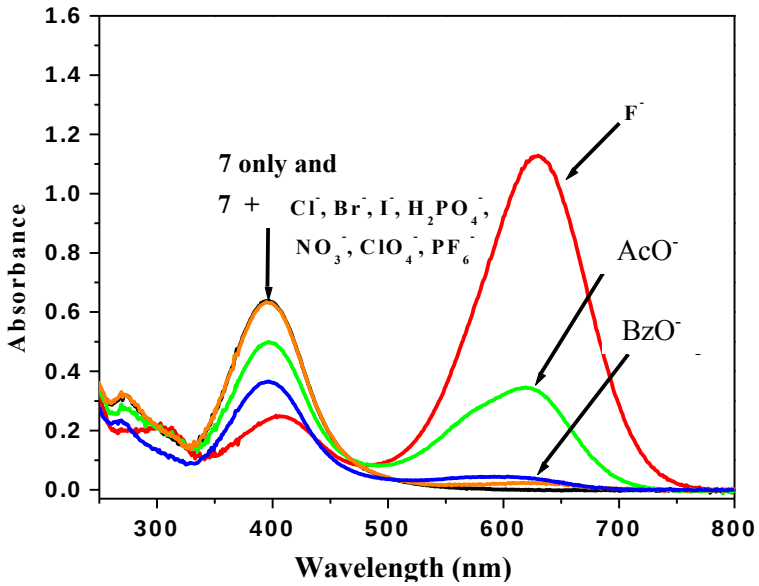

Figure 3.17 Wavelength changes of ligand **7** upon the addition of various anions. Condition: ligand **7** (0.02 mM)/CH_3CN; TBAX (6 equiv.)/CH_3CN.

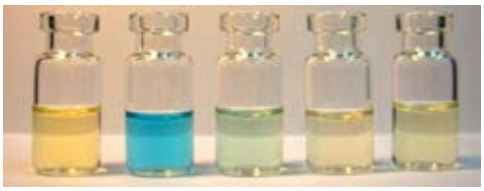

7 F^- AcO^- BzO^- $H_2PO_4^-$

Figure 3.18 Color change of ligand **7** (0.02 mM) with 6 equiv of anions (from left to right ligand **7** only, ligand **7** + F^-, ligand **7** + AcO^-, ligand **7** + BzO^-, ligand + $H_2PO_4^-$).

By the contrast of 6 equivalents addition of all tetrabutylammonium salts, the UV-vis spectra of ligand **7** (0.02 mM) showed only bathochromic shifts to F^-, AcO^- over other anions and showed only weak bathochromic shift to BzO^- (Figure 3.17) with different magnitude. It is known that ligand **7** has azonitrobenzene as a chromophore in the molecule as same as to ligand **9**. Upon anion complexation**,** the electronic excitation of an azonitrobenzene occurred by a charge transfer from the donor oxygen of the phenolic unit through the acceptor substitute (NO_2) of the chromophore [61,139]. Then, the excited state would be more strongly stabilized by the anion resulting in a bathochromic shift as well as color changes [61,140].

As expected from the UV-vis spectra, different color changes occurred after addition of F^- and AcO^- (6 equivalents) into the solution of ligand **7** (0.02 mM). The color changes from light yellow to blue, green and yellow for F^-, AcO^- and BzO^-, respectively (Figure 3.18). The anionic sensing is in accordance to a maximum absorption intensity of $F^- > AcO^- > BzO^-$.

3.3.2 By using ^{1}H-NMR spectroscopy

The anion binding ability of ligand **7** with a series of F^-, AcO^- and BzO^- was also studied to compare the anion binding abilities with ligand **7** by using ^{1}H-NMR spectroscopy. The different amount of F^-, AcO^- and BzO^- (tetrabutylammonium as a counter ions) was added into the CD_3CN solution of ligand **7** (0.65 mM), shaken at room temperature for 30 seconds, and then the ^{1}H-NMR spectrum were collected in each experiment.

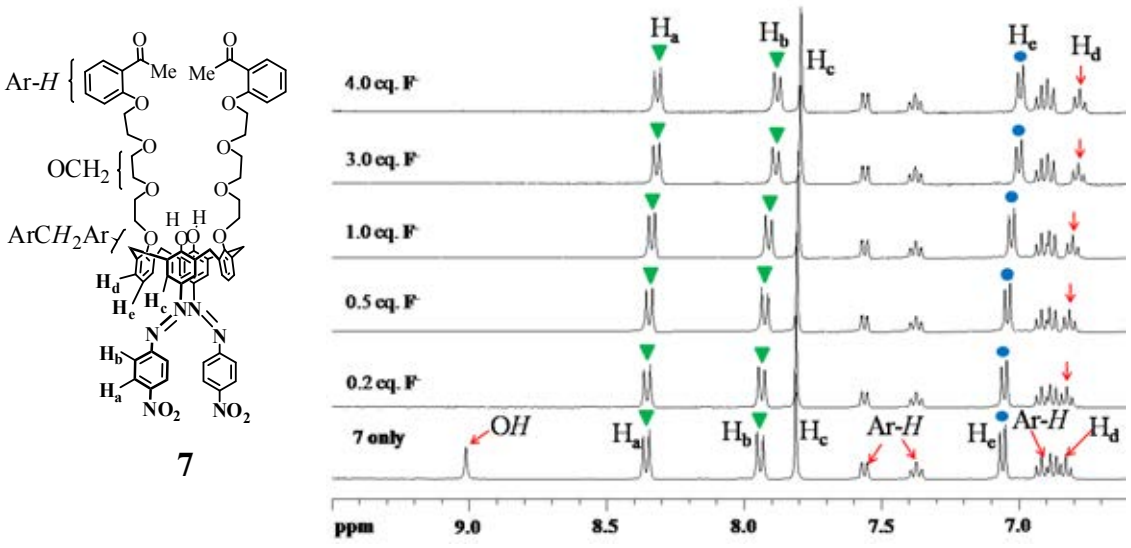

Figure 3.19 ^{1}H-NMR spectra (6-10 ppm) of ligand **7** (0.65 mM) in CD_3CN in the presence of different amounts of TBAF.

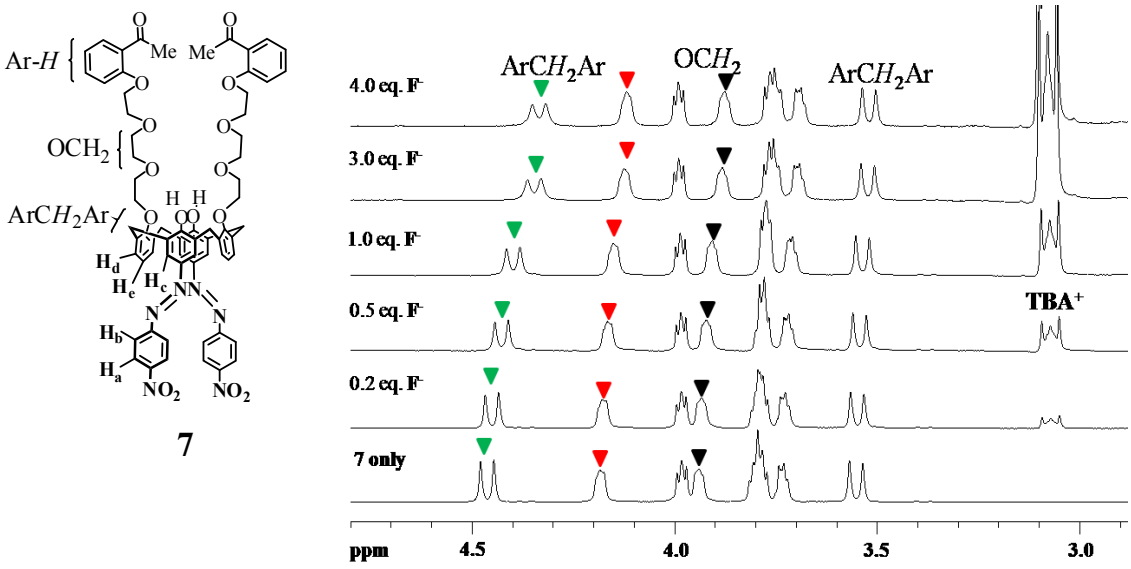

Figure 3.20 ^{1}H-NMR spectra (3-5 ppm) of ligand **7** (0.65 mM) in CD_3CN in the presence of different amounts of TBAF.

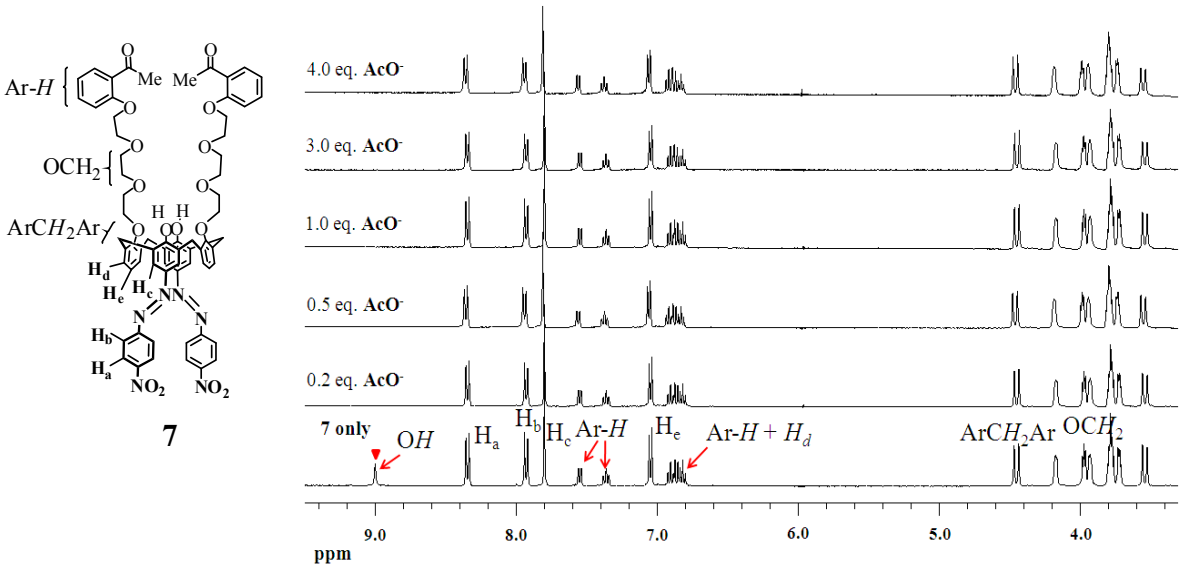

Figure 3.21 ^{1}H-NMR spectra of ligand **7** (0.65 mM) in CD_3CN in the presence of different amounts of $TBA^{+}AcO^{-}$.

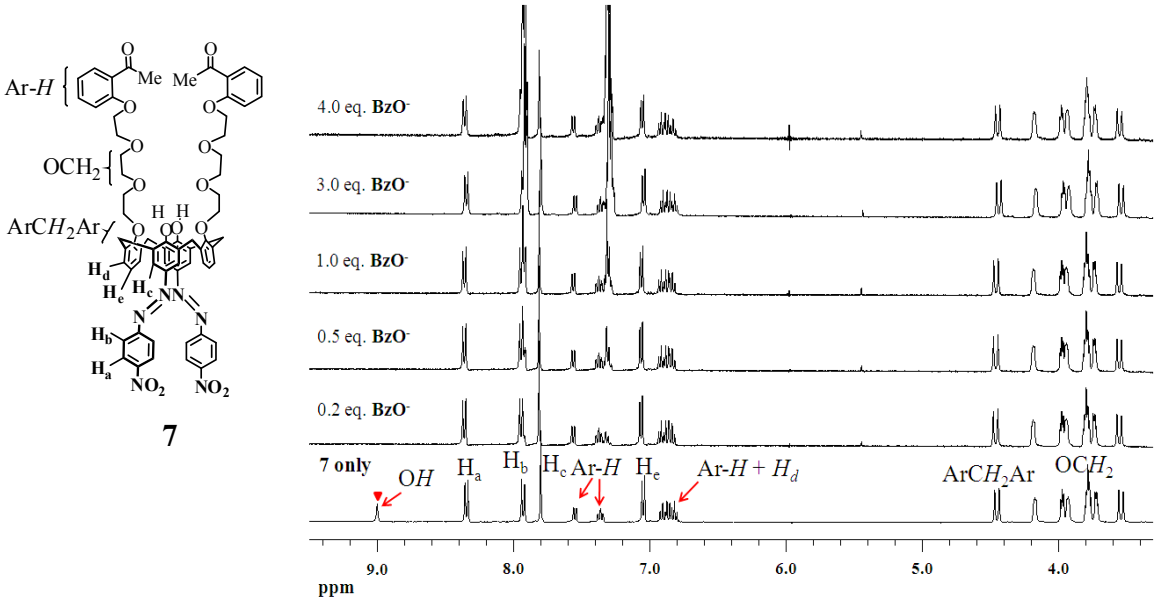

Figure 3.22 ^{1}H-NMR spectra of ligand **7** (0.65 mM) in CD_3CN in the presence of different amounts of $TBA^{+}BzO^{-}$.

According to the ^{1}H-NMR spectra of ligand **7** titrated with F^- (Figure 3.19 and 3.20), the signal of phenol protons also disappeared when added only 0.2 equivalents of F^- into the CD_3CN solution of ligand **7** along with the signal of H_a and H_b protons of azobenzene were shifted upfield. The signal of H_c, H_d and H_e protons of 1,3-alternate calix[4]arene platform were also shifted upfield. The results presented here indicate that the internal charge transfer occurred in the molecule which may the small spherical of F^- can be deprotonated to the phenol protons of ligand **7** along with azocalix[4]arene rearranged to accommodate a small F^- ion.

Contrasting to the ^{1}H-NMR spectra of ligand **7** titrated with AcO^- and BzO^- (Figure 3.21 and 3.22), only disappearance of phenolic protons at 8.90 ppm was observed. However, the signals of H_a, H_b and H_c protons did not shift significantly. It implies that the internal charge transfer did not occur for ligand **7** with AcO^- and BzO^- different to F^- and also ligand **9,** which has the internal charge transfer, occurred in the molecule.

From the results of binding studies of ligand **9** with anions compared with ligand **7**, the binding mode of azocalix[4]arene strapped calix[4]pyrrole **9** with anions can be proposed in Figure 3.23. It may be proposed that the anion could be deprotonated to the two hydroxyl protons of azophenol and encapsulated in side cavity by forming hydrogen bond with calix[4]pyrrole unit. In contrast to azocalix[4]diacetophenone **7** (Figure 3.24), the anion could be deprotonated to the two hydroxyl protons of azophenol but the internal charge transfer may not occurred.

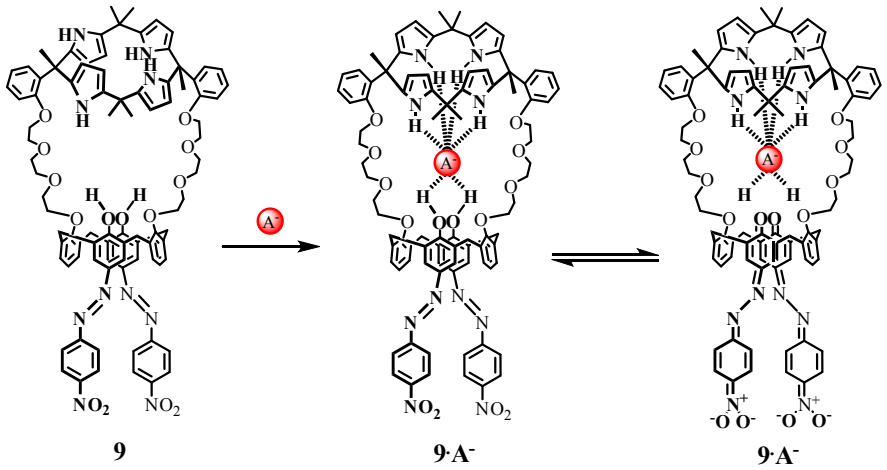

Figure 3.23 Proposed binding mode of ligand **9** + anion (1 : 1).

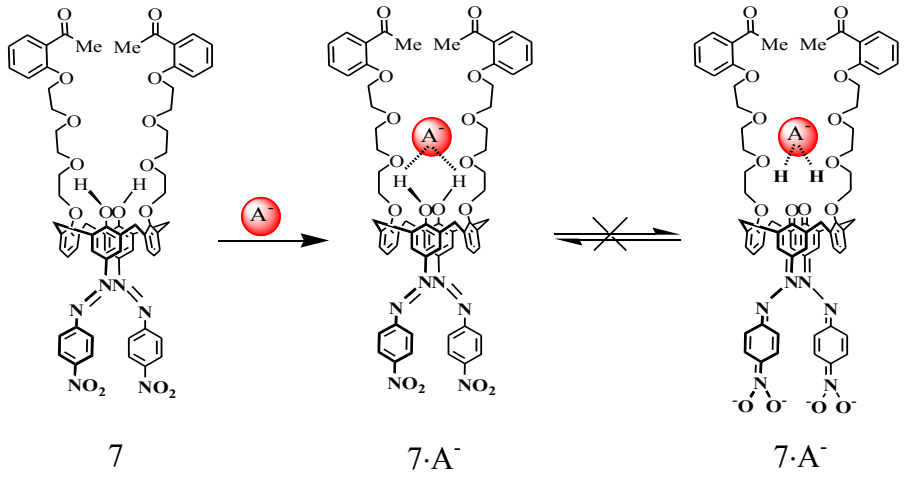

Figure 3.24 Proposed binding mode of ligand **7** + anion (1 : 1).

3.4 UV-vis titration of ligand 9 with F^-, AcO^-, BzO^- and $H_2PO_4^-$

The complexation abilities of ligand **9** with F^-, AcO^-, BzO^- and $H_2PO_4^-$ were investigated by using UV-vis spectrophotometric titration in CH_3CN at 25°C (see Figure 3.25, 3.26, 3.27 and 3.28 respectively). When necessary, Bu_4NPF_6 was employed to keep the ionic strength at 0.01 M. Typically, the solution of 6 equivalents anion was added directly and successively into the cuvette containing ligand **9** (0.02 mM) and the spectral variation was recorded after each addition. The final guest-to-host ratios were varied case by case to obtain the optimal condition for complexation. In all cases, bathochromic shifts were observed upon addition of $NBu4^+X^-$ into solutions of ligand **9**. The stoichiometries and stability constants of the complexes could be determined by the SIRKO program [134] and are summarized in Table 3.1. The changes in absorbance of CH_3CN solution between 300-400 nm were used for evaluating of complex formation constants and stoichiometries of ligand **9** with anions.

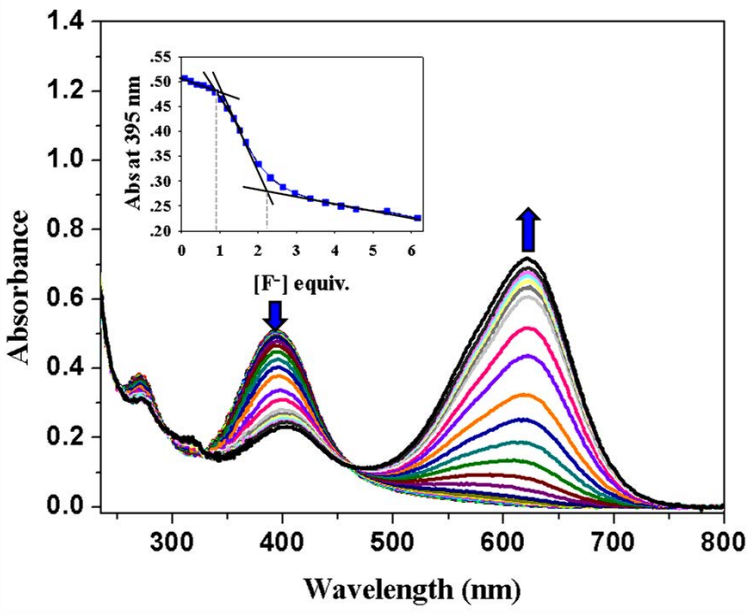

Figure 3.25 UV-vis titration of ligand **9** (0.02 mM) in CH_3CN upon addition of F^- (0-6 equiv). (Inset) Absorbance at 395 nm as a function of F^- concentration, indicating in 1:1 and 1:2 ratios for ligand **9**: F^-.

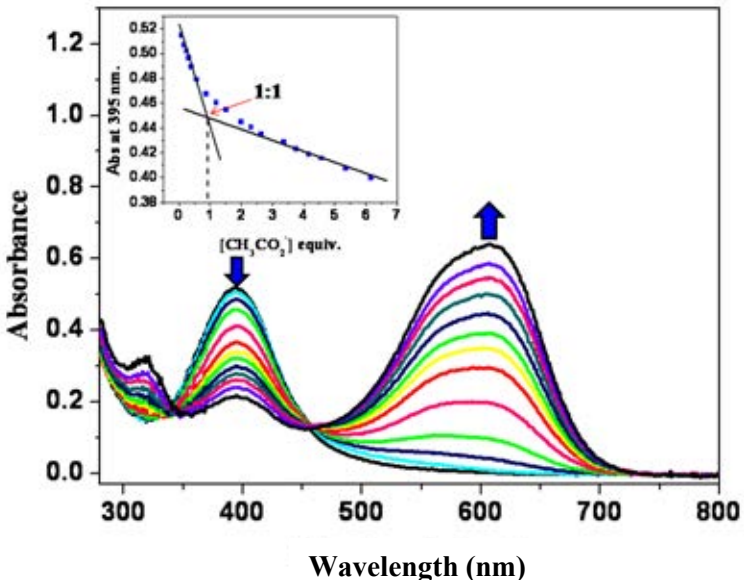

Figure 3.26 UV-vis titration of ligand **9** (0.02 mM) in CH_3CN upon addition of AcO^- (0-6 equiv). (Inset) Absorbance at 395 nm as a function of AcO^- concentration, indicating in 1:1 ratios for ligand **9**:AcO^-.

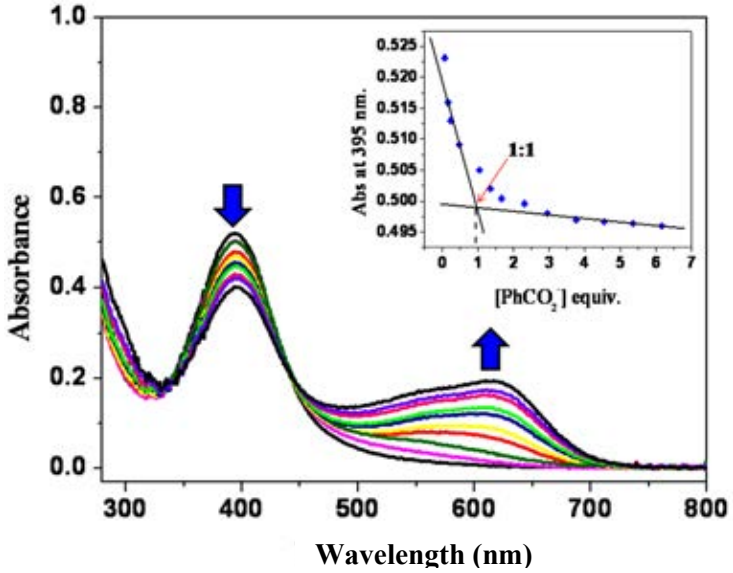

Figure 3.27 UV-vis titration of ligand **9** (0.02 mM) in CH_3CN upon addition of BzO^- (0-6 equiv). (Inset) Absorbance at 395 nm as a function of BzO^- concentration, indicating in 1:1 ratios for ligand **9**:BzO^-.

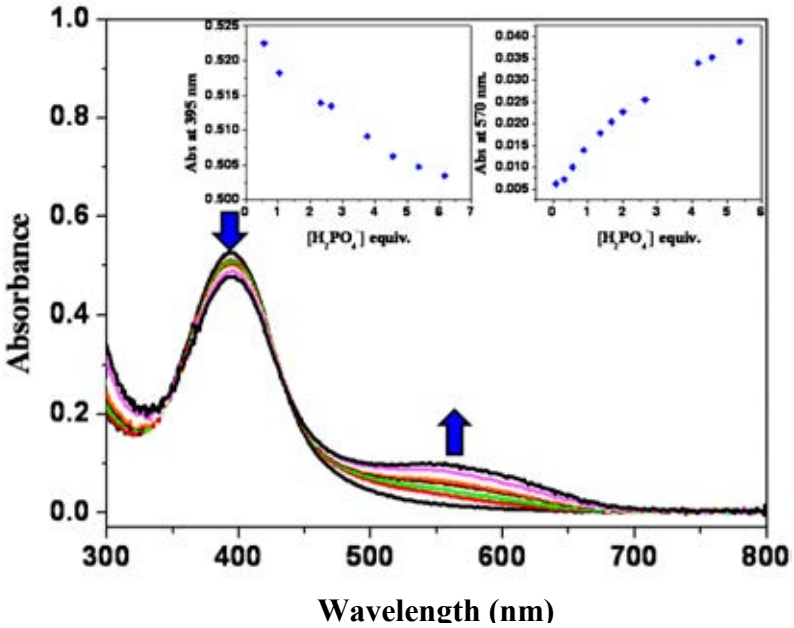

Figure 3.28 UV-vis titration of ligand **9** (0.02 mM) in CH_3CN upon addition of $H_2PO_4^-$ (0-6 equiv). (Inset) Absorbance at 396 nm versus the $H_2PO_4^-$ concentration.

Table 3.1 Stability constants (log β) of complexes of ligand **9** with anions in CH_3CN by the UV-vis titration method (T = 25 °C, I = 0.01 M Bu_4NPF_6).

anions	log β [a]
F^-	3.07 (0.08)[b], 11.09 (0.07)[c]
$H_2PO_4^-$	2.55 (0.02)[b]
AcO^-	4.81 (0.06)[b]
BzO^-	5.64 (0.09)[b]

[a]Mean values of $n \geq 2$ (for anions) of independent determination with standard deviation σ_{n-1} [143,144] on the mean in parentheses, [b]1:1 complex (AL). [c]2:1 complex (A_2L).

For F^-, two binding constants (log β = 3.07 and 11.09) were found due to two species of complexes 1:1 and 2:1 (anion/ligand)(see inset in Figure 3.25), respectively. In case of AcO^-, BzO^- and $H_2PO_4^-$, only 1:1 complexes were found with log β = 4.81,

5.64 and 2.55 , respectively, which could be rationalized on the basis of guest basicity [Table 3.2]. In case of F^-, AcO^-, BzO^- and $H_2PO_4^-$, which almost have a similar basicity but have a spherical for F^- trigonal planar for AcO^- and BzO^- and tetrahedral for $H_2PO_4^-$ can do the same binding mode to ligand **9**. From the titration method, it may be concluded that ligand **9** prefer to bind BzO^- in 1:1 ratio over other anions studied. The selectivity can be explained by the geometry of BzO^- and the π-π stacking interaction between phenyl ring of BzO^- and aromatic ring current of calix[4]pyrrole unite .

Table 3.2 Geometry and basicity of various anions. [145]

Anions	Geometry	pK_a (298 K)
F^-	Spherical	3.3
Cl^-	Spherical	-10.0
Br^-	Spherical	-9.0
I^-	Spherical	-8.0
AcO^-	Trigonal planar	4.8
BzO^-	Trigonal planar	4.2
$H_2PO_4^-$	Tetrahedral	2.1, 6.2, 12.4
ClO_4^-	Tetrahedral	-
NO_3^-	Trigonal planar	-1.4
PF_6^-	Octahedral	-

3.5 Cation complexation studies of 1,3-di-*p*-nitrophenylazo-calix[4]arene-calix[4]pyrrole (9)

3.5.1 By using UV-vis spectrophotometry

The ability of azocalix[4]arene-strapped calix[4]pyrrole **9** to act as cation receptor was also studied. It is known that azocalix[4]crown ether can be used for a metal chelating unit, [146-149] so excess (300 equiv.) nitrate salts of Li^+, Na^+, K^+, Mg^{2+}, Ca^{2+}, Sr^{2+}, Ba^{2+}, Zn^{2+}, Pb^{2+}, Cr^{3+} and Co^{2+} were employed to evaluate the metal-ion binding properties of **9**. Furthermore, upper-rim arylazo functionalized calix[4]arenes, which play not only as a chromophore but also as a metal ion binding site [150-152]. The upper-rim arylazo calix[4]arene toward metal ions enhances the tautomerization of the azophenols to quinine-hydrazones [153] then the excess (300 equiv.) nitrate salts of Ag^+, Hg^{2+}, Ni^{2+}, Cd^{2+} and Cu^{2+} were also investigated. Ligand concentration was fixed at 0.02 mM in CH_3CN.

(a) **(b)**

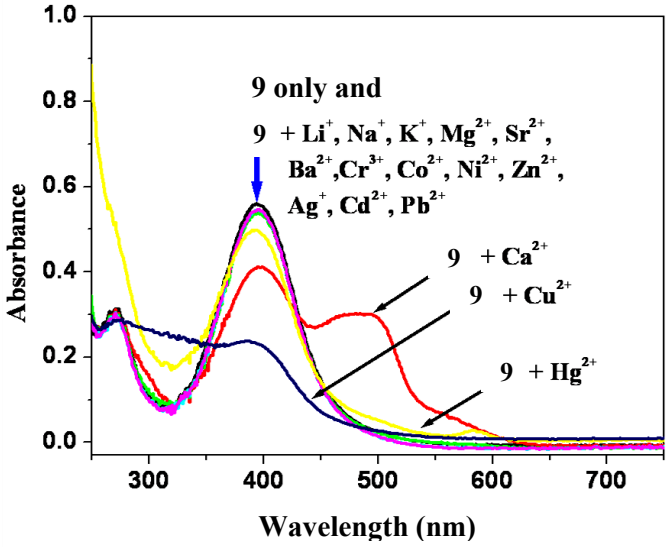

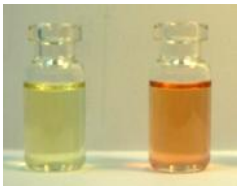

9 **9**·Ca^{2+}

Figure 3.29 UV-vis spectra of ligand **9** (0.02 mM) before and after adding 300 equivalents of various metals nitrate in CH_3CN (a) and color changes upon addition of 300 equivalents of $Ca(NO_3)_2$ into the solution of ligand **9** (b).

From the UV-vis spectra, ligand **9** also exhibited absorption bands at 395 nm in CH_3CN. The addition of 300 equivalents of Ca^{2+} induced a large bathochromic shift of the azocalix[4]arene-strapped calix[4]pyrrole **9** from λ_{max} = 395 nm to 491 nm (Figure 3.29(a)). The light yellow color solution of ligand **9** turned to an orange color upon complexation with Ca^{2+} (Figure 3.29(b)). In addition, UV-vis spectra of ligand **9** showed only weak bathochromic shift with Hg^{2+} and hypsochromic shift with Cu^{2+}. However, the hypsochromic shift of ligand **9** with Cu^{2+} seemed to be the absorption spectrum of Cu^{2+} [154].

3.5.2 By using ^{1}H-NMR spectroscopy

The complexation behavior of azocalix[4]arene-strapped calix[4]pyrrole **9** with Ca^{2+} was also investigated using ^{1}H-NMR spectroscopy as shown in Figure 3.30 and 3.31. Ligand **9** (1.3 mM) with 2 and 10 equivalents of $Ca(NO_3)_2$ showed a slow exchange on the ^{1}H-NMR time scale separate signals for each conformer.

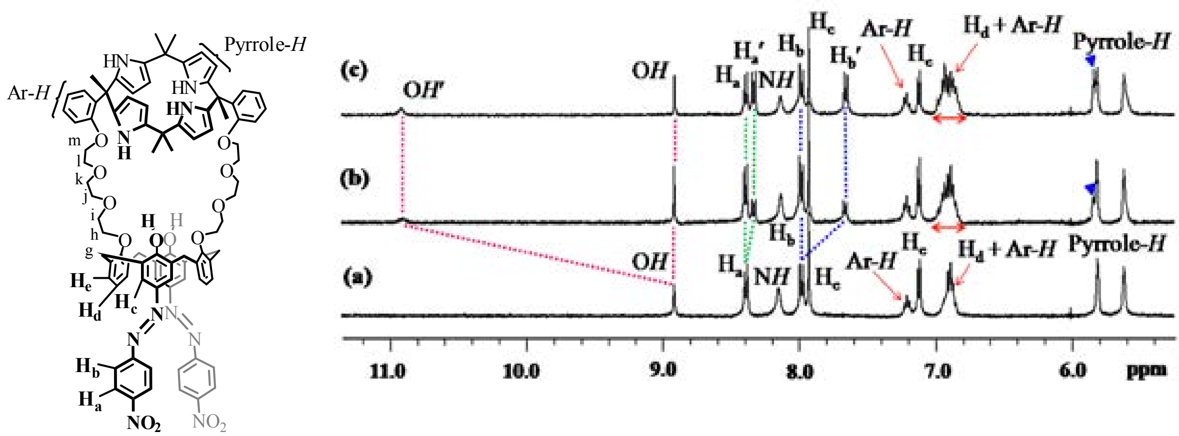

9

Figure 3.30 ^{1}H-NMR spectra (5-12 ppm) of ligand **9** (1.3 mM) in CD_3CN (a) in the presence of 2 equivalents (b) and10 equivalents (c) of $Ca(NO_3)_2$ in which (′) denotes of complexes form.

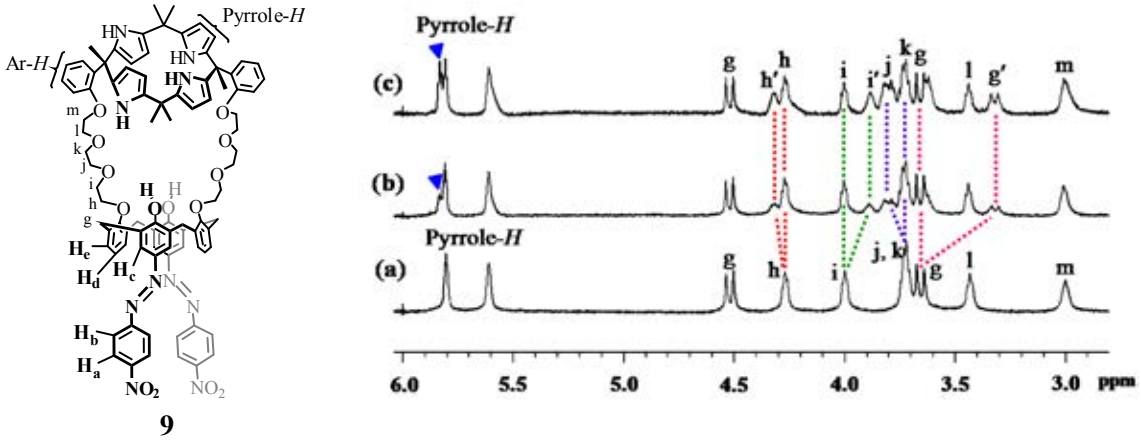

Figure 3.31 ^{1}H-NMR spectra (2-6 ppm) of ligand **9** (1.3 mM) in CD_3CN (a) in the presence of 2 equivalents (b) and 10 equivalents (c) of $Ca(NO_3)_2$ in which (′) denotes of complexes form.

In the presence of 2 and 10 equivalents of Ca^{2+}, O*H*, H_a, H_b and H_g protons of azocalix[4]arene unit showed two sets of the free and complex signals. Furthermore, the spectral changes were also observed for *β*-pyrrolic and aromatic protons. The signal of *β*-pyrrolic protons split to a new signal and the signal of aromatic protons were broader. These imply that both calix[4]arene and calix[4]pyrrole units rearranged themselves to accommodate Ca^{2+} . In addition, H_g, H_h and H_i protons also split into two sets of signals. H_g was split upfield by 0.34 ppm whereas H_h and H_i split and shifted upfield by 0.05 and 0.13 ppm, respectively. These results suggest that two species, free ligand **9** and Ca^{2+} complex, existed in solution and metal oscillation did not occur or cation-binding/decomplexation equilibrium was more rapid than the ^{1}H-NMR timescale and suggested that Ca^{2+} was bound via phenolic and glycolic oxygen atoms.

3.5.3 Time evolution of 1, 3-di-*p*-nitrophenylazo-calix[4]arene-calix[4]pyrrole (9) in the presence of 300 equivalents of $Ca(NO_3)_2$ by using UV-vis spectrophotometry

In addition, the investigation for the time evolution for the responses of ligand **9** (0.02 mM) in the presence of 300 equivalents of $Ca(NO_3)_2$ in CH_3CN was proved by UV-vis spectrophotometry (Figure 3.32). The UV-vis spectra shown the recognition interaction was completed after addition of the $Ca(NO_3)_2$ after 1 hour.

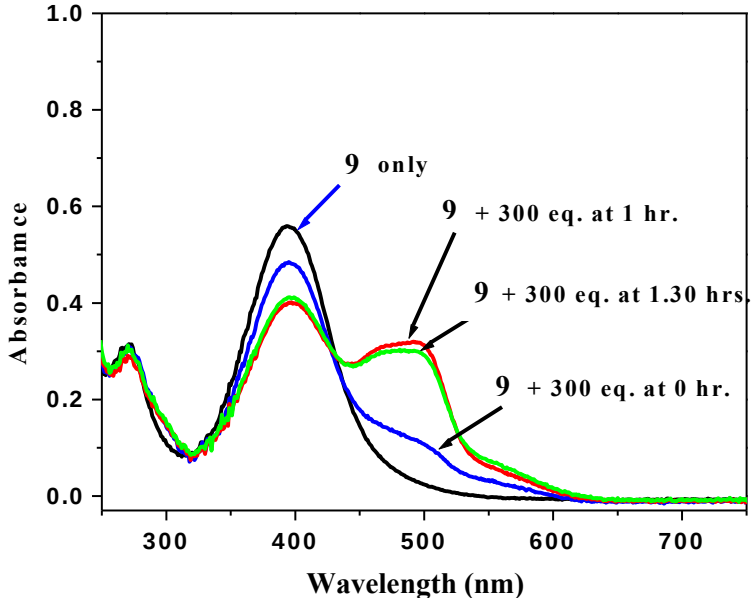

Figure 3.32 UV-vis spectra changes for time evolution of ligand **9** (0.02 mM) in CH_3CN in the presence of 300 equivalents of $Ca(NO_3)_2$.

3.5.4 UV-vis titration of ligand 9 with Ca^{2+}

To study the stoichiometry and association constants between ligand **9** and Ca^{2+}, the UV-vis titration experiment was carried out using 0.02 mM of ligand **9** in CH_3CN and 2 equivalents of $Ca(NO_3)_2$ (Figure3.33). Upon titration with 2 equivalents of $Ca(NO_3)_2$, the CH_3CN solution of chromogenic sensor **9** showed small shoulder band around 450 to 590 nm and exhibited an isosbestic point at 438 nm to confirmed the two species of free and complexes ligand **9** occurred in the solution. Moreover the absorption band around 450 to 590 nm of ligand **9** increased upon gradual addition of Ca^{2+}. The stoichiometry between ligand **9** and Ca^{2+} was determined by mole ratio plot (inset in Figure 3.33) and SIRKO program, which showed a 1:1 stoichiometry.

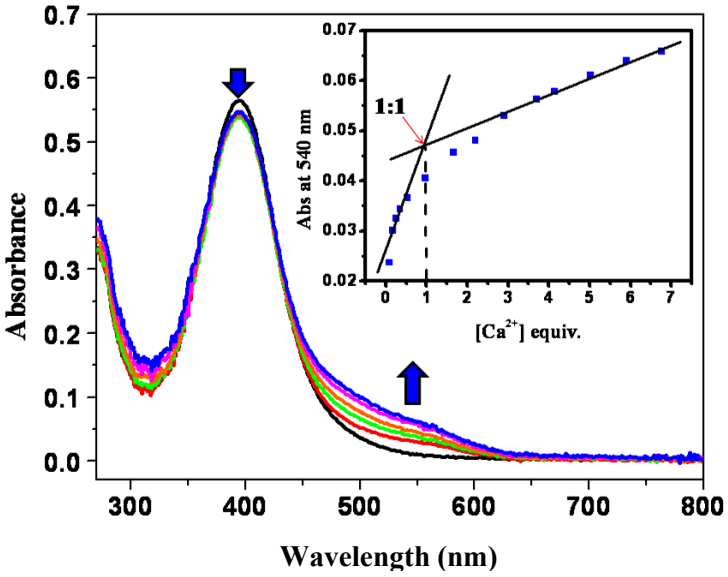

Figure 3.33 UV-vis spectra of ligand **9** (0.02 mM) upon titration with 2 equivalents of $Ca(NO_3)_2$ in CH_3CN.

According to the extent of the observed absorption spectra changes, the association constants of ligand **9** with Ca^{2+} was calculated to be log β = 4.23 M^{-1}. The light yellow color of ligand **9** solution turned to an orange upon complexation with Ca^{2+}.

3.5.5 Ion-pair complexation studies of 1,3-di-*p*-nitrophenylazo-calix[4]arene-calix[4]pyrrole (9) by using ^{1}H-NMR spectroscopy

The ion-pair ligand **9** was designed to bring together both an anion-binding moiety and cation-recognizing subunit in such a way that this molecular platform can serve as a selective ion-pair sensor. Calix[4]pyrrole and azocalix[4]crownether were chosen as the anion- and cation-binding species, respectively. Previous studies have shown that this receptor system could be used individually to affect the binding of fluoride ion and calcium ion, respectively. Accordingly, CaF_2 was selected as the target salt for possible ion-pair complexation. The excess amount of CaF_2 was added into the solution of ligand **9** (3.58 mM), and then keep it at room temperature for 24 hours. The complexation between ligand **9** and CaF_2 was then studied by ^{1}H-NMR spectrum.

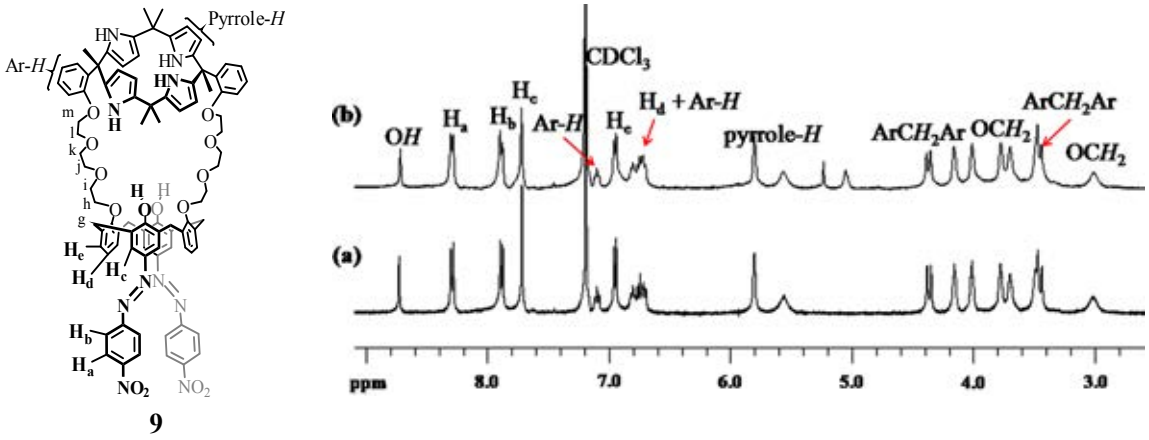

9

Figure 3.34 ^{1}H-NMR spectra of ligand **9** (3.58 mM) in $CDCl_3$ (a) and in the presence of excess CaF_2.

In the presence of excess CaF_2, ^{1}H-NMR spectra showed any change [Figure 3.34]. May the structure of ligand **9** be not suitable to accommodate the ion-pair CaF_2 salt bound into the cavity between calix[4]pyrrole and azocalix[4]crown ether unit.

3.6 Anions binding properties of 1,3-di-*p*-nitrophenylazo-calix[4]arene-calix[4]pyrrole (9) in the presence of calcium cation

3.6.1 By using UV-vis spectrophotometry

The complexation of cation by azophenol crownether is favored under basic condition because of stronger interactions between phenolate anion formed upon deprotonation by a basic guest and cation [155,156]. The azophenolic moieties with ionizable O*H* groups directed inside the cavity require less basic conditions or basic anions to deprotonate and cation may facilitate this process.

Therefore, we investigated the anion binding properties of azocalix[4]arene strapped calix[4]pyrrole **9** with the F^-, AcO^- , BzO^- and $H_2PO_4^-$ in the presence of Ca^{2+}. Two equivalents of $Ca(NO_3)_2$ were added to the sample of ligand **9** (0.02 mM) in CH_3CN, giving 100% saturation of the receptor, and minimizing the amount of free Ca^{2+} in the solution then 6 equivalents of each anions were added into the complex **9**·Ca^{2+} solution. The influence of anion interactions to complex **9**·Ca^{2+} on spectroscopic changes was studied using UV-vis spectrophotometry and ^{1}H-NMR spectroscopy as well as their color changes.

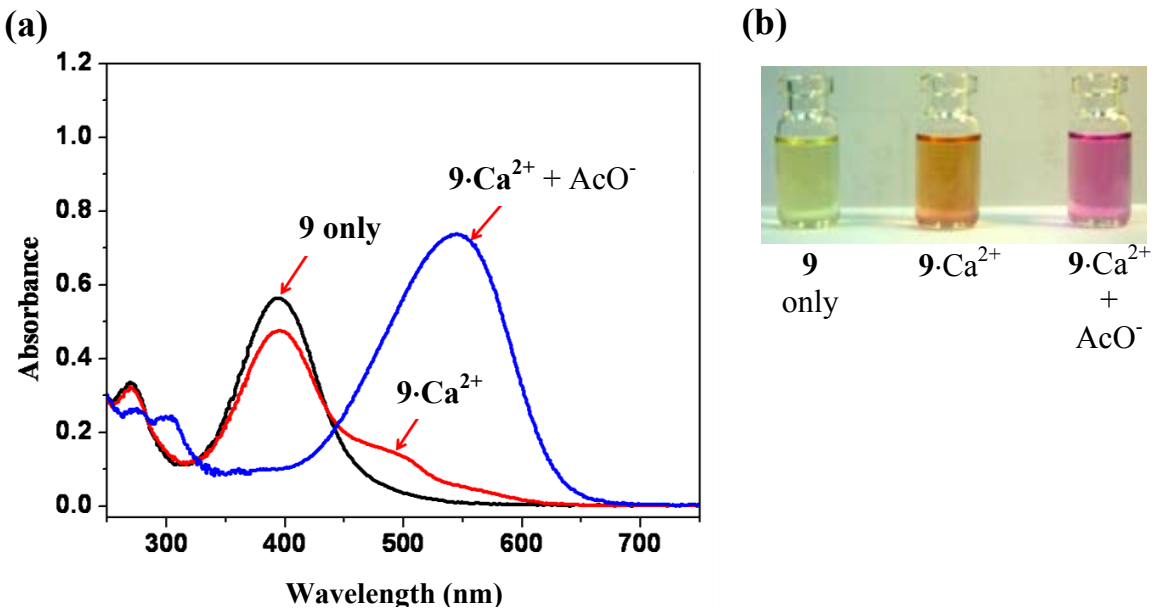

Figure 3.35 Spectral changes in the UV-vis absorption of complex **9**·Ca^{2+} (0.02 mM) upon addition 6 equivalents of AcO^- in CH_3CN.

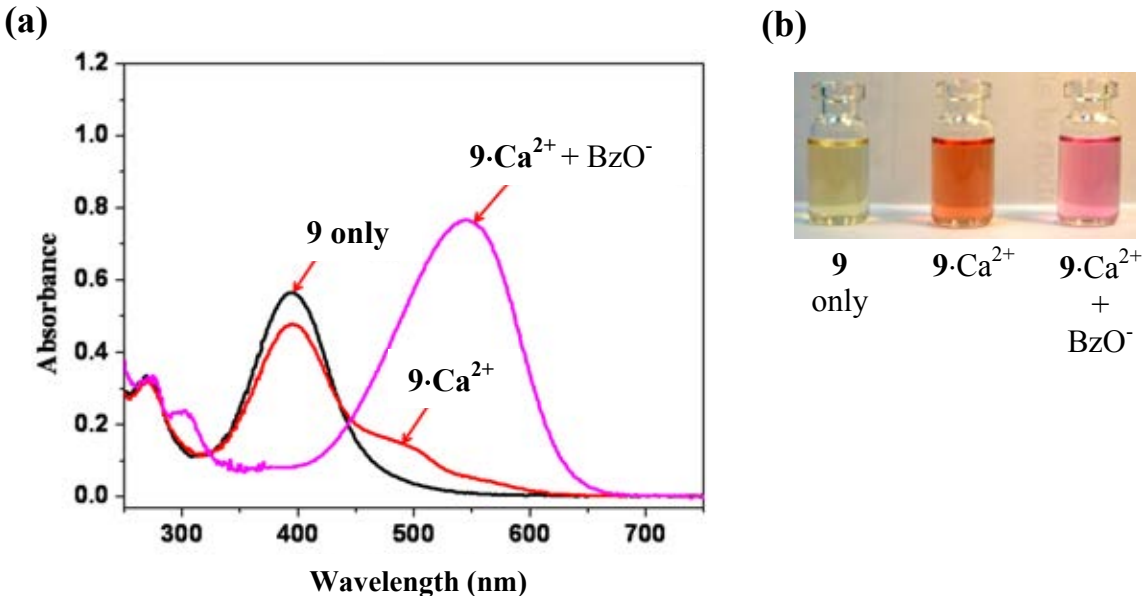

Figure 3.36 Spectral changes in the UV-vis absorption of complex **9**·Ca^{2+} (0.02 mM) upon addition 6 equivalents of BzO^- in CH_3CN.

Upon interacting complex **9**·Ca^{2+} with AcO^- and BzO^-, complex **9**·Ca^{2+} in CH_3CN solution gave a remarkable bathochromic shift as show in Figure 3.35(a) and 3.36(a). The absorption maximum at 395 nm gradually decreased and a new absorption band at approximately 545 nm gradually increased from the shoulder band around 450 to 590 nm which ascribed to a charge density shift in the direction of the acceptor substituent (NO_2) of the chromophore. In other words, increasing in the dipole moment took place leading to bathochromic band shift. [157,158] In addition, the orange color solution of complex **9**·Ca^{2+} switched to the pink color solution of the complex **9**·Ca^{2+} + AcO^- and **9**·Ca^{2+}+ AcO^- (Figure 3.35(b) and 3.36(b)).

3.6.2 By using ^{1}H-NMR spectroscopy

^{1}H-NMR spectroscopy was also used to determine the anion binding properties of complex **9**·Ca^{2+}. As seen in figure 3.37 and 3.38, after addition of 6 equivalents of TBA^+AcO^- into the solution of complex **9**·Ca^{2+}, the disappearance of N*H* signal and significant upfield-shift of pyrrolic protons of calix[4]pyrrole binding site suggested that AcO^- ion was encapsulated by calix[4]pyrrole unit. The signals of H_a, H_b and H_c protons shifted upfield significantly which suggested that a basic AcO^- ion may interact to protic phenol proton (O*H*) as well as methylene-bridge protons (H_g) shifted upfield significantly which indicates that the geometry of calix[4]arene was rearranged. The more AB system signal of methylene-bridge protons separated in ^{1}H-NMR spectrum of **9**·Ca^{2+}·AcO^- which implied that the more phenolic units of calix[4]arene pinched [153]. Moreover, the upfield shift of pyrrolic (pyrrole-H, $\Delta\delta$ = 0.06 ppm) and glycolic (H_l, $\Delta\delta$ = 0.10 ppm) protons of complex **9**·Ca^{2+} confirmed that AcO^- ion locate nearby calix[4]pyrrole unit. In addition, signals of H_j, H_k and H_i protons shifted downfield by 0.02, 0.02 and 0.12 ppm, respectively which suggested that Ca^{2+} ion was more strongly bound by glycolic oxygen atoms. The mentioned proton signal changes of complex **9**·Ca^{2+} suggested that AcO^- was bound inside the crown ether loop of complex **9**·Ca^{2+} near by Ca^{2+} ion which may interact each other. Furthermore, compared the binding mode between **9**·Ca^{2+}·AcO^- and **9**·AcO^- by ^{1}H-NMR spectrum in Figure 3.37(c) and 3.38(c) of **9**·AcO^-. The spectrum has shown the signal of N*H*, pyrrole-*H*, methylene-

bridge protons (H_g) and glycolic protons completely different to **9**·Ca^{2+}·AcO^-. These results suggest that the ion pair complex of **9**·Ca^{2+}·AcO^- was occurred in the solution of acetonitrile.

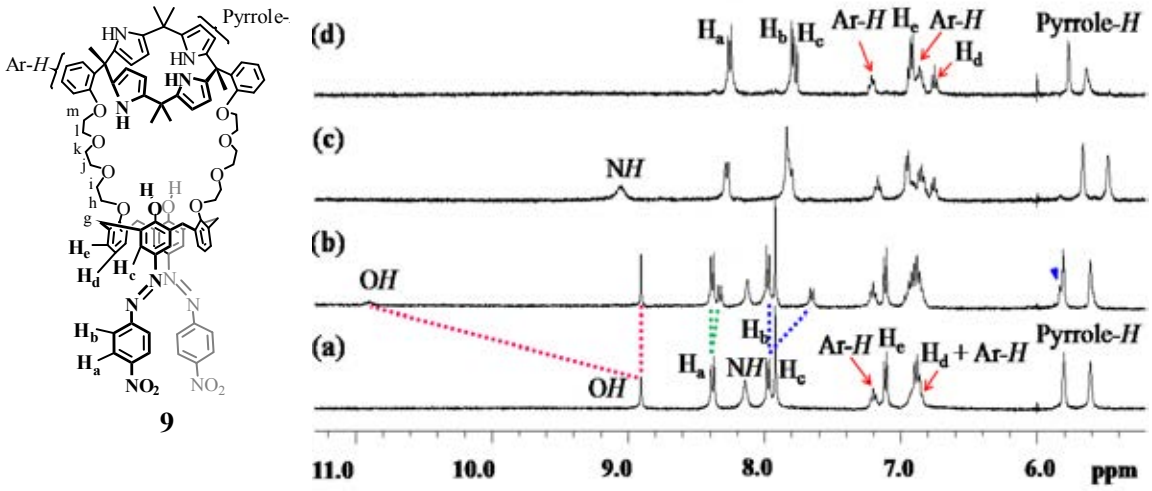

Figure 3.37 ^{1}H-NMR spectra (5-11 ppm) of ligand **9** (1.3 mM) in CD_3CN (a) in the presence of 2.0 equiv. of $Ca(NO_3)_2$ (b) in the presence of 3.0 equiv. of TBA^+AcO^- (c) and ^{1}H-NMR spectra of complex **9**·Ca^{2+} (1.3 mM) in CD_3CN in the presence of 6 equiv of TBA^+AcO^- (d).

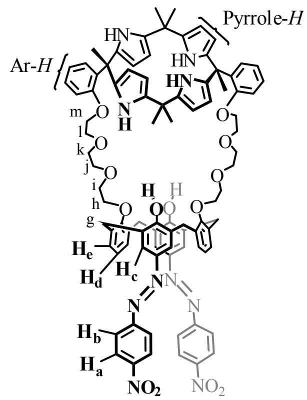

9

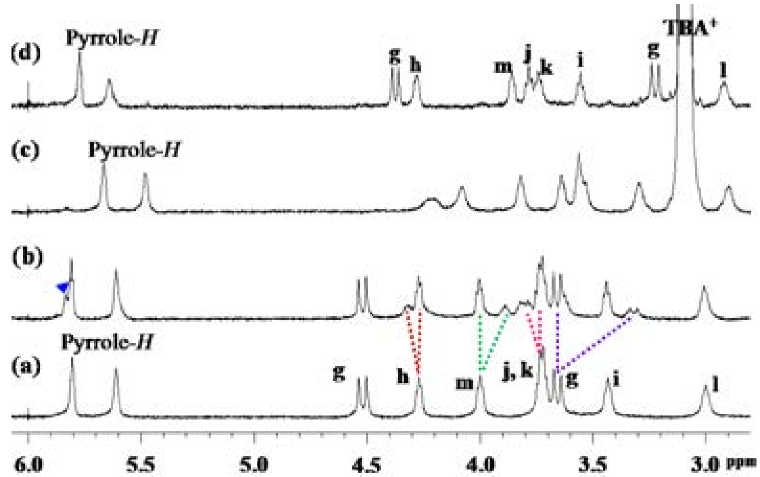

Figure 3.38 ^{1}H-NMR spectra (2.5-6 ppm) of ligand **9** (1.3 mM) in CD_3CN (a) in the presence of 2.0 equiv. of $Ca(NO_3)_2$ (b) in the presence of 3.0 equiv. of $TBA^{+}AcO^{-}$ (c) and ^{1}H-NMR spectra of complex **9**·Ca^{2+} (1.3mM) in CD_3CN in the presence of 6 equiv. of $TBA^{+}AcO^{-}$ (d).

3.6.3 By using UV-vis titration

The stoichiometries and association constants between ligand **9**·Ca^{2+} with AcO^{-} and BzO^{-}, the UV-vis titration experiments were carried out using 0.02 mM of complex **9**·Ca^{2+} with 6 equivalents of $TBA^{+}AcO^{-}$ and $TBA^{+}BzO^{-}$ in CH_3CN solutions. Figure 3.39 shows spectral change of titration of complex **9**·Ca^{2+} with AcO^{-} which demonstrates a decrease of λ_{max} at 397 nm and an appearance of new λ_{max} at 550 nm leading to an isosbestic point at 448 nm. The plot of absorbance of these two peaks in the function of equivalent AcO^{-} added (see inset in Figure 3.39) gives an intersection at 0.5 equivalent of AcO^{-} added which implies that the stoichiometry between complex **9**·Ca^{2+} and AcO^{-} is 1:1.

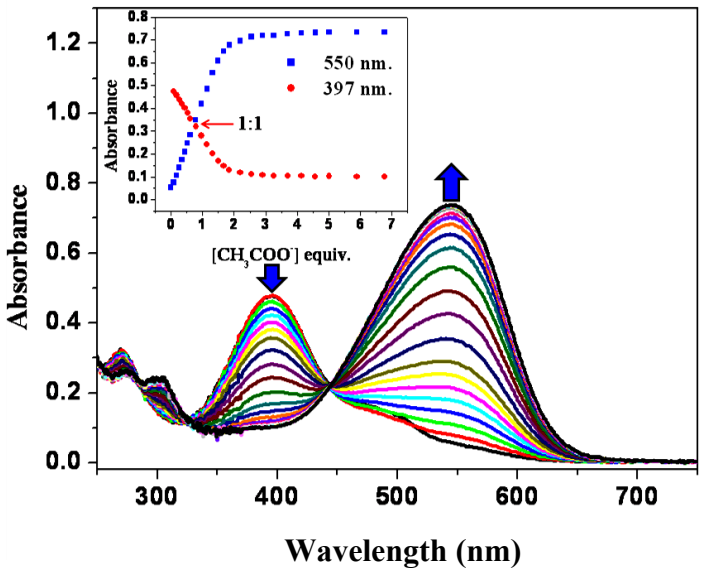

Figure 3.39 UV-vis spectra of complex **9**·Ca^{2+} (0.02 mM) upon titration with 6 equiv. of AcO^- in CH_3CN.

Similarly, in the case of BzO^-, Figure 3.40 and the inset included also display an isosbestic point at 448 nm and a stoichiometry of 1:1 (complex **9**·Ca^{2+}:BzO^-).

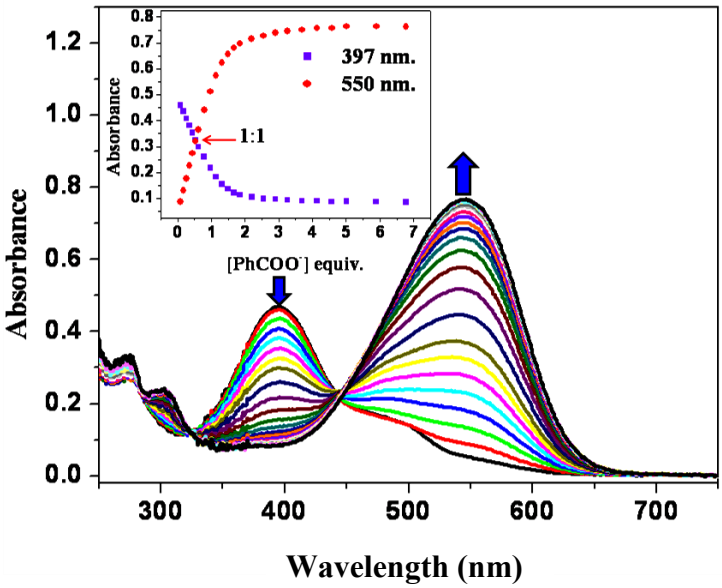

Figure 3.40 UV-vis spectra of complex **9**·Ca^{2+} (0.02 mM) upon titration with 6 equiv. of BzO^- in CH_3CN.

The association constants of complex **9**·Ca^{2+} with anions using the titration method were obtained and summarized in Table 3.4. By comparison, in the case of BzO^- complexation, the stability constants of 1:1 complex of complex **9**·Ca^{2+} is less than that of ligand **9**, 5.52 and 5.64, respectively, which implies that Ca^{2+} gives a negative allosteric effect [159-162]. By contrast, in the case of AcO^-, the higher stability constants of complex **9**·Ca^{2+} compared to that of ligand **9** suggests a positive allosteric effect [159-162].

Table 3.3 Stability constants (log β) 1:1 of ligand **9** with Ca^{2+} and complex **9**·Ca^{2+} with anions in CH_3CN by the UV-vis titration method (T = 25 °C, I = 0.01 M Bu_4NPF_6).

anions	**9** ; log β [a]	**9**·Ca^{2+} ; log β [a]
$CH_3CO_2^-$	4.81 (0.06)[b]	5.01 (0.01)
$PhCO_2^-$	5.64 (0.09)[b]	5.52 (0.01)

[a]Mean values of $n \geq 2$ (for anions) of independent determination with standard deviation σ_{n-1} [143,144] on the mean in parentheses, [b]1:1 complex.

3.6.4 Anion binding properties of 1,3-di-*p*-nitrophenylazo-calix[4]arene-calix[4]pyrrole (9) with the F^- and $H_2PO_4^-$ in the presence of calcium cation

The influence of F^- and $H_2PO_4^-$ to complex **9**·Ca^{2+} on spectroscopic changes was studied using UV-vis spectrophotometry as well as their color changes. Interestingly, upon adding 6 equivalents of F^- or $H_2PO_4^-$ to the solution of complex **9**·Ca^{2+}, the absorption spectra of ligand **9** reappeared (Figure3.41 and 3.42). In addition, the orange color solution of complex **9**·Ca^{2+} also returned to the original ligand **9**.

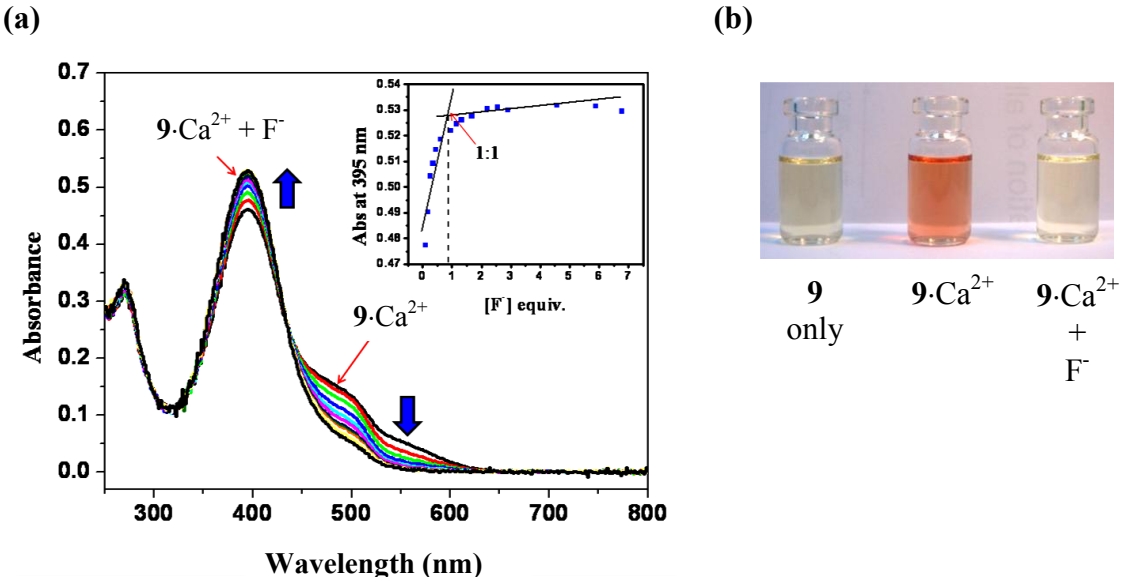

Figure 3.41 (a) UV-vis spectra of complex **9**·Ca^{2+} (0.02 mM) upon titration with 6 equiv. of F^- in CH_3CN and (b) color change of solution of complex **9**·Ca^{2+} added with 6 equiv. of F^-.

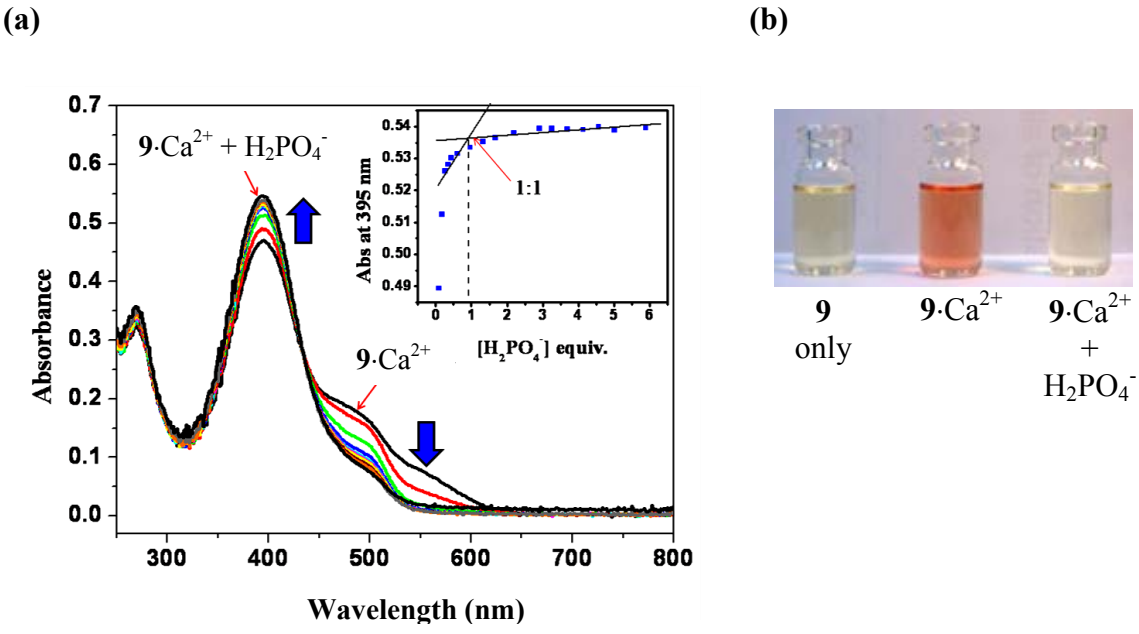

Figure 3.42 (a) UV-vis spectra of complex **9**·Ca^{2+} (0.02 mM) upon titration with 6 equiv. of $H_2PO_4^-$ in CH_3CN and (b) color change of solution of complex **9**·Ca^{2+} added with 6 equiv. of $H_2PO_4^-$.

In the reverse direction, 6 equivalents of TBAF were added to the sample of ligand **9** in CH_3CN first and 2 equivalents of $Ca(NO_3)_2$ followed. The UV-vis spectrum of **9**·F^- complex returned to the original spectrum of ligand **9** and the blue solution of the **9**·F^- complex also returned to the original yellow color of ligand **9** solutions (Figure 3.43).

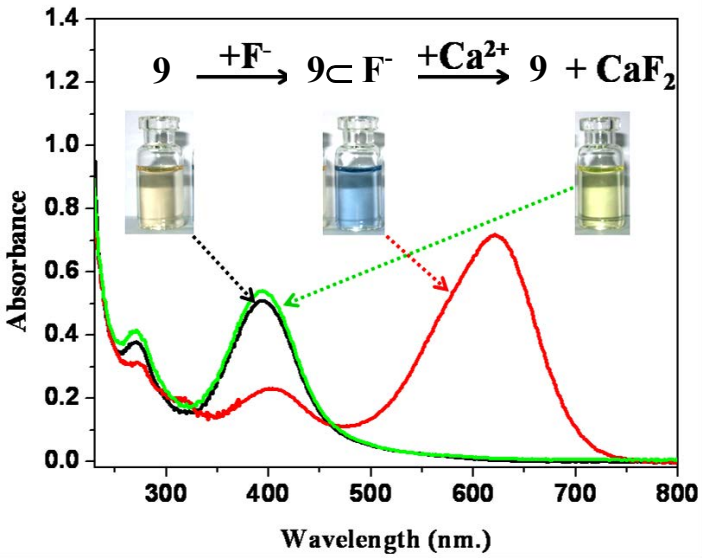

Figure 3.43 UV-vis spectra of ligand **9** (0.02 mM in CH_3CN) (black line), after adding 6 equivalents of F^- (red line) and then 2 equivalents of $CaNO_3$ (green line).

In case of the ^{1}H-NMR spectroscopic study, the original spectrum of ligand **9** also returned after adding excess Ca^{2+} into the solution of **9**·F^{-}complex (Figure 3.44).

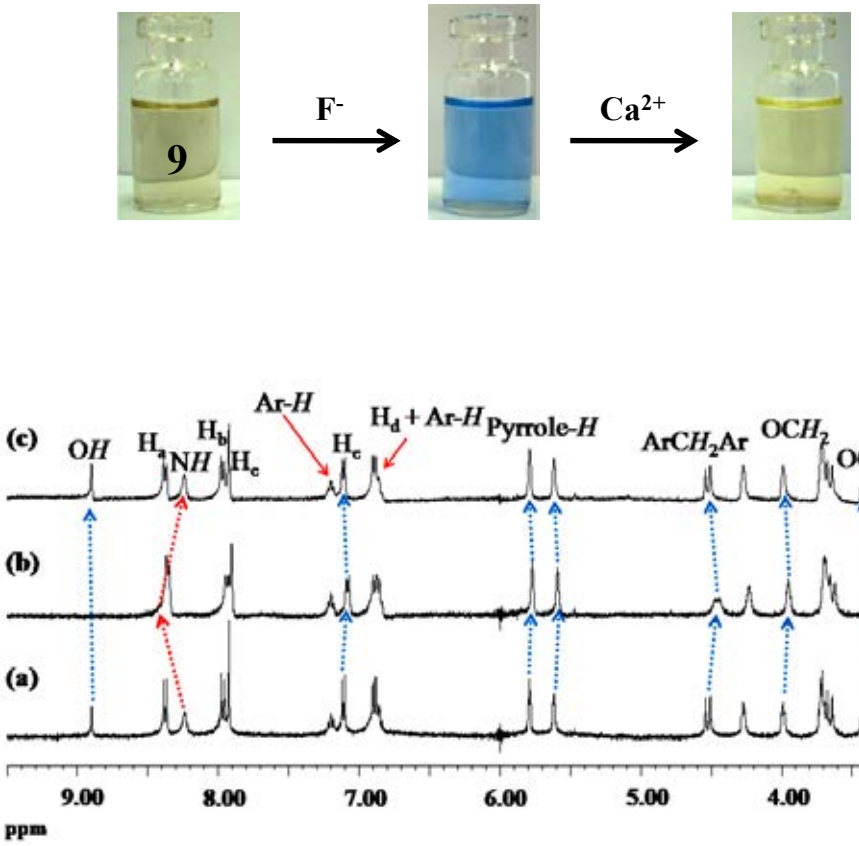

Figure 3.44 ^{1}H-NMR spectra of **9** (2.0 mM) (a) after addition of 3 equiv. of F^{-} in CD_3CN (b) and excess $Ca(NO_3)_2$ were add to the **9**·F^{-} complex (c) and the pathway of color changed (inset).

Smith et al. [163,164] have described a related effect in which binding of anion by a simple neutral host was inhibited in the presence of metal cation in solution as a result of preferential ion-pairing. These clearly indicated that addition only one equivalent of anion or cation leads to a stripping a more stable ion-pair from the receptor in solution, and anion or cation binding to the receptor is effectively inhibited by this process. The ion-pairing effect shows by the cartoon picture in Figure 3.45.

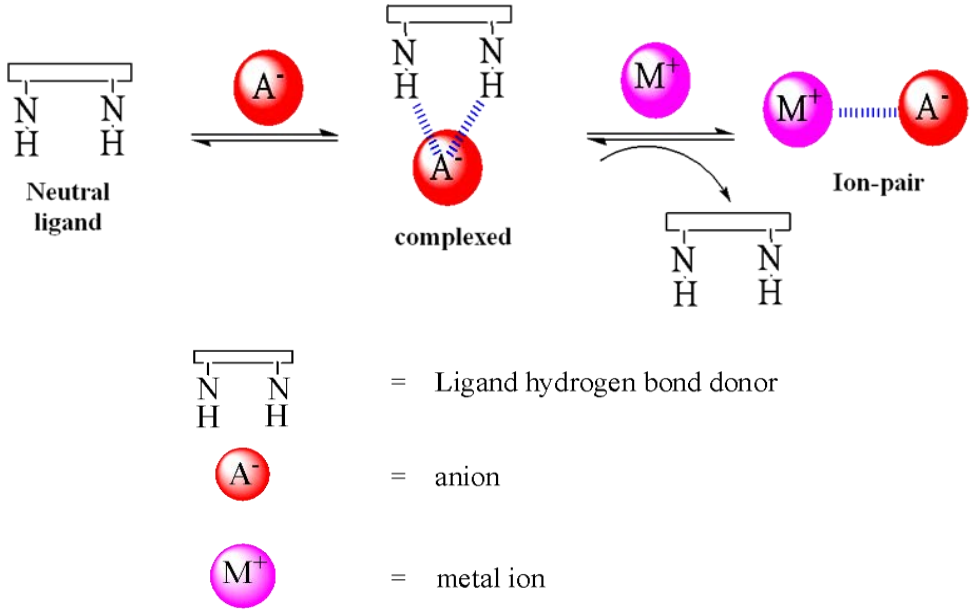

Figure 3.45 The ion-pairing effect.

On the basis of the above observation, we would like to investigate the potential applications of ligand **9**, as an anion sensor. To explore this, we will prepare a test paper (Whatman-40) coat with CH_3CN solution of ligand **9** and then dry in air. Put the solution of each anion on the ligand **9** paper coat. In case of F^-, AcO^-, BzO^- and $H_2PO_4^-$ must show color changes on the test paper. In addition, the prepare test paper can be reused for the detection of anions or not by washing the anion containing test paper with $Ca(NO_3)_2$ solution. By these processes we can recycle the test paper (kits) in several times, for the detection of anions in environment medium.

3.7 Complexation studies of ligand 7 with AcO^-, BzO^-, F^- and $H_2PO_4^-$ in the presence of Ca^{2+} using UV-vis spectrophotometry and ^{1}H-NMR spectroscopy.

To compare the ion-pairing effect of complex **9**·Ca^{2+} with complex **7**·Ca^{2+}, the influence of anion interactions to complex **7**·Ca^{2+} on spectroscopic changes was also studied using UV-vis spectrophotometry and ^{1}H-NMR spectroscopy as well as their color changes. Added 2 equivalents of $Ca(NO_3)_2$ into the CH_3CN solution of ligand **7**, giving 100% saturation of the receptor, and minimizing the amount of free Ca^{2+} in the solution and then 6 equivalents of each anions were added into the complex **7**·Ca^{2+} solution.

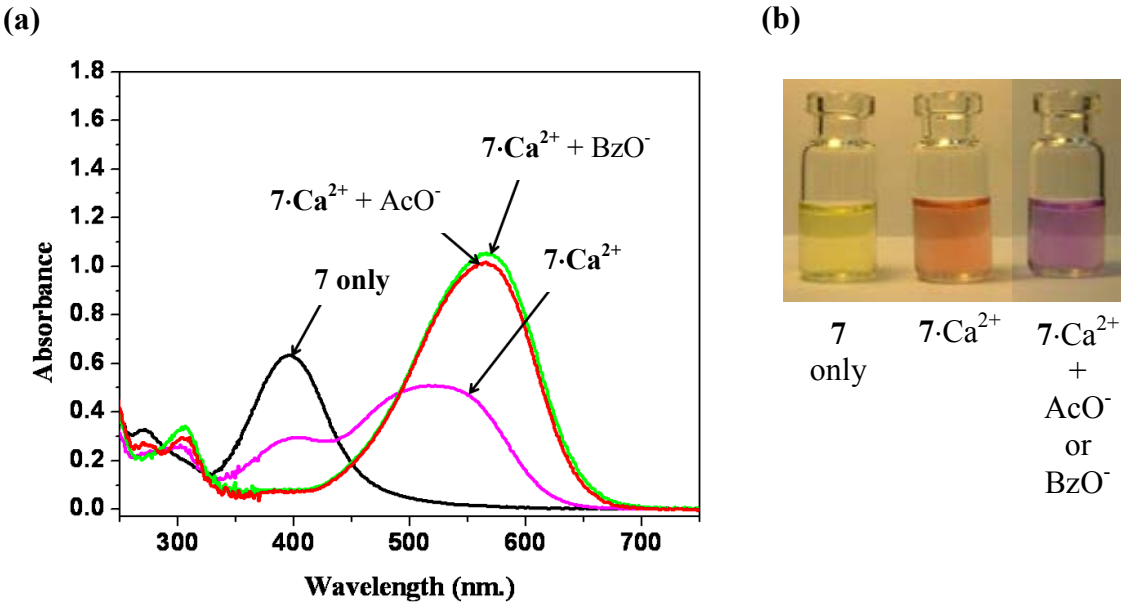

Figure 3.46 Spectral changes in the UV-vis absorption of complex **7**·Ca^{2+} (0.02 mM) upon addition 6 equiv. of AcO^- and BzO^- in CH_3CN (a) and color changes of ligand **7** (0.02 mM) in CH_3CN after adding 2 equiv. of $Ca(NO_3)_2$ and addition 6 equiv. of AcO^- or BzO^- respectively (b).

In case of complex **7**·Ca^{2+} (0.02 mM), the UV-vis spectra showed a bathochromic shift when adding 6 equivalents of AcO^- or BzO^- into the solution (Figure 3.46(a)). However, the absorption band was fixed at 565 nm (different from complex **9**·Ca^{2+} with

AcO^- or BzO^-, 545 nm.) and the orange solution of complex **7**·Ca^{2+} changed to violet (Figure 3.46(b)). This implies that the complex **7**·Ca^{2+} interacted with AcO^- and BzO^- in a different manner as compared to complex **9**·Ca^{2+}. The internal charge transfer did not occur in the absence of calix[4]pyrrole binding unit.

Furthermore, in the case of **7**·F^- complex, 3 equivalents of TBAF were added to the sample of ligand **7** in CD_3CN and then excess of $Ca(NO_3)_2$ was added into the solution of **7**·F^- complex. The signal of **7**·F^- complex did not return to its original spectrum of ligand **7** upon the addition of excess Ca^{2+}. ^{1}H-NMR spectrum of ligand **7** (5.46 mM) upon adding 3 equivalents of F^- showed only deprotonation at phenol protons. Excess Ca^{2+} was then added to the solution of complex **7**·F^- but no evidence of binding was observed (Figure3.47). The phenol protons reappeared after 3 days upon keeping the **7**·F^- complex with Ca^{2+} at room temperature. This lack of reversal process clearly stemmed from the absence of the calix[4]pyrrole unit.

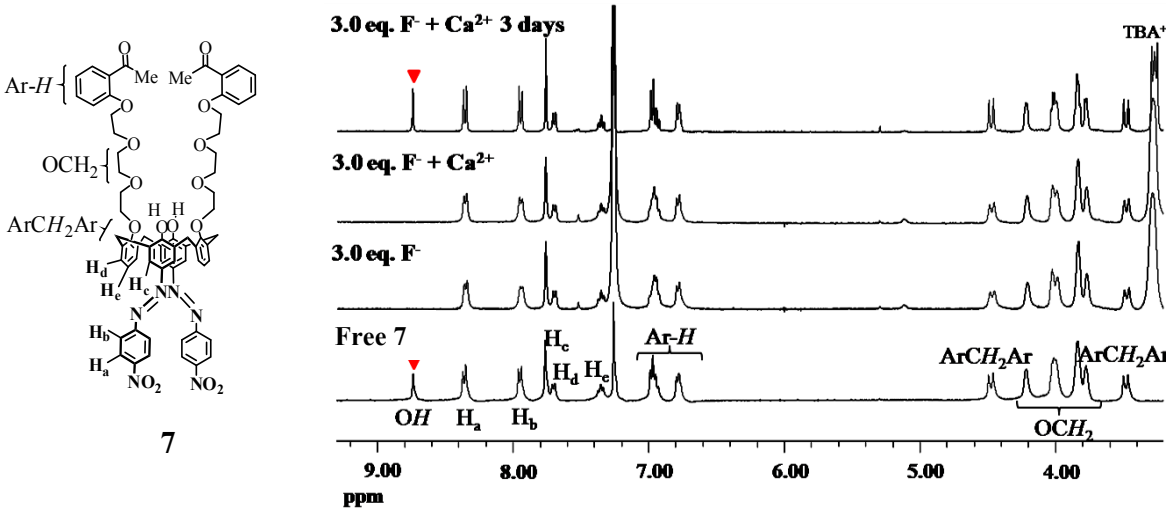

Figure 3.47 ^{1}H-NMR spectra of ligand **7** (5.46 mM) upon titration with 3 equiv. of F^- in $CDCl_3$ and excess $CaNO_3$ was added to the **7**·F^- complex.

CHAPTER IV

CONCLUSION

The chromogenic anion sensor, 1,3-di-*p*-nitrophenylazo-calix[4]arene-calix[4]pyrrole (**9**), has been successfully synthesized in 4 steps. The synthetic pathway starting from a condensation of 2-(triethyleneglycol tosylate)acetophenone (**2**) with calix[4]arene to afford 1,3-calix[4]-diacetophenone (**3**). After condensation of diketone **3** with pyrrole, the obtained 1,3-calix[4]-bis(dipyrrolethane) (**4**) was then cyclized with acetone to provide calix[4]arene-calix[4]pyrrole (**5**). The diazo-coupling reaction of **5** with *p*-nitrobenzene-diazonium tetrafluoroborate gave the undesired product calix[4]arene-*p*-nitrophenylazo-calix[4]pyrrole (**6**), which contains azobenzene ring in β-pyrrolic position. Coupling of nitrobenzene-diazonium tetrafluoroborate with 1,3-calix[4]-diacetophenone (**3**) gave 1,3-di-*p*-nitrophenylazo-calix[4]-diacetophenone (**7**), which has azobenzene ring in para position of the phenol ring. The obtained 1,3-di-*p*-nitrophenylazo-calix[4]-diacetophenone (**7**) was condensed with pyrrole to provide 1,3-di-*p*-nitrophenylazo-calix[4]arene-bis-dipyrroethane (**8**). The obtained product **8** was then cyclized with acetone gave a chromogenic sensor **9** in a total yield of 1.13 %. Regarding the geometry of ligand **9**, the calix[4]arene unit constrains in cone conformation whereas calix[4]pyrrole one fixes in 1,3-alternate fashion with *trans*-linkages of the two units.

The binding abilities of ligand **9** studied by UV-vis spectrophotometry was found to differentiate F^-, AcO^-, BzO^- and $H_2PO_4^-$ based on their sizes and shapes. ^{1}H-NMR spectrum showed the deprotonation from base anions occurred at the phenolic part of azocalix[4]arene leading to the internal charge transfer of the molecule. Calix[4]pyrrole seemed to modulate the anion binding properties with preorganized hydrogen-bonding or coordinating to anions. Ligand **9** was highly selective to Ca^{2+} by using azocalix[4]crown ether as a metal chelating unit. The binding abilities of complex **9**·Ca^{2+} with AcO^- and BzO^- showed a bathochromic shift which ascribed to the complexation of complex **9**·Ca^{2+} with AcO^- and BzO^-. However, F^- and $H_2PO_4^-$ induced the original spectrum of ligand **9** due to the formation of more stable ion-pairs inhibition in solution. Azocalix[4]diacetophenone **7**, which lack of calix[4]pyrrole was used to compare the

binding abilities to ligand **9** . The internal charge transfer did not occur in the case of ligand **7** when complexes with AcO^-, BzO^-. In addition, adding Ca^{2+} to the solution of complex **7**·F^- did not give back the free ligand **7**. We thus demonstrated that the presence of calix[4]pyrrole unit would effect binding and sensing properties of ligand **9** towards cations and anions.

REFERENCES

[1] Lehn, J-M. Supramolecular Chemistry: Concepts and Perspectives. Weinheim: VCH, 1995.

[2] Beer, P. D.; Gale, P. A. and Smith, D. K. Supramolecular Chemistry. Oxford: Oxford University Press, 1999.

[3] G. A. An Introduction to Hydrogen bonding. Oxford: Oxford University Press, 1997.

[4] Arduini, A.; Secchi, A. and Pochini, A. Recognition of amides by new rigid calix[4]arene-based cavitands. The Journal of Organic Chemistry 65 (2000): 9085-9091.

[5] Bodenant, B.; Weil, T.; Businelli-Pourcel, M.; Fages, F.; Barbe, B.; Pianet, I. and Laguerre, M. Synthesis and solution structure analysis of a bispyrenyl bishydroxamate calix[4]arene-based receptor, a fluorescent chemosensor for Cu^{2+} and Ni^{2+} metal ions. The Journal of Organic Chemistry 64 (1999): 7034-7039.

[6] Ikeda, A.; Shinkai, S. Novel cavity design using calix[n]arene skeletons:Toward molecular recognition and metal binding. Chemical Reviews 97 (1997): 1713-1734.

[7] Kral, V.; Sessler, J. L.; Shishkanova, T. V.; Gale, P. A. and Volf, R. Molecular recognition at an organic-aqueous interface: Heterocalixarenes as anion binding agents in liquid polymeric membrane ion-selective electrodes. Journal of the American Chemical Society 121 (1999): 8771-8775.

[8] Lee, D. H.; Lee, H. Y.; Lee, K. H. and Hong, J.-I. Selective anion sensing based on a dual-chromophore approach. Chemical Communications (2001): 1188-1189.

[9] Lee, D. H.; Lee, K. H. and Hong, J.-I. An azophenol-based chromogenic anion sensor. Organic Letters 3 (2001): 5-8.

[10] Hennrich, G.; Sonnenschein, H. and Resch-Genger, U. Fluorescent anion receptors with iminoylthiourea binding sites-selective hydrogen bond mediated recognition of CO_3^{2-}, HCO_3^- and HPO_4^{2-}. Tetrahedron Letters

42(2001): 2805-2808.

[11] Valeur, B.; Leray, I. Design principles of fluorescent molecular sensors for cation recognition. Coordination Chemistry Reviews 210(2000): 3-40.

[12] Perderson, C. J. Cyclic polyethers and their complexes with metal salts. Journal of the American Chemical Society 87(1967): 7017.

[13] Kodansh Ltd. Their Characteristic and Application. Tokyo: Crown Compound, 1982.

[14] Dietrich, B.; Lehn, J. M. and Sauvage, J. P. Diaza-polyoxa-macrocycles et macrobicycles. Tetrahedron Letters 10(1969): 2885.

[15] Stoddart, J. F. Cyclodextrins, off-the-shelf components for the construction of mechanically interlocked molecular systems. Angewandte Chemie International Edition in English (1992): 846.

[16] Kobayashi, N.; Mizuno, K. and Osa, T. A. A calix[4]arened porphyrin as a new host and an oxygen carrier model. Inorganica Chimica Acta 224(1994): 1.

[17] Pochini, A.; Ungaro, R. Calixarenes and Related Hosts Executive Eds. Elsevier: Comprehensive Supramolecular Chemistry, 1996.

[18] Shriver, D. F.; Atkins, P. W. and Langford, C. H. Inorganic Chemistry 3rd ed. New York: W. H. Freeman, 1990.

[19] Sessler, J. L.; Gebauer, A. and Gale, P. A. Anion binding and electrochemical properties of calix[4]pyrrole ferrocene conjugates. Gazzetta Chimica Italiana 127(1997): 723.

[20] Sessler, J. L.; Anzenbacher Jr. P.; Jursikova, K.; Miyaji, H.; Genge, J. W.; Tvermoes, N. A.; Allen, W. E. and Shriver, J. A. Functionalized calix[4]pyrroles. Pure and Applied Chemistry 70(1998) : 2401.

[21] de Silva, S. A.; Zavaleta, A.; Baron, D. E.; allam, O.; Isidor, E. V.; Kashimura, N. and Percapio, J. M. A. Fluorescent photoinduced electron transfer sensor for cations with an off-on-off proton switch. Tetrahedral Letters 38(1997): 2237.

[22] Antonisse, M. G. M.; Reinhoudt, D. N. Neutral anion receptors: Design and application. Chemical communications 4(1998): 443.

[23] Atwood, J. L.; Steed, J. W. Supramolecular Chemistry of Anions. New York:

Wiley-VCH, 1997.

[24] Koh, K. N.; Imada, T.; Nagasaki, T. and Shinkai, S. Molecular design of hard-soft ditopic metal-binding sites on a calix[4]arene platform. Tetrahedral Letters 35(1994): 4157-4160.

[25] Chartres, J. D.; Groth, A. M.; Lindoy, L. F.; Lowe, M. P. and Meehan, G. V. New heteroditopic, linked macrocyclic systems derived from selectively protected $N_2S_2^-$, $N_3O_2^-$ and N_4^-donor macrocycles. Journal of the Chemical Society, Perkin Transaction 1 (2000): 3444-3450.

[26] Fabbrizzi, L.; Montagna, L.; Poggi, A.; Kaden, T. A. and Liselotte, C. Bicyclam [6, 6′-bi(1,4,8,11-tetra-azacyclotetradecane)]: A ditopic receptor for homo- and hetero-bimetallic complexes. Journal of the Chemical Society Dalton Transactions (1987): 2631-2634.

[27] Fages, F.; Desvergne, J.-P. and Bouas-Laurent, H. Synthesis, structural, spectroscopic, and alkali-metal cations complexation studies of a bis-anthracenediyl macrotricyclic ditopic receptor. The Journal of Organic Chemistry 59(1994): 5264-5271.

[28] Fages, F.; Desvergne, J.-P.; Bouas-Laurent, H.; Lehn, J.-M.; Konopelski, J. P.; Marsau, P. and Barrans, Y. Synthesis and fluorescence emission properties of a bis-anthracenyl macrotricyclic ditopic receptor. Crystal structure of its dinuclear rubidium cryptate. Journal of the Chemical Society, Chemical Communications (1990): 655-658.

[29] Sutherland, I. O. Molecular recognition by synthetic receptors. Pure and Applied Chemistry 61(1989): 1547-1554.

[30] Ray, J. K.; Gupta, S.; Pan, D. and Kar, G. K. Molecular recognition: Studies on the synthesis of some bis thiophene carboxamide derivatives as ditopic receptors for long chain dicarboxylic acids. Tetrahedron 57(2001): 7213-7219.

[31] Graf, E.; Hosseini, W. and Ruppert, R. Synthesis of macrocyclic ditopic receptors designed for simultaneous binding of alkaline and transition metal cations. Tetrahedral Letters 35(1994): 7779-7782.

[32] Rudkevich, D. M.; Mercer-Chalmers, J. D.; Verboom, W.; Ungaro , R.; de Jong,

F. and Reinhoudt, D. N. Bifunctional recognition: Simultaneous transport of cations and anions through a supported liquid membrane. Journal of the American Chemical Society 117(1995): 6124-6125.

[33] Beer, P. D.; Dent, S. W. Potassium cation induced switch in anion selectivity exhibited by heteroditopic ruthenium(II) and rhenium(I) bipyridyl bis(benzo-15-crown-5) ion pair receptors. Chemical Communications (1998): 825-826.

[34] Nabeshima, T.; Hanami, T. Synthesis of a novel multi-receptor containing hydrogen bonding sites and ion binding sites**.** Heterocycles 50(1999): 1091-1096.

[35] Love, J. B.; Vere, J. M.; Glenny, M. W.; Blake, A. J. and Schröder, M. Ditopic azathioether macrocycles as hosts for transition metal salts. Journal of the Chemical Society, Chemical Communications (2001): 2678-2679.

[36] Liu, X.; Kilner, C. A. and Halcrow, M. A. 3{5}-*tert*-Butylpyrazole is a ditopic receptor for zinc(II) halides. Journal of the Chemical Society, Chemical Communications (2002): 704 -705.

[37] Park, C. E.; Jung, Y.-G. and Hong, J.-I. Efficient dopamine transport by a crown phosphonate. Tetrahedral Letters 39(1998): 2353-2356.

[38] Kirkovits, G. J.; Shriver, J. A.; Gale, P. A. and Sessler, J. L. Synthetic ditopic receptors. Journal of Inclusion Phenomena and Macrocyclic Chemistry 41(2001): 69-75.

[39] Cooper, J. B.; Drew, M. G. B. and Beer, P. D. Heteroditopic rhenium(I) and rhuthenium(II) bipyridyl calix[4]arene receptors for binding cation-anion ion pairs. Journal of the Chemical Society Dalton Transactions (2001): 392-401.

[40] Beer, P. D.; Dent, S. W. Potassium cation induced switch in anion selectivity exhibited by heteroditopic ruthenium(II) and rhenium(I) bipyridyl bis(benzo-15-crown-5) ion pair receptors. Journal of the Chemical Society, Chemical Communications (1998): 825-826.

[41] Nishizawa, S.; Shigemori, K. and Teramae, N. A thiourea-functionalized benzo-15-crown-5 for cooperative binding of sodium ions and anions. Chemistry Letters (1999): 1185-1186.

[42] Sessler, J. L.; Gale, P. A. and Cho, W.-S. Anion Receptor Chemistry. Cambridge: Royal Society of Chemistry, 2006.

[43] Gale, P. A.; García-Garrido, S. E. and Garric, J. Anion receptors based on organic frameworks: highlights from 2005 and 2006. Chemical Society Review 37(2008): 151–190.

[44] Gale, P. A.; Quesada, R. Anion coordination and anion-templated assembly: Highlights from 2002 to 2004 Coordination Chemistry Reviews 250(2006): 3219–3244.

[45] Bianchi, A.; Bowman-James, K. and García-Espanã, E. Supramolecular Chemistry of Anions. New York: Wiley-VCH, 1997.

[46] Gale, P. A.; Atwood, J. L. and Steed, J. W. The Encyclopedia of Supramolecular Chemistry. New York: Dekker, 2004.

[47] Beer, P. D.; Gale, P. A. Anion recognition and sensing: The state of the art and future perspectives. Angewandte Chemie International Edition 40(2001): 486–516.

[48] Caltagirone, C.; Gale, P. A. Anion receptor chemistry: highlights from 2007. Chemical Society Review 38(2009): 520–563.

[49] Martínez-Máñez, R. Sancenán, F. Fluorogenic and Chromogenic Chemosensors and Reagents for Anions. Chemical Reviews 103(2003): 4419–4476.

[50] Smith, B. D. Ion Pair Recognition by Ditopic Receptors, Macrocycli Chemistry. London: Current Trends and Future Prospectives, 2005.

[51] Kirkovits, G. J.; Shriver, J. A.; Gale, P. A. and Sessler, J. L. Synthetic ditopic receptors. Journal of Inclusion Phenomena and Macrocyclic Chemistry 41(2001): 69–75.

[52] Antonisse, M. M. G.; Reinhoudt, D. N. Neutral anion receptors: design and application. Chemical Communications (1998): 443–448.

[53] Mahoney, J. M.; Stucker, K. A.; Jiang, H.; Carmichael, I.; Brinkmann, N. R.; Beatty, A. M.; Noll, B. C. and Smith, B. D. Molecular recognition of trigonal oxyanions using a ditopic salt receptor: evidence for anisotropic shielding surface around nitrate anion. Journal of the American Chemical Society 127(2005): 2922–2928.

[54] Mele, A.; Metrangolo, P.; Neukirch, H.; Pilati, T. and Resnati, G. A Halogen-bonding-based heteroditopic receptor for alkali metal halides. Journal of the American Chemical Society 127(2005): 14972–14973.

[55] Reeske, G.; Schürmann, M. and Jurkschat, K. Charge separation by ditopic complexation in the solid state: molecular structure of $\{Ph_2(I)SnCH_2Sn(Ph)(I)CH_2$-[16]-crown-5$\}\cdot NaF\cdot CH_3OH$. Dalton Transactions (2008): 3398–3400.

[56] Löhr, H.-G.; Vögtle, F. Chromo- and fluoroionophores. A new class of dye reagents. Account of Chemical Research 18(1985): 65.

[57] Inouye, M. Color. Nontext. Appl., 2000.

[58] Takagi, M.; Ueno, K. Topics in Current Chemistry: Host-Guest Complex Chemistry. Berlin: Springer, 1984.

[59] Zollinger, H. Color Chemistry. Weinheim: VCH, 1991.

[60] Lee, K. H.; Lee, H.-Y.; Lee, D. H. and Hong, J.-I. Fluoride-selective chromogenic sensors based on azophenol. Tetrahedron Letters 42(2001): 5447.

[61] Lee, D. H.; Lee, K. H. and Hong, J.-I. An azophenol-based chromogenic anion sensor. Organic Letters 3(2001): 5.

[62] Lee, D. H.; Lee, H. Y.; Lee, K. H. and Hong, J.-I. Selective anion sensing based on a dual-chromophore approach. Chemical Communications (2001): 1188.

[63] Asfari, Z; Böhmer, V.; Harrowfield, J. and Vincens, J. Calixarenes 2001. Dordrecht: Kluwer Academic Publishers, 2001.

[64] Wieser, C.; Dieleman, D. B. and Matt, D. Calixarene and resorcinarene ligands in transition metal chemistry. Coordination Chemistry Reviews 165(1997): 93-161.

[65] Wolbers, M. P. O.; van Veggel, F. C. J. M.; Peters, F. G. A.; van Beelen, E. S. E.; Hofstraat, J. W.; Geurts, F. A. J. and Reinhoudt, D. N. Sensitized near-infrared emission from Nd^{3+} and Er^{3+} complexes of fluorescein-bearing calix[4]arene cages. Chemistry-A European Journal 5(1998): 772-780.

[66] Cuevas, F.; Stefano, S. D.; Magrans, J. O.; Prados, P.; Mandolini, L. and de Mendoza, J. Toward an artificial acetylcolinesterase. Chemistry - A European Journal 6(2000): 3228-3234.

[67] Collins, E. M.; McKervey, M. A.; Madigan, E.; Moran, M. B.; Owens, M.; Ferguson, G. and Harris, S. J. Chemically modified calix[4]arenes. regioselective synthesis of 1,3-(distal) derivatives and related compounds. X-ray crystal structure of a diphenol-dinitrile. Journal of the Chemical Society, Perkin Transaction 1 (1991): 3137-3142.

[68] Arnaud-Neu, F.; Browne, J. K.; Byrne, D.; Marrs, D. J.; McKervey, M. A.; O"Hagan, P. Schwing-Weill, M. J. and Walker, A. Extraction and complexation of alkali, alkaline earth, and f-element cations by calixaryl phosphine oxides. Chemistry-A European Journal 5(1999): 175-186.

[69] Ludwig, R.; Kunogi, K.; Dung, N. and Tachimori, S. A calixarene-based extractant with selectivity for Am^{III} over Ln^{III}. Journal of the Chemical Society, Chemical Communications 20(1997): 1985-1986.

[70] Tuntulani, T.; Tumcharern, G. and Ruangpornvisuti,V. Recognition studies of a pyridine-pendant calix[4]arene with neutral molecules: Effects of non-covalent interactions on supramolecular structures and stabilities. Journal of Inclusion Phenomena and Macrocyclic Chemistry 39(2001): 47-53.

[71] Diamond, D.; Nolan, K. Peer reviewed: Calixarenes: Designer ligands for chemical sensors. Analytical Chemmistry (2001): 22A-29A.

[72] Molenveld, P.; Engbersen, J. F. J.; Kooijman, H. J.; Spek, A. L. and Reinhoudt, D. N. Efficient catalytic phosphate diester cleavage by the synergetic action of two Cu(II) centers in a dinuclear *cis*-diaqua Cu(II) calix[4]arene enzyme model. Journal of the American Chemical Society 120(1998): 6726-6737.

[73] Haino, T.; Akii, H. and Fukazawa, Y. An artificial receptor based on monodeoxy calix[4]arene. Synlett. 9(1998): 1016-1018.

[74] Hioki, H.; Yamada, T.; Fujioka, C. and Kodama, M. Peptide library based on calix[4]arene. Tetrahedron Letters 40(1999): 6821-6825.

[75] Lee, D. H.; Im, J. H.; Son, S. U.; Chung, Y. K. and Hong, J. I. An azophenol-based chromogenic pyrophosphate sensor in water. Journal of the American Chemical Society 125(2003): 7752.

[76] Lee, D. H.; Lee, H. Y.; Lee, K. H. and Hong, J.-I. Selective anion sensing based on a dual-chromophore approach. Chemical Communications (2001): 1188-1189.

[77] Lee, D. H.; Lee, K. H. and Hong, J. I. An azophenol-based chromogenic anion sensor. Organic Letters 3(2001): 5.

[78] Lee, K. H.; Lee, H.-Y.; Lee, D. H. and Hong, J. I. Fluoride-selective chromogenic sensors based on azophenol. Tetrahedron Letters 42(2001): 5447.

[79] Shinkai, S.; Shimizu, H.; Iwamoto, K. and Fujimoto, K. Chromogenic calix[4]arene. Chemistry Letters 20(1991): 2147-2150.

[80] Chang, K.-C.; Su, I.-H.; Lee, G.-H. and Chung, W.-S. Triazole- and azo-coupled calix[4]arene as a highly sensitive chromogenic sensor for Ca^{2+} and Pb^{2+} ions. Tetrahedron Letters 48(2007): 7274–7278.

[81] Reinhoudt, D. N.; van der Veen, N. J.; Egberink, R. J. M.; Engberson, J. F. J. and van Veggel, F. J. C. M. Conformationally flexible calix[4]arene chromoionophores: optical transduction of soft metal ion complexation by cation–π interactions. Chemical Communications (1999): 681-682.

[82] Kim, J. Y.; Kim, G.; Kim,C. R.; Lee, S. H.; Lee, J. H. and Kim, J. S. UV band splitting of chromogenic azo-coupled calix[4]crown upon cation complexation. The Journal of Organic Chemistry 68(2003): 1933-1937.

[83] Kim, H. J.; Kim, S. K.; Lee, J. Y. and Kim, J. S. Fluoride-sensing calix-luminophores based on regioselective binding. The Journal of Organic Chemistry 71(2006): 6611-6614.

[84] Chung, W.-S.; Chang, K.-C.; Su, I.-H. and Wang, Y.-Y.; A bifunctional chromogenic calix[4]arene chemosensor for both cations and anions: A potential Ca^{2+} and F^{-} switched INHIBIT logic gate with a YES logic function. European Journal of Organic Chemistry (2010): 4700–4704.

[85] Baeyer, A. Ueber ein condensationsproduct von pyrrol mit aceton. Berichte der deutschen chemischen Gesellschaft 19(1886): 2184-2185.

[86] Gale, P. A.; Sessler, J. L.; Král, V. and Lynch, V. Calix[4]pyrroles: Old yet new anion-binding agents. Journal of the American Chemical Society 118(1996): 5140-5141.

[87] Allen, W. E.; Gale, P. A.; Brown, C. T.; Lynch, V. M. and Sessler, J. L. Binding of neutral substrates by calix[4]pyrroles. Journal of the American Chemical Society 118(1996): 12471-12472.

[88] Gale, P. A.; Sessler, J. L. and Král, V. Calixpyrroles. Chemical Communications (1998): 1-8.

[89] Gale, P. A.; Aazenbacher, P., Jr. and Sessler, J. L. Calixpyrroles II. Coordination Chemistry Reviews 222(2001): 57-102.

[90] Sessler, J. L.; Andrievsky, A.; Gale, P. A. and Lynch, V. Anion binding: Self-assembly of polypyrrolic macrocycles. Angewandte Chemie International Edition in English 35(1996): 2782-2785.

[91] Miyaji, H.; An, D. and Sessler, J. L. Mono halogen substituted calix [4lpyrroles: Fine-tuning the anion binding properties of calix[4]pyrrole. Supramolecular Chemistry 13(2001): 661-669.

[92] Gale, P. A.; Sessler, J. L.; Allen, W. E.; Tvermoes, N. A. and Lynch, V. Calix[4]pyrroles: *C*-rim substitution and tunability of anion binding strength. Chemical Communications (1997): 665-666.

[93] Warriner, C. N.; Gale, P. A.; Light, M. E. and Hursthouse, M. B. Pentapyrrolic calix[4]pyrrole. Chemical Communications (2003): 1810-1811.

[94] Camiolo, S.; Gale, P. A. Fluoride recognition in „super-extended cavity" calix[4]pyrroles. Chemical Communications (2000): 1129-1130.

[95] Gale, P. A.; Sessler, J. A.; Lynch, V. and Sansom, P. I. Synthesis of a new cylindrical calix[4]arene-calix[4]pyrrole pseudo dimer. Tetrahedron Letters 37(1996): 7881-7884.

[96] Sessler, J. L.; Cho, W. S.; Gross, D. E.; Shriver, J. A.; Lynch, V. M. and Marquez, M. Anion binding studies of fluorinated expanded calixpyrroles. The Journal of Organic Chemistry 70(2005): 5982-5986.

[97] Piatek, P.; Lynch, V. M. and Sessler, J. L. Calix[4]pyrrole[2]carbazole: A new kind of expanded calixpyrrole. Journal of the American Chemical Society 126(2004): 16073-16076.

[98] Cafeo, G.; Kohnke, F. H.; La Torre, G. L.; White, A. J. P. and Williams, D. J. The complexation of halide ions by a calix[6]pyrrole. Chemical Communications (2000): 1207-1208.

[99] Turner, B.; Botoshansky, M. and Eichen, Y. Extended calixpyrroles: meso-Substituted calix[6]pyrroles. Angewandte Chemie International Edition 37(1998): 2475-2478.

[100] Sessler, J. L.; An, D.; Cho, W.-S. and Lynch, V. Calix[2]bipyrrole[2]furan and calix[2]bipyrrole[2]thiophene: New pyrrolic receptors exhibiting a preference for carboxylate anions. Journal of the American Chemical Society 125(2003): 13646-13647.

[101] Sessler, J. L.; An, D.; Cho, W.-S. and Lynch, V. Calix[n]bipyrroles: Synthesis, characterization, and anion-Binding studies. Angewandte Chemie International Edition 42(2003): 2278-2281.

[102] Panda, P. K.; Lee, C. H. Metalloporphyrin-capped calix[4]pyrroles: Heteroditopic receptor models for anion recognition and ligand fixation. The Journal of Organic Chemistry 70(2005): 3148-3156.

[103] Panda, P. K.; Lee, C.-H. Calix[4]pyrrole-capped metalloporphyrins as ditopic receptor models for anions. Organic Letters 6(2004): 671-674.

[104] Yoon, D.-W.; Hwang, H. and Lee, C.-H. Synthesis of a strapped calix[4]pyrrole: structure and anion binding properties. Angewandte Chemie International Edition 41(2002): 1757-1759.

[105] Sato, W.; Miyaji, H. and Sessler, J. L. Calix[4]pyrrole dimers bearing rigid spacers: towards the synthesis of cooperative anion binding agents. Tetrahedron Letters 41(2000): 6731-6736.

[106] Bucher, C.; Zimmerman, R. S.; Lynch, V. and Sessler, J. L. First cryptand-like calixpyrrole: synthesis, X-ray structure, and anion binding properties of a bicyclic[3,3,3]nonapyrrole. Journal of the American Chemical Society 123(2001): 9716-9717.

[107] Sessler, J. L.; Gale, P. A. and Genge, J. W. Calix[4]pyrroles: new solid-phase HPLC supports for the separation of anions. Chemistry-A European Journal 4(1998): 1095-1099.

[108] Levitskaia, T. G.; Marquez, M.; Sessler, J. L.; Shriver, J. A.; Vercouter, T. and Moyer, B. A. Fluorinated calixpyrroles: anion-binding extractants that reduce the Hofmeister bias. Chemical Communications (2003): 2248-2249.

[109] Miyaji, H.; Sato, W. and Sessler, J. L. Naked-eye detection of anions in dichrolomethane: colorimetric anion sensors based on calix[4]pyrrole. Angewandte Chemie International Edition 39(2000): 1777-1780.

[110] Miyaji, H.; Sato, W.; Sessler, J. L. and Lynch, V. M. A „building block" approach to functionalized calix[4]pyrroles. Tetrahedron Letters 41(2000): 1369-1373.

[111] Gale, P. A.; Bleasdale, E. R. and Chen, G. Z. Synthesis and electrochemical polymerisation of calix[4]pyrroles containing N-substituted pyrrole moieties. Supramolecular Chemistry 13(2001): 557-563.

[112] Gale, P. A.; Hursthouse, M. B.; Light, M. E.; Sessler, J. L.; Warriner, C. N. and Zimmerman, R. S. Ferrocene-substituted calix[4]pyrrole: a new electrochemical sensor for anions involving CH-anion hydrogen bonds. Tetrahedron Letters 42(2001): 6759-6762.

[113] Nishiyabu, R.; Anzenbacher, P. J. Sensing of antipyretic carboxylates by simple chromogenic calix[4]pyrroles. Journal of the American Chemical Society 127(2005): 8270-8271.

[114] Lee, C.-H.; Miyaji, H.; Yoon, D.-W. and Sessler, J. L. Strapped and other topographically nonplanar calixpyrrole analogues. Improved anion receptors. Chemical Communications (2008): 24-34.

[117] Gale, P. A.; Warriner, C. N.; Light, M. E. and Hursthouse, M. B. Pentapyrrolic calix[4]pyrrole. Chemical Communications (2003): 1810-1811.

[118] Spartan "02, Wavefunction Inc., Irvine CA, USA.

[119] Sessler, J. L.; Anzenbacher, Jr. P.; Miyaji, H.; Jursíková, K.; Bleasdale, E. R. and Gale, P. A. Modified calix[4]pyrroles. Industrial & Engineering Chemistry Research 39(2000): 3471-3478

[120] Camiolo, S.; Gale, P. A. Fluoride recognition in „super-extended cavity" calix[4]pyrroles. Chemical Communications (2000): 1129-1130.

[121] Anzenbacher, P.; Jursíková, K.; Lynch, V. M.; Gale, P. A. and Sessler, J. L. Calix[4]pyrroles containing deep cavities and fixed walls. Synthesis, structural studies, and anion binding properties of the isomeric products derived from the condensation of *p*-hydroxyacetophenone and pyrrole. Journal of the American Chemical Society 121(1999): 11020-11021.

[122] Gale, P. A.; Sessler, J. L.; Lynch, V. and Sansom, P. I. Synthesis of a new cylindrical calix[4]arene-calix[4]pyrrole pseudo dimer. Tetrahedron Letters 37(1996): 7881-7884.

[123] Yoon, D. W.; Gross, D. E.; Lynch, V. M.; Sessler, J. L.; Hay, B. P. and Lee, C. H. Benzene-, pyrrole-, and furan-containing diametrically strapped calix[4]pyrroles-an experimental and theoretical study of hydrogen-bonding effects in chloride anion recognition. Angewandte Chemie International Edition 47(2008): 5038–5042.

[124] Lee, C.-H.; Jeong, S.-D.; Yoo, J.; Na, H.-K. and Chi, D. Y. Strapped-calix[4]pyrroles bearing acridine moiety. Supramolecular Chemistry 19(2007): 271–275.

[125] Sessler, J. L.; Miyaji, H.; Kim, H. K.; Sim, E. K.; Lee, C. K.; Cho, W. S. and Lee, C. H. Coumarin-strapped calix[4]pyrrole: A fluorogenic anion receptor modulated by cation and anion binding. Journal of the American Chemical Society 127(2005): 12510-12512.

[126] de Silva, A. P.; Gunaratne, H. Q. N. and McCoy, C. P. A Molecular photoionic AND gate based on fluorescent signaling. Nature 364(1993): 42-44.

[127] de Silva, A. P.; McClean, G. D. and Pagliari, S. Direct detection of ion pairs by fluorescence enhancement. Chemical Communications (2003): 2010-2011.

[128] Yoo, J.; Kim, M. S.; Hong, S. J.; Sessler, J. L. and Lee, C. H. Selective sensing of anions with calix[4]pyrroles strapped with chromogenic dipyrrolylquinoxalines. The Journal of Organic Chemistry 74(2009): 1065–1069.

[129] Ruangchaitaweesuk, S. Synthesis of bis-calix[4]arene-calix[4]pyrrole as ion pair receptor. Master„s Thesis. Department of Chemistry, Faculty of Science, Chulalongkorn University, 2004.

[130] Sessler, J. L.; Kim, S. K.; Gross, D. E.; Lee, C. H.; Kim, J. S. and Lynch, V. M. Crown-6-calix[4]arene-Capped Calix[4]pyrrole: An Ion-Pair Receptor for Solvent-Separated CsF Ions. Journal of the American Chemical Society 130(2008): 13162–13166.

[131] Kim, S. K.; Sessler, J. L.; Gross, D. E.; Lee, C. H.; Kim, J. S.; Lynch, V. M.; Delmau, L. H. and Hay, B. P. A Calix[4]arene Strapped Calix[4]pyrrole: An Ion-Pair Receptor Displaying Three Different Cesium Cation Recognition Modes. Journal of the American Chemical Society 132(2010): 5827–5836.

[132] Gutche, C. D.; Iqbal, M. *p-tert*-butylcalixarene. Organic Synthesis 68(1990): 234.

[133] Vogel, A. I. A tex-book of Quantitative Inorganic Analysis, Norfolk: Longman, 1975.

[134] Vetrogon, V. I.; Lukyanenko, N. G.; Schwing-well, M. J. and Arnaud-Neu, F. A PC compatible computer program for calculation of equilibrium constants by the simultaneous processing of different sets of experiment results. Talanta 41(1994): 2105-2112.

[135] Jaime, C.; de Mendoza, J.; Prados, P.; Nieto, P. M. and Sánchez, C. ^{13}C NMR chemical Shifts. A single rule to determine the conformation of calix[4]arenes. The Journal of Organic Chemistry 56(1991): 3372 – 3376.

[136] Miyaji, H.; Sato, W. and Sessler, J. L. Naked Eye Detection of Anions in Dichroromethane: Colorimetric Anion Sensors Based on Calix[4]pyrrole. Angewandte Chemie International Edition 39(2000): 1777.

[137] Lee, C. H.; Lindsey, J. S. One-flask synthesis of meso-substituted dipyrromethanes and their application in the synthesis of trans-substituted porphyrin building blocks. Tetrahedron 50(1994): 11427.

[138] Steed, J. W.; Atwood, J. L. Supramolecular Chemistry. Chichester, England: John Willey & Sons, 2000.

[139] Chen, C.-F.; Chen, Q.-Y. Azocalix[4]arene-based chromogenic anion probes. New Journal of Chemistry 30(2006): 143-147.

[140] Löhr, H. G.; Vögtle, F. Chromo- and fluoroionophores. A new class of dye reagents. Accounts of Chemical Research 18(1985): 65-72.

[141] Nishizawa, S.; Kato, R.; Hayashita, T. and Teramae, N. Anion Sensing by a Thiourea Based Chromoionophore *via* Hydrogen Bonding. Analytical Sciences 14(1998): 595−597.

[142] Chang, K.-C.; Su, I.-H.; Wang, Y.-Y. and Chung, W.-S. A bifunctional chromogenic calix[4]arene chemosensor for both cations and anions: A potential Ca^{2+} and F^{-} switched inhibit logic gate with a yes logic function. European Journal of Organic Chemistry (2010): 4700.

[143] Kaewtong, C.; Fuangswasdi, S.; Muangsin, N.; Chaichit, N.; Vicens, J. and Pulpoka, B. Novel C_{3v}-symmetrical N_7-hexahomotriazacalix[3]cryptand: a highly efficient receptor for halide anions. Organic Letters 8(2006): 1561-1564.

[144] Kaewtong, C.; Muangsin, N.; Chaichit, N. and Pulpoka, B. Conformation-selective synthesis and binding properties of *N*-benzylhexahomotriaza-*p*-chlorocalix[3]trinaphthylamide. The Journal of Organic Chemistry 73(2008): 5574-5577.

[145] Ionization Constants of Organic Acids in Solution, IUPAC Chemical Data Series No. 23. Oxford: Pergamon Press, 1979.

[146] Gordon, J. L. M.; Biihmer, V. and Vogt, W. **A** Calixarene-based chromoionophore for the larger alkali metals. Tetrahedron Letters 36(1995): 2445

[147] Shimizu, H.; Iwamoto, K.; Fujimoto, K. and Shinkai, S. Chromogenic calix[4]arene. Chemistry Letters (1991): 2147

[148] Yamamoto, H.; Ueda, K.; Sandanayake, K. R. A. S. and Shinkai, S. Molecular design of chromogenic calix[4]crowns which show very high Na^{+} selectivity. Chemistry Letters (1995): 497

[149] van der Veen, N. J.; Egberink, R. J. M; Engbersen, J. F. J.; van Veggel, F. J. C. M. and Reinhoudt, D. N. Conformationally flexible calix[4]arene

chromoionophores: optical transduction of soft metal ion complexation by cation–π interactions. Chemical Communications (1999): 681

[150] Bingol, H; Kocabas, E; Zor, E and Coskun, A. A novel benzothiazole based azocalix[4]arene as a highly selective chromogenic chemosensor for Hg^{2+} ion: A rapid test application in aqueous environment. Talanta 82(2010): 1538-1542.

[151] Ho, I.-T.; Lee, G.-H. and Chung, W.-S. Synthesis of upper-rim allyl- and *p*-methoxyphenylazocalix[4]arenes and their efficiencies in chromogenic sensing of Hg^{2+} ion. The Journal of Organic Chemistry 72(2007): 2434-2442.

[152] Nomura, E.; Taniguchi, H. and Tamura, S. Selective ion extraction by a calix[6]arene derivative containing azo groups. Chemistry Letters 18(1989): 1125-1126.

[153] Kishimoto, S.; Kitahara, S.; Manabe, O. and Hiyama, H. Studies on coupling reactions of 1-naphthol. 6. tautomerism and dissociation of 4-arylazo-1-naphthols in various solvents. The Journal of Organic Chemistry 43(1978): 3882-3886.

[154] Measured UV/vis absorption of $Cu(NO_3)_2$ 0.16 mM. in CH_3CN solution only compared with ligand **9** complex 300 equiv. of $Cu(NO_3)_2$ in CH_3CN solution. UV/vis absorption of $Cu(NO_3)_2$ 0.16 mM. in CH_3CN solution only has shown the same characteristic with ligand **9** complex 300 equiv. of $Cu(NO_3)_2$.

[155] Chapoteau, E.; Czech, B. P.; Gebauer, C. R.; Kumar, A.; Leong, K.; Mytych, D. T.; Zazulak, W.; Desai, D. H.; Luboch, E.; Krzykawski, J. and Bartsch, R. A. Phenylazophenol-quinone phenylhydrazone tautomerism in chromogenic cryptands and corands with inward-facing phenolic units and their acyclic analogs. The Journal of Organic Chemistry 56(1991): 2575.

[156] Luboch, E.; Wagner-Wysiecka, E. and Rzymowski, T. 4-Hexylresorcinol-derived hydroxyazobenzocrown ethers as chromoionophores. Tetrahedron 65(2009): 10671.

[157] Vögtle, F. New ligand systems for ions and molecules - and electronic effects upon complexation. Pure and Applied Chemistry 52(1980): 2405.

[158] Löhr, H. G.; Vögtle, F. Chromo- and fluoroionophores. A new class of dye

reagents. Accounts of Chemical Research 18(1985): 65.

[159] Ni, X.-L.; Tahara, J.; Rahman, S.; Zeng, X.; Hughes, D. L.; Redshaw, C. and Yamato, T. Ditopic Receptors based on Lower- and Upper-Rim Substituted Hexahomotrioxacalix[3]arenes: Cation-Controlled Hydrogen Bonding of Anion. Chemistry – An Asian Journal 3(2012): 519-527.

[160] Tumcharern,G; Tuntulani, T.; Coles, S. J.; Hursthouse, M. B. and Kilburn, J. D. A Novel Ditopic Receptor and Reversal of Anion Binding Selectivity in the Presence and Absence of Bound Cation. Organic Letters 5(2003): 4971-4974.

[161] dos Santos, C. M. G.; McCabe, T.; Watson, G. W.; Kruger, P. E. and Gunnlaugsson, T. The Recognition and Sensing of Anions through "Positive Allosteric Effects" Using Simple Urea-Amide Receptors. The Journal of Organic Chemistry 73(2008): 9235-9244.

[162] Kovbasyuk, L.; Krämer, R. Allosteric Supramolecular Receptors and Catalysts. Chemical Reviews 104(2004): 3161-3187.

[163] Shukla, R.; Kida, T. and Smith, B. D. Effect of Competing Alkali Metal Cations on Neutral Host‟s Anion Binding Ability. Organic Letters 2(2000): 3099;

[164] Camiolo, S.; Coles, S. J.; Gale, P. A.; Hursthouse, M. B. and Tizzard, G. J. Crown ether appended amidopyrrole clefts. Supramolecular chemistry 15(2003): 231.

APPENDICES

APPENDIX A

Table A1. Crystal data and structure refinement for 1,3-di-*p*-nitrophenylazo-calix[4]-diacetophenone (7).

	Ligand **7**
Identification code	s531953_2_0m
Empirical formula	$C_{69}H_{68}C_{l2}N_6O_{16}$
Formula weight	1308.19
Temperature	293(2) K
Wavelength	0.71073 A
Space group	P 21/n
Unit cell dimensions	a = 17.9165(5) Å, b = 16.5501(4) Å, c = 22.8972(6) Å, α = 90°, β = 101.726°, γ = 90°
Volume	6647.8(3) $Å^3$
Z	4
Calculated density	1.307 Mg/m^3
Absorption coefficient	0.170 mm^{-1}
F(000)	2744
θ range for data collection	1.32 - 26.44°
Index ranges	$-20 \le h \le 22$, $-20 \le k \le 19$, $-28 \le l \le 28$
Reflections collected	42073
Independent reflections	13664 [R_{int} = 0.0471]
Completeness to θ = 26.44°	99.6 %
Absorption correction	None
Refinement method	Full-matrix least-squares on F^2
Data / restraints / parameters	13664 / 820 / 830
Goodness-of-fit on F^2	1.741
Final R indices [$F^2 > 2\sigma(F^2)$]	*R1* = 0.1642, *wR2* = 0.4595
R indices (all data)	*R1* = 0.2452, *wR2* = 0.5122
Largest diff. peak and hole	5.040 and -1.399 e $Å^{-3}$

Table A2. Atomic coordinates [x 10^4], and equivalent isotropic displacement parameters [$Å^2$ x 10^3]. *U*(*eq*) is defined as one third of the trace of the orthogonalized U^{ij} tensor.

Atom	*x*	*y*	*z*	*U*(*eq*)
C(1)	302(4)	844(4)	2656(3)	38(1)
C(2)	544(4)	858(4)	3272(3)	44(2)
C(3)	104(4)	469(4)	3620(3)	45(2)
C(4)	-545(4)	77(4)	3361(3)	45(2)
C(5)	-781(4)	68(4)	2750(3)	45(2)
C(6)	-376(4)	455(4)	2383(3)	44(2)
C(7)	-640(4)	453(5)	1710(3)	52(2)
C(8)	-143(4)	-95(4)	1410(3)	42(2)
C(9)	-205(5)	-935(5)	1437(4)	59(2)
C(10)	284(5)	-1423(4)	1213(3)	61(2)
C(11)	862(5)	-1096(4)	982(3)	49(2)
C(12)	938(4)	-268(4)	927(3)	42(1)
C(13)	415(4)	213(4)	1137(3)	37(1)
C(14)	1586(4)	79(4)	666(3)	48(2)
C(15)	2363(4)	5(4)	1068(3)	41(1)
C(16)	2870(4)	-580(4)	941(3)	41(2)
C(17)	3601(4)	-657(4)	1309(3)	37(1)
C(18)	3782(4)	-169(4)	1815(3)	44(2)
C(19)	3281(4)	410(4)	1951(3)	38(1)
C(20)	2589(4)	488(3)	1573(3)	38(1)
C(21)	3501(4)	922(4)	2517(3)	50(2)
C(22)	3057(4)	681(4)	2987(3)	39(1)
C(23)	3247(4)	-39(4)	3301(3)	52(2)
C(24)	2803(5)	-299(5)	3698(3)	62(2)
C(25)	2182(5)	150(4)	3788(3)	55(2)
C(26)	1989(4)	850(4)	3481(3)	42(1)
C(27)	2452(4)	1124(3)	3096(3)	36(1)
C(28)	1263(4)	1314(5)	3541(3)	57(2)
C(29)	-1867(4)	-1199(5)	3872(3)	58(2)

C(30)	-2113(5)	-1993(5)	3696(4)	66(2)
C(31)	-2525(5)	-2419(5)	4034(4)	67(2)
C(32)	-2694(4)	-2071(5)	4537(4)	59(2)
C(33)	-2479(5)	-1278(5)	4707(4)	64(2)
C(34)	-2057(5)	-859(5)	4369(4)	62(2)
C(35)	4574(4)	-2127(4)	636(3)	40(1)
C(36)	4374(4)	-2693(4)	180(3)	48(2)
C(37)	4888(4)	-3215(4)	28(3)	53(2)
C(38)	5618(4)	-3185(4)	342(3)	49(2)
C(39)	5863(4)	-2616(5)	807(4)	60(2)
C(40)	5321(4)	-2107(5)	942(3)	59(2)
C(41)	41(4)	1345(4)	512(3)	46(2)
C(42)	152(5)	2220(4)	480(3)	61(2)
C(43)	-66(7)	3471(5)	881(4)	87(3)
C(44)	-331(7)	3930(5)	1335(4)	91(3)
C(45)	260(5)	3166(5)	2206(4)	63(2)
C(46)	-467(5)	2758(4)	2274(4)	64(2)
C(47)	-1569(5)	3064(5)	2684(3)	58(2)
C(48)	-2021(4)	3640(4)	2865(3)	54(2)
C(49)	-2691(5)	3399(6)	3036(4)	74(2)
C(50)	-2879(6)	2573(7)	3032(5)	93(3)
C(51)	-2449(6)	2036(6)	2825(5)	86(3)
C(52)	-1787(5)	2232(5)	2651(4)	67(2)
C(53)	-1874(5)	4537(5)	2906(4)	62(2)
C(54)	-1076(6)	4849(6)	2940(6)	97(3)
C(55)	2581(5)	2553(4)	3095(4)	63(2)
C(56)	2654(8)	3193(5)	2677(5)	101(3)
C(57)	3664(7)	3507(6)	2254(6)	101(3)
C(58)	4301(9)	3283(9)	1972(6)	138(5)
C(59)	4833(7)	2408(8)	1403(5)	112(3)
C(60)	4636(6)	1618(8)	1041(5)	103(3)
C(61)	3619(6)	1198(6)	242(5)	79(2)
C(62)	2874(6)	1328(5)	-52(4)	73(2)

C(63)	2549(7)	744(6)	-465(4)	86(2)
C(64)	2932(9)	69(7)	-573(5)	106(3)
C(65)	3640(8)	-59(7)	-279(6)	103(3)
C(66)	3979(7)	521(7)	115(5)	96(3)
C(67)	2372(7)	2010(6)	46(5)	86(3)
C(68)	2552(6)	2521(6)	605(5)	95(3)
C(69)	-625(13)	6193(5)	854(5)	630(40)
N(1)	-961(3)	-332(4)	3752(3)	53(2)
N(2)	-1439(4)	-819(4)	3492(3)	64(2)
N(3)	-3096(4)	-2536(6)	4924(4)	77(2)
N(4)	4163(3)	-1177(3)	1202(2)	43(1)
N(5)	3975(3)	-1618(3)	747(3)	48(1)
N(6)	6197(4)	-3741(4)	199(4)	68(2)
O(1)	723(3)	1247(3)	2323(2)	47(1)
O(2)	469(2)	1050(2)	1076(2)	40(1)
O(3)	2061(3)	1060(3)	1661(2)	49(1)
O(4)	2260(3)	1837(2)	2779(2)	47(1)
O(5)	-3184(4)	-3253(5)	4801(4)	103(2)
O(6)	-3315(5)	-2213(6)	5321(4)	122(3)
O(7)	6000(4)	-4193(4)	-227(3)	102(2)
O(8)	6831(4)	-3723(5)	489(4)	113(3)
O(9)	-184(3)	2636(3)	896(2)	61(1)
O(10)	110(3)	3934(3)	1903(3)	67(2)
O(11)	-920(3)	3326(3)	2524(3)	63(1)
O(12)	-2378(4)	4997(4)	2956(3)	90(2)
O(13)	3350(7)	2982(5)	2473(5)	169(4)
O(14)	4272(4)	2533(5)	1725(3)	104(2)
O(15)	3942(4)	1771(4)	617(3)	95(2)
O(16)	1777(5)	2149(5)	-335(5)	136(3)
Cl(1)	-1219(3)	5580(3)	202(2)	161(2)
Cl(2)	-1327(5)	5817(5)	1349(4)	266(3)

Table A3. Bond lengths [Å] and angles [°].

C(1)-O(1)	1.354(7)
C(1)-C(6)	1.405(9)
C(1)-C(2)	1.389(9)
C(2)-C(3)	1.389(9)
C(2)-C(28)	1.511(10)
C(3)-C(4)	1.358(10)
C(4)-C(5)	1.377(10)
C(4)-N(1)	1.445(8)
C(5)-C(6)	1.376(8)
C(6)-C(7)	1.517(10)
C(7)-C(8)	1.527(9)
C(8)-C(13)	1.379(9)
C(8)-C(9)	1.399(10)
C(9)-C(10)	1.365(11)
C(10)-C(11)	1.367(11)
C(11)-C(12)	1.386(9)
C(12)-C(13)	1.388(9)
C(12)-C(14)	1.522(9)
C(13)-O(2)	1.398(7)
C(14)-C(15)	1.509(10)
C(15)-C(16)	1.398(8)
C(15)-C(20)	1.397(9)
C(16)-C(17)	1.411(9)
C(17)-N(4)	1.384(8)
C(17)-C(18)	1.396(9)
C(18)-C(19)	1.392(9)
C(19)-C(20)	1.366(9)
C(19)-C(21)	1.531(9)
C(20)-O(3)	1.382(7)
C(21)-C(22)	1.517(9)
C(22)-C(23)	1.396(9)
C(22)-C(27)	1.373(9)
C(23)-C(24)	1.392(10)
C(24)-C(25)	1.388(11)
C(25)-C(26)	1.363(10)
C(26)-C(27)	1.401(8)
C(26)-C(28)	1.539(10)
C(27)-O(4)	1.392(7)
C(29)-C(30)	1.417(11)
C(29)-C(34)	1.373(11)
C(29)-N(2)	1.419(9)
C(30)-C(31)	1.369(11)
C(31)-C(32)	1.376(12)
C(32)-C(33)	1.400(11)
C(32)-N(3)	1.467(10)
C(33)-C(34)	1.373(10)
C(35)-C(40)	1.379(10)
C(35)-C(36)	1.394(9)

C(35)-N(5)	1.427(8)
C(36)-C(37)	1.358(9)
C(37)-C(38)	1.359(10)
C(38)-C(39)	1.424(10)
C(38)-N(6)	1.472(9)
C(39)-C(40)	1.367(10)
C(41)-O(2)	1.446(7)
C(41)-C(42)	1.466(10)
C(42)-O(9)	1.407(9)
C(43)-O(9)	1.399(9)
C(43)-C(44)	1.443(13)
C(44)-O(10)	1.378(11)
C(45)-O(10)	1.446(9)
C(45)-C(46)	1.504(11)
C(46)-O(11)	1.434(8)
C(47)-O(11)	1.359(9)
C(47)-C(48)	1.370(10)
C(47)-C(52)	1.428(11)
C(48)-C(49)	1.394(11)
C(48)-C(53)	1.508(11)
C(49)-C(50)	1.408(14)
C(50)-C(51)	1.324(14)
C(51)-C(52)	1.366(13)
C(53)-O(12)	1.204(9)
C(53)-C(54)	1.507(13)
C(55)-O(4)	1.447(8)
C(55)-C(56)	1.451(12)
C(56)-O(13)	1.460(14)
C(57)-O(13)	1.198(11)
C(57)-C(58)	1.469(17)
C(58)-O(14)	1.360(14)
C(59)-O(14)	1.377(12)
C(59)-C(60)	1.550(16)
C(60)-O(15)	1.436(13)
C(61)-O(15)	1.330(12)
C(61)-C(66)	1.354(14)
C(61)-C(62)	1.385(14)
C(62)-C(63)	1.394(13)
C(62)-C(67)	1.489(14)
C(63)-C(64)	1.360(14)
C(64)-C(65)	1.326(18)
C(65)-C(66)	1.371(16)
C(67)-O(16)	1.254(13)
C(67)-C(68)	1.512(15)
C(69)-Cl(2)	1.958(16)
C(69)-Cl(1)	1.936(14)
N(1)-N(2)	1.236(8)
N(3)-O(6)	1.188(11)
N(3)-O(5)	1.223(10)
N(4)-N(5)	1.261(7)

N(6)-O(8)	1.193(10)
N(6)-O(7)	1.223(9)
O(1)-C(1)-C(6)	120.3(6)
O(1)-C(1)-C(2)	118.0(6)
C(6)-C(1)-C(2)	121.6(6)
C(3)-C(2)-C(1)	118.6(6)
C(3)-C(2)-C(28)	122.3(6)
C(1)-C(2)-C(28)	119.1(6)
C(4)-C(3)-C(2)	120.4(6)
C(3)-C(4)-C(5)	120.6(6)
C(3)-C(4)-N(1)	117.2(6)
C(5)-C(4)-N(1)	122.2(6)
C(6)-C(5)-C(4)	121.7(7)
C(5)-C(6)-C(1)	117.1(6)
C(5)-C(6)-C(7)	121.8(6)
C(1)-C(6)-C(7)	121.1(6)
C(6)-C(7)-C(8)	111.6(5)
C(13)-C(8)-C(9)	117.3(6)
C(13)-C(8)-C(7)	121.8(6)
C(9)-C(8)-C(7)	120.7(6)
C(10)-C(9)-C(8)	120.5(7)
C(9)-C(10)-C(11)	120.4(7)
C(12)-C(11)-C(10)	121.5(7)
C(11)-C(12)-C(13)	116.7(6)
C(11)-C(12)-C(14)	120.4(6)
C(13)-C(12)-C(14)	122.8(6)
C(8)-C(13)-C(12)	123.2(6)
C(8)-C(13)-O(2)	118.8(5)
C(12)-C(13)-O(2)	117.9(5)
C(15)-C(14)-C(12)	114.4(5)
C(16)-C(15)-C(20)	118.5(6)
C(16)-C(15)-C(14)	119.2(6)
C(20)-C(15)-C(14)	122.3(6)
C(17)-C(16)-C(15)	120.1(6)
C(16)-C(17)-N(4)	124.8(5)
C(16)-C(17)-C(18)	118.4(6)
N(4)-C(17)-C(18)	116.8(6)
C(19)-C(18)-C(17)	122.1(6)
C(18)-C(19)-C(20)	117.9(6)
C(18)-C(19)-C(21)	120.2(6)
C(20)-C(19)-C(21)	121.9(5)
O(3)-C(20)-C(19)	122.2(6)
O(3)-C(20)-C(15)	114.9(6)
C(19)-C(20)-C(15)	122.9(5)
C(22)-C(21)-C(19)	111.9(5)
C(23)-C(22)-C(27)	118.7(6)
C(23)-C(22)-C(21)	118.8(6)
C(27)-C(22)-C(21)	122.4(6)
C(24)-C(23)-C(22)	119.2(7)
C(25)-C(24)-C(23)	120.9(7)

C(24)-C(25)-C(26)	120.4(7)
C(25)-C(26)-C(27)	118.6(6)
C(25)-C(26)-C(28)	120.5(6)
C(27)-C(26)-C(28)	120.9(6)
O(4)-C(27)-C(22)	118.6(5)
O(4)-C(27)-C(26)	119.1(5)
C(22)-C(27)-C(26)	122.1(6)
C(2)-C(28)-C(26)	112.4(5)
C(30)-C(29)-C(34)	120.0(7)
C(30)-C(29)-N(2)	114.4(7)
C(34)-C(29)-N(2)	125.6(7)
C(29)-C(30)-C(31)	119.3(8)
C(32)-C(31)-C(30)	119.6(8)
C(31)-C(32)-C(33)	121.9(7)
C(31)-C(32)-N(3)	120.3(8)
C(33)-C(32)-N(3)	117.8(8)
C(34)-C(33)-C(32)	118.0(7)
C(33)-C(34)-C(29)	121.1(7)
C(40)-C(35)-C(36)	118.1(6)
C(40)-C(35)-N(5)	125.7(6)
C(36)-C(35)-N(5)	116.2(6)
C(37)-C(36)-C(35)	122.3(7)
C(36)-C(37)-C(38)	118.2(6)
C(37)-C(38)-C(39)	122.4(6)
C(37)-C(38)-N(6)	120.5(7)
C(39)-C(38)-N(6)	117.1(7)
C(38)-C(39)-C(40)	116.8(7)
C(35)-C(40)-C(39)	122.1(7)
O(2)-C(41)-C(42)	109.0(6)
O(9)-C(42)-C(41)	111.6(6)
O(9)-C(43)-C(44)	115.4(8)
O(10)-C(44)-C(43)	118.2(9)
O(10)-C(45)-C(46)	111.4(7)
O(11)-C(46)-C(45)	108.6(6)
O(11)-C(47)-C(48)	116.8(7)
O(11)-C(47)-C(52)	122.2(7)
C(48)-C(47)-C(52)	121.0(7)
C(47)-C(48)-C(49)	118.8(8)
C(47)-C(48)-C(53)	126.7(7)
C(49)-C(48)-C(53)	114.5(7)
C(50)-C(49)-C(48)	119.6(8)
C(51)-C(50)-C(49)	119.9(9)
C(50)-C(51)-C(52)	123.2(9)
C(51)-C(52)-C(47)	117.3(8)
O(12)-C(53)-C(48)	120.2(8)
O(12)-C(53)-C(54)	120.0(8)
C(48)-C(53)-C(54)	119.5(7)
O(4)-C(55)-C(56)	110.4(7)
O(13)-C(56)-C(55)	103.6(9)
O(13)-C(57)-C(58)	118.3(11)

O(14)-C(58)-C(57)	116.4(9)
O(14)-C(59)-C(60)	107.5(8)
O(15)-C(60)-C(59)	106.5(10)
O(15)-C(61)-C(66)	124.5(11)
O(15)-C(61)-C(62)	116.9(9)
C(66)-C(61)-C(62)	118.6(11)
C(63)-C(62)-C(61)	116.8(10)
C(63)-C(62)-C(67)	116.5(10)
C(61)-C(62)-C(67)	126.6(10)
C(64)-C(63)-C(62)	122.4(12)
C(65)-C(64)-C(63)	120.3(13)
C(64)-C(65)-C(66)	118.2(12)
C(65)-C(66)-C(61)	123.6(13)
O(16)-C(67)-C(62)	119.2(10)
O(16)-C(67)-C(68)	119.4(10)
C(62)-C(67)-C(68)	121.3(10)
Cl(2)-C(69)-Cl(1)	87.9(8)
N(2)-N(1)-C(4)	113.7(6)
N(1)-N(2)-C(29)	113.7(6)
O(6)-N(3)-O(5)	124.5(8)
O(6)-N(3)-C(32)	120.3(9)
O(5)-N(3)-C(32)	115.3(9)
N(5)-N(4)-C(17)	115.1(6)
N(4)-N(5)-C(35)	113.8(6)
O(8)-N(6)-O(7)	123.2(7)
O(8)-N(6)-C(38)	119.7(7)
O(7)-N(6)-C(38)	117.2(8)
C(13)-O(2)-C(41)	112.8(5)
C(27)-O(4)-C(55)	113.7(5)
C(42)-O(9)-C(43)	112.3(6)
C(44)-O(10)-C(45)	117.6(6)
C(47)-O(11)-C(46)	118.9(6)
C(57)-O(13)-C(56)	117.8(10)
C(58)-O(14)-C(59)	112.8(9)
C(61)-O(15)-C(60)	120.9(9)

APPENDIX B

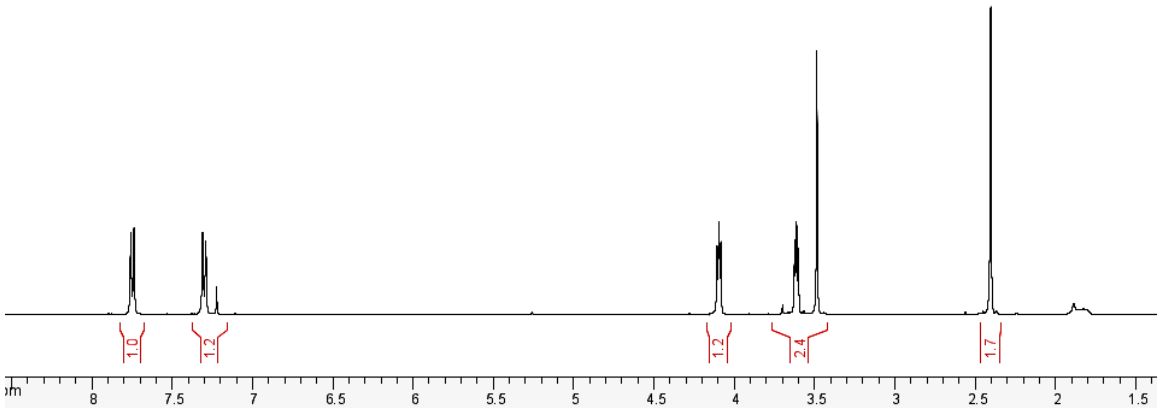

Figure B1. ^{1}H-NMR ($CDCl_3$, 400 MHz) spectrum of triethyleneglycol ditosylate (**1**).

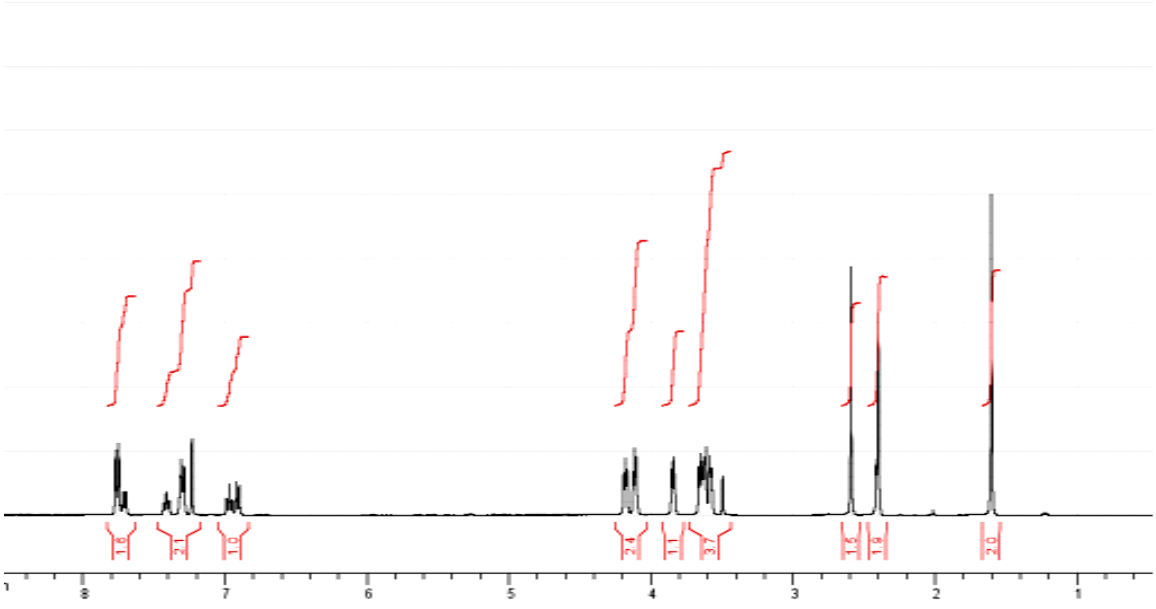

Figure B2. ^{1}H-NMR ($CDCl_3$, 400 MHz) spectrum of 2-(8-tosyltriethyleneglycol)acetophenone (**2**).

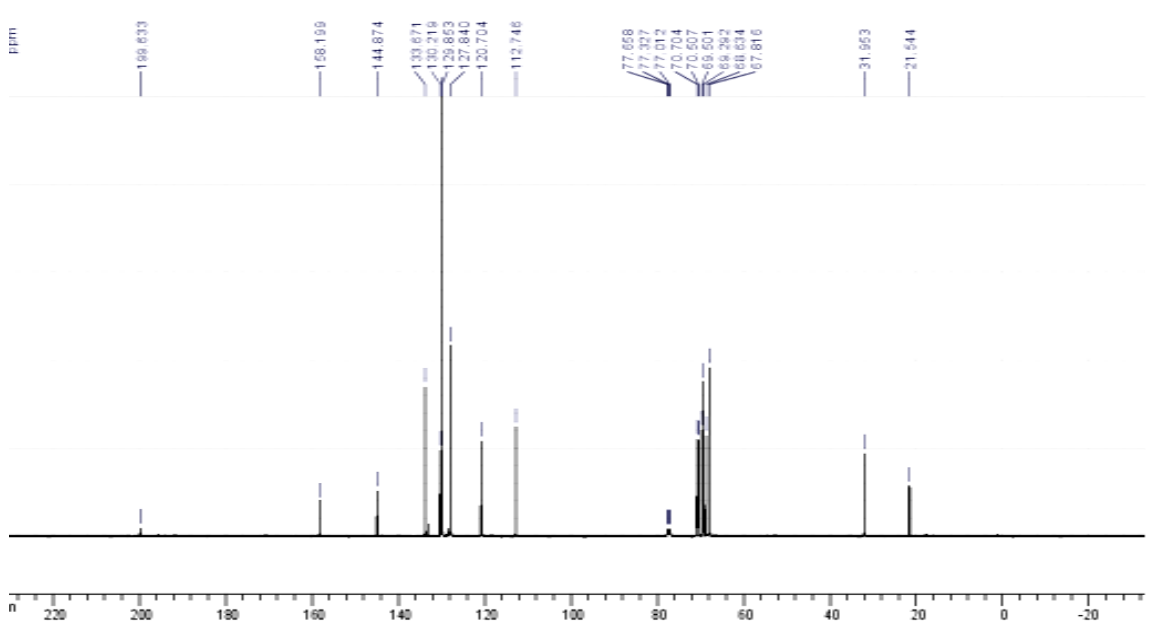

Figure B3. ^{13}C-NMR ($CDCl_3$, 400 MHz) spectrum of 2-(8-tosyltriethyleneglycol)acetophenone (**2**).

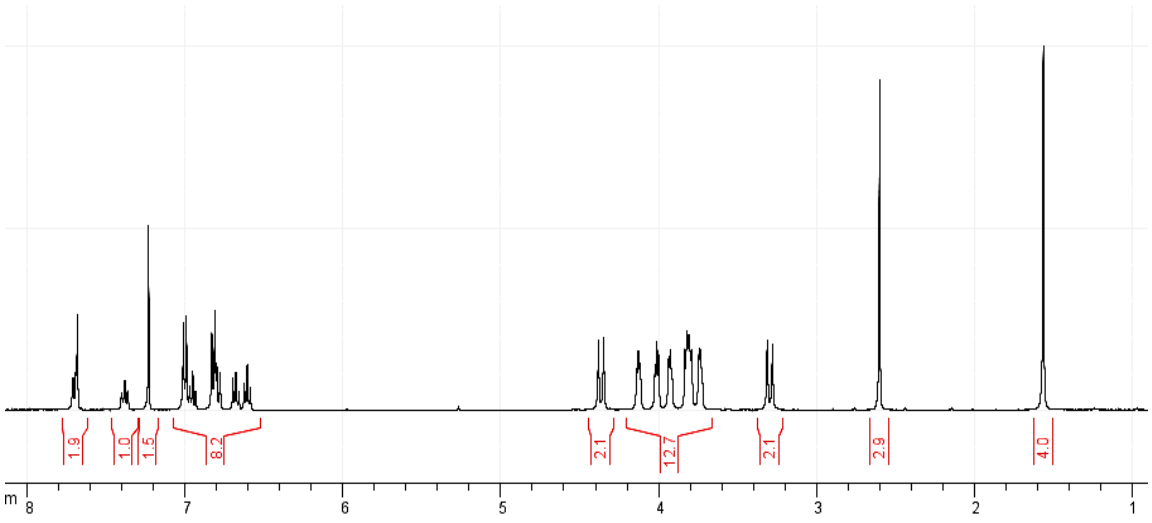

Figure B4. ^{1}H-NMR ($CDCl_3$, 400 MHz) spectrum of 1,3-calix[4]-diacetophenone (**3**).

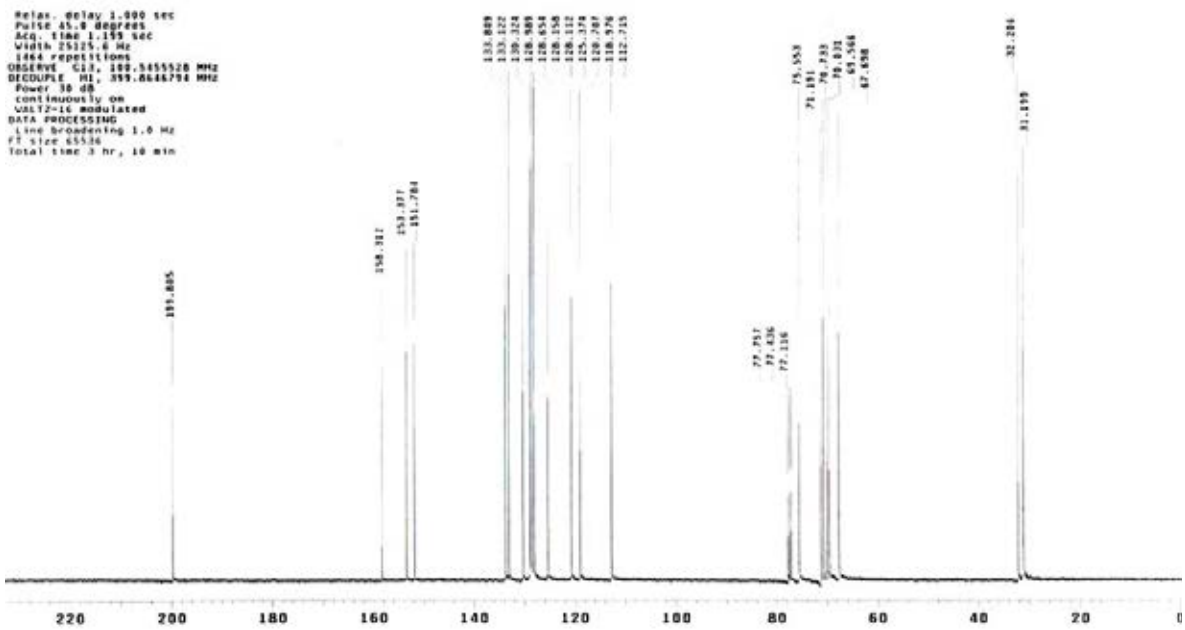

Figure B5. ^{13}C-NMR ($CDCl_3$, 400 MHz) spectrum of 1,3-calix[4]-diacetophenone (3).

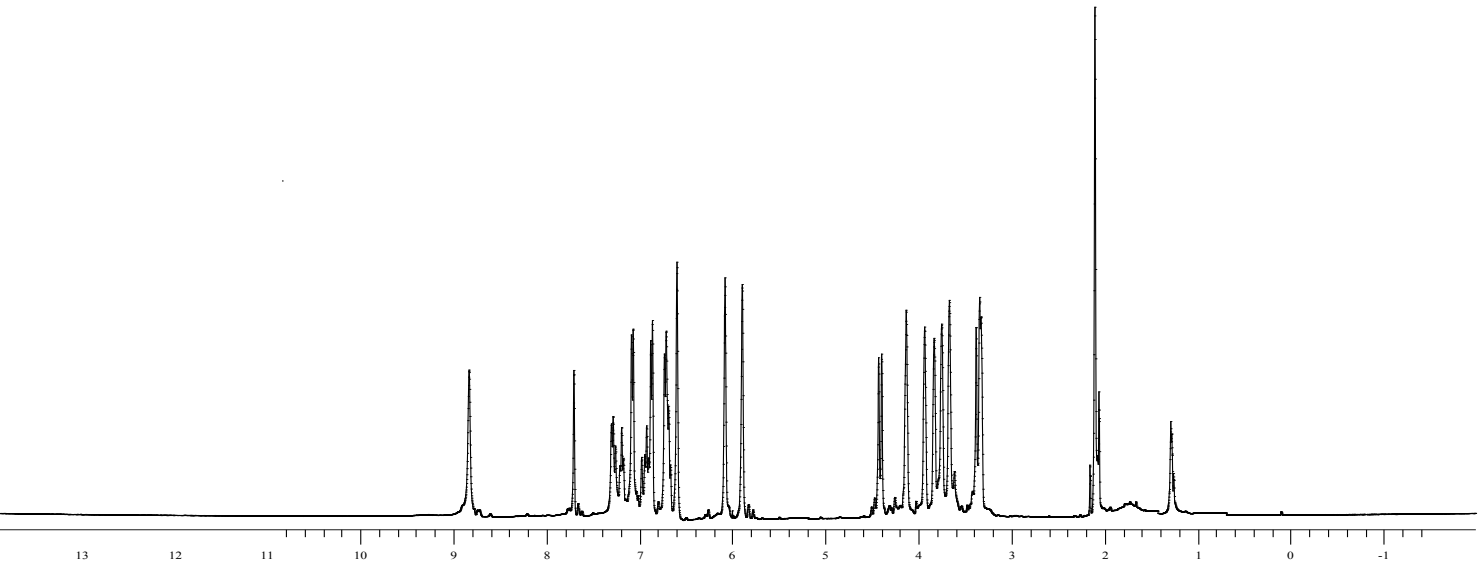

Figure B6. ^{1}H-NMR ($CDCl_3$, 400 MHz) spectrum of 1, 3-calix[4]arene-bis-dipyrroethane (**4**)

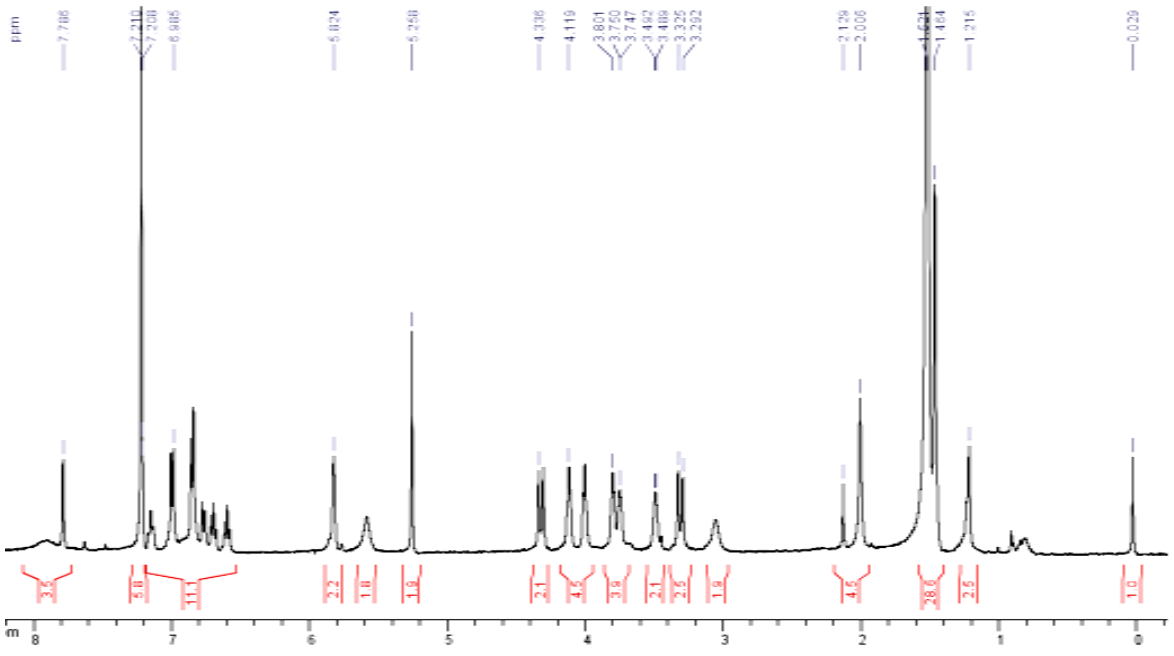

Figure B7. ^{1}H-NMR ($CDCl_3$, 400 MHz) spectrum of calix[4]arene-calix[4]pyrrole (**5**)

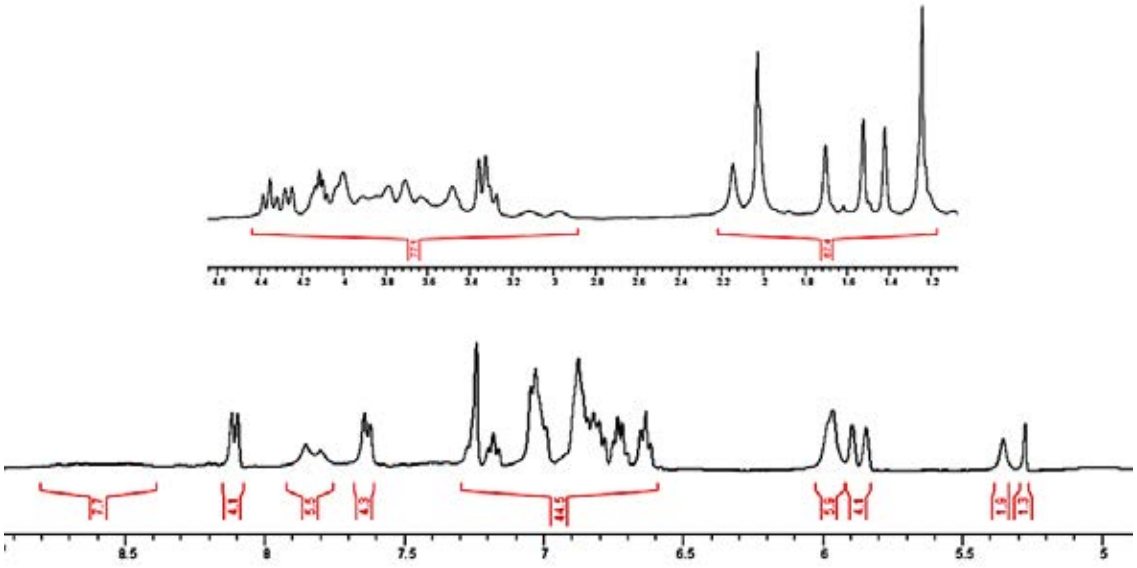

Figure B8. ^{1}H-NMR ($CDCl_3$, 400 MHz) spectrum of calix[4]arene-p-nitrophenylazo-calix[4]pyrrole (**6**)

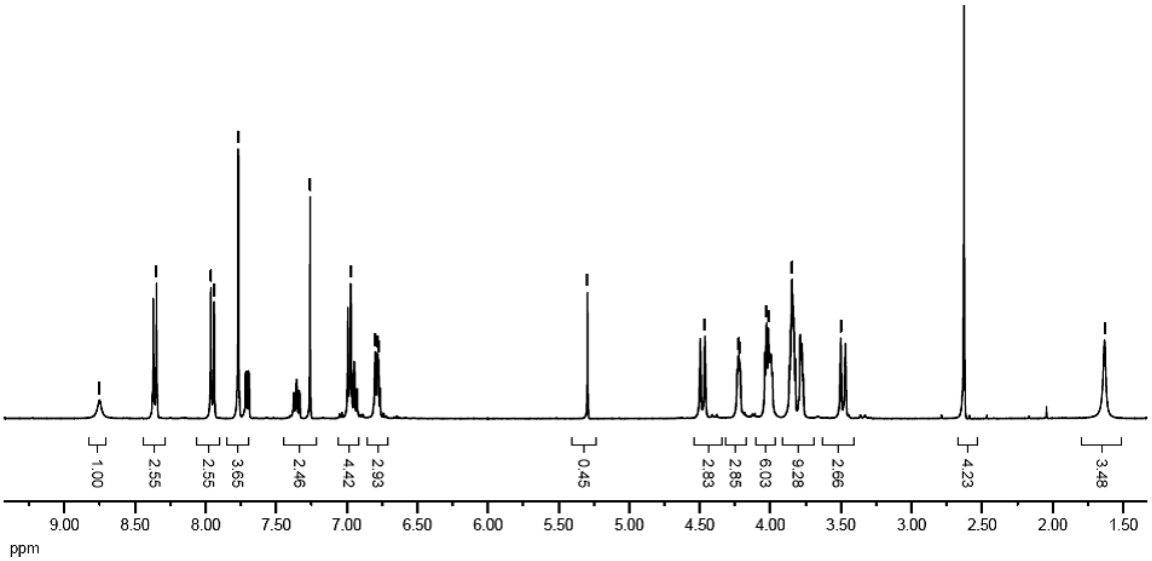

Figure B9. ^{1}H-NMR ($CDCl_3$, 400 MHz) spectrum of 1,3-di-*p*-nitrophenylazo-calix[4]-diacetophenone (**7**)

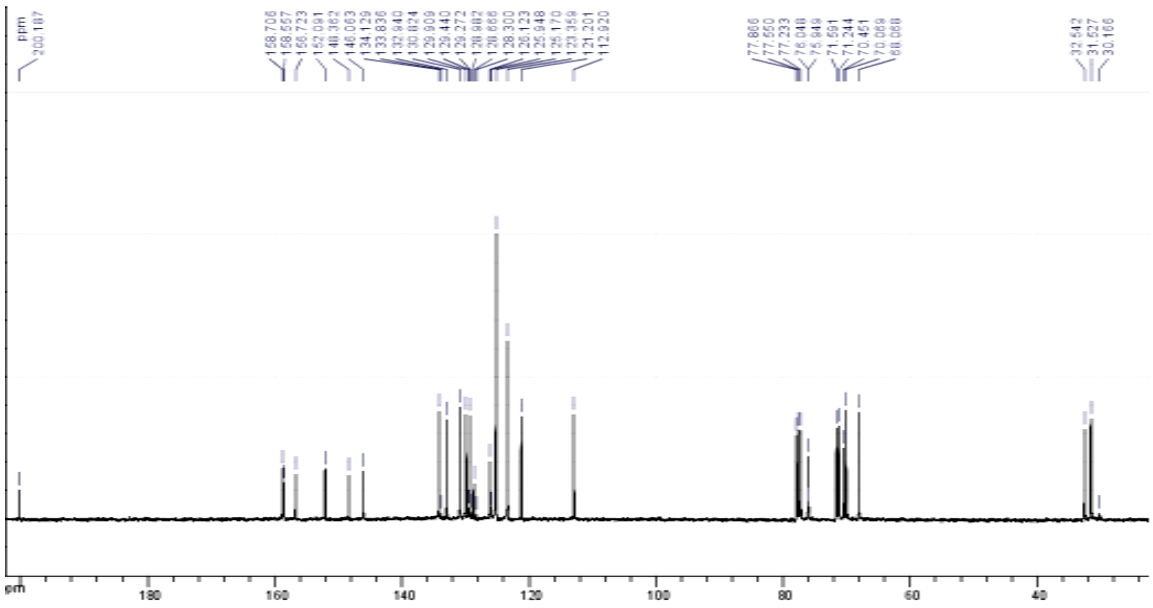

Figure B10. ^{13}C-NMR ($CDCl_3$, 400 MHz) spectrum of 1,3-di-*p*-nitrophenylazo-calix[4]-diacetophenone (**7**)

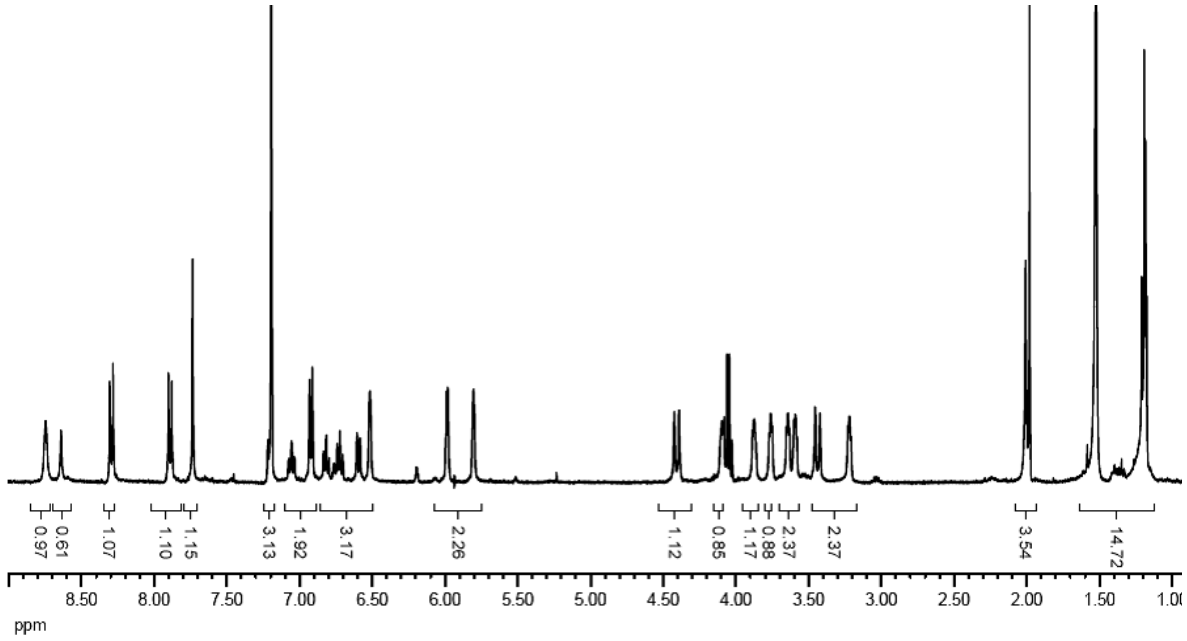

Figure B11. ^{1}H-NMR ($CDCl_3$, 400 MHz) spectrum of 1,3-di-*p*-nitrophenylazo-calix[4]arene-bis-dipyrroethane (**8**).

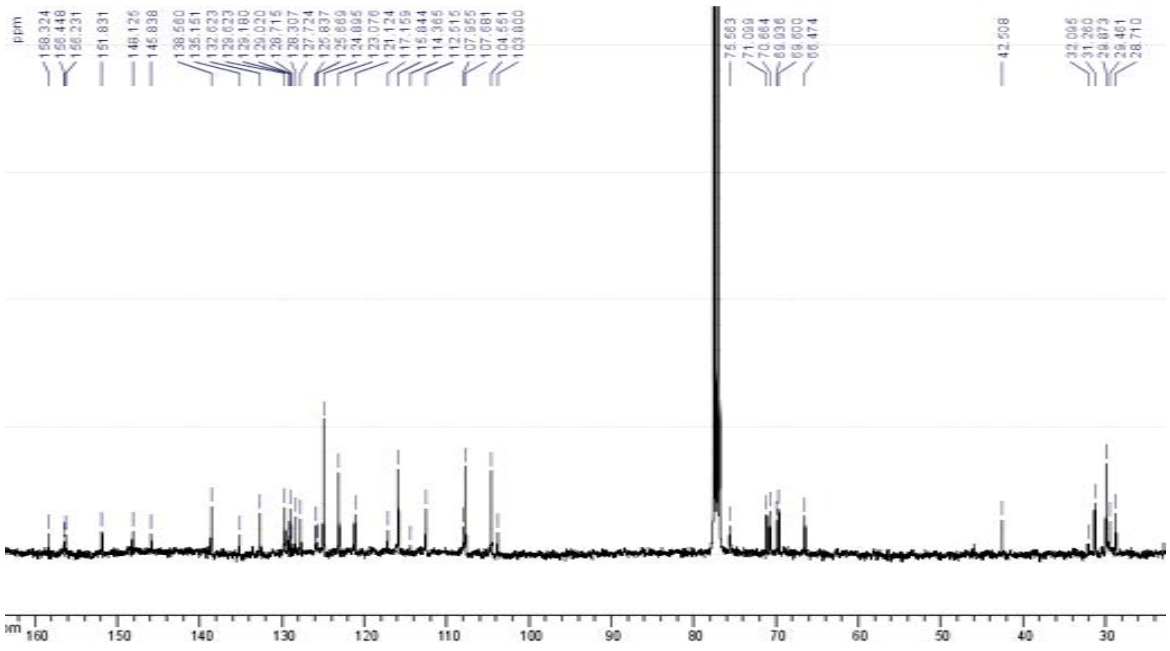

Figure B12. ^{1}H-NMR ($CDCl_3$, 400 MHz) spectrum of 1,3-di-*p*-nitrophenylazo-calix[4]arene-bis-dipyrroethane (**8**).

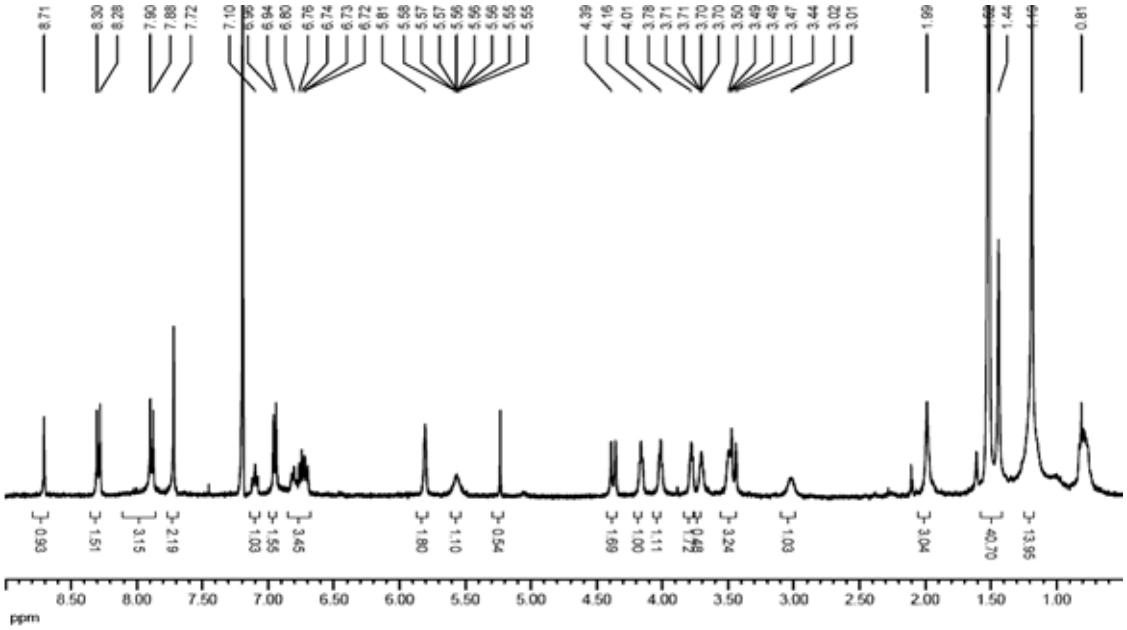

Figure B13. ^{1}H-NMR ($CDCl_3$, 400 MHz) spectrum of 1,3-di-*p*-nitrophenylazo-calix[4]arene-calix[4]pyrrole (**9**).

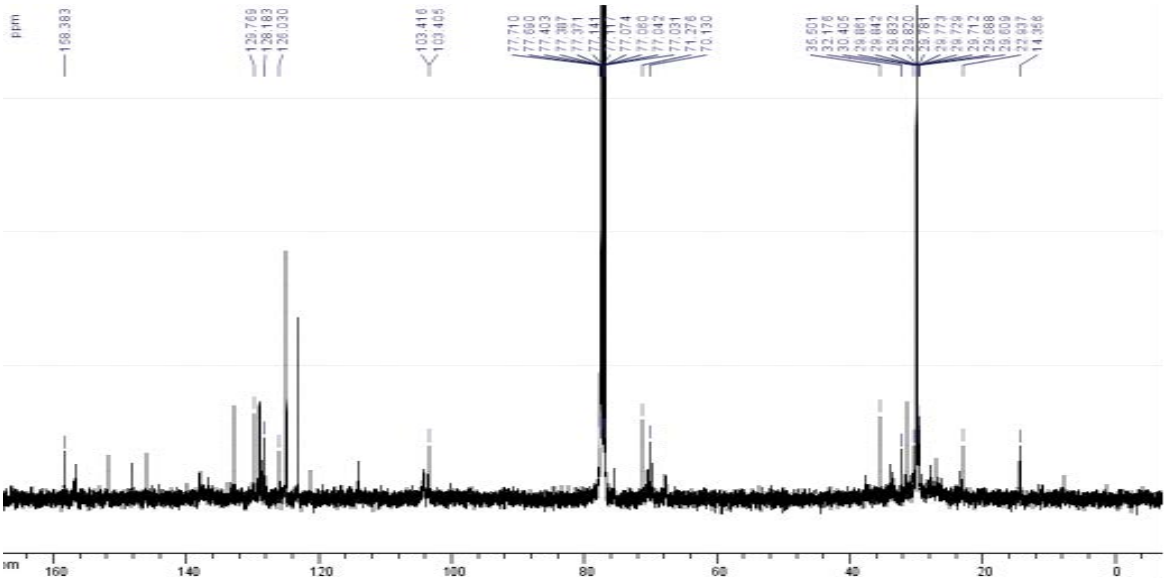

Figure B14. ^{1}H-NMR ($CDCl_3$, 400 MHz) spectrum of 1,3-di-*p*-nitrophenylazo-calix[4]arene-calix[4]pyrrole (**9**).

APPENDIX C

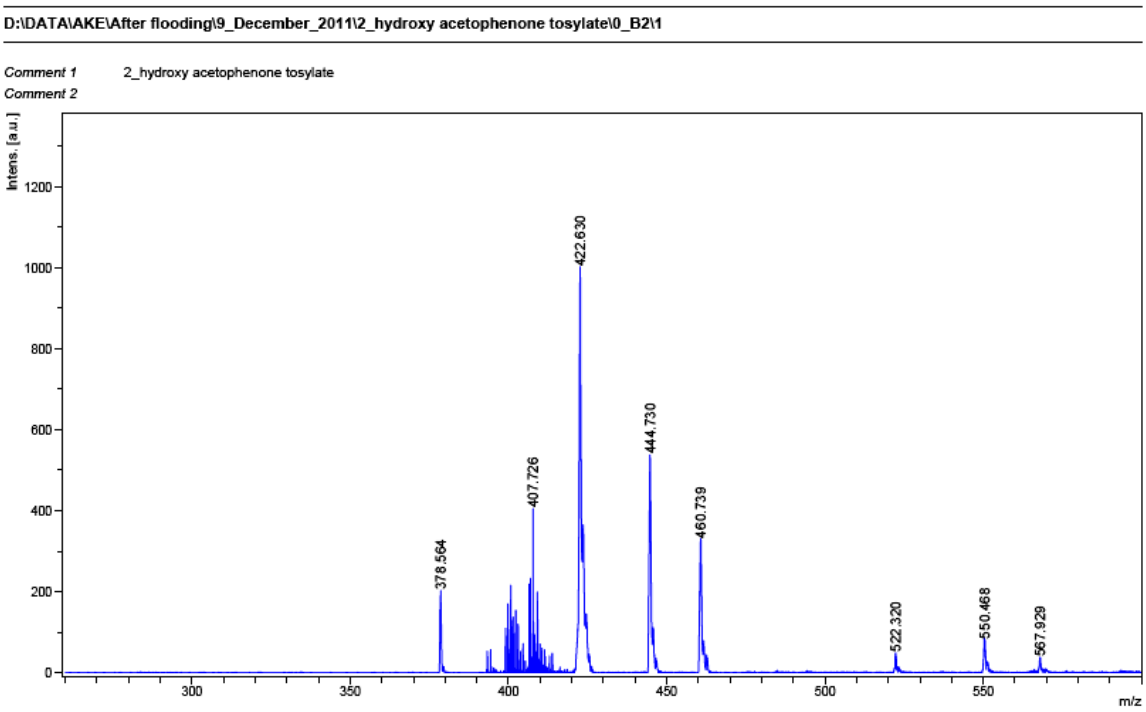

Figure C1. MALDI-TOF mass spectrum of 2-(8-tosyltriethyleneglycol)acetophenone (**2**).

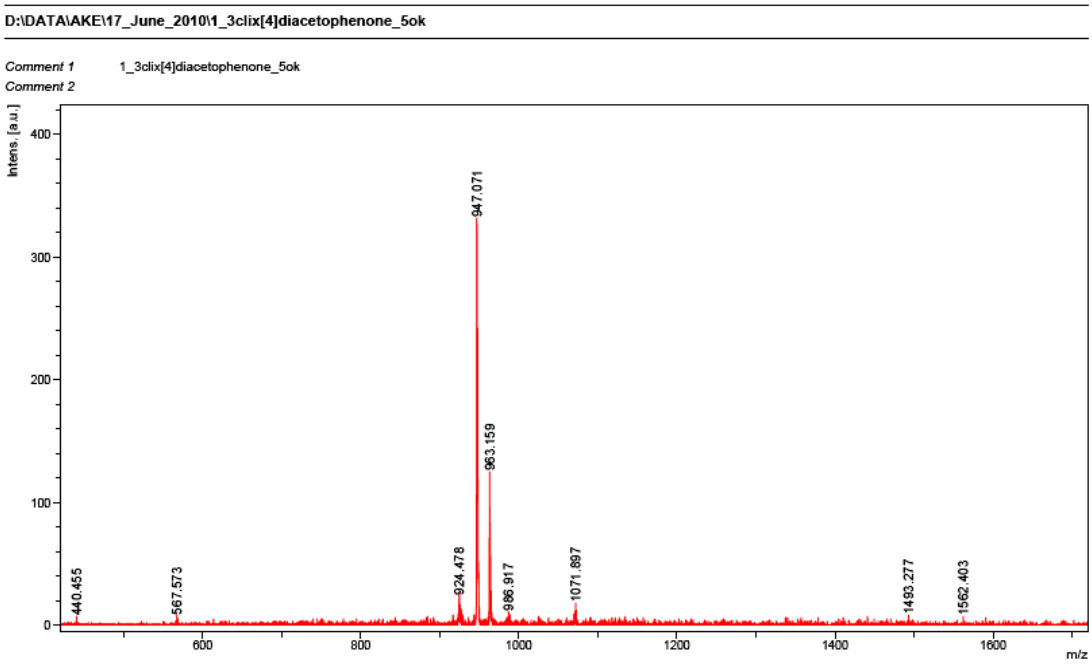

Figure C2. MALDI-TOF mass spectrum of 1,3-calix[4]-diacetophenone (**3**).

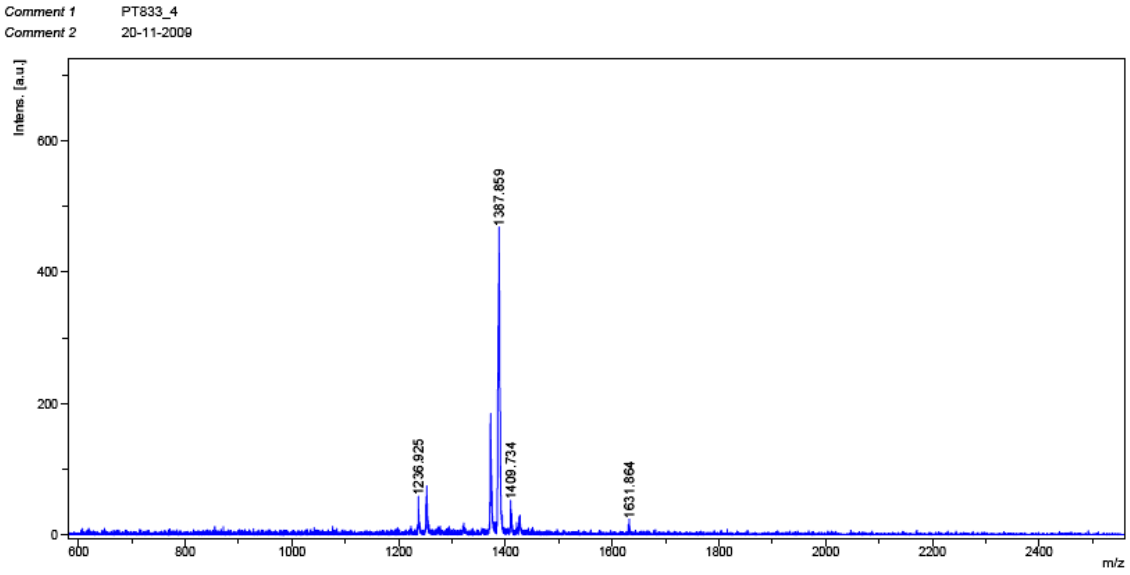

Figure C3. MALDI-TOF mass spectrum of calix[4]arene-*p*-nitrophenylazo-calix[4]pyrrole (**6**).

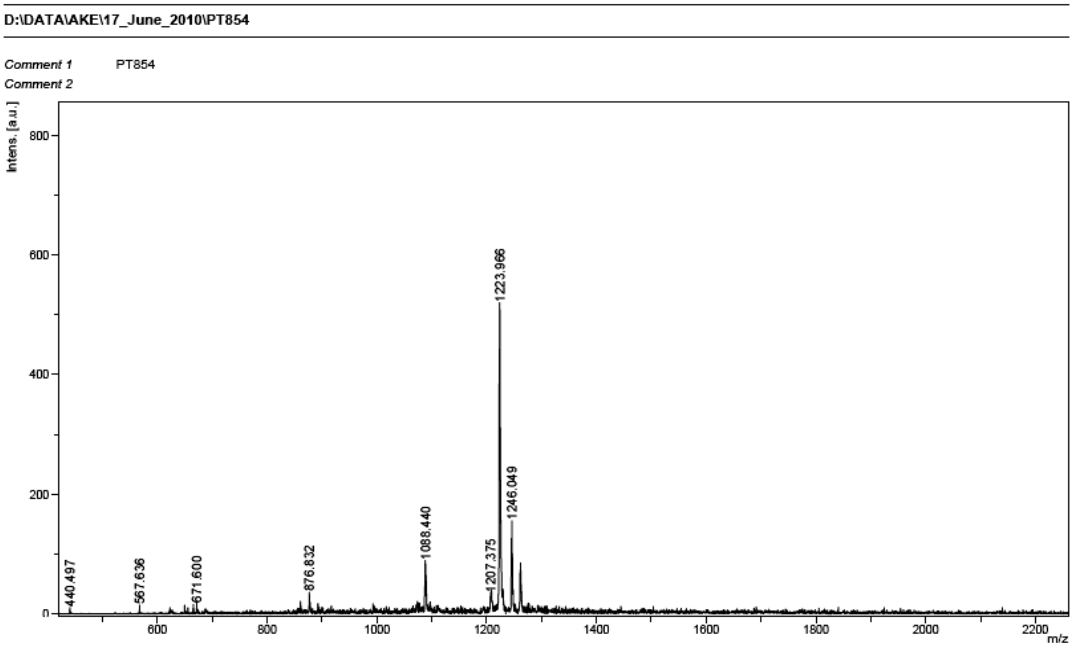

Figure C4. MALDI-TOF mass spectrum of 1,3-di-*p*-nitrophenylazo-calix[4]-diacetophenone (**7**).

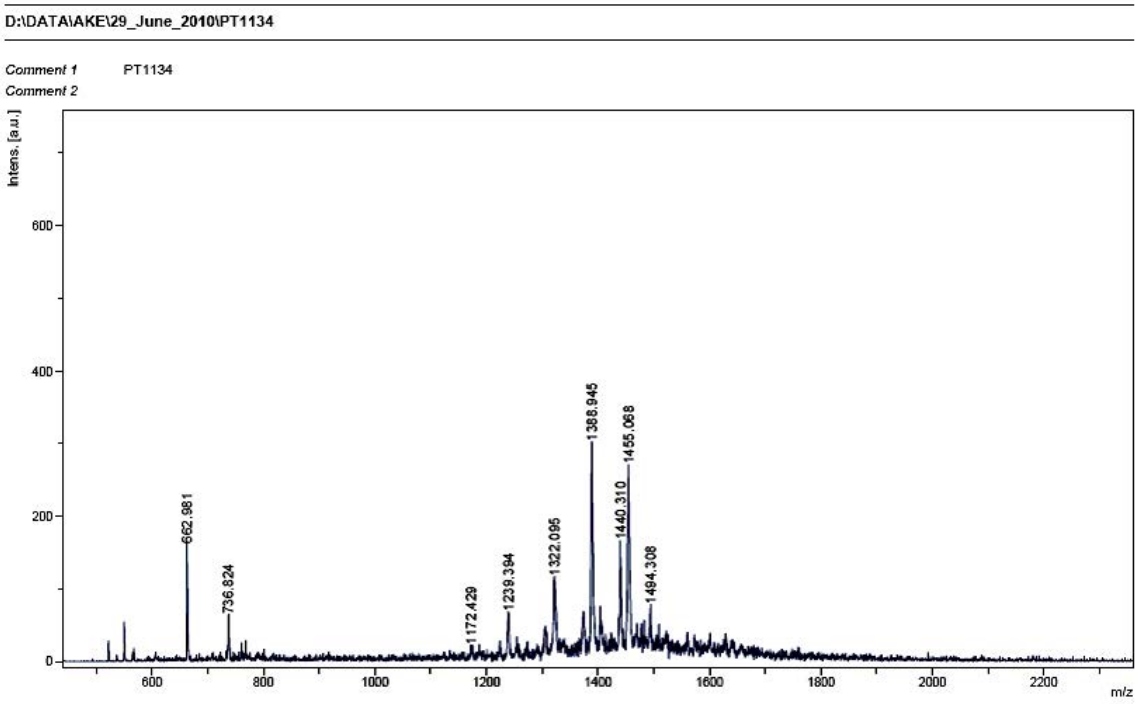

Figure C5. MALDI-TOF mass spectrum of 1,3-di-*p*-nitrophenylazo-calix[4]arene-bis-dipyrroethane (**8)**.

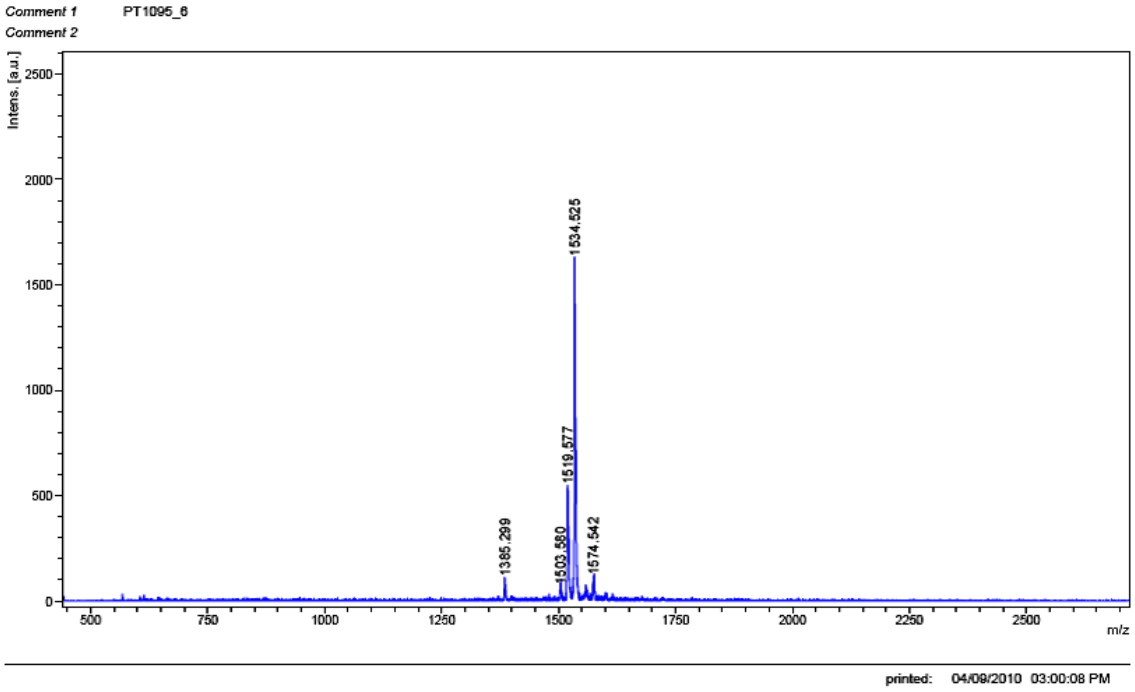

Figure C6. MALDI-TOF mass spectrum of 1,3-di-*p*-nitrophenylazo-calix[4]arene-calix[4]pyrrole (**9**).

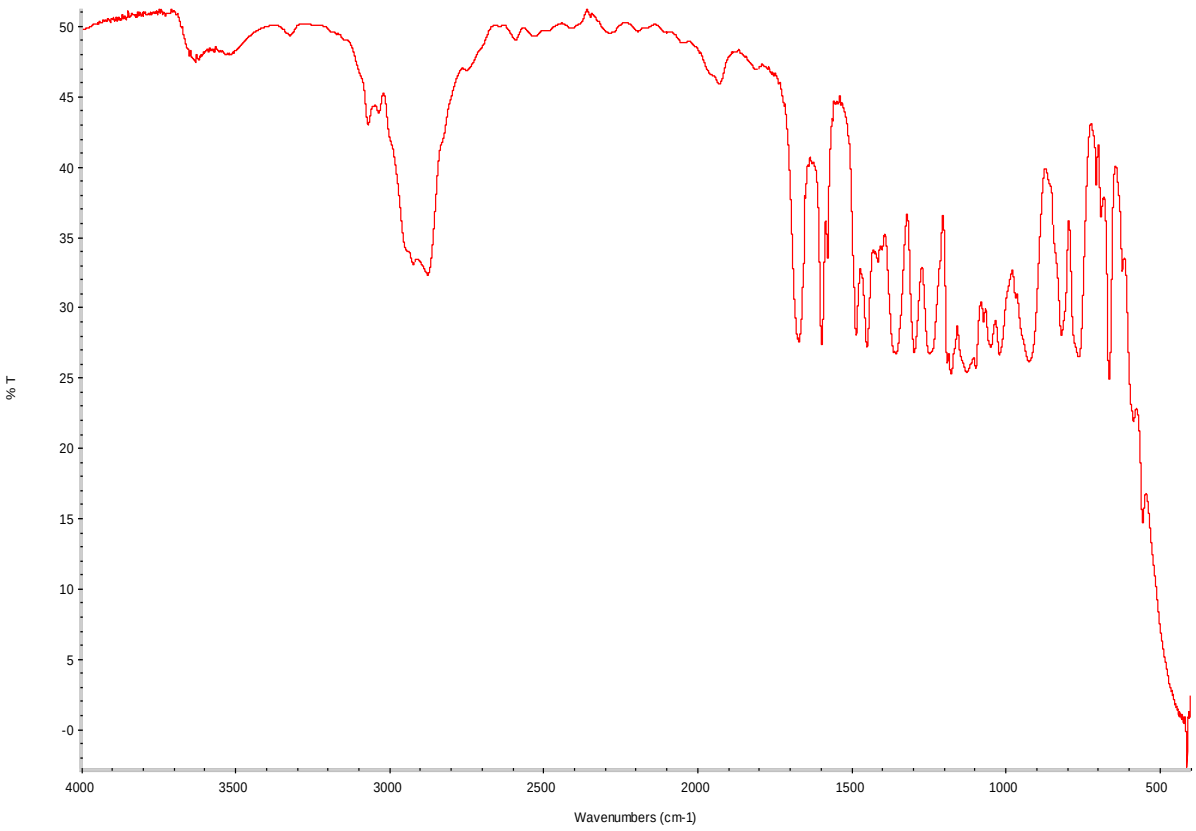

Figure C7. IR spectrum of 2-(8-tosyltriethyleneglycol)acetophenone (**2**).

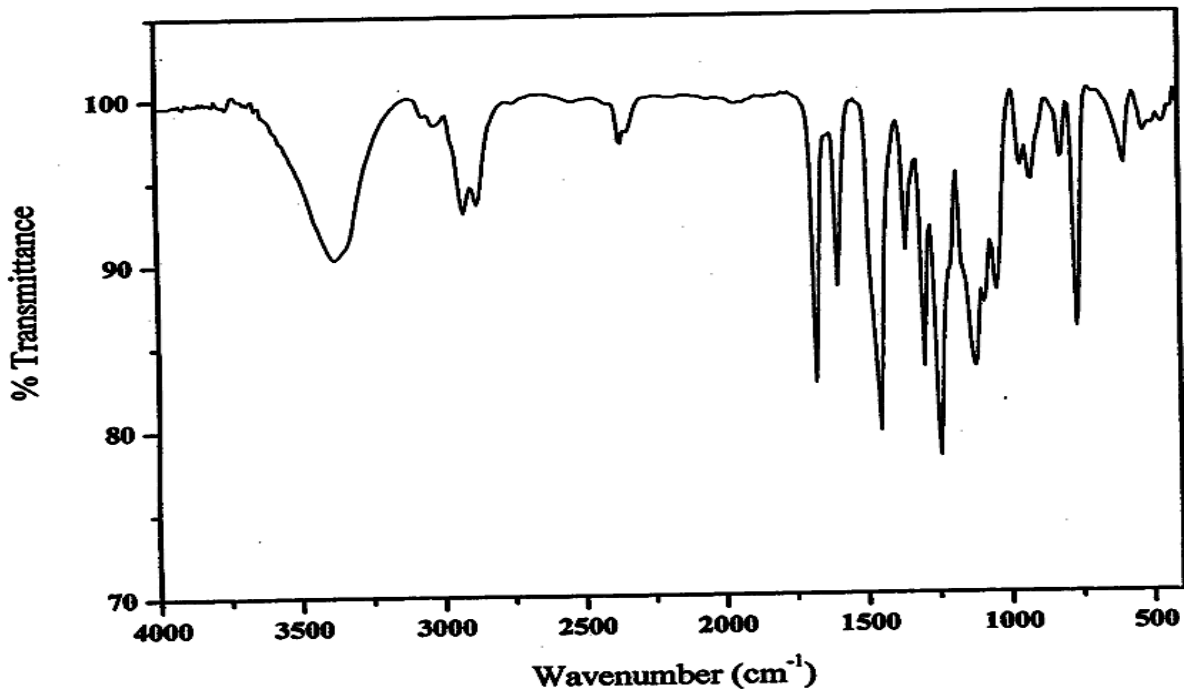

Figure C8. IR spectrum of 1,3 -calix[4]-diacetophenone (**3**).

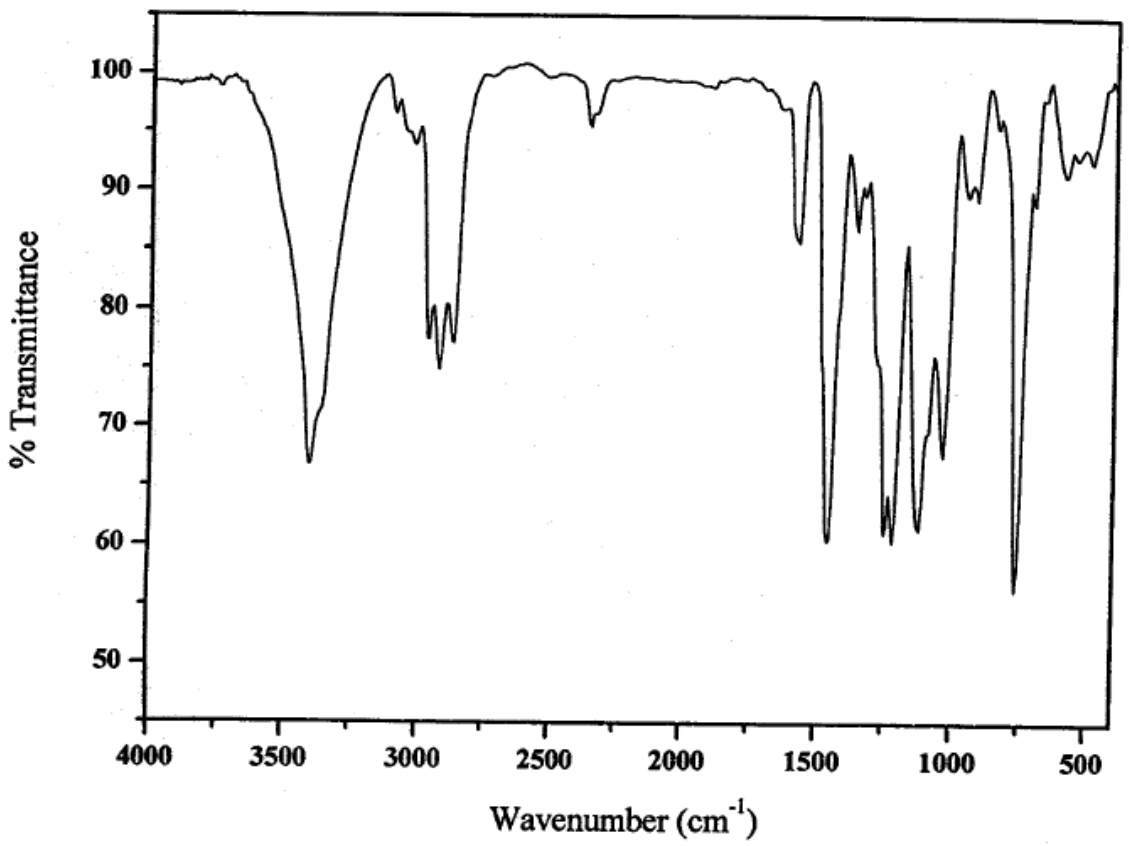

Figure C9. IR spectrum of calix[4]arene-calix[4]pyrrole (**5**).

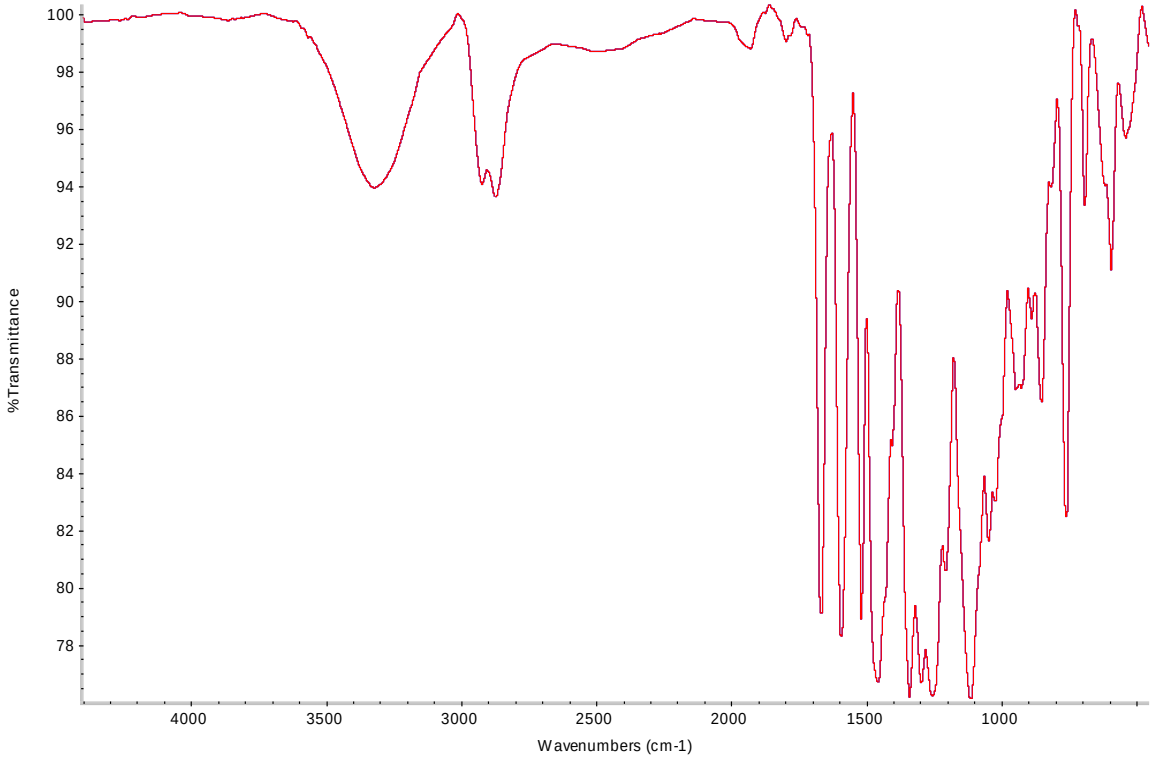

Figure C10. IR spectrum of 1,3-di-*p*-nitrophenylazo-calix[4]-diacetophenone (**7**).

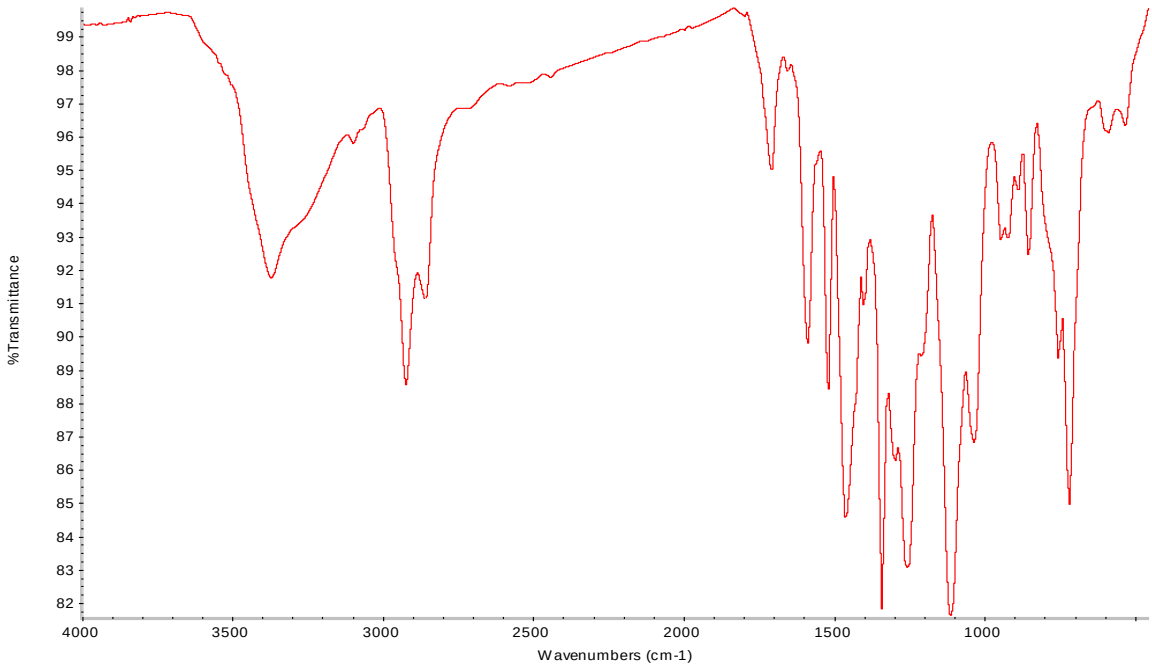

Figure C11. IR spectrum of 1,3-di-*p*-nitrophenylazo-calix[4]arene-bis-dipyrroethane (**8**).

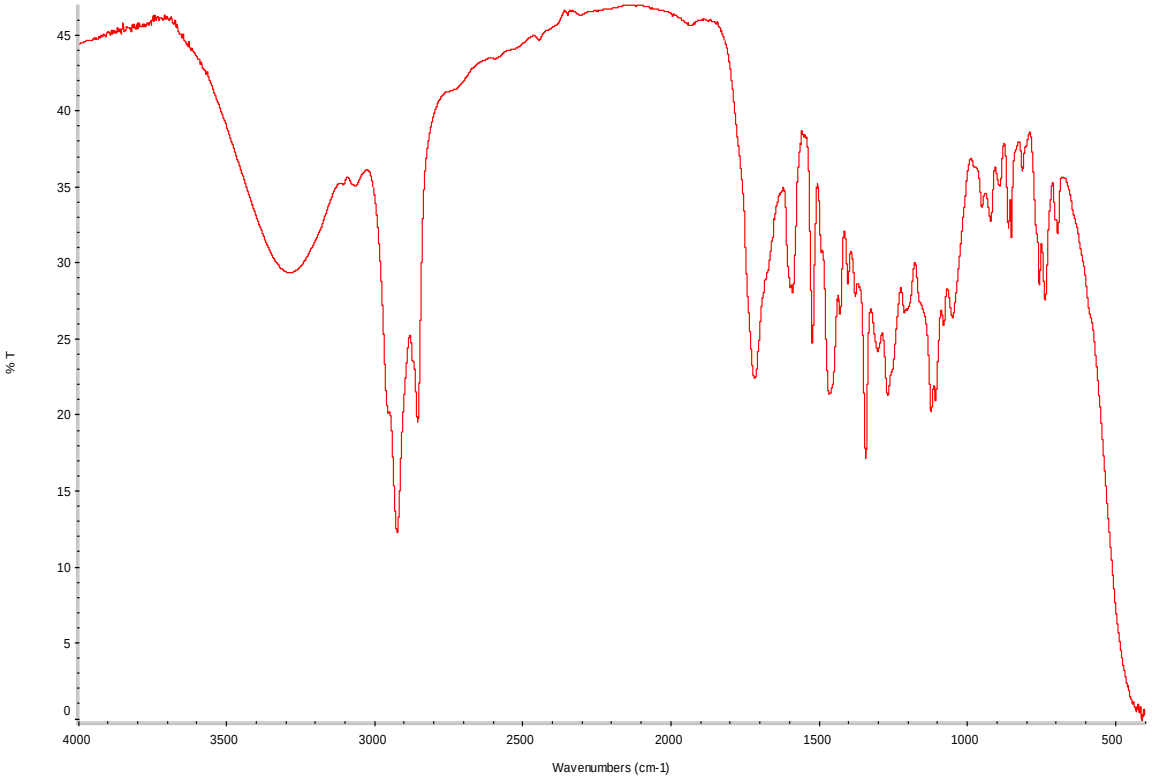

Figure C12. IR spectrum of 1,3-di-*p*-nitrophenylazo-calix[4]arene-calix[4]pyrrole (**9**).

APPENDIX D

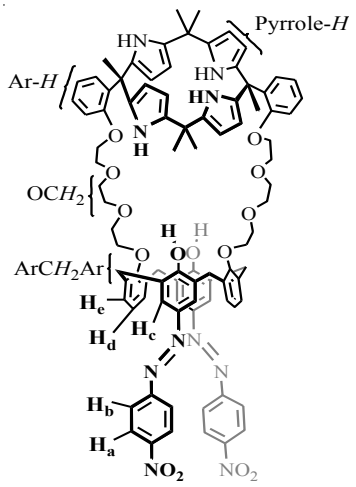

9

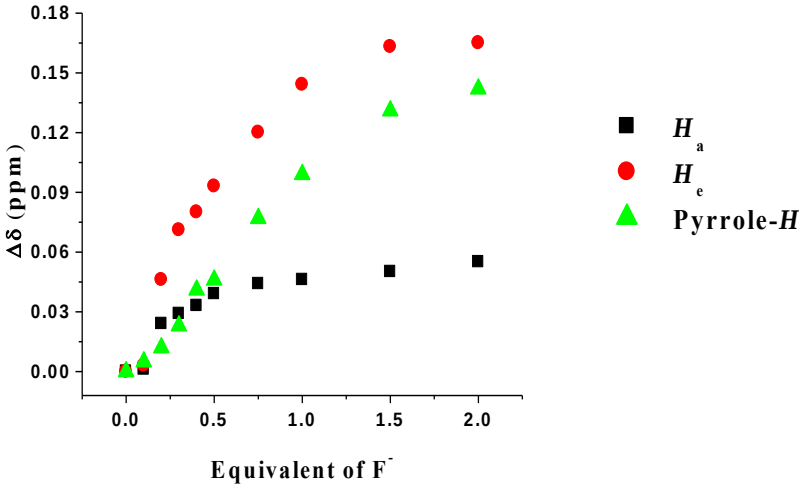

Figure D1. Titration binding curves of receptor **9** (3.58 mM in CD_3CN) with F^- by following the Pyrole-***H*** [▲], proton H_a [■], proton H_e [●].

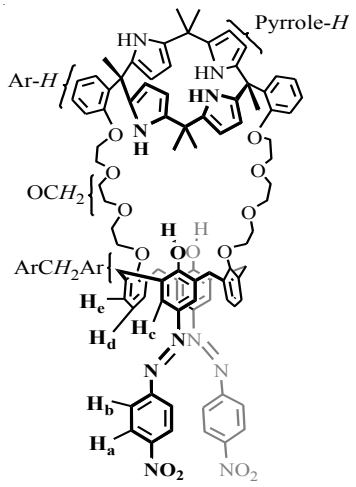

9

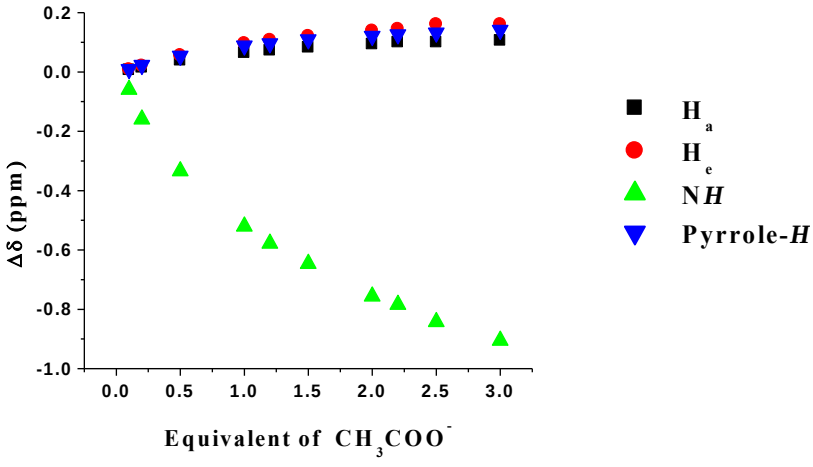

Figure D2. Titration binding curves of receptor **9** (3.58 mM in CD_3CN) with AcO^- by following the N-***H*** [▲], Pyrrole-***H*** [▼], proton H_a [■], proton H_e [●].

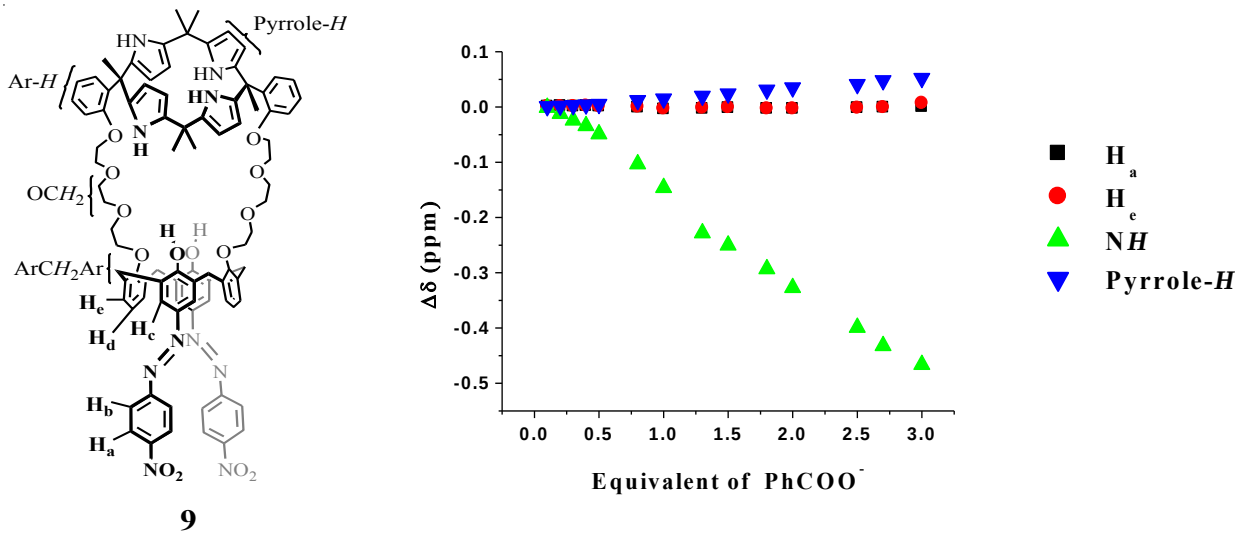

Figure D3. Titration binding curves of receptor **9** (3.58 mM in CD_3CN) with BzO^- by following the N-***H*** [▲], Pyrrole-***H*** [▼], proton H_a [■], proton H_e [●].

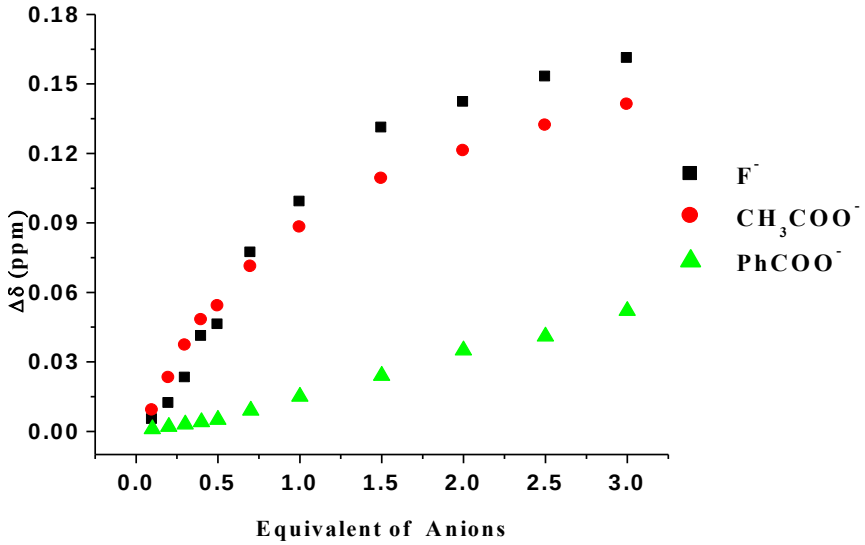

Figure D4. Chemical shift changes of **9** (0.65 mM) in the pyrrole-*H* with the diffrient anions.

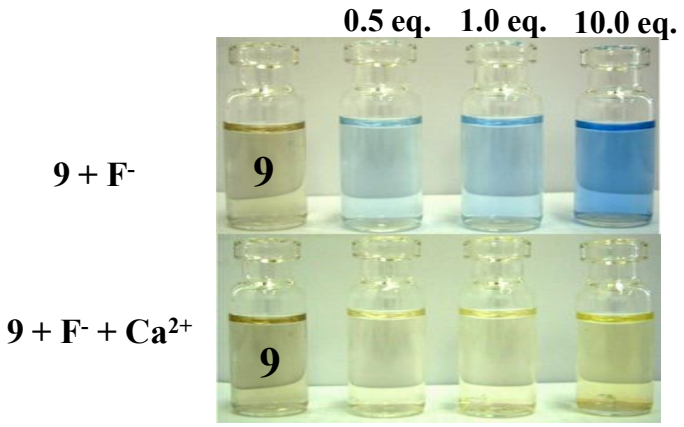

Figure D5. Color change of ligand **9** (0.02 mM) with 0.5, 1.0 and 10 equiv of F^- and then put excess of $CaNO_3$ into each solution of complex **9**.F^- in CH_3CN.

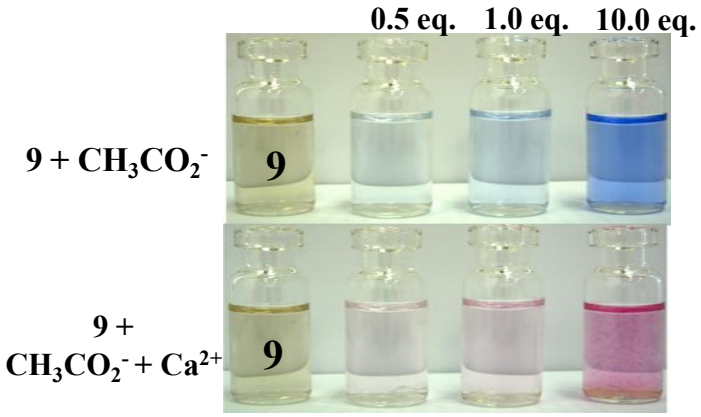

Figure D6. Color change of ligand **9** (0.02 mM) with 0.5, 1.0 and 10 equiv of $CH_3CO_2^-$ and then put excess of $CaNO_3$ into each solution of **9**.$CH_3CO_2^-$ in CH_3CN.

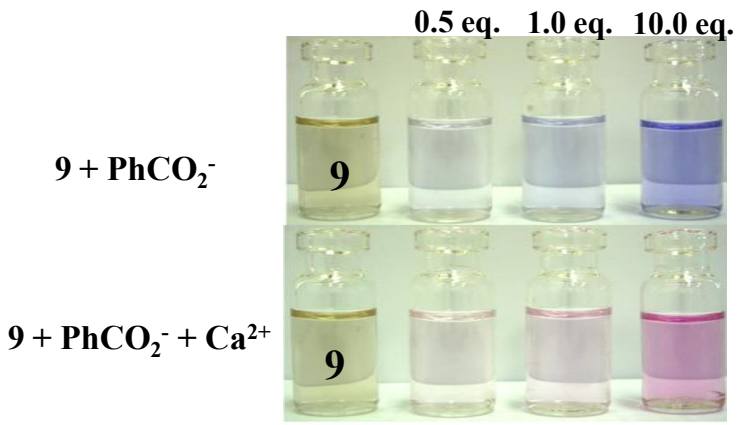

Figure D7. Color change of ligand **9** (0.02 mM) with 0.5, 1.0 and 10 equiv of $PhCO_2^-$ and then put excess of $CaNO_3$ into each solution of **9**.$PhCO_2^-$ in CH_3CN.

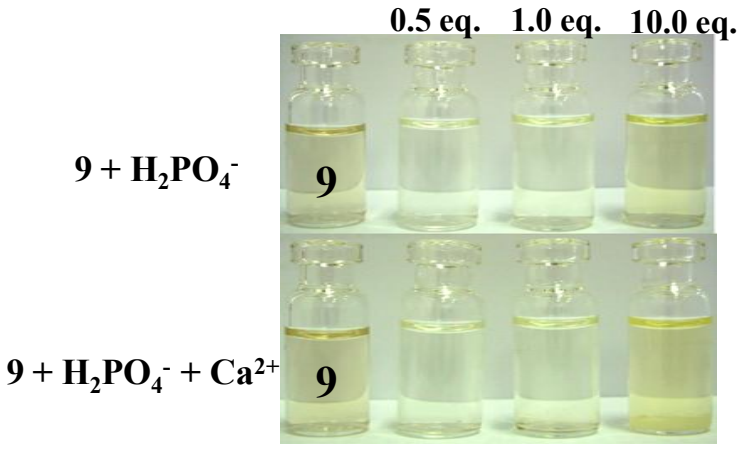

Figure D8. Color change of ligand **9** (0.02 mM) with 0.5, 1.0 and 10 equiv of $H_2PO_4^-$ and then put excess of $CaNO_3$ into each solution of **9**. $H_2PO_4^-$ in CH_3CN.

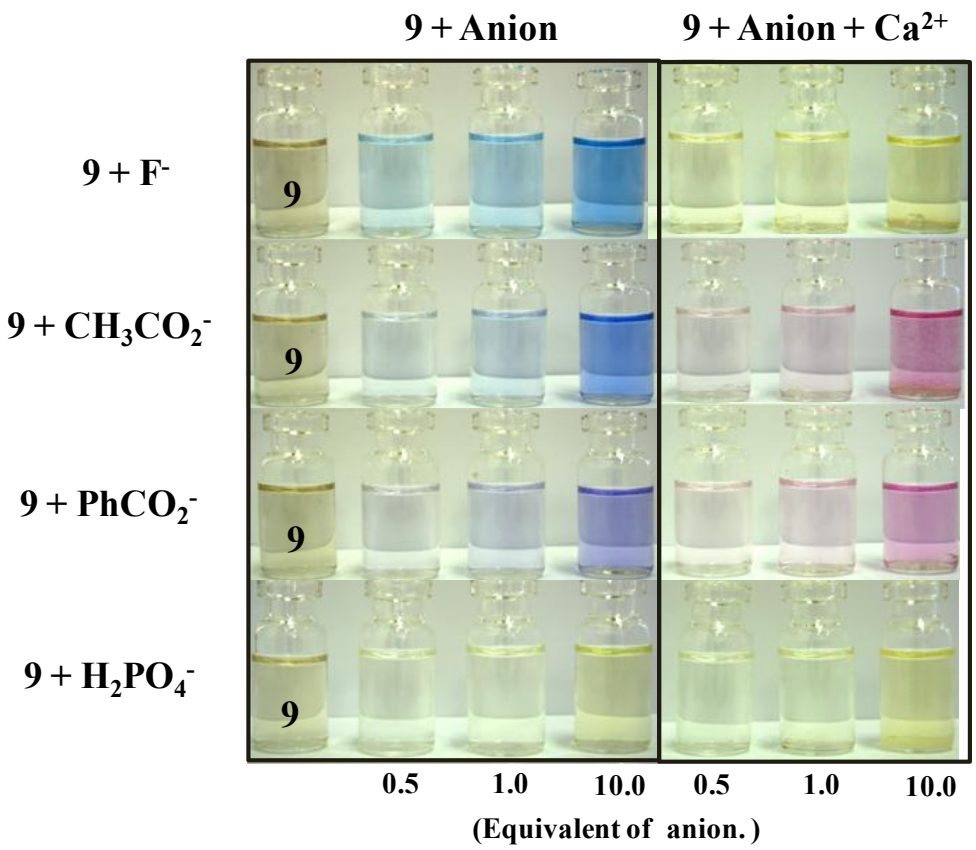

Figure D9. Compare color of the solution in each concentration of anions and cations in ligand **9** (0.02 mM) CH_3CN solution.

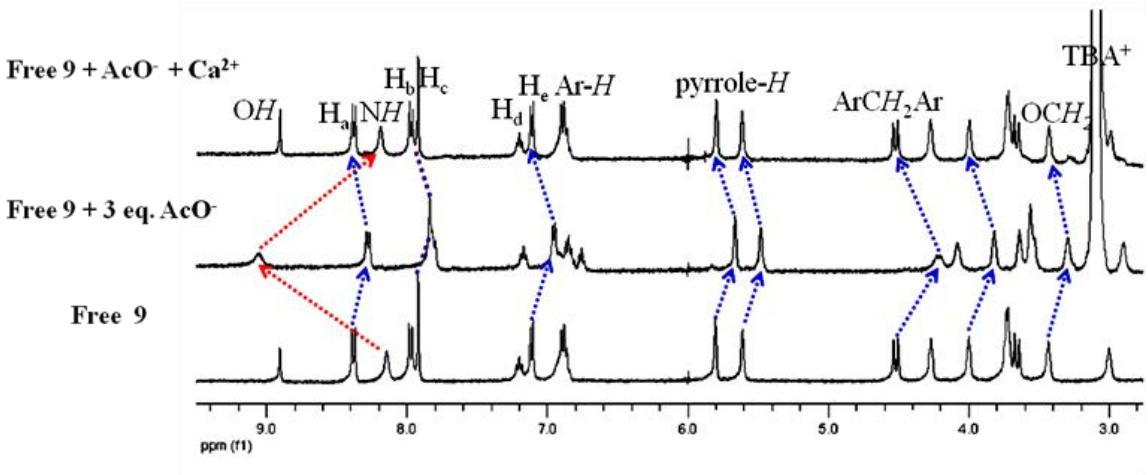

Figure D10. ^{1}H-NMR spectra of ligand **9** (2.0 mM) after addition of 3 equiv. of AcO^- in CD_3CN and then excess $Ca(NO_3)_2$ were add to the **9**·AcO^- complex.

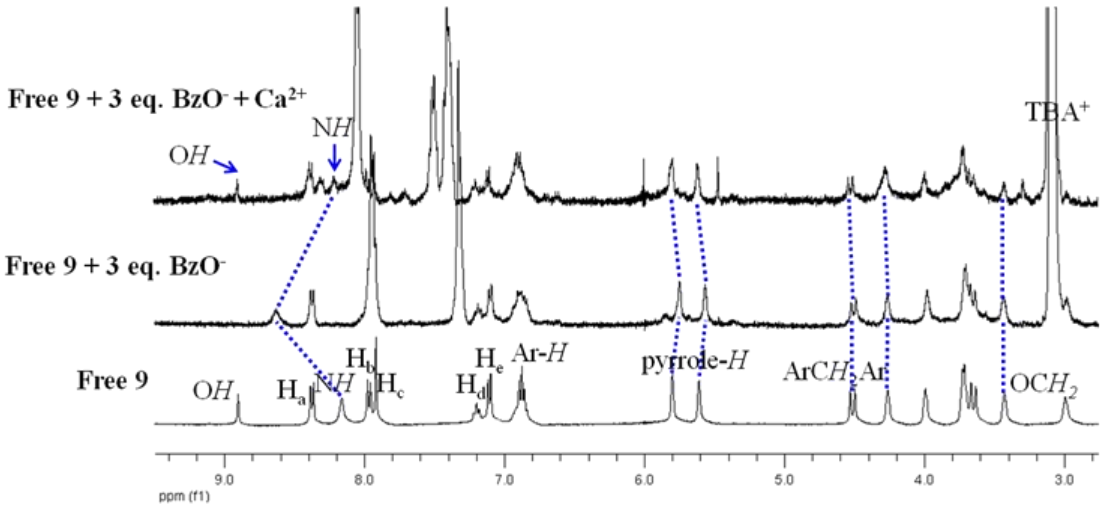

Figure D11. ^{1}H-NMR spectra of ligand **9** (2.0 mM) after addition of 3 equiv. of BzO^- in CD_3CN and then excess $Ca(NO_3)_2$ were add to the **9**·BzO^- complex.

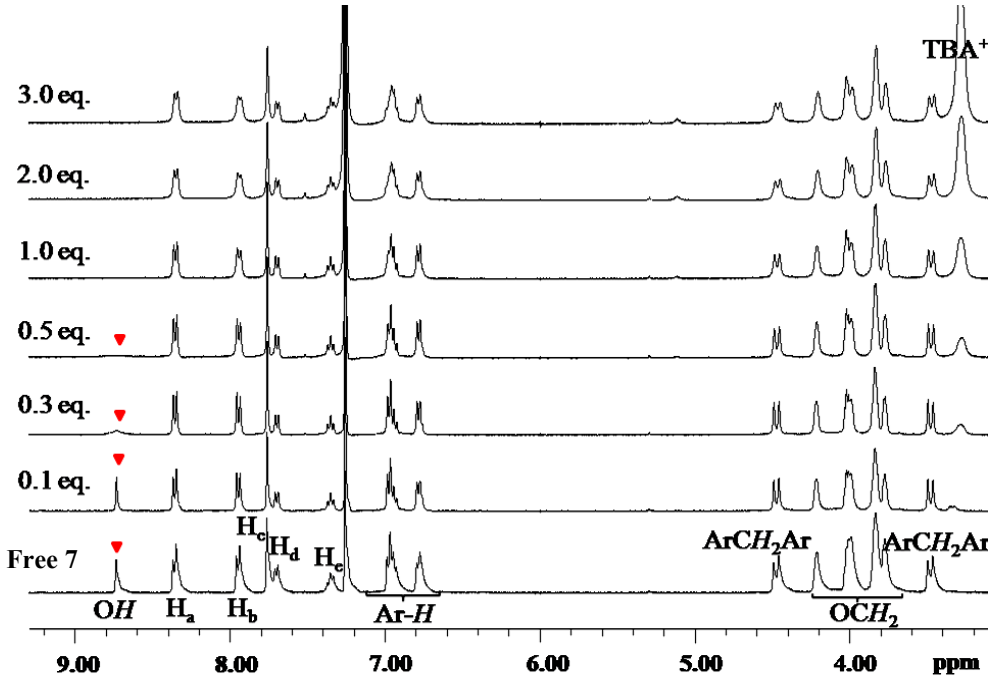

Figure D12. ^{1}H-NMR spectra of ligand **7** (3.58 mM) in $CDCl_3$ in the presence of different amounts of TBAF.

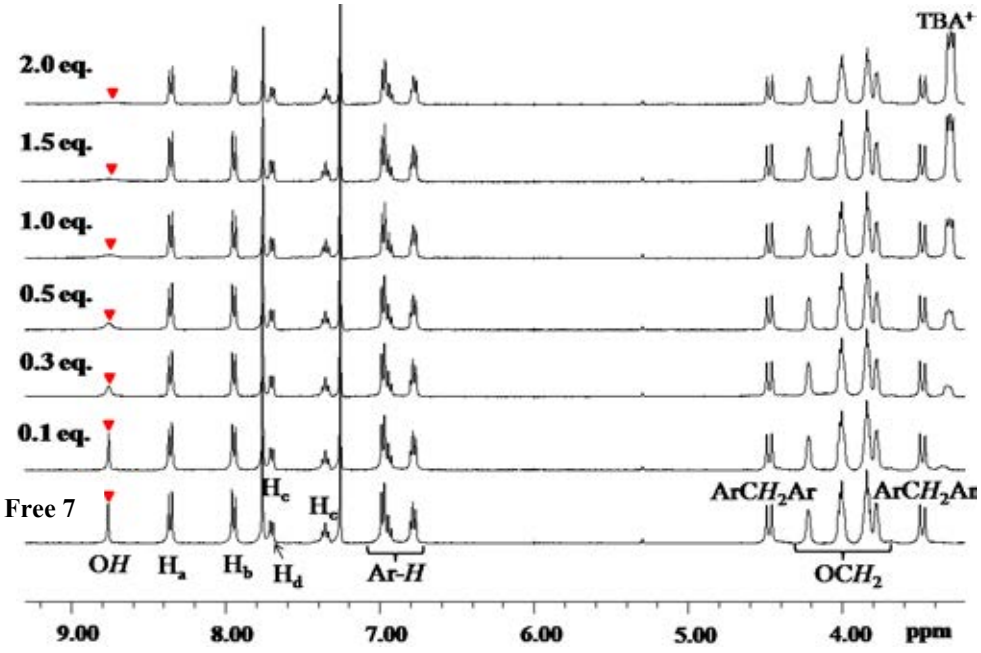

Figure D13. ^{1}H-NMR spectra of ligand **7** (3.58 mM) in $CDCl_3$ in the presence of different amounts of $TBA^{+}AcO^{-}$.

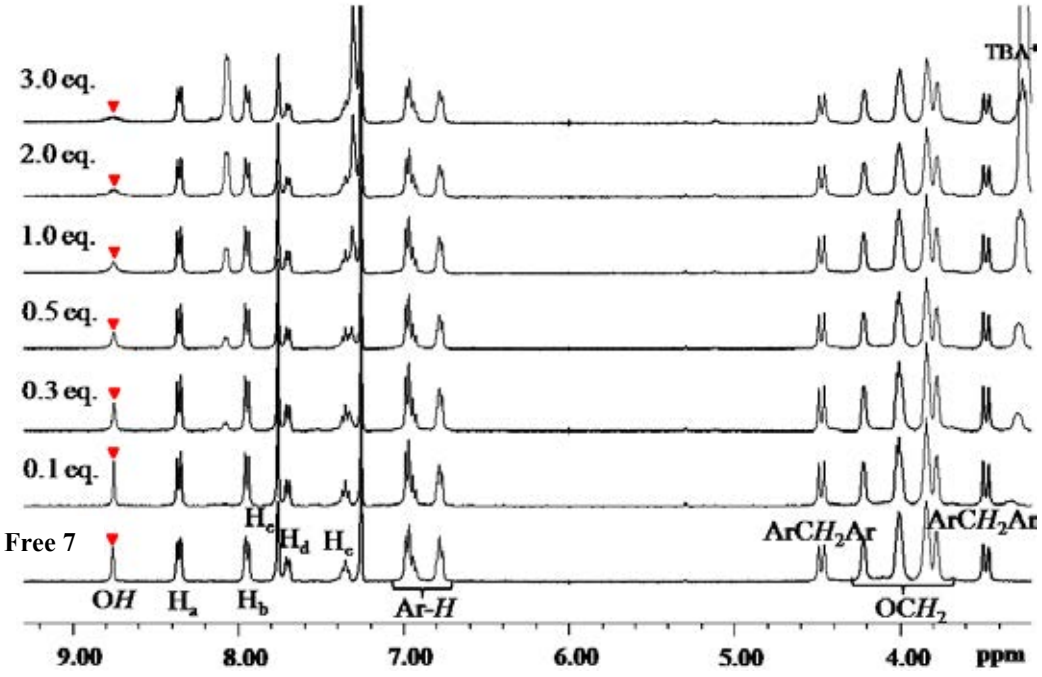

Figure D14. ^{1}H-NMR spectra of ligand **7** (3.58 mM) in $CDCl_3$ in the presence of different amounts of $TBA^{+}BzO^{-}$.

VITAE

Mr.Preecha Thiampanya was born on January 27,1979 in Angthong, Thailand. He graduated with a high school diploma from Angthong Phattamaroj Witthayakhom School, Angthong in 1996. He received his Bachelor's degree of Science in Chemistry from Ramkhamheang University in 2001. In the year of 2002-2003, he worked at the Center of protein structure and function, Faculty of Science, Mahidol University with Associate Professor Dr. Palangpon Kongsaeree. Since 2004, he has been a graduate student at the Department of Chemistry, Chulalongkorn University and become a member of the Supramolecular Chemistry Research Unit under Supervision of Associate Professor Dr. Buncha Pulpoka. He finished his Master's degree of Science in the academic year 2006. Since 2007 until 2012, he is a Ph.D. student of chemistry at the Department of Chemistry, Chulalongkorn University and become again to a member of the Supramolecular Chemistry Research Unit under Supervision of Associate Professor Dr. Buncha Pulpoka.